ABSTRACT

Title of dissertation: THE EFFECTS OF OXYGEN TRANSITION ON COMMUNITY METABOLISM AND NUTRIENT CYCLING IN A SEASONALLY STRATIFIED ANOXIC ESTUARY

Dong-Yoon Lee, Doctor of Philosophy, 2014

Directed By: Research Professor Jeffrey C. Cornwell
Marine Estuarine and Environmental Science

Gradients of dissolved oxygen concentrations in seasonally stratified estuarine water columns directly influence microbial composition and metabolic pathways, resulting in annually recurring spatiotemporal chemical gradients of redox-active species. Understanding such microbial responses to variable geochemical conditions and elucidating the diversity of microbial processes are needed to comprehensively identify ecosystem functions. At first this study describes an investigation of the relationships between microbial processes and geochemical conditions. To assess the contribution of different biological redox processes on carbon and nitrogen cycles in the Chesapeake Bay, we used observational and experimental approaches as well as utilization of monitoring datasets to facilitate an assessment of ecosystem-level metabolism. Observations revealed a general positive association of community metabolism with strong gradients of redox-related variables and hydrodynamic

characteristics, although geochemical and environmental conditions varied seasonally across oxic transitions and interannually across degrees of stratification. The most distinct evidence supporting the positive association were vertical distributions of community respiration with the highest average rates in the most stratified regions coincident with the depths of the steepest gradient of chemical compounds. Although organic matter availability may be enhanced due to hydrodynamically induced stability, our investigation of factors driving the pattern revealed that differential responses and metabolic strategies of microbial communities result in high respiration near oxyclines. Investigation of vertical profiles of redox-related variables also revealed that the coexistence of oxidants and reduced compounds further provides an optimal condition for other electron accepting processes, including chemoautotrophy and anoxygenic photoautotrophy. The strong interdependence between environmental conditions and variability in microbial metabolism also reflected in patterns of plankton assemblages. An ammonium mass-balance analysis revealed that increases in vertical ammonium dispersion during severe hypoxia cause a shift of plankton assemblages towards heterotrophy, subsequently supporting a deep secondary microbial food web in the vicinity of oxic/anoxic interface. Overall, results from this research indicate that the estimation of more accurate net ecosystem metabolism should take into consideration of the highly variable nature of community metabolism associated with both geochemical gradients and stratification.

THE EFFECTS OF OXYGEN TRANSITION ON COMMUNITY METABOLISM AND NUTRIENT CYCLING IN A SEASONALLY STRATIFIED ANOXIC ESTUARY

By

Dong-Yoon Lee

Dissertation submitted to the Faculty of the Graduate School of the
University of Maryland, College Park, in partial fulfillment
of the requirements for the degree of
Doctor of Philosophy
2014

Advisory Committee:
Dr. Jeffrey C. Cornwell, Chair
Dr. Byron C. Crump
Dr. Raleigh R. Hood
Dr. Todd M. Kana
Dr. Alyson E. Santoro
Dr. Karen L. Prestegaard, Dean's Representative

Dedication

My wife, *Yoo Kyung Song*,

My mother-in-law, *Mee Ra Park*

My mother, *Soon Hee Kim*

My grandmother, *Bong Ae Kim*

, who have never stopped praying for me.

Acknowledgements

I would like to begin by thanking my adviser, Jeffrey Cornwell, who had accepted me as a student but has treated me as a colleague. As far as I remember, he has never once said 'No' to my requests or has never ignored my opinions. We did not need a scheduled meeting because we had discussed a broad range of science topics from my dissertation research to other ecological issues almost every day. He had continuously introduced new or interesting topics, and they always led to novel insight into my research. I do and will always think that I could not have reached this far without his endless encouragement. In this regard, he is my role model as a scientist and a person. I would also like to give full appreciation to Michael Owens for providing a series of invaluable lectures for every detail of my experiments. His professionalism and perfectionism in series of scientific experiments had influenced my dissertation research without a doubt.

I would also like to give deep appreciation to my unofficial co-adviser Byron Crump for his time, advice, and expertise dedicated to my dissertation research. Byron helped to keep me in touch with microbial ecology and his insight always led to substantial improvement of my dissertation research. I would also like to thank the other members of my graduate advisory committee (Alyson Santoro, Todd Kana, and Raleigh Hood) for their expertise, time, comment, guidance, and encouragement that had undoubtedly influenced my dissertation research.

I would also like to thank many faculties at Horn Point Laboratory; Larry Sanford for joyfully answering for my thousand questions with full of enthusiasm, Michael Kemp for providing insight in ecosystem metabolism, Tom Fisher for his

contribution of background methodology and insight on stratification, Pat Glibert for improving my understanding on plankton physiology, Diane Stoecker and Jamie Pierson for providing invaluable insight in plankton dynamics.

I thank you all.

Table of Contents

List of Tables

List of Figures

Chapter 1: Introduction and Overview

Introduction

Seasonal depletion of dissolved oxygen (DO) is an important driver of biogeochemical cycles in eutrophic shallow ecosystems (Diaz and Rosenberg 2008; Middelburg and Levin 2009). The intensity and duration of DO depletion in areas commonly called Dead Zones has exponentially increased worldwide from the 1960s. These Dead Zones are strongly associated with industrialization and urbanization of adjacent watersheds supplying excessive nutrient loads. In Chesapeake Bay, United States of America, geochemical sediment records indicate that anthropogenic activities and human population have progressively increased the areal extent of hypoxia (<62.5 μmol l^{-1}, <2 mg l^{-1}) by changing many aspects of geochemical and biological conditions (Cooper and Brush 1993; Cooper 1995; Cornwell et al. 1996; Zimmerman and Canuel 2000). A particular interest has been paid to understanding how such inputs regulate a balance between primary production and respiration. The balance, which is called net ecosystem metabolism (NEM), is a measure of ecosystem functions and is highly influenced by biophysical factors, such as geochemical gradients (e.g., temperature, salinity), residence time, and composition of organic substrates, macrobenthos, and microbes (Holland et al. 1987; Hopkinson and Vallino 1995; Pomeroy and Wiebe 2001; Abril et al. 2002; Jordan et al. 2008; Giblin et al. 2010; Fortunato and Crump 2011).

To understand ecosystem functions, it is critical to know the relationships between various environmental factors and microbial metabolism because carbon and nitrogen cycling are predominantly mediated by microbes. However, we have a relatively weak understanding in how the spatiotemporal depletion of DO affects

microbial metabolic responses. Previous studies have paid more attention to anabolic than catabolic processes due to an assumed tight coupling between the two processes (e.g., Odum 1956) although respiration is an index of total sink (loss) of organic matter. We know that a spatiotemporal imbalance of NEM is a common feature along geochemical gradients in most estuaries due to high variability in factors controlling respiration (Kemp et al. 1997; Caffrey 2004). Such limited understanding in the loss term can be particularly problematic when we are trying to predict global carbon and nitrogen budgets because of disproportionately large impacts of estuarine processes (Bauer et al. 2013). These shallow environments (i.e., land-ocean aquatic continuum) have not been considered as an important sink of anthropogenic production on a global scale (Regnier et al. 2013) despite a rapid response of estuarine and coastal communities to environmental disturbances (Baird et al. 2004). To ensure accurate estimation of carbon and nitrogen budgets, therefore, future estimates will require an improved knowledge in various microbial metabolic pathways in low DO environments.

The decline of DO across vertical (i.e. depth) and horizontal (i.e. time or space) geochemical gradients gradually shifts energy (e.g. inorganic, organic compounds) from higher to lower trophic levels. Regardless of oxic conditions, a strong association of bacterial biomass and production with particulate organic matter during hypoxia suggests that pelagic respiration is mostly driven by bacterioplankton (Jonas and Tuttle 1990; Jonas 1997). Some microbes span a narrow range of oxic conditions due to microaerophilic or aerotolerant characteristics (Morris and Schmidt 2013), while other microbes can use alternate electron acceptors and go through a

gradual succession of respiratory processes to produce energy. For example, when DO is not available, a characteristic sequence of terminal electron acceptors is used in microbial respiratory processes in order of NO_3^-, Mn(IV), Fe(III), SO_4^{2-}, and CO_2 according to energy yield (Canfield et al. 2005).

Microbial respiratory processes recycle organic compounds that can further stimulate autotrophic and heterotrophic growth. In stratified water columns, however, pycnocline formation restricts vertical mixing and creates steep gradients of geochemical constituents. As a result, estuarine pycnoclines can be populated with both autotrophic and heterotrophic communities due to the coincidence of reduced compounds with oxidants (Fig. 1.1). Pycnocline formation and function is somewhat analogous to thin layers that are ubiquitously found in aquatic environments. Thin layers typically accumulate high concentrations of particulate and dissolved organic matter, including phytoplankton, zooplankton, and free and particle-attached microbes (Alldredge et al. 2002; McManus et al. 2005). Thus, we would likely observe similar dynamic mechanisms in stratified estuarine water columns, with efficient carbon and nitrogen cycling during hypoxia a likely result.

Nutrient cycling in estuarine systems has been of both scientific and management interest. Limited observations on the variability of both anaerobic processes and environmental structures in relation to hypoxia (e.g., depth of pycnoclines, strength of stratification) have been made. Understanding the cycling of dissolved compounds in hypoxic layers can be difficult because of a tight coupling between biogeochemical and physical factors simultaneously controlling the flux of chemical constituents (Kemp et al. 1992). Thus, the research presented in this

dissertation focuses on the effects of seasonal DO transition on community metabolism to improve our understanding in the dynamic interaction between biogeochemical and physical factors controlling estuarine nutrient cyclings.

Research Objective and Approach

The overall goal of this dissertation is to understand how microbial metabolism changes in response to the transition of DO, which is regulated by other hypoxia-related environmental conditions. My research focuses on the cycling of dissolved inorganic carbon (DIC) and nitrogen (DIN) in a broad array of geochemical gradients in pelagic and benthic communities. The different modes of primary and secondary production in the vicinity of oxyclines have been identified. I described biochemical and physical aspects of DIN cycling by integrating long-term monitoring data with experimental data acquired from metabolic analyses. Below is a summary of the objectives and approaches for each chapter.

Chapter 1:

Introduction and Overview

Chapter 2:

Indirect analytical methods have been used to assess anaerobic processes in pelagic and benthic ecosystems, and that could bias NEM in the seasonally stratified Chesapeake Bay. Respiratory pathways produce DIC regardless of surrounding oxic

conditions as a respiratory product along with other chemical compounds. So to determine if anaerobic metabolism plays an important role in estuarine nutrient cycling and NEM from spring to fall, I quantified the change in respiration activity in vertical and horizontal dimensions using simultaneous measurements of respiratory products. To collect samples for DIC, DO, N_2, H_2S, Fe, and Mn, water sampling methods with finer spatiotemporal scales than those typically examined in estuaries (i.e., meter vs. layer, month vs. season) were developed. High resolution observations of respiration in this chapter facilitate the comparison between total pelagic respiration (i.e., aerobic and anaerobic) and benthic processes. This process was used to increase our understanding of the role of anaerobic processes in carbon and nitrogen cycling. For estimating the flux of electron donors and acceptors across oxyclines and to propose other electron accepting processes that occurring in stratified water columns, profiles of geochemical constituents were analyzed.

Chapter 3:

Different modes of electron accepting processes in stratified water columns have an important role in supporting secondary microbial food webs with a profound effect on nutrient cycling. The study presented in this chapter examined the effects of these metabolic processes by using a radio-labeled carbon incubation experiment in addition to the metabolic measurements used in Chapter 2. To comprehensively identify ecosystem functions in oxic/anoxic interfaces, this chapter focuses on

understanding microbial responses to changing geochemical conditions and elucidating the diversity of microbially-mediated processes.

Chapter 4:

The relationship of microbial DIN regeneration with environmental conditions becomes complex because ammonium recycling per unit total nitrogen load was boosted in ecosystems with a history of hypoxia (Turner et al. 2008; Testa and Kemp 2012). The elevated recycling efficiency can further exert a positive feedback effect on the incidence and duration of hypoxia due to enhanced phytoplankton growth (Conley et al. 2007). Furthermore, biological changes can be tightly coupled to physical dispersion of ammonium fluxes below oxyclines because of a fundamental interdependence between chemical gradients and physical dispersion of geochemical compounds. The study examined the interaction of biological ammonium fluxes based on research conducted in Chapter 2 and 3 in relation to physical fluxes based on data from multiple monitoring programs using a mass-balance framework in bottom anoxic layers. One of the main objectives of this study was to quantify how long-term changes and variability in summer stratification altered the balance of biophysical ammonium fluxes.

Chapter 5:

Summary

Figure Legend

Fig. 1.1: The schematic diagram of energy flow and metabolic responses in stratified ecosystems. Anthropogenic nitrogen (N) and phosphorous (P) inputs cause a bloom of phytoplankton which is a key driver of seasonal hypoxia below strong density (ρ) gradients. Functional and phylogenetic diversity of microbes are denoted with different colors in the closeup pycnocline.

Figure

Fig. 1.1

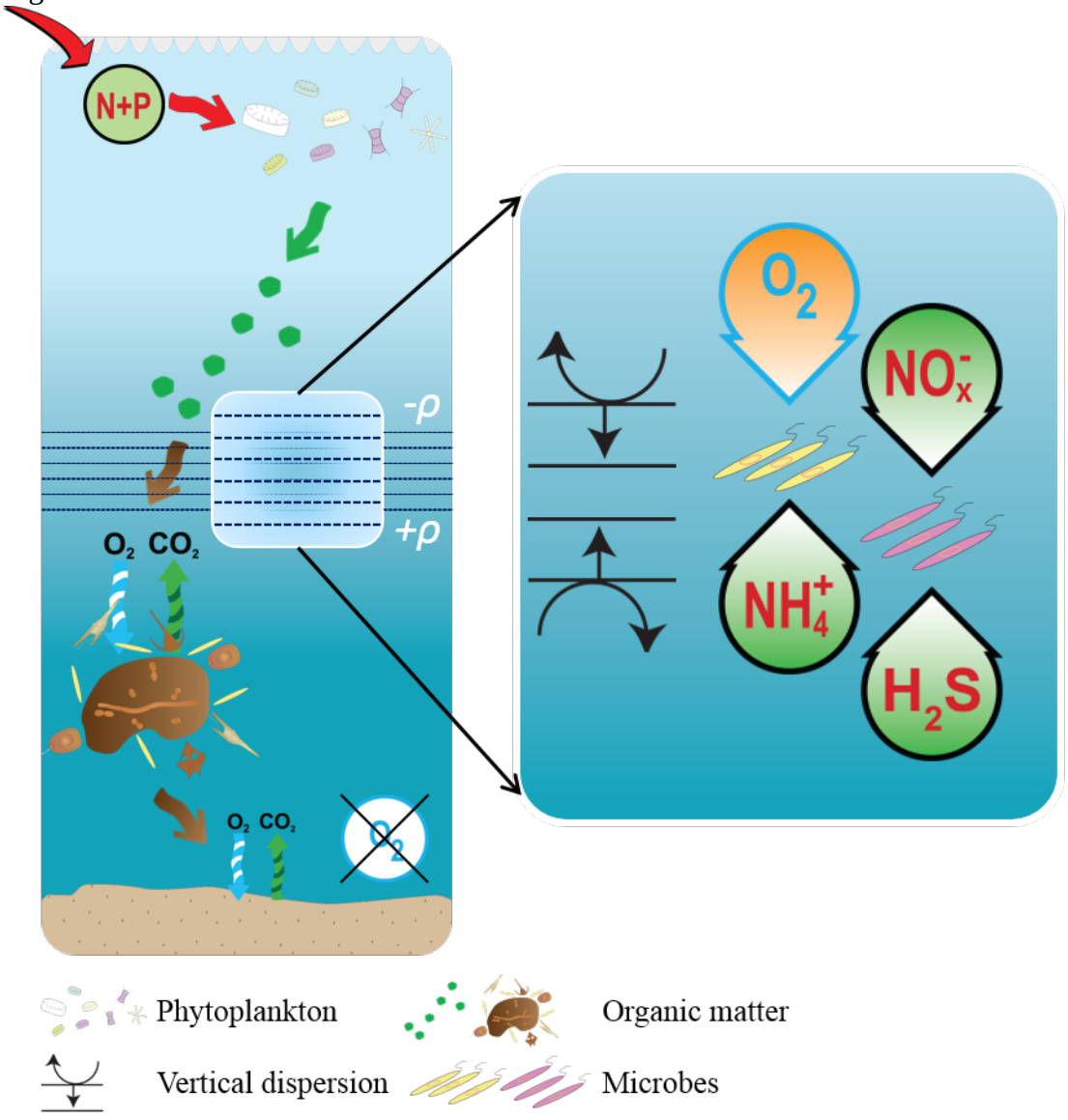

Chapter 2: The effects of oxygen transition on community respiration and potential chemoautotrophic production in a seasonally stratified anoxic estuary

Reference citation:

Lee, D. Y., M. S. Owens, M. Doherty, E. M. Eggleston, I. Hewson, B. C. Crump, and J. C. Cornwell. 2014. The effects of oxygen transition on community respiration and potential chemoautotrophic production in a seasonally stratified anoxic estuary. Estuaries and Coasts, DOI:10.1007/s12237-014-9803-8

Abstract

To assess the effects of seasonal oxygen transition on microbial metabolism, we measured spatiotemporal changes in total dissolved inorganic carbon, respiratory products, and geochemical constituents in the mesohaline region of Chesapeake Bay from May to October 2010. Vertical redox zonation was examined and a spatial transect survey was also conducted from the southern to northern limit of the mesohaline region in July providing an alternative approach for assessing the temporal dynamics of oxygen transition. The transitions from oxic to hypoxic to anoxic and back to oxic were illustrated by the pattern of nitrogen redox species. Respiration, measured from changes in total dissolved inorganic carbon (ΔDIC) and dissolved oxygen (ΔDO) during incubations, had an average respiratory quotient (ΔDIC / ΔDO) of 1.04 ± 0.06 under oxic conditions and 1.58 ± 0.48 under hypoxic conditions. The difference in the respiratory quotients suggested that oxygen-based respiration measurements would underestimate community respiration rates in hypoxic conditions. In the present study, we observed within the surface mixed layer 3 to 7-fold differences in temporal and vertical variation of community respiration, while net respiration across oxyclines and anaerobic respiration in deep waters had lower rates and variability. In some anoxic samples there was a net decrease in dissolved inorganic carbon that was exacerbated with experimental augmentation of terminal electron acceptors. Potential carbon fixation rates of chemoautotrophs within and below oxyclines were estimated and ranged from 0.63 to 116.9 mg C m^{-2} d^{-1} depending on growth conditions. These results indicate that anaerobic metabolism

during the seasonal anoxic transition and at oxic/anoxic interface can play an important role in the estuarine carbon cycle.

Introduction

Estuaries receive organic matter fluxes from terrestrial, oceanic, and estuarine sources. Most organic matter undergoes the process of biotic degradation and remineralization that are the outcomes of respiration. Respiration is an index of the flux of total organic carbon (Williams and del Giorgio 2005) and represents the largest sink of total organic carbon in estuaries (Kemp et al. 1997). Although respiration is a major component of carbon budgets (Smith and Hollibaugh 1993), the expansion of human perturbations (Cooper and Brush 1993; Zimmerman and Canuel 2000) and anoxic events (Diaz and Rosenberg 2008) appear to cause large uncertainties in respiratory carbon budgets (Gattuso et al. 1998).

There are inter and intra ecosystem differences in factors controlling pelagic and benthic respiration in estuaries. Environmental controls include the distance from the source of freshwater (*i.e.*, salinity), governing geochemical conditions (*e.g.*, pH, ionic strength, redox condition) (Jordan et al. 2008; Middelburg and Levin 2009; Giblin et al. 2010), metabolic diversity (Capone and Kiene 1988), the composition of organic substrates (Abril et al. 2002), macrobenthic activity (Holland et al. 1987), and pelagic microbial community composition (Fortunato and Crump 2011). Temperature and substrate supply are considered key factors because of physiological effects of temperature on cellular respiration fuelled by the degradation of organic substrates (Pomeroy and Wiebe 2001). For example, picoplankton respiration, which accounts

for >50 % of community respiration (Jonas and Tuttle 1990; Jonas 1997), exhibits strong temperature dependence at water temperatures <20 °C (Sampou and Kemp 1994; Smith and Kemp 2001; Apple et al. 2006) while both temperature and organic substrates exert equally important controls on respiration variability at water temperature >20 °C (Shiah and Ducklow 1994). In sediments, aerobic degradation is affected by temperature, but not rates of anaerobic degradation (Sun et al. 1993; Cowan and Boynton 1996).

Current understanding of environmental controls on anaerobic respiration is limited because seasonal oxygen transitions result in seasonal changes in phylogeny and respiratory processes (Kan et al. 2006; Crump et al. 2007; Lin et al. 2008; Zaikova et al. 2010). Cellular respiration requires electron flow through membrane-associated transport systems from electron donors to acceptors to generate a proton gradient and ultimately energy. Facultative aerobes and obligate anaerobes can produce energy in anoxic conditions using a sequence of terminal electron acceptors (other than oxygen) such as NO_3^-, Mn(IV), Fe(III), or SO_4^{2-}. As pelagic respiration depletes oxygen in the water column, anaerobes initiate a succession of respiratory processes (Wright et al. 2012). In shallow aquatic systems, the cycling of terminal electron acceptors is determined by microbially-mediated reactions (McCarthy et al. 1984), depletion of energetically-favored terminal electron acceptors (Nealson and Myers 1992), diffusion or mixing rates (Horrigan et al. 1990; Bourgault et al. 2012), phytobenthic processes (Epping et al. 1998), and ionic composition (Capone and Kiene 1988).

Anaerobic respiration rates have previously been estimated using isotopic techniques or stoichiometric mass balances of respiratory metabolites. For instance, sulfate reduction can be estimated with either utilization of $^{35}SO_4^{2-}$ radiotracers (Roden et al. 1995; Marvin-DiPasquale and Capone 1998) or from the vertical distribution of metabolites across redoxclines (Kemp et al. 1992). However, dependence on the stoichiometric equivalent of oxygen consumption associated with sulfide flux can bias sulfate reduction rates because of iron sulfide formation (Roden and Tuttle 1992; Marvin-DiPasquale and Capone 1998) or a coupling of sulfide oxidation with metal reduction (Nealson and Myers 1992; Burdige 1993).

Observations of biologically-driven changes in total dissolved inorganic carbon (DIC = $[H_2CO_3] + [HCO_3^-] + [CO_3^{2-}]$) have improved our understanding of estuarine carbon budgets regardless of redox conditions (Hargrave and Phillips 1981; Anderson et al. 1986; Wissel et al. 2008; Jiang et al. 2010). Although DIC concentrations may vary conservatively with salinity in a quasi-steady-state estuary (Zhai et al. 2007), non-conservative behavior occurs through factors such as air-sea exchange, and both pelagic and benthic autotrophic and heterotrophic processes (Cai and Wang 1998). To assess the non-conservative pattern of DIC in a seasonally stratified environment, fine-scale (*i.e.*, less than the thickness of pycnocline) or discrete interval vertical sampling is necessary because of high spatiotemporal variability of microbial abundance, community composition, and metabolism above, below and across oxyclines (McDonough et al. 1986; Jonas 1997; Hamdan and Jonas 2006; Robinson 2008). DIC measurements also improve our systematic

understanding of net ecosystem metabolism because both primary production and respiration can be measured with DIC (Oviatt et al. 1986b).

Here we report fine-scale DIC-based community respiration rates measured in the water column and sediment of seasonally stratified anoxic Chesapeake Bay to determine the influence of changing environmental and redox conditions on respiration. We hypothesized that microbial respiration below oxyclines would vary both seasonally and vertically. Specifically, lower rates would be observed in summer due to the depletion of electron acceptors with high energy yields. We further hypothesized that higher rates would be observed near the oxycline due to close proximity of algal organic carbon and electron acceptors with higher energy yields. Moreover, to examine multiple limiting factors for anaerobic respiration, anoxic water samples were augmented with terminal electron acceptors to investigate metabolic responses to the possible diffusion or advection of electron acceptors.

Materials and Methods

This study was conducted in the mesohaline region of Chesapeake Bay where spring blooms (Harding 1994) and seasonal anoxia (Hagy et al. 2004) occur annually. The main site (S4: 38° 22'N, 76° 24'W) for temporal observations near the mouth of the Little Choptank River, Maryland (Fig. 2.1) has extensive background data on water column and sediment processes (Cornwell et al. 1996; Cowan and Boynton 1996; Marvin-DiPasquale and Capone 1998; Zimmerman and Canuel 2000; Smith and Kemp 1995). Sampling at S4 was conducted seven times (17 May, 7 June, 16 June, 11 July, 5 August, 31 August, and 18 October 2010) using a small boat. In

addition, we conducted an axial transect survey along the central channel of Chesapeake Bay from S1 (mouth of the Rappahannock River) to S5 (Chesapeake Bay Bridge) on the R/V *Hugh R. Sharp* on 10-14 July 2010 (Fig. 2.1). This transect survey mapped spatial geochemical properties as bottom water slowly flowed northward. The times and locations of sampling were determined to capture specific oxic conditions: oxic, hypoxic, anoxic (*i.e.*, no reduced sulfur compounds), and sulfidic conditions below oxyclines.

Sampling and Incubation

A Sea-Bird conductivity-temperature-depth (CTD) system with dissolved oxygen (SBE 25 on a small boat and SBE 911plus on R/V *Hugh R. Sharp*; Sea-Bird Electronics) and fluorescence (WETStar, WET Labs) sensors was used to select eight sampling depths including three above, two within, and three below the oxyclines. When an oxycline was absent in May and October, changes in salinity were used to apportion the sample depths. As a result, it should be noted that sampling depths changed on each cruise. Post-processing of CTD data corrected the time delay between sensors, and sample parameters were averaged by time (SBE Data Processing v.7.21d). Samples were collected between 08:30 and 11:30 and we spent <20 min at each depth. We used a diaphragm pump with a 2.5 cm diameter hose attached to the CTD frame and ended with a conical PVC manifold distributing water to 16 tubings to fill sample vials.

Dark bottle incubations were used to estimate respiration. Initial samples were preserved with 2 µl per ml of 50 % saturated mercuric chloride in either 12 ml vials with silicon septum caps or 7 ml test tubes with ground-glass stoppers.

Simultaneously, incubations were conducted in triplicate 60 ml biochemical oxygen demand (BOD) bottles covered with opaque plastic bags. Bottles were incubated in either a thermostated bath or a temperature-controlled environmental chamber (±1°C of *in situ* water temperatures) for 24 h. The linear increase of DIC was examined with water samples collected in different oxic conditions (Fig. 2.2). At the end of incubation, samples were siphoned from the BOD bottles to the vials and preserved with mercuric chloride, submerged in water at below-ambient temperatures, and analyzed within 1 wk. Respiration rates were measured as differences in DIC and dissolved oxygen concentrations between initial and final samples divided by incubation times.

Sediment cores were collected at all sampling sites (except on 5 August) with an acrylic/PVC Soutar-design box corer to determine sediment-water fluxes. The sediment was sub-cored using two 7×30 cm (inner diameter × height) acrylic cylinders to a depth of ~15 cm. Sediment and water column blank cores were preincubated in a temperature-controlled walk-in chamber or incubator at bottom water temperatures (±1 °C) for 6 h for oxic conditions and for 18 h for anoxic conditions to allow any initial core disturbance artifacts to dissipate. Each core was equipped with a Teflon magnetic stir bar rotating at 20 rpm to mix overlying water without resuspension. Overlying water was collected four times during 4-6 h incubations (oxic) or 24 h incubations (anoxic): gas and solute samples were collected in triplicate 6 ml Exetainer vials and 20 ml syringes, respectively. During each subsampling, 5 % water volume in each core was replaced with collected bottom water through a second port so that no bubbles formed within the tubes. Sediment-

water fluxes were calculated using linear regressions of gas or solute concentrations and the slopes of blank cores were used to account for water column processes. The sediment-water flux experiments resulted in high regression coefficients: linear regression of DIC flux resulted in $r^2 > 0.95$ ($p < 0.01$) in 15 out of 20 cores and the lowest value ($r^2 = 0.91$, $p < 0.05$) was measured on 31 August.

Analytical Methods

Solute samples were filtered using 0.4 µm pore size cellulose acetate syringe filters. Solutes measured were ammonium (NH_4^+), soluble reactive phosphorus (SRP), total dissolved sulfide (DS = $[S^{2-}] + [HS^-] + [H_2S]$), nitrite ($NO_2^-$), nitrate ($NO_3^-$), and dissolved manganese (DM). Concentrations of NH_4^+, SRP, DS, and DM were analyzed colorimetrically (Brewer and Spencer 1971; Parsons et al. 1984). Concentrations of NO_2^- and NO_3^- were determined by segmented flow analysis after cadmium reduction (Lane et al. 2000).

An infrared-based analyzer (Apollo SciTech; Cai and Wang 1998) was used for DIC analysis because of its low sample volume (0.75 ml), high throughput (<2 min per analysis), and high precision (Goyet and Snover 1993; Huang et al. 2012). Standard solutions of sodium carbonate were prepared using distilled water over a range from 1000 to 2000 µmol C l^{-1} and preserved with mercuric chloride. The standard solution was transferred to autoclaved borosilicate glass tubes fitted with a septum. Standardization was repeated several times prior to analyzing the first sample of each cruise and daily during the transect survey as described in Goyet and Hacker (1992). The standard's precision was 0.04-0.12 % depending on sampling volume, with higher precision (0.04-0.06 %) when 0.75 ml of sample was analyzed. The

calibration was also checked twice with certified reference material (CRM; 2064.11 µmol C l^{-1}; A. Dickson, Scripps Institution of Oceanography). A comparison of standard solution and CRM resulted in a difference of <2 µmol C l^{-1} (<0.1 %).

Dissolved oxygen to argon ratios were measured with a membrane inlet mass spectrometer (Kana et al. 1994) yielding a precision of <0.05 %. Thermostated (±0.02 °C of incubation temperature) deionized water was used for standardization and gas ratios were converted to gas concentrations using temperature and salinity-based argon concentrations (Colt 1984).

Terminal Electron Acceptor Addition Experiment

Samples collected at S2 (anoxic/non-sulfidic) and S5 (sulfidic) bottom water were augmented with dissolved oxygen and NO_3^- during the transect survey. For oxygen augmentation, bottom water was rapidly mixed in a 20 l carboy to increase dissolved oxygen to near-saturation concentrations (6.7 mg l^{-1}). Samples were subsequently siphoned into triplicate 300 ml BOD bottles. For NO_3^- augmentation, bottom water in 300 ml BOD bottles was spiked with an anaerobic $NaNO_3$ solution to a final concentration of 20 µmol l^{-1}. After a 24 h incubation, we preserved samples with mercuric chloride and measured DIC concentrations.

Statistical Analyses

All tests were performed using R (version 2.13.0, R Foundation): regression, Tukey's Studentized range test, and principal component analysis (PCA). Homogeneity of variances and normality of residuals were tested for regression analysis with Anderson-Darling and Bartlett's test, respectively. PCA was employed

to identify spatiotemporally simultaneous changes in environmental indices associated with DIC respiration. The data include 88 observations of 11 variables (*e.g.*, dissolved oxygen, fluorescence, temperature, salinity, DIC respiration, NO_2^-, NO_3^-, NH_4^+, DS, SRP, DM) and eigenvectors of PCA results were plotted to examine relationships between variables. Geochemical water properties were mapped with contour plots using EasyKrig V3.0 in MATLAB (Mathworks). We used kriging with an isotropic nonlinear semi-variogram model as a gridding method that performed statistical interpolation at every 5 cm in the y-direction, and 12 h and 1 km in the x-direction for temporal and transect survey, respectively.

Results

During the temporal survey we observed a transition of sub-pycnocline redox conditions from oxic to hypoxic to anoxic to sulfidic, and back to oxic (Fig. 2.3 a). The average pycnocline thickness was 4.2 m (18 % of total depth) and usually coincided with rapid geochemical changes (*e.g.*, halocline, oxycline, nutricline) (Fig. 2.3 b-j). Similar transitions of redox conditions were also observed in the transect survey in July when northward oxygen depletion reflected the aging of bottom water as it moves up-estuary (Fig. 2.3 k). Pycnocline thicknesses across this spatial transect averaged 4.8 m (23 % of total depth) with rapid lateral changes in geochemical distributions (Fig. 2.3 l-t).

In May and June, the dominant dissolved inorganic nitrogen (DIN) species was NO_3^- in the surface mixed layer and NH_4^+ below the pycnocline with NO_2^- concentrations usually <1 μmol l^{-1} (Fig. 2.3 e-g). In July and early August, the sum of

DIN was usually low (<1 µmol l^{-1}) in the surface mixed layer, but high below the pycnocline due to elevated NH_4^+ concentrations, which coincided with high DS, DM, and SRP (Fig. 2.3 h-j). Under the anoxic non-sulfidic conditions on 31 August high NO_2^- concentrations dominated total DIN (85%) within and below the pycnocline. In September and October destratification appeared to cause vertical mixing of dissolved oxygen, NO_2^-, and DM. During the transect survey DIN was dominated by NH_4^+ (Fig. 2.3 o-q). Bottom water NO_2^- and NO_3^- disappeared northward under anoxic conditions and high NH_4^+ and SRP concentrations were observed in a narrow region (~10 km) between S2 (38.224° N) and S3 (38.312° N). Both DS and DM concentrations increased northward from S3 (Fig. 2.3 r-t).

The concentration of DIC in the water column ranged from 1140 to 1860 µmol l^{-1} under stratified conditions and was usually higher in deeper saline water except after destratification (Fig. 2.4). The relationship between DIC and salinity was best described by a second degree polynomial function because the curve leveled off below the pycnocline (*i.e.*, >20 psu). Considering high seasonal variation in river discharge and respiratory processes which can result in DIC variability (Jiang et al. 2008), the regression analysis yielded a high coefficient of determination presumably due to much higher background DIC concentrations. The non-conservative pattern and moderate variability at all salinities suggests the strong influence of biogeochemical processes.

Above the pycnocline, the significant correlation between respiration rates measured with dissolved oxygen and DIC yielded a mean respiratory quotient of 1.04 ± 0.06 (standard error) (Fig. 2.5). Incorporating results from hypoxic sample

incubations (n = 17) without complete oxygen depletion, lower regression coefficients (r^2 = 0.84) were observed with a higher and more variable respiratory quotient of 1.58 ± 0.48.

Under water column stratification, respiration rates were higher above the pycnocline than within and below the pycnocline (Fig. 2.6); lower variability was observed when the water column was mixed (Fig. 2.6 a, g). In July and August a 3 to 7-fold increase of respiration rates was measured near the upper oxycline. In contrast, anaerobic respiration was consistently low with no detectable spatiotemporal pattern. We measured negative respiration rates (*i.e.*, the decrease of DIC concentrations during incubation) in some field observations below the oxycline (Fig. 2.6 a, b, e, k). During the transect survey (Fig. 2.6 e, h-k) high subsurface respiration rates were also measured at S3 and S4 near the upper oxycline.

The first four principal components (PC) used for the PCA analysis explained 44, 21, 14, and 12 % of total variability (Fig. 2.7). The results of PC1 suggest that oxygen and fluorescence increased in the opposite directions from salinity and reduced compounds (NH_4^+, DS, SRP), reflecting a spatiotemporal gradient of oxic condition. The results of PC2 suggest that respiration and temperature increased in the opposite directions from chlorophyll fluorescence, NO_2^-, and NO_3^-, reflecting a spatiotemporal discrepancy between the zone of high respiration and phytoplankton abundance.

Areal sediment-water fluxes were compared to water column respiration rates derived from a trapezoidal mid-point integration calculation (Fig. 2.8). We assumed that pelagic respiration below the deepest sampling depth was uniform and equal to

respiration rate of the deepest sampling depth in each cruise. Water column respiration during the temporal and transect surveys averaged 80 and 86 % of total produced DIC, respectively. Temperature dependence was observed in the sediment efflux of DIC and DIN during the temporal survey (Fig. 2.9). The ratio of DIC : DIN flux averaged 6.3 ± 0.8 when overlying water was anoxic and sulfidic (*i.e.*, June to August), 4.3 ± 2.2 when overlying water was oxic, and 5.6 ± 1.5 when all data were considered. The flux of NO_x (NO_2^- and NO_3^-) was usually negative (*i.e.*, into sediments) and contributed negligibly to total DIN flux.

The experimental augmentation of dissolved oxygen and NO_3^- (*i.e.*, terminal electron acceptors) resulted in an increase of DIC concentration under anoxic/non-sulfidic incubations (Fig. 2.10). Respiration in the control and oxygen addition treatments was not significantly different, while NO_3^- addition increased respiration significantly with respect to the control. In contrast, augmentation of both electron acceptors resulted in a decrease of DIC concentration under sulfidic conditions. Significant differences from the control were only observed with NO_3^- addition.

Discussion

Pelagic respiration was seasonally variable with high rates in the surface mixed layer, while the contribution of sediment-water DIC flux was <20 % of total DIC production, consistent with observations in eutrophic estuaries (Hopkinson and Smith 2005). Maximum hypoxic volume was 13.5 km^3 in 2010 which was similar to the long-term (1985-2010) average of 13.2 km^3 (Bever et al. 2013). Other studied years included in Table 2.1 also had either similar or lower hypoxic volumes than the

long-term average. Thus, it is likely that our data and previous studies in Table 2.1 represent community respiration in an average hypoxic year. However, with the spatiotemporally finer resolution of this study, we were able to assess the influence of seasonal anoxic transitions on diverse microbial metabolism pathways including aerobic and anaerobic respiration, and biological oxidation of reduced species across oxyclines. The variability in vertical profiles of respiration rate was most distinct in mid-summer when strong redox gradients across the oxycline were evident (Fig. 2.3 and 2.6). The highest DIC respiration rate of 6.2 ± 0.4 μmol l^{-1} h^{-1} was measured on 5 August, which is approximately 5-fold higher than the monthly mean of previous studies (Table 2.1). The peak abundances of bacterioplankton (Crump et al. 2007) and mesozooplankton (Pierson et al. 2009) in the oxycline are consistent with high subsurface respiration. The high abundance of heterotrophs in this zone have not been taken into account in previous community respiration studies. The higher respiratory quotient within the oxycline relative to surface mixed layers suggests that oxygen-based respiration measurements underestimate community respiration across the oxycline (Wissel et al. 2008).

Influence of Temperature and Substrate Supply

Chesapeake Bay microbial respiration is predominantly controlled by temperature in spring, but in summer both temperature and substrate are important (Shiah and Ducklow 1994). Those observations are inconsistent with the PCA results showing a negative relationship between temperature and fluorescence although most of our studies were conducted in summer (Fig. 2.7). However, the negative correlation between pelagic respiration and fluorescence is likely caused by

subsurface high aerobic respiration in mid-summer and a minimal dependence of anaerobic respiration on 'fresh' phytoplankton. Previous studies suggest mesohaline bacterial abundance and metabolism were not correlated with chlorophyll *a* during summer (Jonas and Tuttle 1990) but were positively correlated with dissolved organic carbon originating from phytoplankton during seasonal hypoxia in the Potomac River (Hamdan and Jonas 2006). Thus, differential carbon utilization by aerobic and anaerobic microbes may yield the contrasting response we observed of respiration to phytoplankton abundance.

Temperature appeared to be an important control on sediment-water fluxes of DIC and DIN (Fig. 2.9). However, the sediment-water flux was more likely affected indirectly by vernal river flow stimulating phytoplankton production. The Susquehanna River flow in winter-spring is positively correlated with a deposition of chlorophyll *a* in the mesohaline region of the Chesapeake Bay (Boynton and Kemp 2000). If an average river flow of 1574 $m^3 s^{-1}$ in winter 2009-2010 is used (United States Geological Survey at the Conowingo Dam; http://waterdata.usgs.gov/md/nwis), it results in a loading of 1.06 g chlorophyll *a* m^{-2} from mid-February through the end of April, which is equivalent to 54.18 g C m^{-2} using a carbon to chlorophyll *a* ratio of 51 (Wienke and Cloern 1987). All of these carbon equivalents would be consumed by benthic processes roughly by the end of June (within 61 d) using a linear interpolation of sediment-water fluxes between cruises. However, higher sediment-water DIC and DIN fluxes observed in late summer suggest that there was continuous input of organic carbon. It is likely that algal organic carbon (*i.e.*, phytodetritus) rather than terrestrial organic carbon drives

metabolic rates; sediment $\delta^{13}C$ data (Cornwell and Sampou 1995) are consistent with phytoplankton as the major organic matter source in the mid-bay. The peak biomass of planktonic organisms coincide with the formation and persistence of the pycnocline because of low vertical mixing rates (Etemad-Shahidi and Imberger 2002; Bochdansky and Bollens 2009). Additionally, with >50 % of bay surface area occurring within shallow flanks (Cronin and Pritchard 1975), lateral inputs of algal organic carbon could contribute to total organic carbon in the main channel (Malone et al. 1986; McCallister et al. 2006; Scully 2010). Both chemoautotrophic or anoxygenic photoautotrophic production have been identified as an important source of organic carbon in many stratified lagoons (Llirós et al. 2011), lakes (Cloern et al. 1983), and estuaries (Casamayor et al. 2001). Therefore, the variability of sediment-water DIC and DIN fluxes during seasonal anoxia appears to be driven by an interaction between temperature and organic carbon loading mainly from phytoplankton, rather than redox conditions.

Oxidation of Reduced Species Below and Across Oxyclines

The net DIC uptake observed during some hypoxic and anoxic periods (Fig. 2.6) were consistent with the results of terminal electron acceptor additions into sulfidic bottom water (Fig. 2.10). The net uptake of DIC suggests that chemoautotrophic growth and DIC fixation occurred when sub-pycnocline reduced nitrogen or sulfur compounds mixed with dissolved oxygen or NO_3^- (Labrenz et al. 2005). The transect survey showed a rapid transition of NH_4^+ within the oxycline, while that of DS occurred below the oxycline (Fig. 2.11). Since nitrification is inhibited by reduced sulfur compounds (Joye and Hollibaugh 1995), this spatial

displacement of reduced nitrogen and sulfur gradients would allow both nitrifiers and sulfur oxidizers to grow simultaneously in different redox conditions (Trouwborst et al. 2006).

To estimate the potential chemoautotrophic production in the study region, we have compared cross-oxycline NH_4^+ fluxes derived from NH_4^+ gradients and an eddy diffusion estimate (Kemp et al. 1992) with sediment-water NH_4^+ fluxes (Table 2.2). The average ratio of NH_4^+ fluxes between those measured across the sediment-water interface and those estimated across the oxycline was 1.24 in May and June, suggesting biological oxidation or uptake of NH_4^+ in the oxycline or bottom waters. Uptake of DIC was observed consistently below the oxycline on 7 June (Fig. 2.6 b) when 3.1 µM NO_3^--N was observed in anoxic conditions. If we assume that nitrifiers, chemoautotrophic microorganisms, were solely responsible for the DIC incorporation, potential DIC fixation rates can be estimated using yield factors (*i.e.*, mol of DIC fixed per mol of oxidized substrate molecule) ranging from 0.02 to 0.50 mol C (mol NH_4^+)$^{-1}$ depending on growth conditions (Andersson et al. 2006 and references therein). Thus, potential DIC fixation rates associated from nitrification could range from 0.01 to 0.32 µmol C l^{-1} d^{-1} (0.63 to 19.0 mg C m^{-2} d^{-1}) within the oxycline (mean depth of 4.9 m) in May and June.

The ratios of transect survey sediment-water NH_4^+ flux : oxycline NH_4^+ flux were highly variable, ranging from 0.55 to 7.08, and the highest ratio at S4 was caused by maximum sediment-water flux with minimum flux across the oxycline. The large spatial variability in the ratios suggests that nitrification was not limited by electron donors (*i.e.*, NH_4^+) during maximum summer stratification but rather by

either their growth rate, species distribution, or environmental conditions (Andersson et al. 2006; Crump et al. 2007). Potential DIC fixation rates estimated using the same assumption as above ranged from 0.13 to 3.8 μmol C l^{-1} d^{-1} (3.9 to 116.9 mg C m^{-2} d^{-1}) within the oxycline (mean depth of 2.6 m) during the transect survey. These potential nitrification rates were similar to NH_4^+-oxidation rates in the Delaware River estuary ranged from 0.01 to 4.1 μmol C l^{-1} d^{-1} (Lipschultz et al. 1986). Likewise, we also estimated potential DS oxidation rates using a range of yield factors from 0.11 to 0.58 mol C (mol DS)$^{-1}$ (Zopfi et al. 2001) resulting from 0.59 to 3.1 μmol C l^{-1} d^{-1} (18.5 to 97.7 mg C m^{-2} d^{-1}) within the oxycline.

Although large variabilities and uncertainties still remain in vertical diffusivity (Li et al. 2007) and chemoautotrophic yield factor (Veuger et al. 2013), the estimated potential chemoautotrophic rates are comparable to maximum values measured in other oxic/anoxic interfaces such as 17.2 μmol C l^{-1} d^{-1} the Coromina Lagoon (Llirós et al. 2011), 21.8 μmol C l^{-1} d^{-1} in the Big Soda Lake (Cloern et al. 1983), and 10.3 μmol C l^{-1} d^{-1} in the Ebro River salt wedge (Casamayor et al. 2001). Despite environmental variability in different stratified ecosystems, consistent ranges of chemoautotrophic production rates suggest that chemoautotrophic production is predominantly limited by growth rate, oxidizing activity, or supply of oxidants.

The large accumulation of NO_2^- we observed in late August-September also suggests active nitrification in the Chesapeake Bay water column. A previous study (Horrigan et al. 1990) attributing high NO_2^- in fall to nitrification suggested that the accumulation of NO_2^- may occur annually due to an increasing frequency and magnitude of winds. Although high NO_2^- concentrations can result from

phytoplankton excretion due to growth limitation (Lomas and Lipschultz 2006), the mechanism was unlikely in this region because of the absence of chlorophyll fluorescence at the depth of high NO_2^- (>11 m in Fig. 2.3 d, g). Accumulation of NO_2^- during nitrification may be due to several factors. The oxidation of NH_4^+ to NO_2^- has a higher affinity for oxygen than that from NO_2^- to NO_3^- (Martens-Habbena et al. 2009). Further, marine nitrite oxidizing bacteria, responsible for the second step of nitrification, are slow growing organisms (Watson et al. 1986) that may not be able to immediately respond to pulses of NO_2^-. Thus, differential reaction rates may result in the transient accumulation of NO_2^- (water column average of 2.57 µmol l^{-1} on 31 August) followed by NO_3^- (water column average of 1.69 µmol l^{-1} on 18 October).

While our data suggest that chemoautotrophic production may serve as an energy source in oxyclines, the estimated rates during the transect survey are an order of magnitude lower than typical summer phytoplankton production in the bay. If we assumed the highest yield factor for the oxidation of NH_4^+ and DS, potential chemoautotrophic production was 214.6 mg C m^{-2} d^{-1}, while gross phytoplankton production was approximately 2600 mg C m^{-2} d^{-1} in the mesohaline region in July (Malone et al. 1996; Kemp et al. 1997), indicating that the contribution of chemoautotrophic production would be <8 % of total primary production. In addition, chemoautotrophic processes would have a small effect on estuarine DIC cycling due to high background DIC concentrations and lower chemoautotrophic DIC fixation rates than heterotrophic DIC production rates. Although more data from experiments with finer spatiotemporal scale are needed to draw conclusions, it is likely that high

respiration rates above the oxycline resulted from degradation of complex organic matter predominantly composed of phytoplankton-derived organic matter.

Conclusion

Even on the meter scale that we sampled, the difference in aerobic respiration between near surface and upper oxycline depths resulted in up to a 7-fold difference, which can lead to an underestimation of the respiratory carbon budget. The elevated respiration near upper oxyclines has potentially significant environmental and ecological consequences, including increased extent and duration of hypoxia and enhanced interactions between aerobic and anaerobic organisms. Within the oxycline terminal electron accepting processes can lead to both heterotrophic organic carbon consumption rates and chemoautotrophic carbon fixation rates. Below the oxycline respiration resulted in low spatiotemporal variability but the pattern of respiratory products suggests the changes in microbial function and composition. Thus, large variabilities in all aspects of microbial populations make it hard to predict relationships between environmental variables and microbial metabolism during seasonal anoxic transition. However, with our new findings we may elucidate the interaction between reduced compounds and oxidants using higher resolution vertical sampling within oxyclines. We hypothesize that a zone of chemoautotrophic production may exist throughout spring and summer in the vicinity of the oxycline where the organisms can thrive due to the coincidence of reduced compounds with oxidants during seasonal oxygen transition. This chemoautotrophic primary production can potentially serve as an energy source in estuarine microbial food web.

Tables

Table 2.1: Summary of studies presenting monthly mean respiration rates in surface and bottom layers of water column separated by pycnoclines in the mesohaline of Chesapeake Bay. In previous studies, samples were collected from a depth of ~1 m below the air-water interface and from ~1 m above the sediment-water interface only when oxygen was present. A respiration quotient of 1.04 was used to convert oxygen-based respiration rates to carbon equivalents. Maximum values are included in parentheses. (nd: no data).

	May	Jun	Jul	Aug	Sep	Oct	Source
	(μmol C l^{-1} h^{-1})						
Surface	0.50	0.68	1.90	1.08	0.54	0.41	Kemp et al. 1992
	0.72	nd	2.21	1.11	nd	nd	Sampou and Kemp 1994
	0.73	1.14	1.71 (2.52)	1.63	1.38	0.98	Smith and Kemp 1995
	0.78	nd	1.41	nd	nd	0.63	Smith and Kemp 2001[a]
	0.83	1.16	1.61 (2.53)	1.82 (6.20)	nd	0.42	This study
(mean)	0.71	0.99	1.77	1.41	0.96	0.61	
Bottom	0.50	0.68	1.90	1.08	0.54	0.41	Kemp et al. 1992[b]
	0.44	0.59	0.91	0.68 (1.46)	nd	nd	Sampou and Kemp 1994[c]
	0.49	0.16	nd	nd	0.33 (0.65)	0.49	Smith and Kemp 1995
	0.24	-0.07	0.12	0.71 (1.24)	nd	0.17	This study in oxyclines
(mean)	0.42	0.34	0.98	0.82	0.44	0.35	

[a]: Mean values of year 1996 and 1997
[b]: When bottom water was anoxic, samples were collected from the steepest region of oxyclines
[c]: Samples were collected from a depth of pycnocline in July and August

Table 2.2: Sediment fluxes of NH_4^+ and total dissolved sulfide (DS) relative to those across oxyclines to investigate the decrease (if the ratio in the last column is >1) or increase (if the ratio is <1) of reduced compounds across the oxycline. Gradients of reduced compounds were estimated using a slope of reduced compounds. Cross-oxycline fluxes were estimated using an assumed vertical diffusivity of 1.73 $m^2\ d^{-1}$ according to Kemp et al. (1992).

Date	Station	Solute	Sediment-water flux	Gradient	Cross-oxycline flux	Sediment-water flux : Cross-oxycline flux
			(mmol $m^{-2}\ h^{-1}$)	(mmol m^{-4})	(mmol $m^{-2}\ h^{-1}$)	
17 May	S4	NH_4^+	0.28 ± 0.07	3.1	0.22	1.26
7 June	S4	NH_4^+	0.28 ± 0.07	3.6	0.26	1.06
16 June	S4	NH_4^+	0.21 ± 0.02	2.1	0.15	1.39
13 July	S3	NH_4^+	0.32 ± 0.02	7.9	0.57	0.55
		DS	0.23 ± 0.09	0.6	0.04	5.65
11 July	S4	NH_4^+	1.32 ± 0.04	2.6	0.19	7.08
		DS	0.48 ± 0.08	1.2	0.08	5.65
14 July	S5	NH_4^+	0.14 ± 0.01	2.9	0.21	0.68
		DS	0	0.3	0.02	0

Figure Legends

Fig. 2.1: Sampling stations along axial transect in the mesohaline region of Chesapeake Bay. Temporal surveys at S4 (main station; star symbol) were conducted from May to October while the spatial transect survey from S1 to S5 occurred on 10-14 July 2010.

Fig. 2.2: Time courses of dissolved inorganic carbon concentration normalized by initial concentration. Samples were collected at S4 on 17 May (9.7 mg O_2 l^{-1}), 7 June (1.5 mg O_2 l^{-1}), and 11 July (anoxic).

Fig. 2.3: Temporal (a-j) and spatial (k-t) transitions of biogeochemical variables reflecting redox conditions in the water column of Chesapeake Bay. Note that temporal surveys were conducted at a single station (S4) seven times while the transect survey was conducted at five stations (S1 to S5) in July. Oxygen concentrations (a, k) presented here were determined by membrane inlet mass spectrometry. Minimum and maximum values of color scale are identical for each variable. Gray circles represent sampling depths. Dotted lines on fluorescence maps represent the depth of 1 % of surface irradiance. (DS: total dissolved sulfide; SRP: soluble reactive phosphorus; DM: dissolved manganese).

Fig. 2.4: Relationship between salinity and dissolved inorganic carbon (DIC) in the water column from 17 May to 31 August 2010. DIC data on 18 October (gray circles) were not included in regression estimates.

Fig. 2.5: Relationship between respiration rates measured with dissolved oxygen and DIC. The straight line shows the result of linear regression analysis with oxic samples and the dotted line represents the 1:1 relationship. The highest respiration rate measured on 5 August was omitted in the plot but taken into account in the regression analysis. Error bars represent standard errors of the mean for a set of triplicate samples.

Fig. 2.6: Seasonal and spatial patterns of community respiration rates measured with DIC and dissolved oxygen. Horizontal dotted and dashed line represents the depth of 3 and 0.5 mg O_2 l^{-1}, respectively. Error bars represent standard errors of the mean for a set of triplicate samples.

Fig. 2.7: A bi-plot of principal component loadings of biochemical and environmental factors in water columns. (O_2: dissolved oxygen; Temp: temperature; R_{DIC}: pelagic respiration measured with DIC; Fluo: chlorophyll fluorescence; Sali: salinity).

Fig. 2.8: Comparison between sediment-water flux and water column respiration using a trapezoidal mid-point integration method for the latter in (a) temporal and (b) transect survey. Error bars represent standard errors of the mean for a set of duplicate cores for sediment-water flux and equal estimates of the propagated standard error for either eight (total water column) or four (below pycnoclines) sets of triplicate samples.

Fig. 2.9: Relationship between temperature and sediment-water flux of (a) DIC and (b) dissolved inorganic nitrogen (DIN flux = $NH_4^+ + NO_2^- + NO_3^-$ fluxes). Error bars represent standard errors of the mean for a set of duplicate cores.

Fig. 2.10: DIC respiration results augmented with terminal electron acceptors in anoxic at S2 (light gray bars) and sulfidic at S5 (dark gray bars). Tukey's Studentized range test was used to investigate statistical differences between treatments. Different letters indicate significant differences ($p < 0.05$) in each group. Error bars equal estimates of the propagated standard error for a set of triplicate samples.

Fig. 2.11: Vertical water column profiles of dissolved oxygen, NH_4^+, and DS measured at (a) S5, (b) S4, and (c) S3 during the transect survey.

Figures

Fig. 2.1

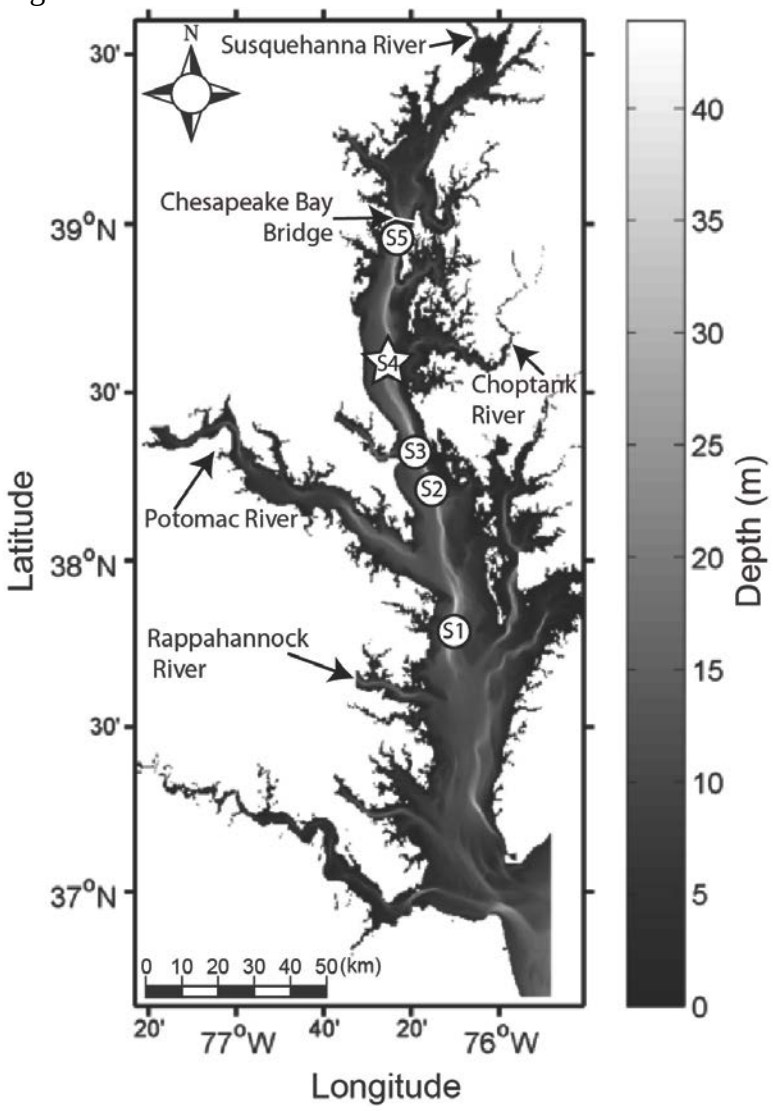

Fig. 2.2

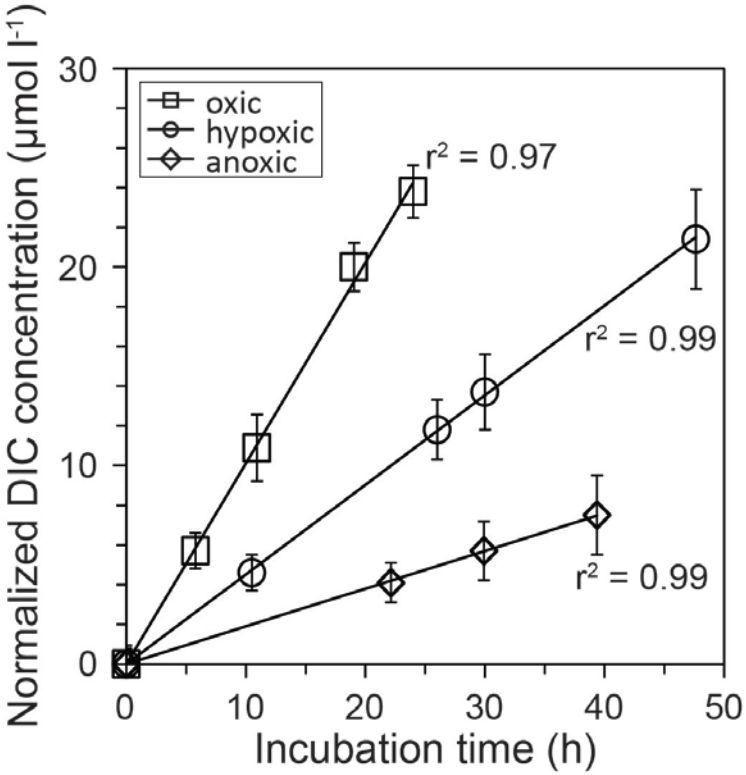
Normalized DIC concentration (µmol l-1)
Incubation time (h)
oxic
hypoxic
anoxic
r2 = 0.97
r2 = 0.99
r2 = 0.99
0
10
20
30
40
50

Fig. 2.3

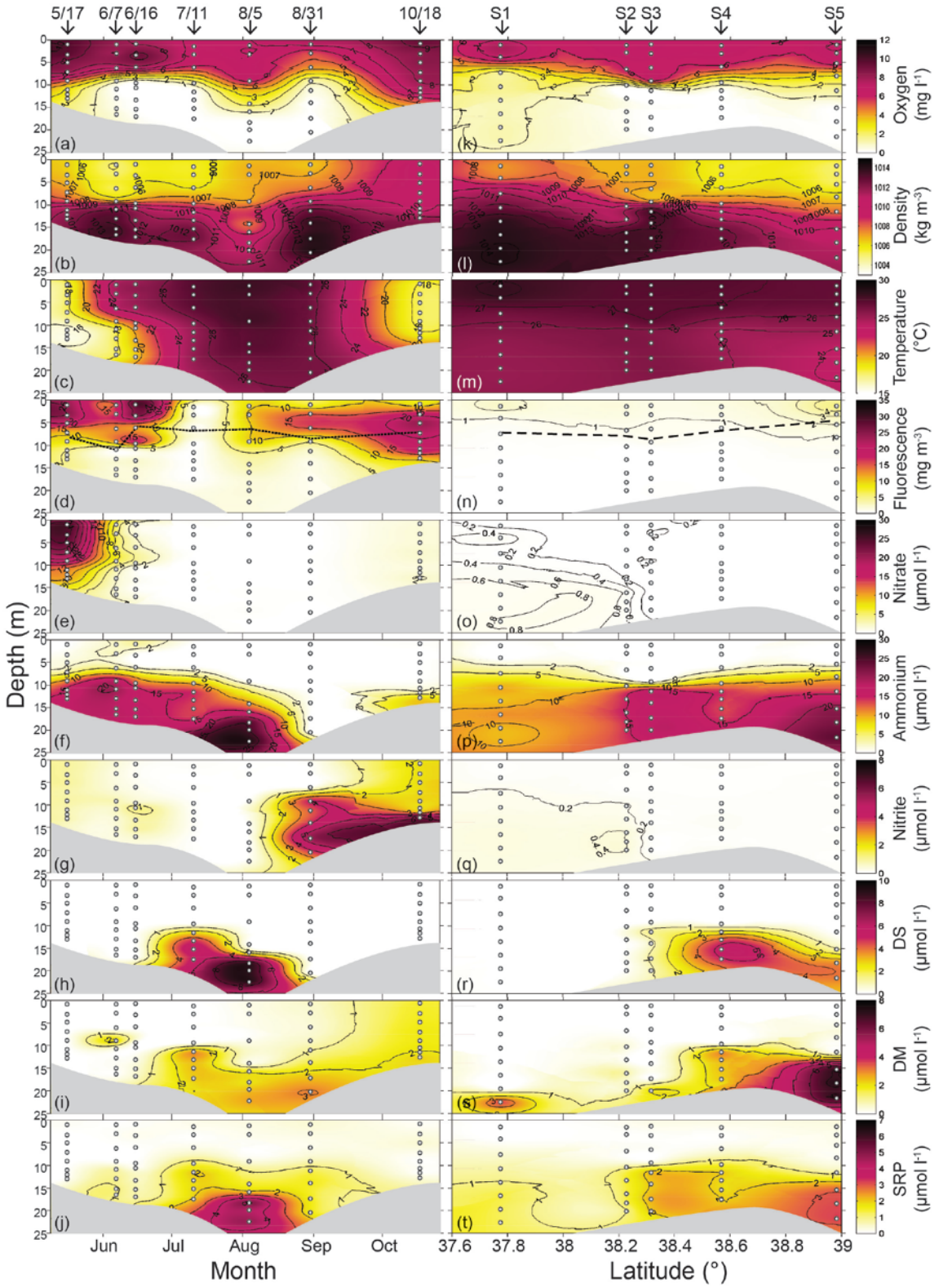
5/17
6/7
6/16
7/11
8/5
8/31
10/18
S1
S2
S3
S4
S5
Depth (m)
Month
Jun
Jul
Aug
Sep
Oct
Latitude (°)
37.6
37.8
38
38.2
38.4
38.6
38.8
39
Oxygen (mg l-1)
Density (kg m-3)
Temperature (°C)
Fluorescence (mg m-3)
Nitrate (µmol l-1)
Ammonium (µmol l-1)
Nitrite (µmol l-1)
DS (µmol l-1)
DM (µmol l-1)
SRP (µmol l-1)
(a)
(b)
(c)
(d)
(e)
(f)
(g)
(h)
(i)
(j)
(k)
(l)
(m)
(n)
(o)
(p)
(q)
(r)
(s)
(t)

Fig. 2.4

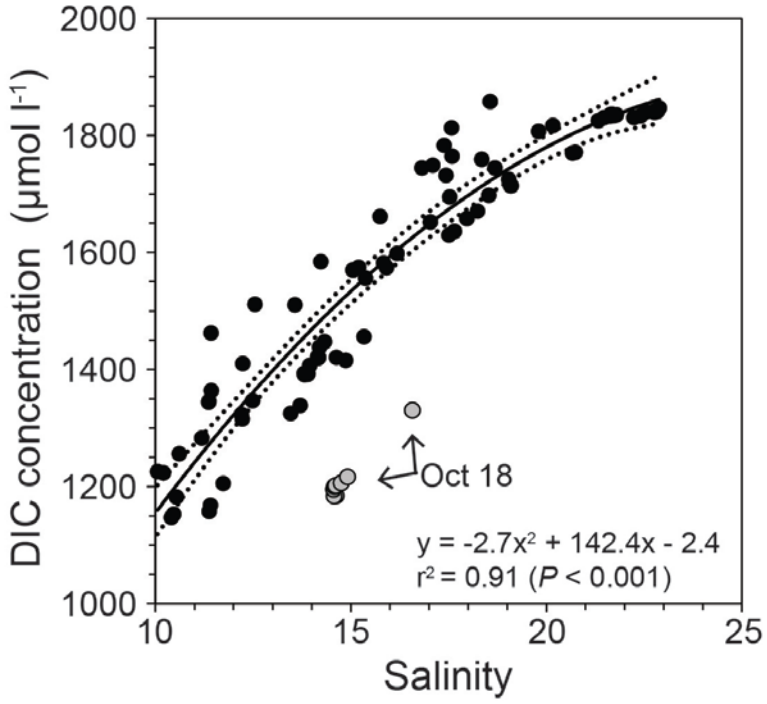
DIC concentration (µmol l-1)
2000
1800
1600
1400
1200
1000
10
15
20
25
Salinity
Oct 18
y = -2.7x2 + 142.4x - 2.4
r2 = 0.91 (P < 0.001)

Fig. 2.5

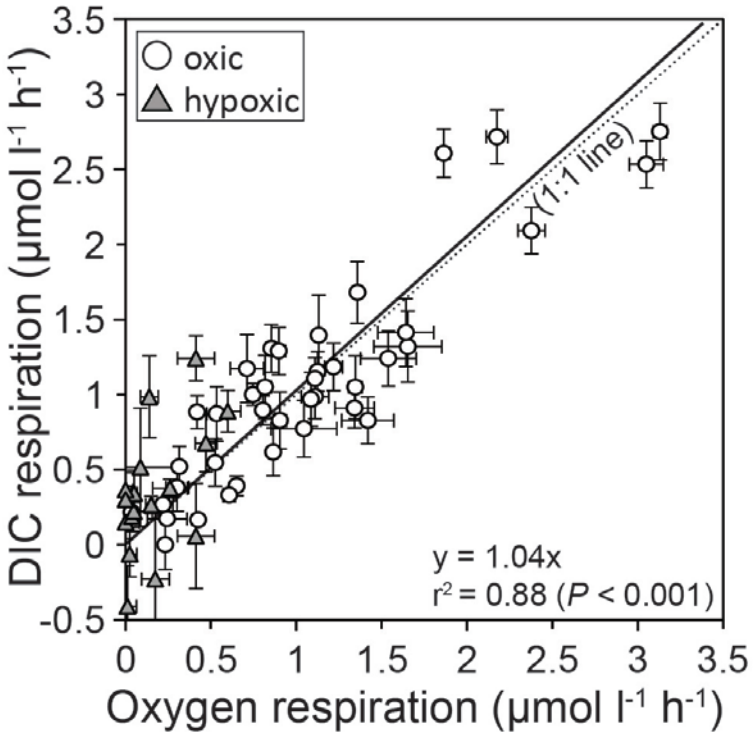
oxic
hypoxic
(1:1 line)
y = 1.04x
r² = 0.88 (P < 0.001)
DIC respiration (µmol l⁻¹ h⁻¹)
Oxygen respiration (µmol l⁻¹ h⁻¹)
3.5
3
2.5
2
1.5
1
0.5
0
-0.5
0
0.5
1
1.5
2
2.5
3
3.5

Fig. 2.6

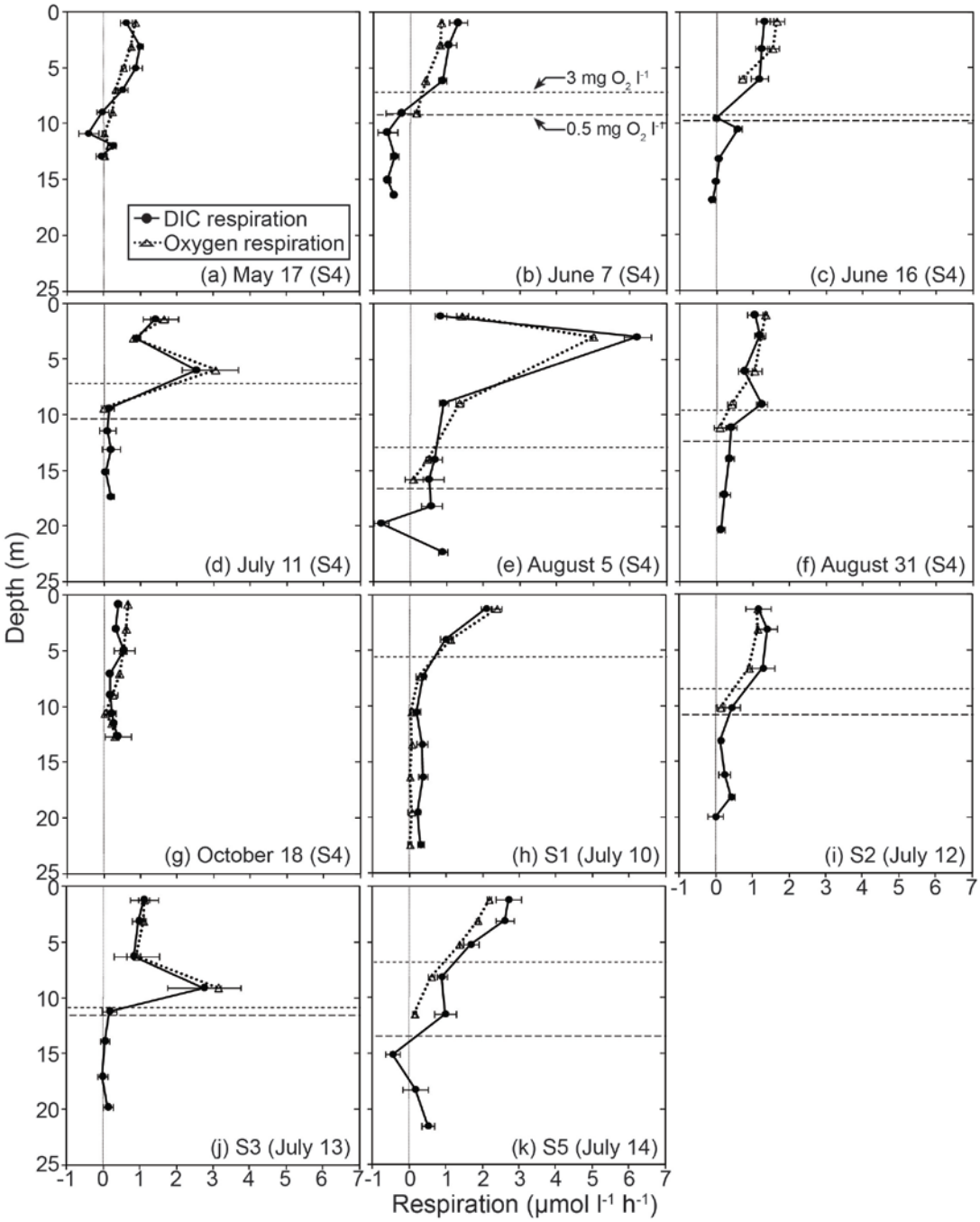
DIC respiration
Oxygen respiration
3 mg O2 l-1
0.5 mg O2 l-1
(a) May 17 (S4)
(b) June 7 (S4)
(c) June 16 (S4)
(d) July 11 (S4)
(e) August 5 (S4)
(f) August 31 (S4)
(g) October 18 (S4)
(h) S1 (July 10)
(i) S2 (July 12)
(j) S3 (July 13)
(k) S5 (July 14)
Depth (m)
Respiration (µmol l-1 h-1)

Fig. 2.7

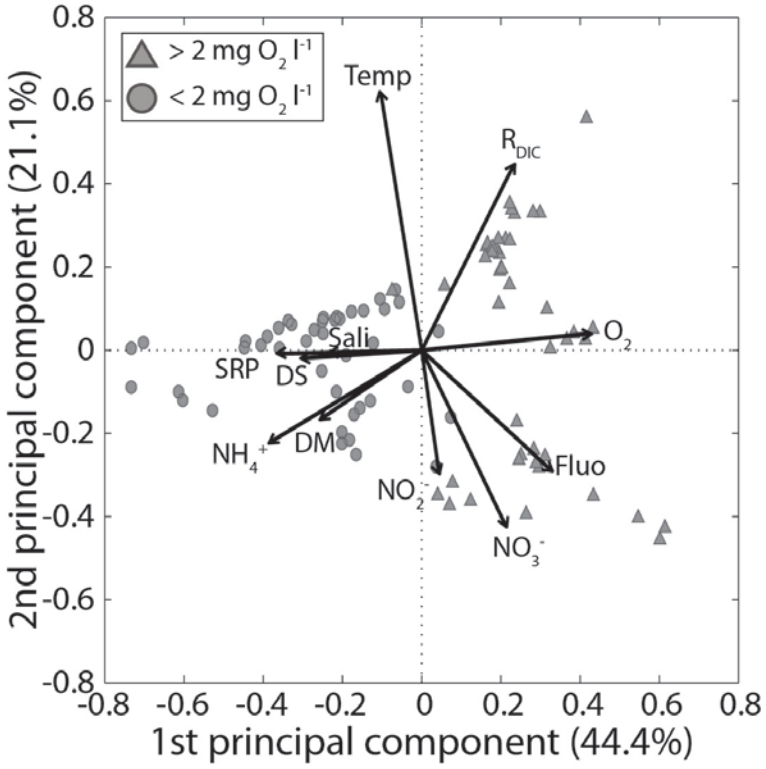
> 2 mg O2 l-1
< 2 mg O2 l-1
Temp
RDIC
O2
Sali
SRP
DS
DM
NH4+
NO2-
NO3-
Fluo
2nd principal component (21.1%)
1st principal component (44.4%)
0.8
0.6
0.4
0.2
0
-0.2
-0.4
-0.6
-0.8
-0.8 -0.6 -0.4 -0.2 0 0.2 0.4 0.6 0.8

Fig. 2.8

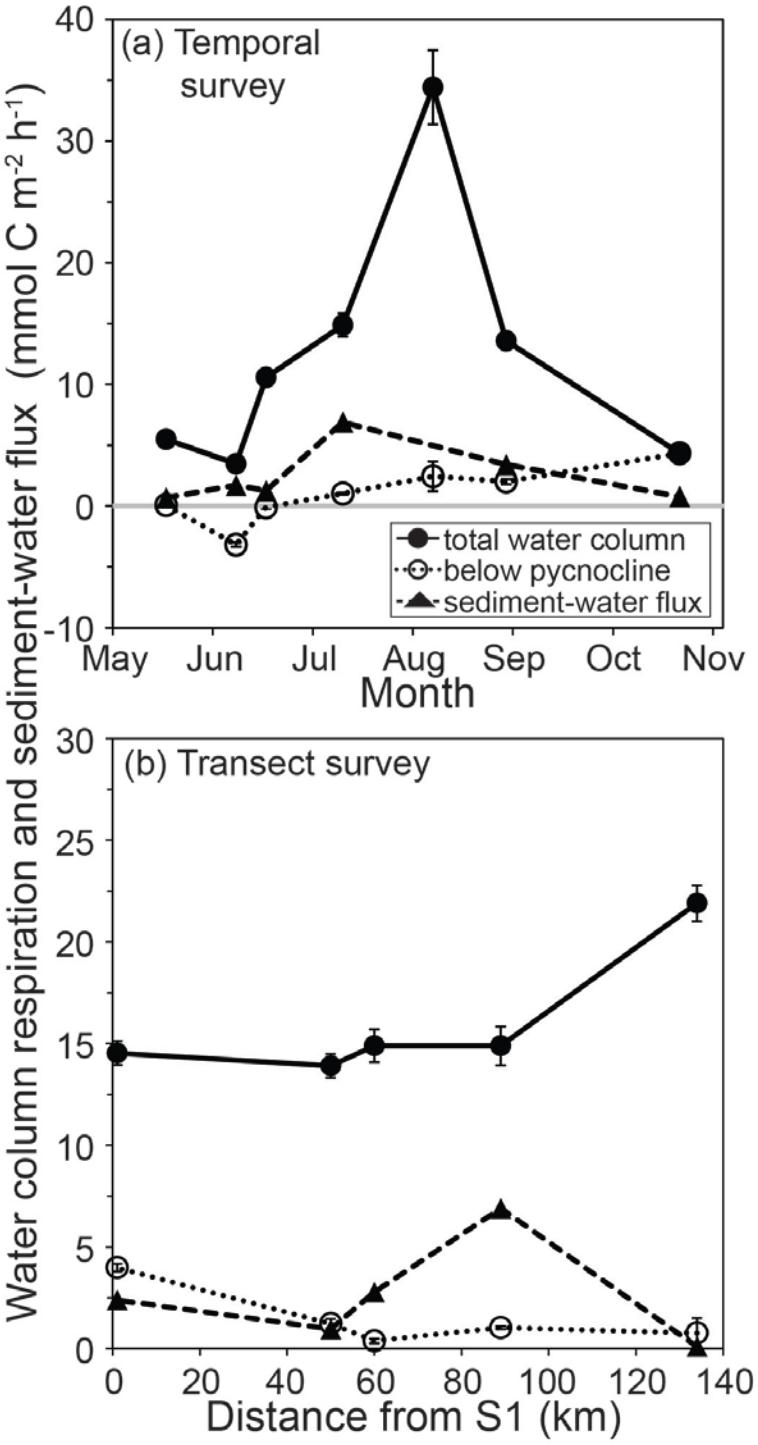
(a) Temporal survey
Water column respiration and sediment-water flux (mmol C m-2 h-1)
40
30
20
10
0
-10
May
Jun
Jul
Aug
Sep
Oct
Nov
Month
total water column
below pycnocline
sediment-water flux
(b) Transect survey
30
25
20
15
10
5
0
0
20
40
60
80
100
120
140
Distance from S1 (km)

Fig. 2.9

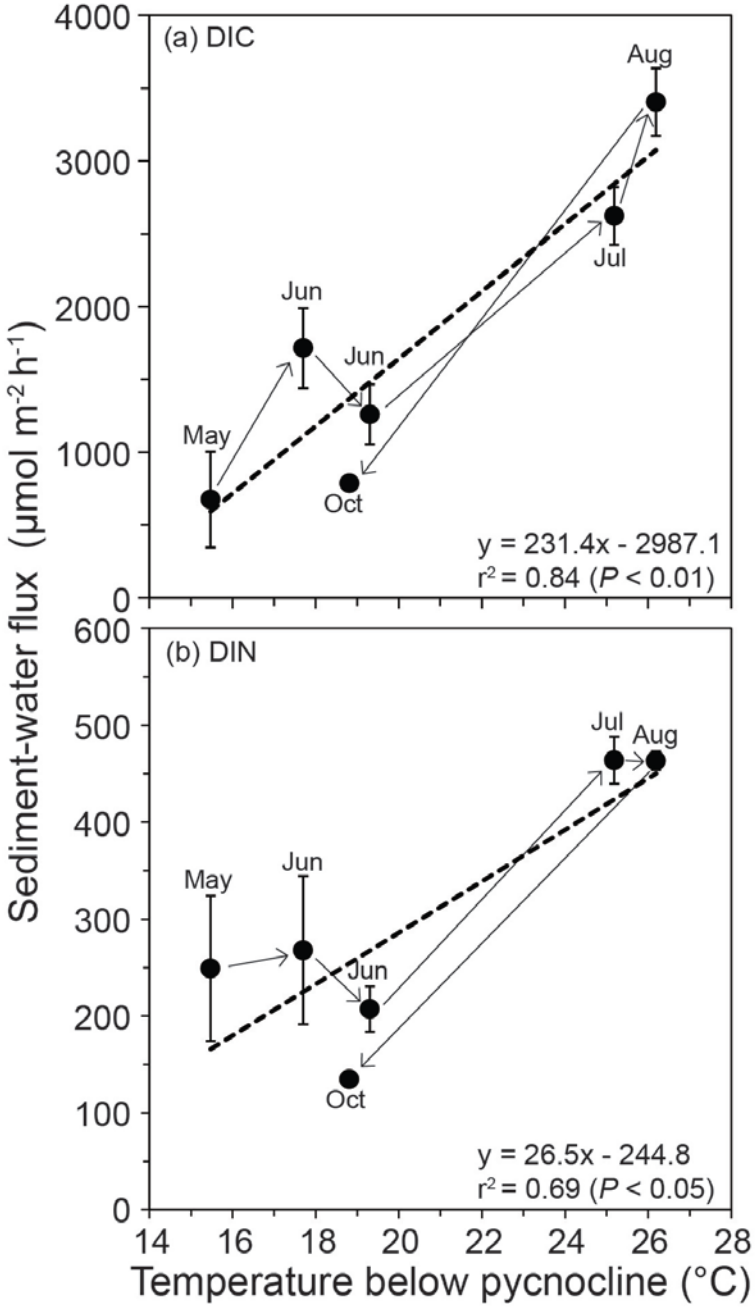
(a) DIC
Aug
Jul
Jun
Jun
May
Oct
y = 231.4x - 2987.1
r² = 0.84 (P < 0.01)
(b) DIN
Jul
Aug
May
Jun
Jun
Oct
y = 26.5x - 244.8
r² = 0.69 (P < 0.05)
Sediment-water flux (µmol m⁻² h⁻¹)
Temperature below pycnocline (°C)
0
1000
2000
3000
4000
100
200
300
400
500
600
14
16
18
20
22
24
26
28

Fig. 2.10

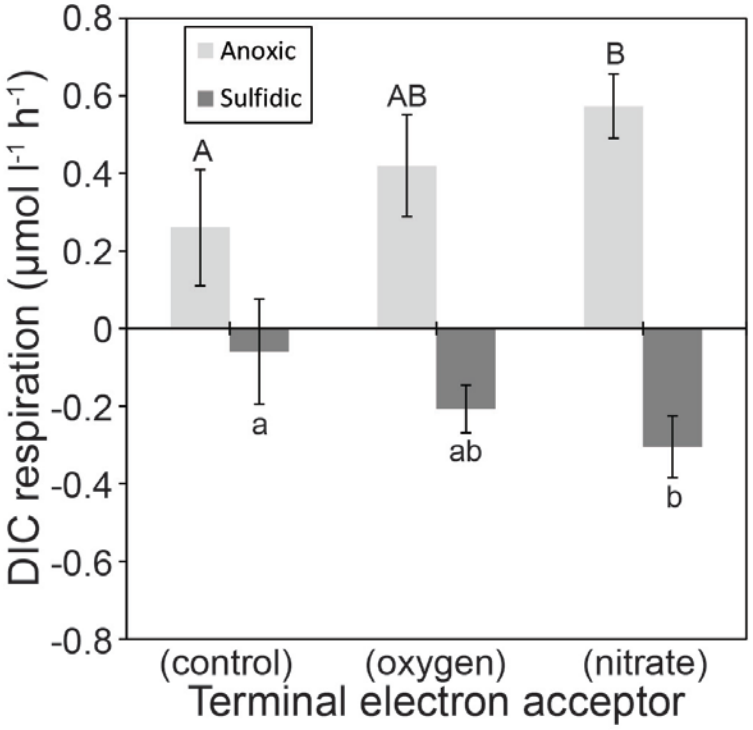
Anoxic
Sulfidic
DIC respiration (µmol l-1 h-1)
0.8
0.6
0.4
0.2
0
-0.2
-0.4
-0.6
-0.8
A
a
AB
ab
B
b
(control)
(oxygen)
(nitrate)
Terminal electron acceptor

Fig. 2.11

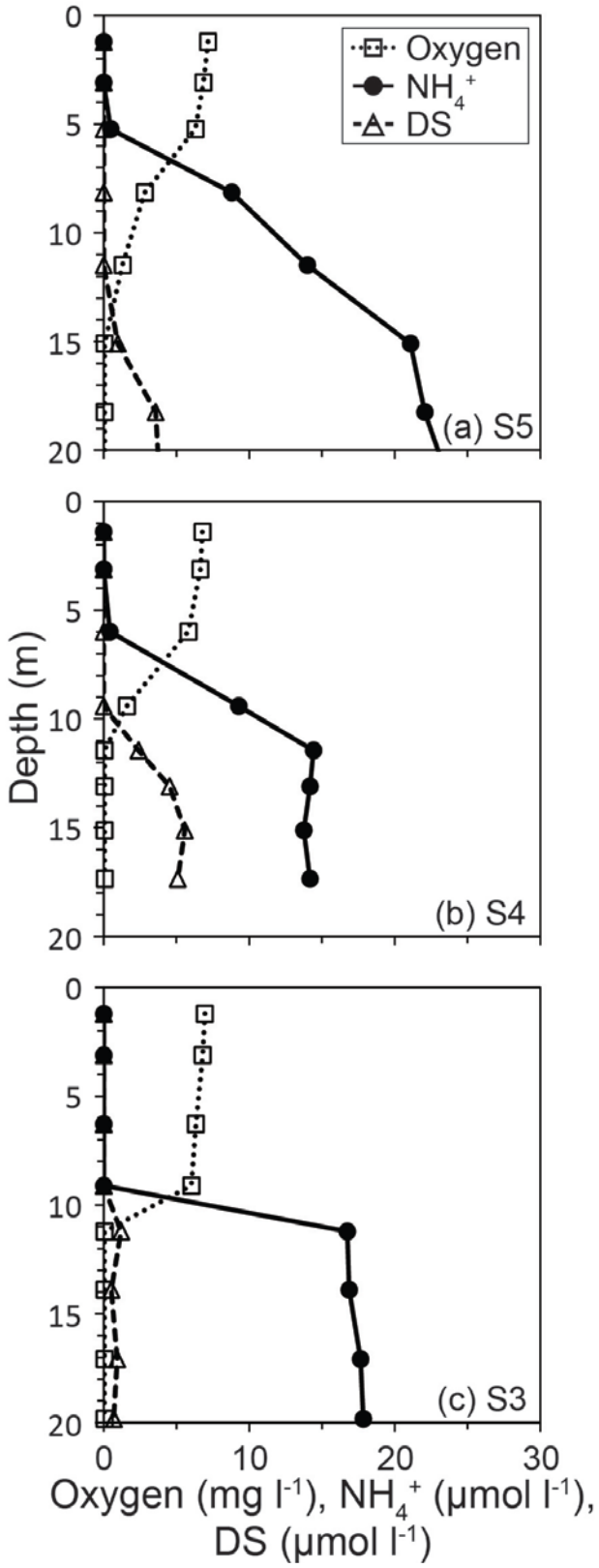
Oxygen
NH4+
DS
(a) S5
(b) S4
(c) S3
Depth (m)
0
5
10
15
20
0
10
20
30
Oxygen (mg l-1), NH4+ (µmol l-1),
DS (µmol l-1)

Chapter 3: Elevated microbial CO_2 production and fixation in the oxic/anoxic interface of estuarine water columns during seasonal anoxia

Abstract

Gradients of dissolved oxygen concentrations in stratified estuarine water columns directly influence microbial composition and metabolic pathways, resulting in vertical and axial chemical gradients of redox-active species. Understanding such microbial responses to changing geochemical conditions and elucidating the diversity of microbially-mediated processes are needed to comprehensively identify ecosystem functions. We tested the hypothesis that metabolic processes in the vicinity of the oxic/anoxic interface in Chesapeake Bay would be elevated due to the coincidence of oxidized and reduced compounds. We measured rates of metabolic processes associated with carbon cycles and quantified geochemical constituents. The transition from oxic to anoxic to oxic conditions was correlated with the pattern of dissolved nitrogen species, with the most reducing conditions comprising the highest concentrations of dissolved chemical compounds. The vertical distribution of community respiration was measured with changes in dissolved inorganic carbon concentrations and was related to water column stratification, with the highest median and variability (1.2 ± 1.4 μmol L^{-1} h^{-1}) in the most stratified conditions. Rates of CO_2 fixation under dark conditions, a measure of chemoautotrophy after correction for anaplerotic carboxylation, were elevated at the base of oxyclines and significantly correlated with a gradient of density and some reduced compounds. Although vertical interpolation must be made with caution due to high vertical variability, chemoautotrophic production averaged 0.5 mmol m^{-2} h^{-1} from May to August and added 5.8 % to autochthonous organic carbon production. Overall, our results suggest that anaerobic community metabolism and chemoautotrophy in the oxic/anoxic interface exert a small impact on estuarine carbon cycles.

Introduction

Estuarine ecosystems contain a series of unique and mixed microbial communities that originate within the estuary and from neighboring ecosystems, such as rivers, oceans, and watershed soils (Crump et al. 2004). These microbes acclimate to stable or widely ranging environmental conditions (Bouvier and Del Giorgio 2002; Fortunato and Crump 2011) and many are capable of fulfilling thermodynamic energy requirements in an annually recurring environmental pattern (Bouskill et al. 2011). For example, if dissolved oxygen (DO) is depleted due to a combination of biochemical (e.g., organic matter oxidation) and physical (e.g., stratification) mechanisms during seasonal anoxic events, microbes use alternative electron acceptors for respiration, such as NO_3^-, Mn(IV), Fe(III), and SO_4^{2-} (Wright et al. 2012). The dynamic response of microbial processes is demonstrated by metatranscriptomic analyses, revealing that successional transitions of respiratory processes corresponded to a given geochemical condition in anoxic waters (Hewson et al. 2014, E. M. Eggleston unpubl.).

The adaptability of the microbial community to changing redox conditions allows microbial specialists to thrive in the vicinity of the oxic/anoxic interface (Brune et al. 2000). One of best-studied examples of microbial adaptations are active chemoautotrophic and anoxygenic photoautotrophic processes attributed to the simultaneous presence of various oxidized and reduced compounds. The vertical distribution of the microbes is strongly related to the vertical structure of oxic/anoxic or oxic/sulfidic interfaces (Sorokin et al. 1995; Casamayor 2010; Casamayor et al. 2012). In some deep ecosystems where photosynthetic production is restricted to upper mixed layers, chemoautotrophic production can support a deep secondary microbial food web

(Ho et al. 2004; Alonso-Saez et al. 2010; Swan et al. 2011). Surprisingly, zooplankton have been shown to fulfill about half of their total carbon requirements through the consumption of chemoautotrophic and anoxygenic photoautotrophic production in a shallow ecosystem (Camacho et al. 2001). Chemoautotrophy and anoxygenic photoautotrophy have been investigated in stratified ecosystems, including lagoons (Llirós et al. 2011), lakes (Cloern et al. 1983), fjords (Zopfi et al. 2001), estuaries (Casamayor et al. 2001), and oceans (Taylor et al. 2001; Labrenz et al. 2005). However, few such studies have been conducted in eutrophic estuaries due to an emphasis on phytoplankton production dominating estuarine food webs and carbon cycling.

Previous studies have suggested spatiotemporal variability in microbial phylogenetic and functional composition reflects the diversity of metabolic processes in the Chesapeake Bay during seasonal anoxic events (Crump et al. 2007; Lee et al. 2014; Hewson et al. 2014). For example, consistently high production of dissolved inorganic carbon (DIC = $[H_2CO_3] + [HCO_3^-] + [CO_3^{2-}]$) near the top of oxyclines and occasional net consumption of DIC in the oxic/anoxic interface suggested not only close proximity between aerobic heterotrophs and chemoautotrophs, but also the formation of a secondary microbial food web. Net consumption of DIC was shown to intensify following experimental augmentation of samples with terminal electron acceptors (e.g., O_2, NO_3^-), suggesting enhanced aerobic and anaerobic chemoautotrophy (Lee et al. 2014). In addition, vertical mixing from frequent and strong winds during autumn was coincident with increases in *Thaumarchaeote* transcripts and NO_2^- concentration in the dissolved inorganic nitrogen (DIN = $[NH_4^+] + [NO_2^-] + [NO_3^-]$) pool. The decrease in denitrification related transcript ratios relative to spring and summer suggested that

nitrification rather than denitrification was responsible for NO_2^- accumulation (Hewson et al. 2014). Further, assuming no limitation of electron acceptors and donors with maximum growth efficiency for chemoautotrophy, the upward flux of reduced nitrogen and sulfur compounds across oxyclines can potentially fix up to 9.7 mmol C m^{-2} day^{-1} in summer (Lee et al. 2014). This study concluded that chemoautotrophy would exert a small impact on estuarine organic and inorganic carbon cycles due to the higher magnitude of phytoplankton production and aerobic respiration. However, it is still important to understand chemoautotrophy because it couples the fixation of CO_2 with oxidation of reduced compounds that can be further recycled for other electron accepting processes. In addition, the strong association of chemoautotrophy with stratification could cause large variability in the extent of chemoautotrophic metabolism due to large interannual variability in river discharge controlling stratification (Hagy et al. 2004).

The goal of the present study was to investigate the spatiotemporal variability of community metabolism across DO and redox gradients to assess the contribution of different biological redox processes on estuarine carbon cycles. Further, we identified and quantified the association of community metabolism with a gradient of environmental and geochemical factors to explain additional variability in various metabolic processes in the oxic/anoxic interface. We hypothesize that anoxygenic photoautotrophic production (AnoxyPP) and primary production in dark (DarkPP) would be elevated during seasonal anoxic events due to the close proximity between the abundant supply of oxidized and reduced compounds in the interface.

Materials and Methods

Location and Sampling

Pelagic and benthic samples were collected during seven temporal surveys at S3 (38°33’54” N, 76°26’32”W) located in the mesohaline region of Chesapeake Bay from spring to fall (18 April, 24 May, 14 June, 8 July, 8 August, 30 August, and 21 September 2011) (Fig. 3.1). We also conducted spatial surveys at five stations (S1 to S5) along the 150-km long main axis from near the mouth of Potomac River to the Chesapeake Bay Bridge on 6-12 July 2011 on board the R/V Hugh R. Sharp.

We measured conductivity, temperature, and depth (CTD) using a profiler (SBE25, SBE 911plus, Sea-Bird Electronics) equipped with DO (SBE 43, Sea-Bird Electronics) and photosynthetically active radiation (PAR) sensors (400-700 nm, Biospherical Instruments). On 6 and 12 July during the transect survey, water column geochemistry was surveyed with an undulating towed vehicle (Scanfish II-1250, GMI Denmark) equipped with CTD (SBE25), DO (SBE 43), and fluorometer (WET Labs) sensors. The surveys began from S1 at the Potomac River mouth to S5 at the Chesapeake Bay Bridge for ~12 hours (h).

We collected samples using a diaphragm pump with a 2.5-cm diameter hose attached to the CTD frame and terminated shipboard with a conical PVC manifold water distribution system which allowed multiple sample vials to be filled simultaneously. Samples were collected at eight depths (three above, two within, and three below oxyclines) between 08:30 h and 11:30 h; when an oxycline was absent salinities were used to apportion sampling depths.

Analytical Analyses

Solute samples were filtered through 0.45 µm cellulose acetate syringe filters and samples collected for NO_2^-, NO_3^-, NH_4^+, total dissolved sulfide (DS = $[S^{2-}]$ + $[HS^-]$ + $[H_2S]$), soluble reactive phosphorus (SRP), dissolved manganese (DMn = [Mn(II)] + [Mn(III)]), and dissolved iron (DFe = Fe(II)+ Fe(III)) in 7 ml polyethylene vials with screw caps. Concentrations of NH_4^+, DS, SRP, DMn, and DFe were determined colorimetrically (Brewer and Spencer 1971; Parsons et al. 1984) with a spectrometer (UVmini-1240, Shimadzu), while NO_2^- and NO_3^- were determined using segmented flow analysis after cadmium reduction by the Horn Point Analytical Services (Lane et al. 2000). Samples for fluorometric pigment analysis (50 ml) were collected in duplicate, filtered through 25 mm GF/F filters and stored at -20 °C. The concentration of chlorophyll a and pheophytin was determined using EPA method 445.0 (Arar and Collins 1997).

Both DO and DIC-based respiration measurements were made in triplicate dark 60 ml BOD bottles. Samples for initial concentrations were preserved with 10 µl of 50 % saturated mercuric chloride in triplicate 12 ml glass vials with butyl rubber septum caps, while the BOD bottles for final concentrations were covered with opaque plastic bags and incubated at in situ water temperatures (±1°C) for 24 h. At the end of incubation samples were siphoned into the vials and preserved with Hg. Capped vials were submerged in an opaque container below incubation temperatures and analyzed within three days. In addition, we filtered the same water samples through a 3 µm polycarbonate membrane filter using a reverse gravity method (Crump et al. 1998) to estimate the contribution of <3 µm microbes to community respiration. This experiment was conducted on 24 May,

14 June, 8 July, and 30 August 2011. Respiration in the filtered samples has been assumed to represent bacterial respiration (BR) in the mesohaline Chesapeake Bay (Smith and Kemp 2003). Respiration rates were computed as concentration differences between initial and final samples divided by incubation time. A linear increase (or decrease) of DIC (DO) in similar samples was observed during previous incubations up to 40 h (Lee et al. 2014).

A DIC analyzer, consisting of an automated digital pump, a mass-flow-controller, and an infrared CO_2 detector (LI-COR), was used (Apollo SciTech; Cai and Wang 1998). Certified reference material (provided by A. Dickson at Scripps Institution of Oceanography) was used to calibrate the analyzer according to Dickson et al. (2007) prior to analyzing the first sample of each cruise and daily during the transect survey. Overall, the calibration coefficient of variation ranged from 0.05 to 0.12 % with an average standard deviation of ±1.5 µmol L^{-1}.

Dissolved oxygen to argon ratios were determined with a membrane inlet mass spectrometer (Kana et al. 1994) yielding a precision of <0.05 %. Thermostated (±0.02 °C of incubation temperature) deionized water was used for standardization and gas ratios were converted to gas concentrations using temperature and salinity-based argon concentrations (Colt 1984).

CO_2 Fixation

Cellular CO_2 fixation was estimated using radiolabeled $NaH^{14}CO_3$ ($^{14}CO_2$, PerkinElmer) as described in previous studies (Kemp et al. 1993; García-Cantizano et al. 2005). A working $^{14}CO_2$ stock was prepared using a sodium carbonate solution before the dilution of $^{14}CO_2$ to a final concentration of 5 µCi per sample in an anoxic glove bag.

Water samples from the third to sixth depths were collected in triplicate 12 ml vials with butyl rubber septum caps for determining photosynthetic fixation, including oxygenic photoautotrophic production (OxyPP) and AnoxyPP. Similarly, water samples were collected from the third to eighth depths for determining DarkPP. The $^{14}CO_2$ stock was added into each vial through the septa with a gas-tight Hamilton syringe in an anoxic glove bag. Four treatments were prepared and incubated for 4 h in the bag in a temperature-controlled environmental chamber.

The first set of samples was covered with neutral-density screens allowing passage of four PAR levels (6.1, 3.7, 2.2, and 1.3 % of surface irradiance (E_0)). The second set of triplicate samples was incubated under the same PAR with an addition of 3-(3', 4'-dichlorophenil)-1,1'-dimethyl urea (DCMU) dissolved in ethanol at a final concentration of 2 μmol L^{-1} to inhibit the photosystem II reaction. The third set of samples was incubated in the dark. The last set of samples was incubated with formaldehyde (4 %, volume:volume) to correct for abiotic reactions. At the end of incubation, samples were immediately filtered onto 0.2 μm polycarbonate membrane filters (Millipore) and dried 24 h. Then, filters were fumed with hydrogen chloride for 30 min and immersed in scintillation cocktail (PerkinElmer).

Radioactivity was counted in a liquid scintillation analyzer (Packard Tri-Carb 3100TR) with quench correction. The $^{14}CO_2$ assimilation by OxyPP was calculated by subtracting the $^{14}CO_2$ activity in illuminated vials with DCMU from that in the illuminated vials. The $^{14}CO_2$ assimilation by AnoxyPP was calculated by subtracting the activity in dark vials from that in illuminated vials with DCMU. The $^{14}CO_2$ assimilation

by DarkPP was calculated by subtracting the $^{14}CO_2$ activity in killed samples from that in dark vials.

Bacterial Production

Water samples for bacterial production (BP) measurements were pumped directly to the bottom of 120 ml BOD bottles and allowed to overflow three times to ensure no bubbles remained. Samples were sealed and stored under water in the dark at ambient bottom water temperature during transport and were processed immediately upon return from the station (<5 h). Heterotrophic BP was measured by determining the rate of ^3H-leucine incorporation during 1-h incubations. All incubations were conducted in an anaerobic chamber (Coy) in sealed plastic syringes with the headspace removed. All plastic was stored in an O_2-free environment 24 h prior to use. Carbon production was calculated based on leucine incorporation using a ratio of cellular carbon to protein of 0.86, a fraction of leucine in protein of 0.073, and an intracellular leucine isotope dilution of two (Kirchman 1993).

Sediment-Water Flux

Sediment cores were collected using a box corer to determine sediment-water flux at S3 during the temporal survey. The sediments were sub-cored using three 7×30 cm (inner diameter × height) acrylic cylinders to a depth of ~15 cm. The sediment cores plus a core filled only with bottom water were incubated in the dark with stirring, and four samples were collected over 6 or 18-h time courses for aerobic or anaerobic incubations, respectively. For DIC analysis samples were collected in glass vials with preservation using Hg as described before. Samples for NH_4^+ and NOx (NO_2^- + NO_3^-) analysis were

collected in syringes and filtered prior to preservation via freezing. Overall, linear regression of overlying water DIC and DIN time courses resulted in high regression coefficients (n = 21, R^2 > 0.90, p < 0.05).

Statistical Analyses

All statistical tests were performed using R (version 2.13.0, R Foundation). Correlation and multiple regression analysis were used to identify the relationship between microbial metabolism and a vertical slope (gradient) of diverse variables. Gradients were calculated by subtracting values of shallower from deeper depth between neighboring sampling depths, and the difference was normalized by depth difference (i.e., $= (C_{i+1} - C_i) \times (Z_{i+1} - Z_i)^{-1}$, where C and Z indicates value and depth, respectively). For multiple regression analysis, absolute values of gradients were used to examine the effect of the magnitude of gradients, rather than both magnitude and direction (i.e., sign). In model selection, we used two criteria to determine best models: the Bayesian information criterion (BIC) and Mallow's Cp (Cp), satisfying both >10 BIC (Kass and Raftery 1995) and <1 difference between Cp values and the number of variables used for each model plus one (Gilmour 1996), respectively. Then, we present one model with the highest regression coefficient from a set of models with the same number of variables. Lastly, geochemical water properties were mapped with contour plots using EasyKrigV3.0 in MATLAB (Mathworks). We used kriging with an isotropic nonlinear semi-variogram model as a gridding method that performed statistical interpolation at every 5 cm in the y-direction, and 12 h and 1 km in the x-direction for temporal and transect survey, respectively.

Results

Environmental Conditions

Seasonal and spatial changes in density gradient reflected the effect of high river discharge with the initial development and persistent formation of pycnoclines in late spring (Fig. 3.2a) and throughout the mesohaline region in summer (Fig. 3.2c), respectively. Average Susquehanna River discharge in March (4,417 $m^3 s^{-1}$) was the highest recorded since monitoring began in 1968 (http://waterdata.usgs.gov/md/nwis). As a result, hypoxic (<2 mg L^{-1}, <62.5 µmol L^{-1}) waters occupied 33 % (7.1 km^3) of the Maryland portion of the mainstem Chesapeake Bay in summer, which is greater than the long-term average of 4.8 km^3 from 1985 to 2010 (http://mddnr.chesapeakebay.net/eyesonthebay). In addition, the depth of maximum buoyancy frequency (i.e., natural logarithm of N^2), an index of vertical stability (Murphy et al. 2011), was observed in the pycnocline and coincided with observations of the oxyclines (Fig. 3.2b, d). The seasonal anoxic event was terminated by Hurricane Irene (28 August), resulting in earlier destratification and reoxygenation of water columns for about a month (Murphy et al. 2011). In addition, the average thickness of oxyclines, determined using a threshold value of conductivity gradient defined by the Chesapeake Bay Program (http://www.chesapeakebay.net/data), was 3.0 m in spring and summer 2011, which is significantly smaller than the 4.5 m observed in 2010 (Lee et al. 2014).

Temporal Survey

Observations of the transition of DO below oxyclines showed a transition through oxic, hypoxic, anoxic (i.e., no DO and DS), sulfidic, and back to oxic condition over

about four months (Fig. 3.3a). Patterns of biogeochemical constituents were similar to those observed in 2010 (Lee et al. 2014), but the depth of the 2 mg O_2 L^{-1} isopleth was 2-4 m shallower in summer 2011 than 2010 probably because higher river discharges generated stronger stratification (i.e., high N^2) and shallower pycnoclines (e.g., comparison between 1998 and 1999 in Testa and Kemp 2012). The distribution of fluorometric pigments suggested that the seasonal oxic transition was initiated by microbial DO consumption of algal-derived organic matter in spring (Fig. 3.3c, d). The same biophysical mechanisms (i.e., respiration, oxycline) were also reflected in the pattern of DIC that accumulated below the oxycline (Fig. 3.3h). Overall, the transition of DIN best reflected that of redox conditions likely due to various microbial-mediated nitrogen processes (Fig. 3.3e, f, g). Oxidized forms of DIN were supplied by rivers in spring and coincided with a spring bloom of phytoplankton, suggesting a rapid consumption of DIN and production of organic nitrogen. Relative increase of lower oxidation states of DIN (i.e., NH_4^+) towards deeper depths and warmer months was likely caused by microbial consumption of organic nitrogen. Finally, NO_2^- and NO_3^- concentrations rebounded after Hurricane Irene and were even higher than the concentration in spring, an observation not previously recorded.

Despite large interannual differences in environmental conditions, the seasonal pattern and magnitude of respiration in 2011 (Fig. 3.4) was similar to those in 2010 (Lee et al. 2014). We observed high vertical variability and maximum respiration rates near the top of the oxycline in summer (Fig. 3.4c, d). On 14 June, the concentrations of NO_2^- (3.3 µmol L^{-1}), DS (1.2 µmol L^{-1}), DMn (1.5 µmol L^{-1}), and DFe (1.2 µmol L^{-1}) approached zero at the depth of the observed subsurface respiration maximum. On 8 July

when the oxycline was the shallowest among the surveys (e.g., 6.9 m for 0.5 mg O_2 L^{-1} isopleth), we also observed the coincidence of maximum respiration and the steepest gradient of reduced species.

DarkPP showed strong vertical gradients when the water column was stratified, with high rates consistently observed below the depth of the 0.5 mg O_2 L^{-1} isopleth (Fig. 3.4). The depth-integrated DarkPP rates below the oxycline were 39.7, 17.9, 26.8, and 9.7 mmol m^{-2} day^{-1} on 24 May, 14 June, 8 July, and 8 August, respectively. To convert volumetric hourly rates to areal daily rates, we assumed a consistent thickness and formation of oxyclines over tidal cycles (24 h), supported by the result of a continuous density survey using an undulating towed vehicle in July (data not shown). However, we must note that vertical interpolation likely overestimated depth-integrated DarkPP in our meter-scale sampling because optimal conditions for chemoautotrophic growth could be heterogeneous possibly with a patchy distribution (Wright et al. 2012). Further, it should be noted that average 4.4 ± 1.4 mmol m^{-2} day^{-1} of $^{14}CO_2$ fixation was also detected in non-stratified/oxic water columns (Fig. 3.4a, f, g), suggesting that non-chemoautotrophic $^{14}CO_2$ fixation consistently occurred regardless of oxic conditions.

Additionally, a comparison between OxyPP and AnoxyPP during the temporal survey is shown in different irradiance levels (Fig. 3.5). High OxyPP rates were observed at 6.1 and 3.7 % E_0 (Fig. 3.5a, b), while similar and even higher AnoxyPP were measured at lower irradiance when sulfidic conditions (>11 μmol L^{-1}) prevailed below the oxycline (Fig. 3.5c, d).

The molar DIC:DIN ratio of sediment fluxes averaged 7.4 ± 0.4, similar to the Redfield ratio of 6.6 (Fig. 3.6). The sediment flux of DIC ranged from 35.2 to 56.3 mmol

m^{-2} day^{-1} with lower fluxes in summer than spring and fall, while that of DIN (i.e., the sum of NH_4^+ and NOx fluxes) ranged from 3.6 to 7.5 mmol m^{-2} day^{-1} with the same seasonal pattern.

Spatial Transect Survey

The pattern of geochemical constituents during the transect survey showed the origin of reduced compounds (between S4 and S5) where anoxia is first observed each year (Fig. 3.7). The 2011 record-high anoxic event resulted in a full coverage of anoxic waters from the northern to southern limits of the mesohaline region. The concentration of reduced compounds (e.g., NH_4^+, DS, SRP, DMn) in bottom waters increased northward as the bottom water aged. However, the transformation of NOx was not observed as in the temporal survey.

Consistent with the results of the temporal survey, higher subsurface respiration rates were observed when high concentrations of reduced compounds were observed below oxyclines (Fig. 3.8c, d, e). In addition, high DarkPP near the base of the oxycline was a consistent feature. Depth-integrated DarkPP below the oxycline were 22.2, 30.3, 26.8, 60.4, and 24.6 mmol m^{-2} day^{-1} from S1 to S5, respectively. The highest DarkPP of 0.43 µmol L^{-1} h^{-1} was measured at S4 and S5 where water depths decrease sharply to the north (Fig. 3.8d, e).

To check the validity of consistent $^{14}CO_2$ fixation, we frequently conducted time course incubations for DarkPP (Fig. 3.9). The experiment supported consistent $^{14}CO_2$ fixation regardless of oxic conditions below oxyclines, suggesting that the short incubation (4 h) was appropriate in the ecosystem. It should be noted that variability between replicates seemed to increase over time and the curve slightly leveled off after

15 h incubation for anoxic and sulfidic samples (Fig. 3.9b, c). However, it is inconclusive whether the deviation over time suggested the decline of metabolic rates (like a growth curve) or was simply caused by experimental error between replicates. Additionally, to check the effect of ethanol in DCMU on $^{14}CO_2$ fixation, we incubated additional sets of samples augmented with the same amount of ethanol in DCMU. Although there was no statistical difference in the change of $^{14}CO_2$ fixation over time between samples with and without ethanol (analysis of covariance: $p > 0.2$, graph not shown), we sometimes observed up to 7 % of elevated fixation in ethanol samples collected near the top of oxyclines. Ethanol augmentation would enhance heterotrophic metabolism; however, autotrophs below the oxycline would not benefit from the recycling of organic matter because of abundant inorganic nutrients in deeper waters. Thus, the most likely reason for elevated fixation would be a positive feedback effect of heterotrophic nutrient recycling for autotrophic metabolism, which likely overestimated AnoxyPP above the oxycline in summer.

Bacterial Growth Efficiency

Contribution of BR to community respiration ranged widely from 0.17 to 0.80 but we could not find a spatiotemporal pattern in the variability. Due to large variability, we used an average estimate (0.54) of current and previous studies (Sampou and Kemp 1994; Smith and Kemp 2001) for oxic and hypoxic conditions, and we used the upper limit (0.80) of our estimate for anoxic conditions because of dominance of microbial metabolism (Wright et al. 2012). As a result, the relationship between total organic carbon consumption and BP (Fig. 3.10) was best fitted with the following model (R^2 = 0.65, df = 88):

$$BP = (0.39 \times (BP + BR) - 0.02) \times ((BP + BR) + 0.30)^{-1}$$

where the sum of BP and BR represents total organic carbon consumption by heterotrophic bacteria. The relationship suggests that bacterial growth efficiency (BGE), which is the slope of regression fitting in Fig. 3.10, decreased as total organic carbon consumption increased.

Statistical Analysis

The influence of stratification on geochemical variables and community metabolism has not been systematically assessed before, although most environmental and geochemical factors are affected by density to some extent in a stratified estuary. Thus, we investigated the relationship using both a value of geochemical variables at depths and a gradient of variables across neighboring sampling depths; the latter appears to be more appropriate for stratified ecosystems because a gradient is proportional to flux. The results of correlation analyses using values (i.e., concentrations) and gradients were notably different for some variables (Table 3.1). For example, temperature correlated with pheophytin, NO_3^- and NH_4^+, but the gradient of temperature correlated with gradients of density, DO, NH_4^+, DS, and DMn. Also, NO_3^- concentration appeared to be a good predictor for several geochemical properties, but the gradient of NO_3^- was not correlated with any variable.

Multiple regression analysis was also conducted using gradients of variables to observe relationships of microbial metabolism with degrees of changes in environmental and geochemical conditions. Note that all gradients were converted to absolute values (i.e., no sign) to only investigate the effect of magnitude and to simplify the interpretation of results. The models selected according to the predetermined criteria (i.e., BIC, Cp)

showed different responses of respiration over oxic conditions (Table 3.2). The gradient in aerobic respiration was positively associated with gradients of temperature and chlorophyll a, while it was negatively associated with gradients of NO_3^- and DMn. Contrary, the gradient of respiration in hypoxic and anoxic condition was only significantly associated with gradients of DFe and DMn. Thus, the results suggest a large discrepancy in the physiological responses of aerobic and anaerobic organisms. On the other hand, the results of multiple regression analysis for gradients of DarkPP suggested that a gradient of geochemical variables can be used to predict DarkPP (Table 3.3); gradients of density, DO, DS, DFe, and DMn particularly exerted a strong influence ($p < 0.05$) on DarkPP variability, suggesting that opposing gradient systems in the diffusion-limited region supported DarkPP.

Discussion

Elevated community metabolism in the oxic/anoxic interface and the strong association with gradients of redox-related variables suggest that during seasonal anoxic events geochemical and hydrodynamic characteristics of the interface support microbial food webs near oxyclines. Despite interannual differences in the extent of stratification and hypoxic volume associated with river discharge, we observed similar patterns of community respiration and geochemical constituents compared to previous studies (e.g., Gavis and Grant 1986; Lee et al. 2014), suggesting phylogenetic or functional redundancy in bacterioplankton communities (Kan et al. 2006; Crump et al. 2007; Hewson et al. 2014). The vertical patterns of respiration, autotrophic dark $^{14}CO_2$ fixation, and BGE, elevated near the maximum stratification, suggest that some subset of the

microbial community was optimally adapted to the interface. Dynamic interactions between environmental conditions and microbial responses that drive productivity at these interfaces are discussed below, along with some implications for estuarine carbon cycles.

Metabolic Response to Stratification Related Variables

In the studied region, river discharge is positively correlated with phytoplankton biomass (Harding 1994; Adolf et al. 2006b) and stratification (Hagy et al. 2004), while it is not correlated with phytoplankton sedimentation (Hagy et al. 2005). In general, high river discharges in 2011 resulted in higher community respiration than average anoxic years: a 1.5-fold increase of depth-integrated respiration in summer 2011 (316.3 mmol m^{-2} day^{-1}) than 2010 (206.5 mmol m^{-2} day^{-1}; Lee et al. 2014). However, sediment-water DIC fluxes were lower in summer 2011 than summer 2010, suggesting a relative increase in pelagic metabolism and decrease in benthic metabolism during severe anoxic events.

Stratification-dependent respiration profiles showed the highest variability and highest median rate in the most stratified water columns (Fig. 3.11a). We hypothesized that dynamic stability of a stratified water column (Durham and Stocker 2012) and high fraction of particulate organic matter in suspended materials (~64 %) in the Bay's summer (Hopkinson et al. 1998) would drive high respiration near the depth of maximum stratification. Phytoplankton-derived dissolved organic matter (Fisher et al. 1998) and coagulated polymerized particles (Passow 2002) can accumulate at this interface by reaching neutral buoyancy. In addition, high respiration would have been supported by high concentrations of viruses (Drake et al. 1998) and bacterioplankton (Hamdan and Jonas 2006; Crump et al. 2007), supporting microbial food webs in the vicinity of

pycnoclines (Pierson et al. 2009). Furthermore, respiration normalized to chlorophyll a concentration yielded the same pattern as un-normalized respiration (Fig. 3.11b), suggesting relative increases in microbial growth efficiency near the maximum stratification.

Considering the importance of temperature on the variability in respiration in summer (Shiah and Ducklow 1994), the elevated respiration in the oxic/anoxic interface is counterintuitive due to a significant inverse relationship between density and temperature (r = -0.79, $p < 0.001$, Table 3.1). The abrupt decrease in temperature could give the microbes in the interface a physiological disadvantage. However, the disadvantage may not have affected community respiration in the interface if a mixed microbial community occupied the region because of the inverse effect of temperature on aerobic and anaerobic respiration (Table 3.2). In addition, it is commonly found that the coexistence of aerobic and anaerobic communities in various environments benefits from syntrophic interactions (Gottschal and Szewzyk 1985; van den Ende et al. 1997). Thus, the coexistence of microbes with different metabolic strategies appears to be a crucial factor resulting in high respiration in the interface.

Our results also demonstrated a similar pattern of bacterial metabolism across density gradients, with the highest median of BP and total organic carbon consumption (i.e., BP + BR) in the most stratified region (Fig. 3.11c, d). In addition, averaged BGE was 0.43, 0.47, and 0.42 in oxic, hypoxic, and anoxic condition, respectively. The BGEs were not significantly different (ANOVA, $p > 0.05$) because of high variability in both aerobic BGE (Fig. 3.10) and total organic carbon consumption (note a 5-fold difference in y-axis in Fig. 3.11c, d). In general, decreases in BGE across geochemical gradients

(e.g., salinity, pH, nutrient) reflects high energy requirements for cell maintenance due to physiological stress (Church et al. 2000; del Giorgio and Bouvier 2002). Thus, the highest BGE in hypoxic waters would suggest either the decline of some stress or the successive adaptation of bacterioplankton assemblages (Bouvier and Del Giorgio 2002). Since hypoxic regions represent the depth of the most abrupt geochemical change, physiological stress would be greater than in oxic and anoxic mixed water columns. Thus, we speculated that microbial communities with physiological advantages or adaptation would account for high BGE in hypoxic waters.

Anoxygenic Photoautotrophy

The results of AnoxyPP support the idea that the oxic/anoxic interface provided an optimal condition for a guild of photoautotrophic organisms (Fig. 3.5). The highest AnoxyPP was measured in summer (14 June, 8 July), suggesting a positive effect of increasing temperature for AnoxyPP (Sieracki et al. 2006). On 14 June, high AnoxyPP was measured at 2.2 % E_0 and coincided with 3.3 µmol L^{-1} of NO_2^-, suggesting NO_2^- might serve as an electron donor for purple sulfur bacteria (Griffin et al. 2007). On 8 July, AnoxyPP at 2.2 and 1.3 % E_0 coincided with DS removal rates of 1.5 and 1.8 µmol L^{-1} h^{-1}, respectively. This observation suggests that 6.0 and 15.1 µmol L^{-1} DS was oxidized to fix 1 µmol L^{-1} CO_2 (i.e., yield factor) at 2.2 and 1.3 % E_0, respectively. The range of yield factors is in agreement with a previous study (Zopfi et al. 2001) and reflects the highly variable nature of AnoxyPP within the oxycline. While the majority of photosynthesis was contributed by OxyPP, our results suggest that the vertical shift of oxic conditions and the concurrent change of water column geochemistry may increase the patchy distribution of AnoxyPP.

However, the interpretation of AnoxyPP results must be made with caution because of likely contamination of cyanobacterial AnoxyPP. Cyanobacteria are capable of switching from oxygenic to anoxygenic metabolism in reducing environments (Jørgensen 1982). Among major taxonomic groups of phytoplankton in the Chesapeake Bay (i.e., diatoms, dinoflagellates, cryptophytes, cyanobacteria), a rapid increase of cyanobacteria from 2 to 26 % of total algal pigments from spring to summer (Adolf et al. 2006b) increases the possibility of cyanobacterial AnoxyPP. Thus, some of our samples with high chlorophyll a were possibly affected by cyanobacterial AnoxyPP in summer: the concentration was >10.0 μg L^{-1} at 6.1 and 3.7 % E_0, while it was <2 μg L^{-1} at 2.2 and 1.3 % E_0. However, it is impossible to quantitatively discriminate the contribution of cyanobacteria on total AnoxyPP for current approaches. Due to this methodological issue and possible overestimation of light-dependent $^{14}CO_2$ fixation, AnoxyPP was not incorporated into the carbon budget.

Chemoautotrophy

Similar to the results of respiration and AnoxyPP, stratification appeared to provide an optimal condition for chemoautotrophic growth because of consistently measured high rates near oxyclines (Fig. 3.4, Fig. 3.8). Despite the apparent vertical and seasonal pattern, most previous studies found weak or no correlation between chemoautotrophy and geochemical variables presumably due to the coexistence of a diverse assemblage of physiological and ecological types of chemoautotrophs (Casamayor 2010; Casamayor et al. 2012). However, we found significant models with a gradient of some geochemical variables, including density, DO, DS, DFe, and DMn for predicting DarkPP variability (Table 3.3); however, it remains difficult to determine the

physiological requirement of DarkPP from the models because the relationship could be coincidental with geochemical changes.

We should note that our DarkPP results include ubiquitous anaplerotic carboxylation (Li 1982), possibly resulting in the overestimation of chemoautotrophy. Heterotrophs can also incorporate CO_2 using carboxylation reactions to synthesize fatty acids, nucleotides, and amino acids. In particular, heterotrophic CO_2 fixation can be enhanced under nutrient-limited conditions (Perez and Matin 1982; Alonso-Saez et al. 2010), which is uncommon for bacterioplankton in the Chesapeake Bay (Jonas 1997). If we assume that measured DarkPP in non-stratified/oxic waters only resulted from the carboxylation reaction, the reaction accounted for 6.4 to 11.7 % of BP in April, August, and September. Previous studies reported a similar range (1.4 to 13 %) depending on physiological and environmental conditions (Perez and Matin 1982; Roslev et al. 2004). Thus, heterotrophic carboxylation was assumed to have occurred throughout this study and all DarkPP results were corrected for averaged carboxylation reaction.

Electron Budget in the Oxic/Anoxic Interface

The quantitative significance of different electron accepting processes was evaluated using the vertical profiles of oxidants and electron donors in the oxic/anoxic interface. This analysis helps us to estimate the balance of various opposing gradients and to assess potential metabolic processes. For examples, the average ratio of DS and NH_4^+ across the oxycline during sulfidic conditions was 0.7, far less than the Redfield ratio of 3.3. The deviation can be caused by either enhanced DS removal pathways, such as reoxidation or iron sulfide formation (Cornwell and Sampou 1995), unaccounted production of NH_4^+ from other anaerobic respiration pathways other than sulfate

reduction (Roden et al. 1995), or possibly dissimilatory nitrate reduction to ammonium (Giblin et al. 2013).

Reduced forms of redox-active species are usually entrapped in the deep channel of Chesapeake Bay, and vertical gradient of chemical concentrations is a key component of vertical dispersion of chemical species during seasonal anoxia as well as vertical advection (Hagy 2002). Kemp et al. (1992) reported a vertical dispersion coefficient of 0.2 $cm^2\ s^{-1}$, which is higher than April-September average value of 0.1 $cm^2\ s^{-1}$ estimated from a salt and water balance analysis (Hagy 2002). We also estimated a vertical dispersion coefficient using a relationship between the flux of chemical species across the sediment-water interfaces and oxyclines:

Sediment-water NH_4^+ flux = K $((\Delta NH_4^+) \times (\Delta Depth)^{-1})$

where K is the vertical dispersion coefficient and $((\Delta NH_4^+) \times (\Delta Depth)^{-1})$ represents a gradient of NH_4^+ across oxyclines. We used NH_4^+ fluxes and concentrations because they were consistently measured throughout this study and had slow biogeochemical turnover rates. Although the equation does not explicitly include a vertical advection term, a gradient of chemical compounds is equally dependent of both diffusion and advection (Kemp et al. 1992). As a result, the estimated average K value of 0.13 $cm^2\ s^{-1}$ from May to August was used for different chemical species (e.g., DO, NO_3^-, NO_2^-, DS, NH_4^+, Mn, Fe) in each cruise.

The flux of electron acceptors and donors across oxyclines (computed by a gradient of chemical species multiplied by K) was converted to electron equivalents to evaluate a redox balance (Table 3.4). The downward flux of electron acceptors usually exceeded the upward flux of electron donors, indicated by net negative balance in Table

3.4, mainly due to excess DO flux. The contribution of electron acceptors other than DO to total electron balance was 5.6 % with the second highest contribution from NO_3^- and NO_2^- (3.5 %). The upward flux of DMn and DFe was assumed to be equal to the downward flux of Mn(IV) and Fe(III)-oxides due to the absence of vertical pattern and a rapid biochemical recycling of the two elements (Nealson and Myers 1992). However, this assumption likely underestimated the downward flux of Fe(III)-oxides during sulfidic conditions due to the formation of Fe-sulfide below the oxycline.

The oxidized products of some inorganic electron donors are efficient redox mediators and can be rapidly recycled for further anaerobic processes (Nealson and Myers 1992; Schippers and Jørgensen 2001; Hulth et al. 2005). For examples, dissolved Mn(III), abundant in the suboxic zone of Chesapeake Bay, can be used as both electron acceptor and donor (Trouwborst et al. 2006). Also, anaerobic DFe oxidation by NO_3^- indicates the importance of iron as a transient electron carrier for organic matter oxidation (Benz et al. 1998). Thus, we hypothesize that efficient recycling would result in higher chemoautotrophic CO_2 fixation than 'potential' rates estimated from the upward flux of electron donors. To estimate chemoautotrophic rates from the pattern of electron donors, we assumed that there was no limitation of electron acceptors as Table 3.4 suggested. We also assume maximum efficiency of yield factors (i.e., least amount of electron donor is oxidized to fix 1 unit of CO_2) for a series of chemoautotrophy, such as 0.58, 0.11, 0.32 for the oxidation of DS, NH_4^+, and metal (Mn, Fe) oxides (Kepkay and Nealson 1987; Zopfi et al. 2001). As a result, the average depth-integrated 'potential' chemoautotrophic rate was 5.4 mmol m^{-2} day^{-1} in summer, while we measured 14.0 mmol m^{-2} day^{-1}. This calculation based on the flux of electron donors underestimated total

chemoautotrophic rates because the model does not account for internal redox recycling. The recycling of metal species as an electron carrier was also supported by the results of the multiple regression of DarkPP (Table 3.3); a gradient of DFe and DMn was positively associated with DarkPP variability. However, these two ways of estimating chemoautotrophic rate are quite different; while the former (from electron balance) only accounts for production across the oxycline, the latter (depth-integrated DarkPP) was based on the interpolation of actual measurement throughout bottom mixed layers.

Longitudinal Redox Gradient

Although a vertical redox gradient is a distinct recurring feature in the Bay during summer, a longitudinal redox gradient (i.e., relatively high DO concentrations in the southern mesohaline region) also forms due to a spatial expansion and reduction of anoxic waters in spring and fall, respectively. One of most likely regions to observe longitudinal redox gradients is between S4 and S5 where water depths decrease sharply to the north because northward expansion of anoxic waters is restricted by topography and downstream freshwater. Note that S4 and S5 had almost identical depth and thickness of oxyclines along with the highest DarkPP below the 0.5 mg O_2 L^{-1} isopleth (Fig. 3.8d, e), suggesting DarkPP could be catalyzed by oxidants other than DO. Persistent formation of Mn(III) maximum under suboxic condition (i.e., O_2 < 3 µmol L^{-1} and DS < 0.2 µmol L^{-1}) was reported between S4 and S5 (Trouwborst et al. 2006). In addition, we consistently measured >2.3 µmol L^{-1} DMn at S5. Thus, these data suggest that the deep DarkPP rates would be caused by reactive anaerobic oxidants (Schippers and Jørgensen 2001; Hulth et al. 2005; Bruckner et al. 2013) because S5 is close to the shallow oligohaline region. It is also suggested that Mn(II) can be used as an electron donor for

autotrophic growth (Tebo et al. 2005). However, since it is not possible for our DMn measurement to quantitatively discriminate between Mn(II) and Mn(III), the role of DMn in the present study cannot be concluded.

Annual NO_2^- Accumulation in Fall

We speculated that autumn occurrence of high NO_2^- followed by NO_3^- result from nitrification; however, this hypothesis was not supported during the two post-Hurricane Irene cruises (Fig. 3.4f, g). DarkPP rates measured on 30 August after Hurricane Irene were not significantly different from those on 18 April in non-stratified/oxic waters. Simultaneous metatranscriptome analysis also revealed that NH_4^+ monooxygenase subunit C gene, which catalyzes the oxidation of ammonia to hydroxylamine, was absent during the cruises while it was abundant in fall 2010 (Hewson et al. 2014). Ironically, an order of magnitude increase of the abundance of Archaea, in which almost all archaeal transcripts were recruited to *Nitrosopumilus marinus* SCM1 (thaumarchaeote), was observed in fall 2010 and 2011 with respect to spring and summer. These contradictory results (i.e., the absence of CO_2 fixation despite the increased abundance of nitrifiers) may suggest that some marine nitrifiers might be capable of growing chemoorganotrophically because heterotrophic nitrification is observed in some terrestrial nitrifiers (Starkenburg et al. 2006). However, chemoorganotrophic (mixotrophic) nitrification is unlikely because the organisms known to use this metabolism require several weeks to months to gain an ability to grow with organic substrates (Bock 1976). On the other hand, it is possible that our temporal resolution of sampling (i.e., monthly) missed a narrow window of active nitrification: previous studies in our studied region and the nearby Delaware River estuary reported NH_4^+ oxidation rates up to 3.4 μmol L^{-1} day^{-1}

in fall (Lipschultz et al. 1986; Horrigan et al. 1990). With this maximum rate, the highest NO_2^- concentration of 4.6 μmol L^{-1}, observed on 30 August, would be formed within 33 h after the Hurricane Irene (28 August) prior to our sampling date (30 August). This suggests that our temporal sampling was insufficient to fully resolve the variance of nitrification in fall.

Carbon Budget during Seasonal Anoxic Event

The most obvious feature in the carbon budget is the dominance of phytoplankton production and pelagic aerobic respiration for the gain and loss of organic carbon, respectively (Fig. 3.12). We used gross phytoplankton production measured using DO balances (Smith and Kemp 2001) and converted to carbon equivalent using a photosynthetic quotient of 1.04 (Lee et al. 2014). The production was measured in 1996 and 1997 when the anoxic volume was close to the long-term average. Despite large interannual variability, a long-term average of gross phytoplankton production is still an order of magnitude greater than chemoautotrophy (Harding et al. 2002) and, thus, it would not affect our conclusion. Any external source of organic carbon is not included because physical transport of organic carbon can only reach 10.8 mmol m^{-2} day^{-1} (= 3.9 mol m^{-2} yr^{-1} × $(365\ day)^{-1}$) in the mesohaline region of tributaries (Kemp et al. 1997); further, considering lower river discharge in summer and low biodegradability of terrestrial organic matter, it would contribute less to the summer labile organic pool. Lastly, as only a fraction of dissolved organic carbon is labile (Jonas and Tuttle 1990) and degradable by anaerobic heterotrophs (Bastviken et al. 2003), we estimated extracellularly released organic carbon (ROC) flux using a relationship with

phytoplankton production as a proxy of labile dissolved organic carbon (Chrost and Faust 1983; Baines and Pace 1991).

Overall, our results suggest that 5.8 ± 0.8 % of total autochthonous organic carbon production was attributed to chemoautotrophy during summer anoxia (Fig. 3.12a). The average chemoautotrophic CO_2 fixation rate was about a 3.4-fold and 4.5-fold smaller than ROC and BP, respectively. This suggests a stronger dependence of heterotrophic metabolism on phytoplankton derived organic carbon than chemoautotrophic production.

We also estimated the budget of organic carbon remineralization and fluxes, including aerobic and anaerobic respiration, sediment-water flux, and sediment burial in terms of carbon (Fig. 3.12b). Anaerobic respiration is the sum of respiration rates measured below oxyclines and the flux of NO_3^-, NO_2^-, Mn(IV), and Fe(III) converted to carbon equivalents across the oxyclines, assuming a complete reduction (e.g., NO_3^- to N_2) of electron acceptors (Table 3.4). Burial of organic carbon is assumed to be ~20 % of sediment-water flux according to previous studies (Roden et al. 1995; Kemp et al. 1997). If we assume a quasi-steady state of physical forces in terms of the input/export of organic carbon during seasonal anoxic events, net ecosystem metabolism, estimated by subtracting the loss from the gain of organic carbon flux, resulted in -43.3, -37.8, -4.2, and 44.8 mmol m^{-2} day^{-1} on 24 May, 14 June, 8 July, and 8 August, respectively (Fig. 3.12b). The magnitude and pattern of ecosystem trophic status from net heterotrophy to autotrophy was almost identical to a previous study that only included phytoplankton production in the production term (e.g., Kemp et al. 1997). Additionally, considering the high variability of phytoplankton production dynamics related to river discharge (Harding

et al. 2002), the fraction of chemoautotrophy to total organic carbon would be even smaller during a year of average river discharge.

Implication of Chemoautotrophy for Carbon Cycles

Chemoautotrophy is a generally inefficient and slow process due to high energy requirement for CO_2 fixation (Shively et al. 1998). Despite slow growth, chemoautotrophy can exert considerable influence on the dynamics of chemical cycles because the low energy yield of chemoautotrophy requires an oxidation of disproportionally large amounts of reduced substrates to fix CO_2. For example, the oxidation of 2 to 60 μmol L^{-1} of NH_4^+ and 1.7 to 9.1 μmol L^{-1} of DS is required by chemoautotrophs to fix 1 μmol L^{-1} CO_2 depending on physiological and environmental conditions controlling growth efficiency (Zopfi et al. 2001; Andersson et al. 2006; Veuger et al. 2013). Assuming only nitrification occurred on 24 May (no DS measured below oxyclines), average DarkPP of 0.1 μmol L^{-1} h^{-1} coincided with an average NH_4^+ oxidation of 3.7 μmol L^{-1} h^{-1}, measured simultaneously using a pair of identical water samples. Similarly, average DarkPP of 0.3 μmol L^{-1} h^{-1} on 8 July coincided with an average DS oxidation of 1.6 μmol L^{-1} h^{-1}. Since our assumption of uniform chemoautotrophy (i.e., either NH_4^+ or DS oxidization) is highly unlikely, it is probable that a guild of chemoautotrophs would simultaneously mediate a conversion of a series of different compounds aerobically and anaerobically (Kepkay and Nealson 1987; Straub et al. 1996; Benz et al. 1998).

Despite the minimal effect of chemoautotrophy on the budget of total organic carbon in the Chesapeake Bay (Fig. 3.12a), previous studies reported an important role of chemoautotrophy in different environments (Table 3.5). The difference in the

contribution of chemoautotrophy to gross phytoplankton production would reflect differences in a gradient of geochemical properties. For example, DarkPP was as high as the production of OxyPP at oxic/anoxic interfaces in the estuarine turbidity maximum (ETM) region of the Ebro River (Casamayor et al. 2001). Similarly, DarkPP was also measured in oxic water columns of the Columbia River ETM due to the formation of micro-scale DO gradients inside suspended particles (Bräuer et al. 2013). Further, higher contribution of chemoautotrophy than phytoplankton to the carbon balance has been observed in some ecosystems (e.g., Taylor et al. 2001; García-Cantizano et al. 2005), suggesting that there is an external source of either electron acceptors or donors. For examples, lateral advection of oxidized waters in the Cariaco Basin (Taylor et al. 2001) and excessive input of reduced sulfur into a monomictic lake (García-Cantizano et al. 2005) can result in higher chemoautotrophy than phytoplankton production. These results along with our data suggest that DarkPP can be a widespread phenomenon in both shallow and deep sections of estuaries and the relative magnitude of DarkPP to total production strongly depends on a gradient of environmental, physical, geochemical, and hydrodynamic characteristics.

Conclusion

We assessed the contribution of different modes of primary production and respiration across a gradient of DO. The results suggest that such processes are highly adapted to the change of redox conditions in the estuarine water column. Although coupled biogeochemical and genomic measurements are required to identify all the processes, our estimation of the budget of electron acceptors/donors across oxyclines

showed potential chemolithoautotrophic and anoxygenic photoautotrophic metabolism. Our results and previous research also support the idea that the region of high chemolithoautotrophic production is not confined in stratified water columns but is widespread throughout estuaries presumably because of phylogenetic and functional diversity of microbes and micro-scale DO gradients. Missing from this analysis is biogeochemical cycling related to elevated carbon consumption by zooplankton on AnoxyPP and DarkPP, linking food webs between anoxic and oxic environments. Considering that average strength of pycnoclines has been increasing during the last two decades (Murphy et al. 2011) and is predicted to increase further (Najjar et al. 2000) in the Chesapeake Bay, environmental factors attributable to climate change would exert a positive influence on the distribution and extent of microbial metabolism associated with stratification.

Tables

Table 3.1: Correlation matrix of biogeochemical values at different depths (lower left) and gradients across neighboring depths (upper right) (n = 88). Only significant ($p < 0.05$) results are present and bold coefficients indicate $p < 0.001$. Units: density (kg m^{-3} or kg m^{-4}); temperature (°C or °C m^{-1}); chlorophyll a and pheophytin (µg L^{-1} or µg L^{-1} m^{-1}); dissolved oxygen and inorganic compounds (µmol L^{-1} or µmol L^{-1} m^{-1}). Abbreviations: Temp: temperature; Chl-a: chlorophyll a; Pheo: pheophytin; DO: dissolved oxygen; SRP: soluble reactive phosphorus; DS: total dissolved sulfide; DFe: dissolved iron; DMn: dissolved manganese.

	Density	Temp	Chl-a	Pheo	DO	NO_2^-	NO_3^-	NH_4^+	SRP	DS	DFe	DMn
Density		**-0.79**	-	-	**-0.65**	-	-	**0.71**	-	0.29	-	**0.51**
Temp	-		-	-	**0.73**	-	-	**-0.86**	-	-0.32	-	**-0.63**
Chl-a	**-0.55**	-		**0.58**	**0.42**	-0.33	-	-	0.27	-	-	-
Pheo	**-0.42**	-0.26	**0.70**		0.24	-	-	-	-	-	-	-
DO	**-0.74**	-	**0.69**	**0.55**		-0.32	-	**-0.69**	-	-	-	**-0.39**
NO_2^-	-	-	-	-	-		-	-	**-0.68**	-	-	-
NO_3^-	-0.35	**-0.56**	-	0.28	**0.49**	0.31		-	-	-	-	-
NH_4^+	**0.58**	-0.23	**-0.45**	-0.33	**-0.76**	-0.28	-0.34		-	0.35	-	**0.70**
SRP	**0.39**	-	-	-0.31	**-0.38**	-0.25	**-0.36**	**0.53**		0.23	-	0.28
DS	**0.43**	-	-0.27	-0.32	**-0.47**	-0.25	-0.23	**0.70**	**0.53**		-	0.33
DFe	-	-	-	-	-	-0.29	-	-	-	-		**0.49**
DMn	**0.35**	-	-0.31	**-0.36**	**-0.60**	-	-0.25	**0.84**	**0.50**	**0.61**	0.32	

Table 3.2: The results of multiple regression analysis to explaining the variability of aerobic and anaerobic respiration measured with changes in dissolved inorganic carbon concentrations (μmol L^{-1} h^{-1}). Bold coefficients indicate $p < 0.05$.

Oxic condition	# of variable	Temp	Chl-a	Pheo	NO_3^-	SRP	DFe	DMn			
		°C m^{-1}	μg L^{-1} m^{-1}		μmol L^{-1} m^{-1}				intercept	R^2	*p*
Oxic	4	**1.69**	**0.11**		**-0.28**			**-1.50**	**0.45**	0.35	<0.001
Oxic	5	**1.66**	**0.10**		**-0.26**	0.27		**-1.63**	**0.41**	0.37	<0.001
Hypoxic & anoxic	3					0.27	**-0.28**	**0.84**	-0.09	0.40	<0.001
	4			0.32		0.21	**-0.27**	**0.78**	-0.11	0.40	<0.001

Table 3.3: The results of multiple regression analysis to explaining the variability of chemoautotrophic production in dark (nmol L^{-1} h^{-1}). Bold coefficients indicate $p < 0.05$.

# of variable	Density	DO	NO_2^-	NO_3^-	NH_4^+	DS	DFe	DMn			
	kg m^{-4}	µmol L^{-1} m^{-1}							intercept	R^2	*p*
4	**141.0**	**-3.0**				**38.3**	**42.3**		**31.4**	0.52	<0.001
5	**142.9**	**-2.8**		-15.1		**35.9**	**42.5**		**37.3**	0.53	<0.001
6	**130.6**	**-2.9**		**-14.1**		**30.0**	**36.6**	**47.2**	**40.5**	0.53	<0.001
7	**134.6**	**-3.0**	-71.4	-12.8		**30.1**	**35.9**	**44.4**	**43.1**	0.53	<0.001
8	**133.4**	**-3.1**	-69.5	-12.8	2.2	**29.7**	**36.3**	**39.5**	**43.6**	0.52	<0.001

Table 3.4: The flux of electron acceptors and donors in terms of mass (mmol m^{-2} day^{-1}) and electron equivalent (mmol e^- m^{-2} day^{-1}) across oxyclines. The number of transferable electron (e^-) is based on the assumption of complete reduction and oxidation of respective electron acceptors and donors.

Date		Electron acceptor					Electron donor				Balance
		DO	NO_3^-	NO_2^-	Mn(IV)	Fe(III)	DS	NH_4^+	DMn	DFe	
	Transferable e^-	4	5	3	2	1	8	8	2	1	
24 May	Mass flux	-46.8	-2.8	-0.2	-0.4	-0.1	0.0	6.8	0.4	0.1	
	Electron flux	-187.3	-13.9	-0.5	-0.9	-0.1	0.0	54.1	0.9	0.1	-147.5
14 June	Mass flux	-13.1	-0.5	-0.5	-0.5	-0.2	1.3	4.1	0.5	0.2	
	Electron flux	-52.2	-2.3	-1.6	-1.0	-0.2	10.3	33.1	1.0	0.2	-12.7
8 July	Mass flux	-31.3	0.0	0.0	-1.7	-0.7	7.6	6.5	1.7	0.7	
	Electron flux	-125.1	-0.1	0.0	-3.4	-0.7	60.6	51.6	3.4	0.7	-13.0
8 August	Mass flux	-62.1	0.0	0.0	-1.8	-2.3	4.8	7.6	1.8	2.3	
	Electron flux	-248.3	-0.2	0.0	-3.7	-2.3	38.1	60.5	3.7	2.3	-150.0

Table 3.5: Depth-integrated chemoautotrophy in different ecosystems and a comparison with gross phytoplankton production (GPP).

	Oxic/anoxic interface interval	Chemoautotrophy	Contribution to GPP	
System	(m)	(mmol m^{-2} day^{-1})	(%)	Source
Ebro River estuary	3-5	3.5	48.0[a]	Casamayor et al. 2001
Ciso´ Lake	0.5-1.5	28.8	52.0	García-Cantizano et al. 2005
Cadagno Lake	10.8-11.4	130.0	50.0	Camacho et al. 2001
Big Soda Lake	3-4	31.5	30.0	Cloern et al. 1983
Cariaco Basin	80-100	82.0	62.0	Taylor et al. 2001
Chesapeake Bay	8.5-10.1	14.0	5.8 ± 0.8	This study
[a]: Within the oxic/anoxic interface				

Figure Legends

Fig. 3.1: The map of Chesapeake Bay with a depth gradient. The stations were located along a shipping channel and stretched from near the mouth of Potomac River to the Chesapeake Bay Bridge.

Fig. 3.2: Density (top) and natural log-transformed buoyancy frequency (bottom) during the temporal (a, b) and transect (c, d) survey. Gray asterisk represents sampling depth and gray area on the transect survey represents bottom topography.

Fig. 3.3: Temporal transition of biogeochemical variables reflecting redox conditions in the mesohaline Chesapeake Bay. Note that the survey was conducted at single station (S3) for seven times. Asterisk represents sampling depth. Dotted line on the map of chlorophyll a represents the depth of 1% of surface irradiance. (DIC: dissolved inorganic carbon; SRP: soluble reactive phosphorus; DS: dissolved sulfide; DM: dissolved manganese; DFe: dissolved iron).

Fig. 3.4: Respiration and primary production in dark at S3 during the temporal survey. Horizontal dotted and dash line represents 2 and 0.5 mg O_2 L^{-1} isopleth, respectively. Error bar represents standard error of triplicate samples.

Fig. 3.5: Photosynthetic production rates near and within oxyclines (or pycnoclines when oxycline was not established on 18 Apr, 30 Aug, and 21 Sep) during the temporal survey. Error bar represents standard error of triplicate samples.

Fig. 3.6: Sediment-water fluxes of dissolved inorganic carbon and nitrogen at S3 collected during the temporal survey.

Fig. 3.7: Spatial transition of biogeochemical variables reflecting redox conditions along the main axis of Chesapeake Bay. Asterisk represents sampling depth. Dotted line on the map of chlorophyll a represents the depth of 1% of surface irradiance. Gray area represents bottom topography. The scale for each variable is identical to that in Fig. 3.3.

Fig. 3.8: Respiration and dark primary production at five stations during the transect survey. Horizontal dotted and dash line represents 2 and 0.5 mg O_2 L^{-1} isopleth, respectively. Error bar represents standard error of triplicate samples.

Fig. 3.9: The results of time course incubations for checking the validity of consistent increases in $^{14}CO_2$ fixation in (a) oxic, (b) anoxic, and (c) sulfidic condition. Dotted line represents a best fit regression analysis.

Fig. 3.10: The relationship between total organic carbon consumption (i.e., the sum of bacterial production and respiration) and production of heterotrophic bacteria in different oxic conditions.

Fig. 3.11: Box-and-Whisker plot presents the variability of (a) community respiration, (b) respiration normalized by chlorophyll a, (c) bacterial production, and (b) bacterial total organic carbon consumption dependent of stratification. The edges of the box are the 25^{th} and 75^{th} percentiles and the center line is the median. Whiskers at the both ends extend to the most extreme data points not including outliers that are marked with '+'.

Fig. 3.12: (a) Percentage contribution of gross phytoplankton production (GPP), extracellularly released organic carbon (ROC), and chemoautotrophy (DarkPP) to total

organic carbon production. (b) Percentage contribution of aerobic respiration (Aerobic R.), anaerobic respiration (Anaerobic R.), sediment-water flux (Sed. flux), and sediment burial to total organic carbon loss. The line graph represents the sum of absolute values in (a), while the dashed graph represents the sum of absolute values in (b); both graphs use a secondary y-axis.

Figures

Fig. 3.1

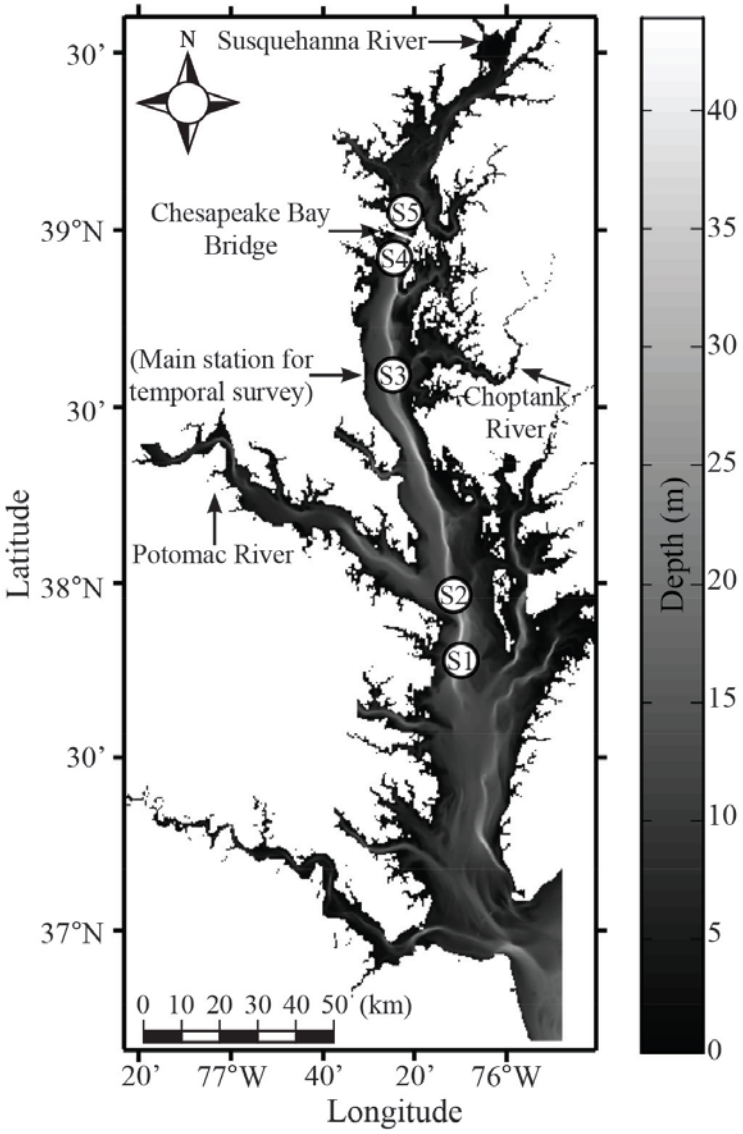

Fig. 3.2

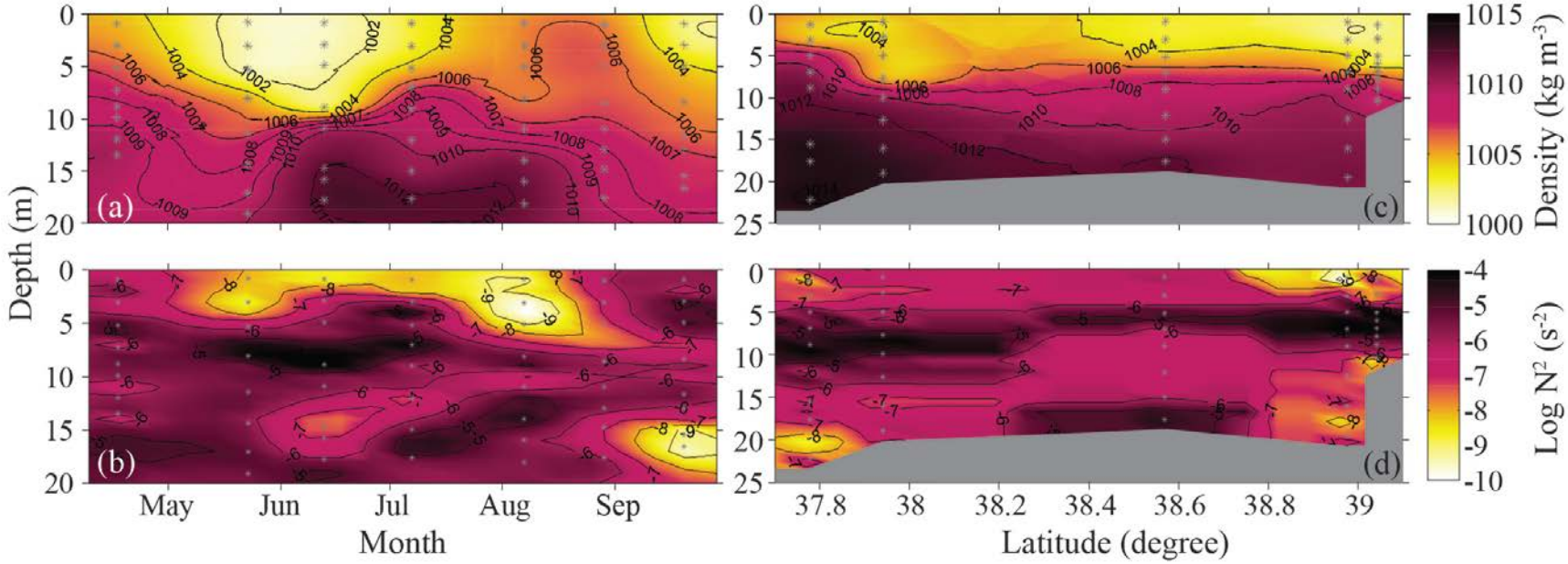
Depth (m)
(a)
(b)
(c)
(d)
May
Jun
Jul
Aug
Sep
Month
37.8
38
38.2
38.4
38.6
38.8
39
Latitude (degree)
Density (kg m-3)
Log N2 (s-2)

Fig. 3.3

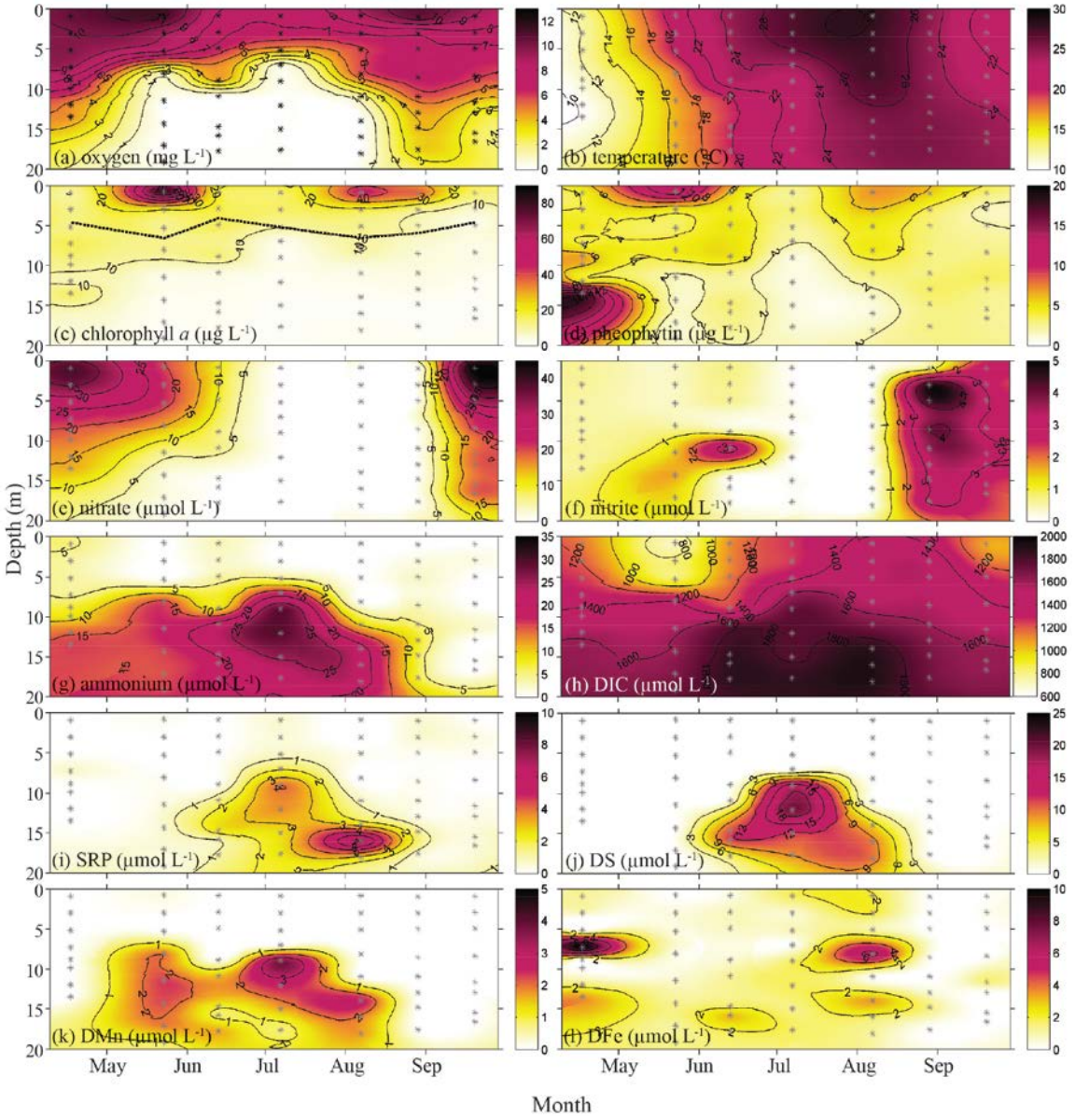
(a) oxygen (mg L-1)
(b) temperature (°C)
(c) chlorophyll a (µg L-1)
(d) pheophytin (µg L-1)
(e) nitrate (µmol L-1)
(f) nitrite (µmol L-1)
(g) ammonium (µmol L-1)
(h) DIC (µmol L-1)
(i) SRP (µmol L-1)
(j) DS (µmol L-1)
(k) DMn (µmol L-1)
(l) DFe (µmol L-1)
Depth (m)
May
Jun
Jul
Aug
Sep
Month

Fig. 3.4

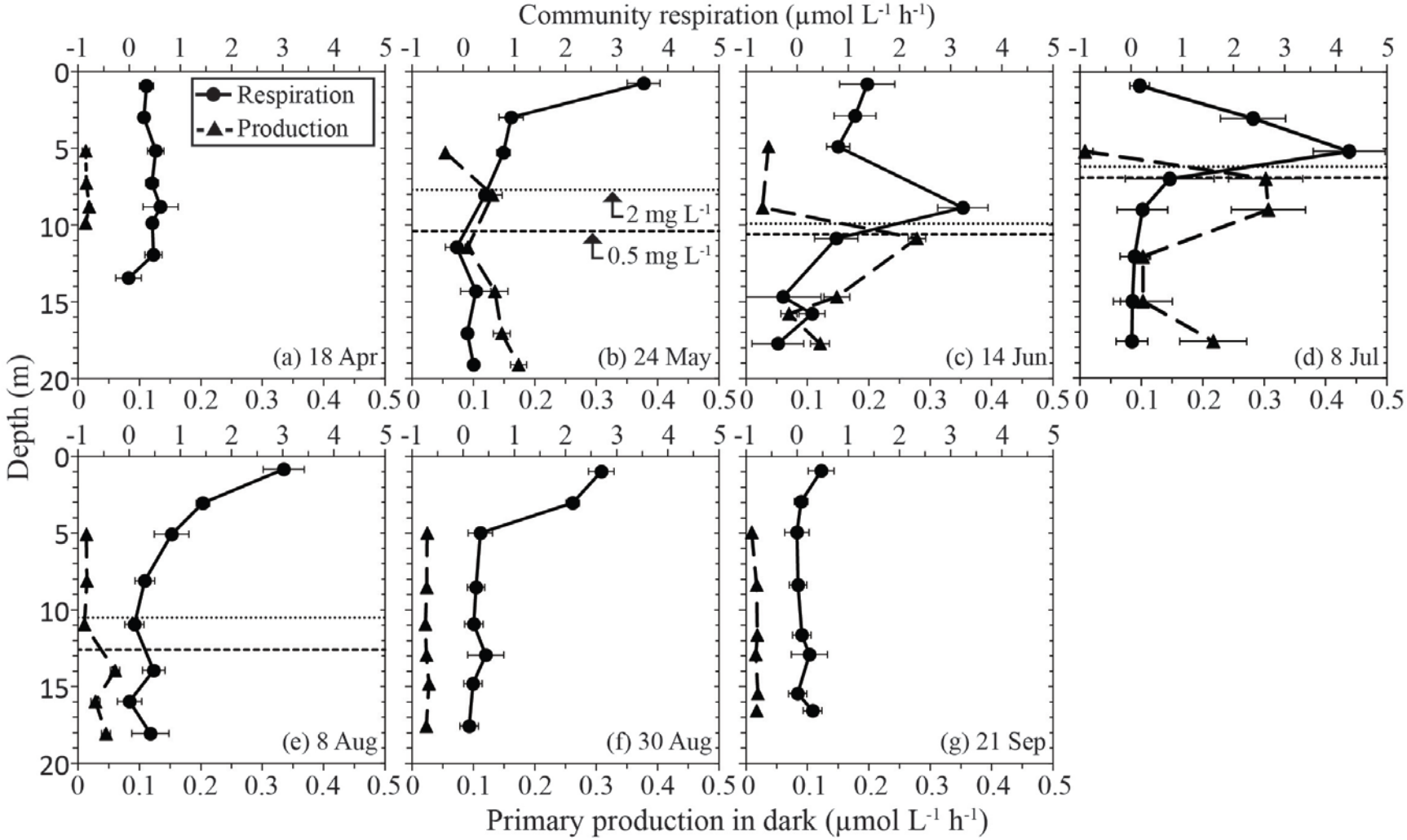
Community respiration (µmol L-1 h-1)
Respiration
Production
2 mg L-1
0.5 mg L-1
(a) 18 Apr
(b) 24 May
(c) 14 Jun
(d) 8 Jul
(e) 8 Aug
(f) 30 Aug
(g) 21 Sep
Depth (m)
Primary production in dark (µmol L-1 h-1)

Fig. 3.5

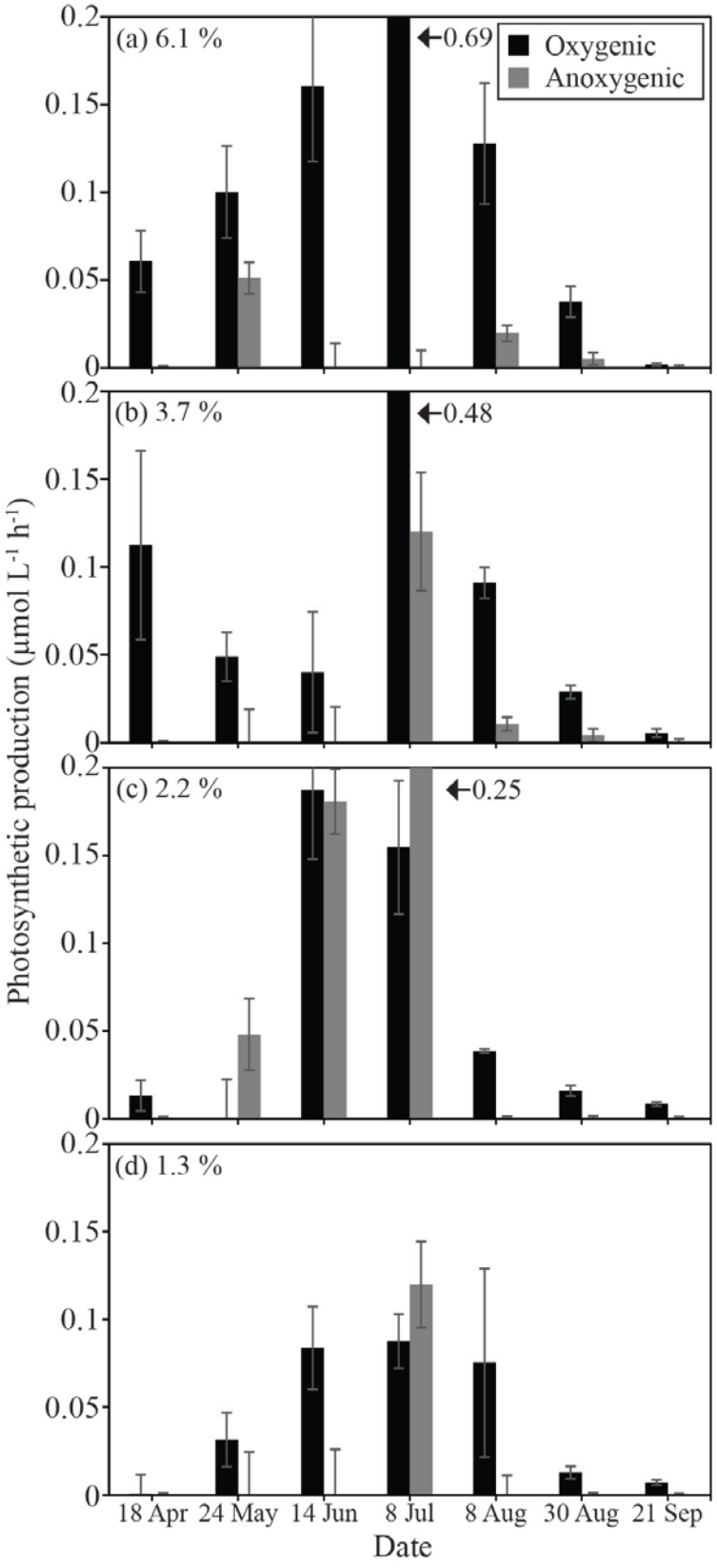
(a) 6.1 %
←0.69
Oxygenic
Anoxygenic
(b) 3.7 %
←0.48
(c) 2.2 %
←0.25
(d) 1.3 %
Photosynthetic production (µmol L-1 h-1)
0.2
0.15
0.1
0.05
0
18 Apr
24 May
14 Jun
8 Jul
8 Aug
30 Aug
21 Sep
Date

Fig. 3.6

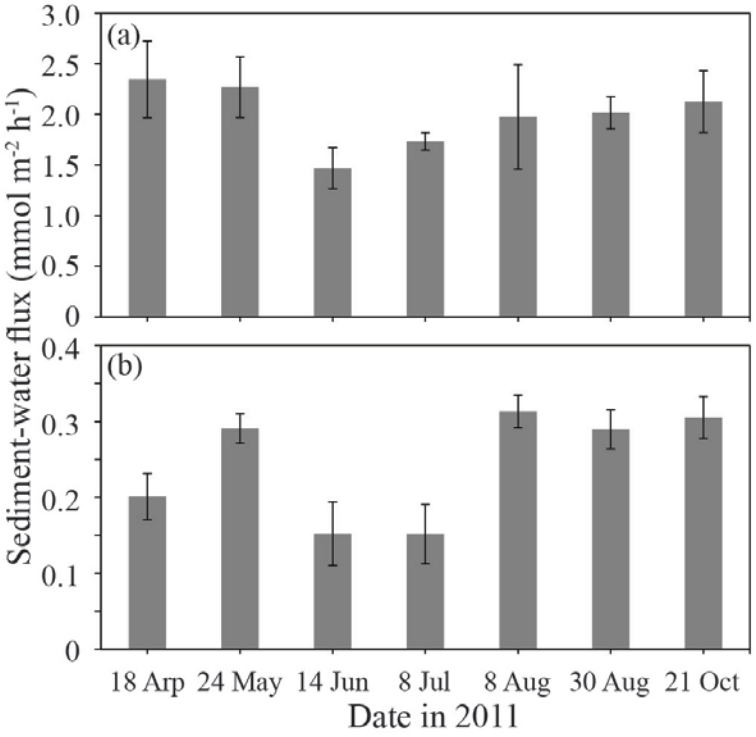
(a)
(b)
Sediment-water flux (mmol m-2 h-1)
3.0
2.5
2.0
1.5
1.0
0.5
0
0.4
0.3
0.2
0.1
0
18 Arp
24 May
14 Jun
8 Jul
8 Aug
30 Aug
21 Oct
Date in 2011

Fig. 3.7

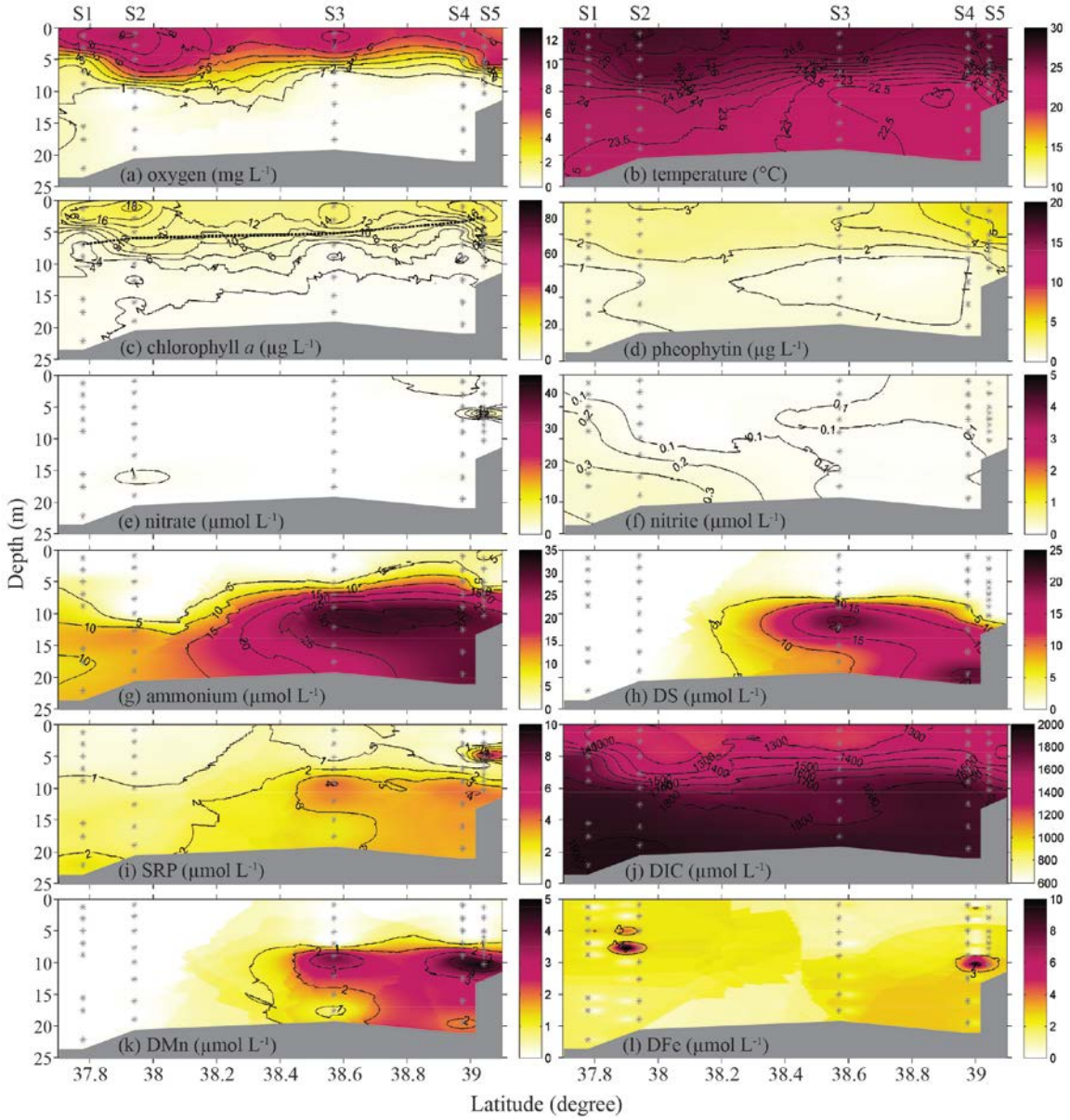
S1
S2
S3
S4
S5
(a) oxygen (mg L-1)
(b) temperature (°C)
(c) chlorophyll a (µg L-1)
(d) pheophytin (µg L-1)
(e) nitrate (µmol L-1)
(f) nitrite (µmol L-1)
(g) ammonium (µmol L-1)
(h) DS (µmol L-1)
(i) SRP (µmol L-1)
(j) DIC (µmol L-1)
(k) DMn (µmol L-1)
(l) DFe (µmol L-1)
Depth (m)
Latitude (degree)
37.8
38
38.2
38.4
38.6
38.8
39

Fig. 3.8

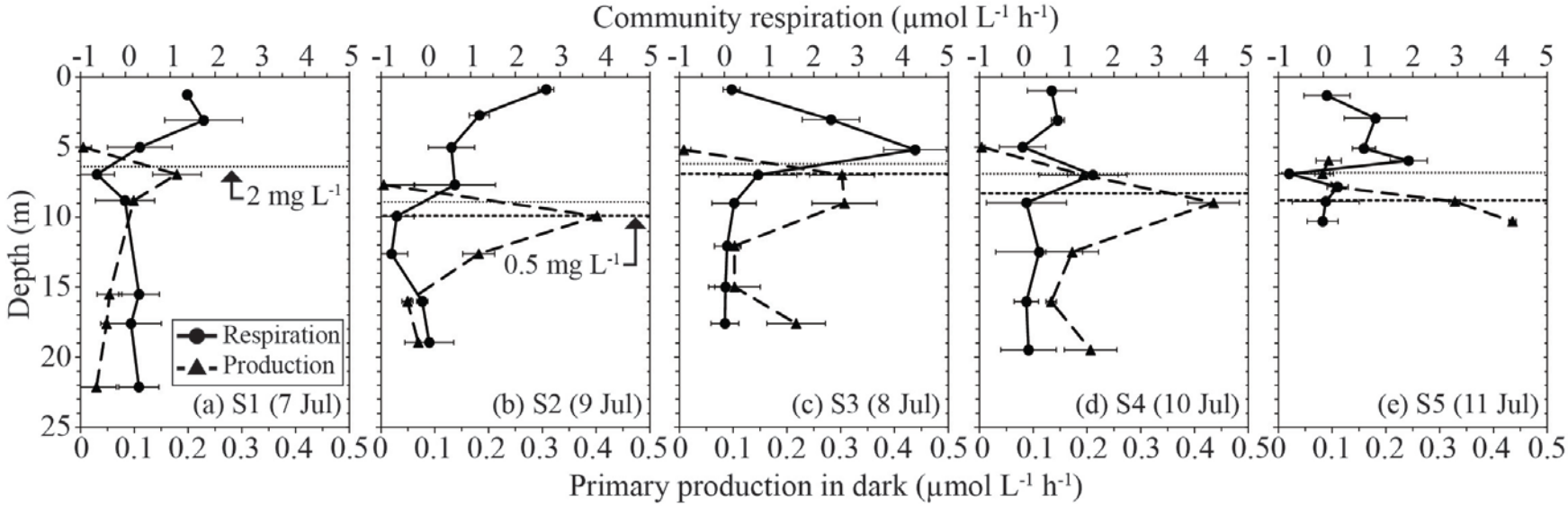
Community respiration (µmol L-1 h-1)
-1 0 1 2 3 4 5
Depth (m)
0 5 10 15 20 25
2 mg L-1
0.5 mg L-1
Respiration
Production
(a) S1 (7 Jul)
(b) S2 (9 Jul)
(c) S3 (8 Jul)
(d) S4 (10 Jul)
(e) S5 (11 Jul)
0 0.1 0.2 0.3 0.4 0.5
Primary production in dark (µmol L-1 h-1)

Fig. 3.9

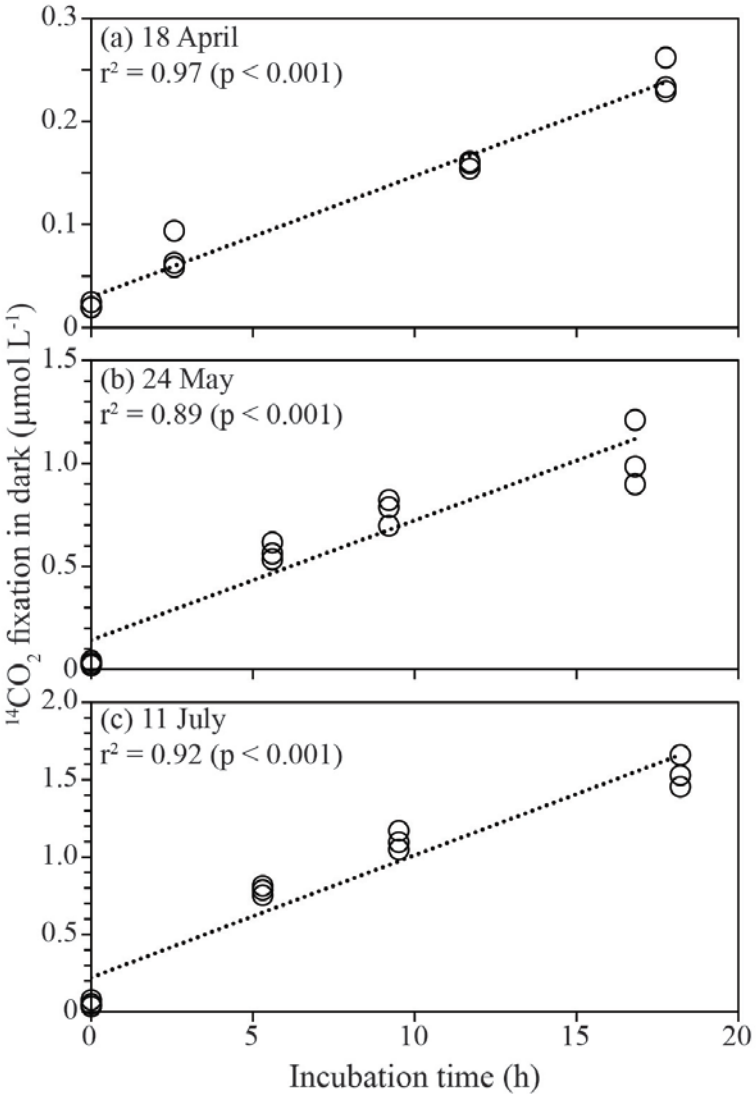
(a) 18 April
r² = 0.97 (p < 0.001)
(b) 24 May
r² = 0.89 (p < 0.001)
(c) 11 July
r² = 0.92 (p < 0.001)
¹⁴CO₂ fixation in dark (µmol L⁻¹)
Incubation time (h)
0.3
0.2
0.1
0
1.5
1.0
0.5
0
2.0
1.5
1.0
0.5
0
0
5
10
15
20

Fig. 3.10

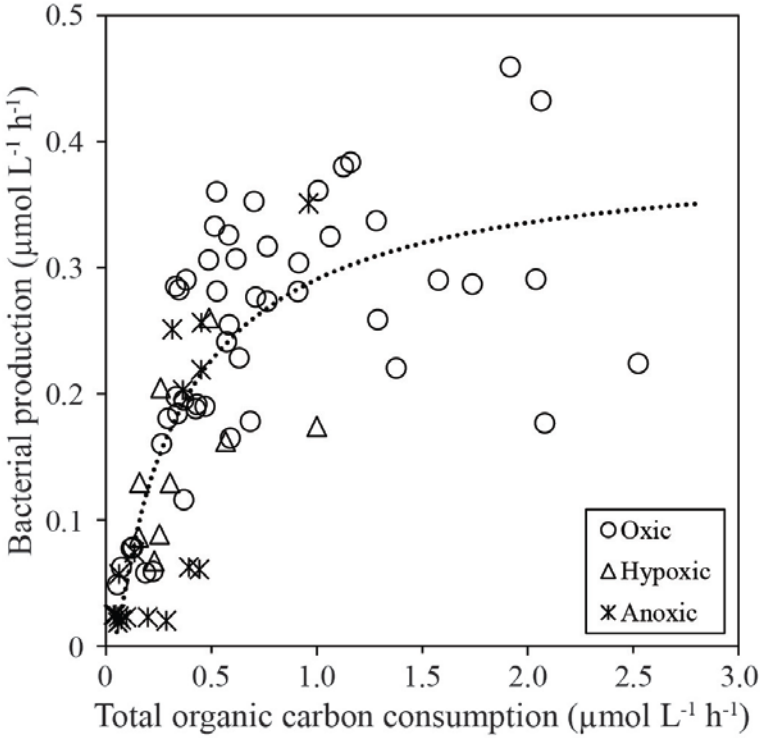
Bacterial production (μmol L-1 h-1)
Total organic carbon consumption (μmol L-1 h-1)
0
0.1
0.2
0.3
0.4
0.5
0.5
1.0
1.5
2.0
2.5
3.0
Oxic
Hypoxic
Anoxic

Fig. 3.11

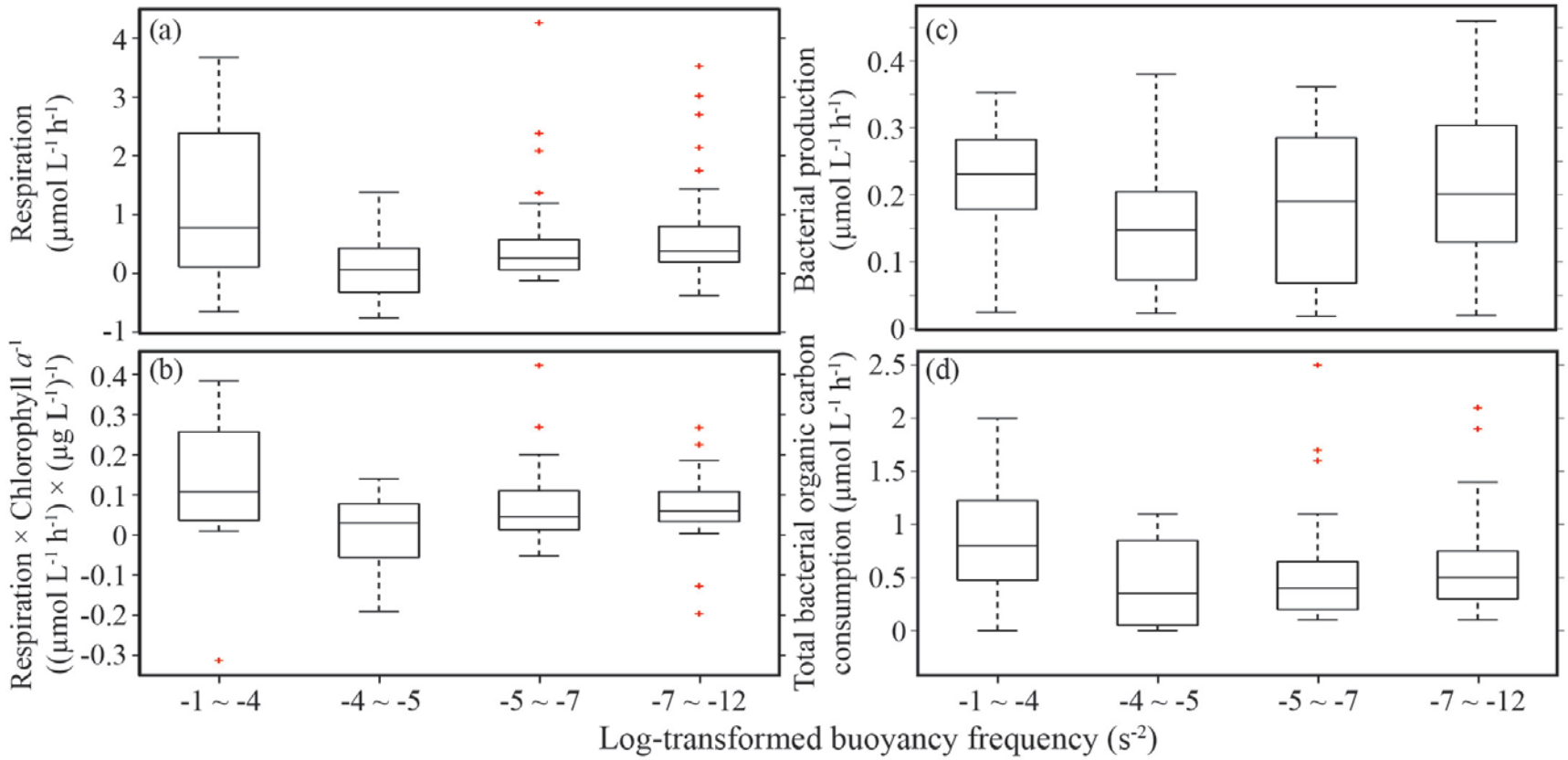
(a)
(b)
(c)
(d)
Respiration (μmol L-1 h-1)
Respiration × Chlorophyll a-1 ((μmol L-1 h-1) × (μg L-1)-1)
Bacterial production (μmol L-1 h-1)
Total bacterial organic carbon consumption (μmol L-1 h-1)
-1 ~ -4
-4 ~ -5
-5 ~ -7
-7 ~ -12
Log-transformed buoyancy frequency (s-2)

Fig. 3.12

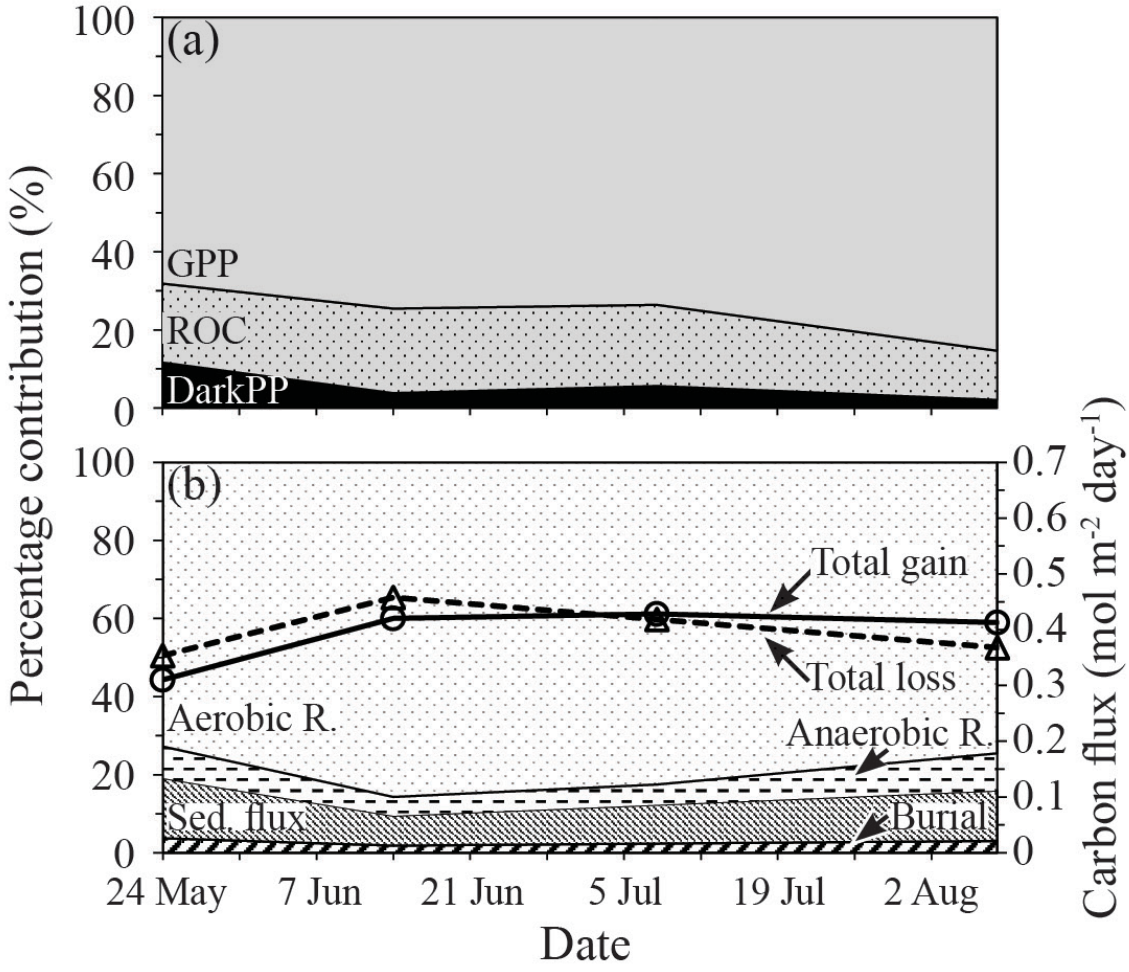
(a)
GPP
ROC
DarkPP
(b)
Total gain
Total loss
Aerobic R.
Anaerobic R.
Sed. flux
Burial
Percentage contribution (%)
Carbon flux (mol m-2 day-1)
24 May
7 Jun
21 Jun
5 Jul
19 Jul
2 Aug
Date

Chapter 4: Ammonium budget estimates during seasonal hypoxia: the relative contribution of biological and physical processes in a coastal plain estuary

Abstract

Biological and physical NH_4^+ budgets were determined across longitudinal and vertical salinity gradients in the bottom mesohaline region of Chesapeake Bay where seasonal hypoxia recurs annually. Vertical NH_4^+ zonation in surface, bottom mixed layer, and in-between (pycnocline) layers varied interannually but has not previously been incorporated into budget estimations. Biological NH_4^+ fluxes, including pelagic anaerobic respiration and benthic fluxes, were either directly measured or estimated using relationships between biogeochemical concentrations and environmental properties. Biogeochemical observations from long-term monitoring measurements (1985-2011) were also used to calculate a gradient of NH_4^+ concentrations to facilitate the estimation of NH_4^+ dispersion below the pycnocline. These fluxes were incorporated into a mass-balance framework to investigate a quantitative relationship between biological and physical NH_4^+ fluxes and determine how variations in the fluxes affect plankton composition, ecosystem production, and food web dynamics in different hypoxic conditions. The four NH_4^+ mass-balance components were in near balance calculations showing average rates of anaerobic respiration (307 μmol NH_4^+-N m^{-2} h^{-1}), sediment-water flux (313 μmol m^{-2} h^{-1}), longitudinal dispersion (370 μmol m^{-2} h^{-1}), and vertical dispersion (207 μmol m^{-2} h^{-1}). The comparison of NH_4^+ fluxes during hypoxic conditions revealed elevated vertical NH_4^+ transport rates during high hypoxic years caused a shift of plankton assemblages toward dinoflagellates and cyanobacteria species, having a competitive advantage under high NH_4^+ concentrations. We conclude that such community change exerts a positive influence on ecosystem production near the top of pycnoclines and redoxclines.

Introduction

Seasonal depletion of dissolved oxygen (DO) is a key driver of biogeochemical cycles (Middelburg and Levin 2009) and becomes a common feature in eutrophied coastal and estuarine ecosystems (Diaz and Rosenberg 2008). Eutrophication in estuarine ecosystems is strongly associated with river discharge (Malone et al. 1988) because excessive nutrient loads from anthropogenic activities result in rapid growth of phytoplankton (Howarth et al. 2011). In the Chesapeake Bay, and most temperate climate partially-stratified estuaries, spring river discharge and surface warming increase the buoyancy of surface water and create strong gradients in water density. While the heterotrophic decomposition of phytoplankton results in the consumption of DO and production of inorganic compounds, stratification plays an important role in maintaining hypoxia (<2 mg l^{-1}) and accumulating inorganic compounds by minimizing vertical mixing (Boicourt 1992; Kemp et al. 1992; Boynton and Kemp 2000). Thus, the spatiotemporal extent of hypoxia and budgets of inorganic chemical compounds may fluctuate interannually due to the variability in the effects of biological and physical factors (Murphy et al. 2011; Bever et al. 2013).

In the Chesapeake Bay, dissolved inorganic nitrogen (DIN) requirements for summer phytoplankton growth are met by the combination of pelagic (Glibert 1982) and sediment-water regeneration (Boynton and Kemp 1985; Baird et al. 1995). These studies reported variable contributions of benthic DIN regeneration relative to phytoplankton DIN requirements (10-40 %) although the growth appears to be consistently limited by DIN in summer (Fisher et al. 1992, 1999). The increase in the intensity and duration of hypoxia, however, likely provides a positive impact on the recycling and retention of

DIN and subsequently alleviates the growth limitation. Elevated sediment-water NH_4^+ fluxes occur under low DO conditions because reduced assimilation and diminished coupled nitrification-denitrification is strongly associated with benthic habitat degradation (Middelburg and Levin 2009). For example, the loss of benthic macrofauna and microphytobenthos decreases sediment redox levels, generally increasing nutrient efflux (Cornwell et al. 1999). Consequently, the absence of DO and NO_3^- limits NH_4^+ oxidation which is coupled to N_2 production (Kemp et al. 1990; Rysgaard et al. 1996; Rich et al. 2008), while an alternative pathway, dissimilatory nitrate reduction to ammonium (DNRA), results in increased DIN fluxes (Christensen et al. 2000; An and Gardner 2002). Further, ecosystems that suffer from hypoxia appear to lose the ability to recover from hypoxia-induced stress and lead to an increase in susceptibility of more severe hypoxia (Cloern 2001; Conley et al. 2009). Such a loss in systematic resistance against hypoxia appears to be accelerated by increases in hypoxic area and NH_4^+ recycling per unit total nitrogen load (Turner et al. 2008; Testa and Kemp 2012), further exacerbating eutrophication-related problems.

Despite increased understanding of the effect of hypoxia on biogeochemical NH_4^+ fluxes, we still have a lack of understanding in the role of physical properties on the transport and fate of NH_4^+. Chesapeake Bay is the moderately stratified estuary where tidal mixing produces a typical two-layer circulation (Pritchard 1967). The oxic/anoxic interface is usually coincident with the pycnocline and located in the middle of water column. Thus, dissolved constituents in estuarine waters are often measured as a function of salinity, assuming one dimensional and steady state mixing between river and seawater (Officer 1979; Gavis and Grant 1986). However, there appears to be no previous studies

describing the relationship of NH_4^+ cycling with physical structures in relation to stratification. While stratification primarily restricts vertical mixing and limits microbial growth in the surface (Stanley and Nixon 1992), episodic and seasonal climate events can result in unusually high primary production and the change in community composition due to excess supply of previously limited nutrients across stratification (Horrigan et al. 1990; Yeager et al. 2005). Therefore, it is likely that seasonal and interannual variability in the property of stratification exert a quantitative influence on nitrogen budget and ecosystem production.

A quantitative relationship between water column physics and DO budget in stratified ecosystems can provide insight into how dynamic physical mechanisms affect NH_4^+ cycling. It is generally assumed that net DO consumption, a fundamental cause of hypoxia, results from biochemical DO utilization exceeding vertical and longitudinal DO supply (Taft et al. 1980). However, the imbalance (i.e., hypoxia) can be attributed to different time-scales in both biogeochemical and physical components. For example, diurnal variations in sediment-water nutrient flux have been attributed to rapid community responses to short-term environmental changes (e.g., light, salinity, temperature) (Sundbäck et al. 2000; Giblin et al. 2010). In contrast, the extent of net residual current velocity and hypoxia is associated with longer-time-scale climate variability (Scully 2010). Despite the different time-scale of ecosystem responses, however, biogeochemical and physical processes are tightly coupled; higher biological DO consumption results in stronger physical DO transport (Kemp et al. 1992). Thus, it appears that we would likely be observing a similar coupling in NH_4^+ fluxes in anoxic waters where biophysical fluxes are constrained by stratification.

The goal of this research is to quantify the relative contribution of biological and physical processes on NH_4^+ fluxes during seasonal hypoxia to improve our knowledge of interannual variability of NH_4^+ transport and fate in relation to stratification. To examine the effect of environmental factors on NH_4^+ cycling and budgets, we used long-term monitoring and sediment flux databases combined with our observations for determining biophysical NH_4^+ fluxes. The specific objectives of this analysis were to: (1) quantify biophysical NH_4^+ fluxes from multiple data sources; (2) assess the relationship between the fluxes and environmental factors (e.g., river discharge, hypoxia); and (3) determine how variations in the fluxes affect ecosystem production and food web dynamics in the vicinity of the oxic/anoxic interface.

Materials and Methods

Pelagic and benthic samples were collected during temporal and spatial surveys along the axial transect of the mesohaline Chesapeake Bay (Table 4.1). We conducted biogeochemical surveys at CB4.3C in 2010 (7, 16 June) and 2011 (14 June). In addition, axial transect surveys were conducted on board the R/V Hugh R. Sharp in 2010 (6-12 July) and 2011 (9-15 July) from the mouth of the Rappahannock River to the Chesapeake Bay Bridge. On the first and last day of the transect survey water properties were surveyed with an undulating towed vehicle (Scanfish II-1250, GMI Denmark) equipped with conductivity-temperature-depth (CTD; Sea-Bird), DO (SBE 43), and fluorometer (WET Labs) sensors. The surveys began from CB5.5 station near the Potomac River mouth to CB3.2 station near the Chesapeake Bay Bridge covering 166 km over 12 hours (h). Water and sediment samples at five stations, including the CB4.3C (R-64) station,

were further analyzed for a series of pelagic and benthic metabolism and geochemical studies (Lee et al. 2014).

Vertical profiles of pelagic respiration, geochemical properties (salinity, temperature, DO), dissolved nitrogen species (NO_2^-, NO_3^-, NH_4^+), total dissolved sulfide (DS = $[S^{2-}] + [HS^-] + [H_2S]$), soluble reactive phosphorus (SRP), dissolved manganese (DMn = [Mn(II)] + [Mn(III)]), and dissolved iron (DFe = Fe(II)+ Fe(III)), and sediment fluxes of dissolved constituents (NH_4^+, dissolved inorganic carbon (DIC)) were measured at each station. A CTD (Sea-Bird) with DO sensor (SBE 911plus) was used to select eight sampling depths including five below surface mixed layers. We used a diaphragm pump with a 2.5 cm diameter hose attached to the CTD frame; a conical PVC manifold distributed water to 16 tubings to fill sample vials.

The samples for NH_4^+ were filtered using 0.4 μm pore size cellulose acetate syringe filters and analyzed colorimetrically (Parsons et al. 1984) with a spectrophotometer (UVmini-1240, Shimadzu). DIC concentrations were measured using an automated analyzer (LI-COR, Apollo SciTech), consisting on an automated digital pump, a mass-flow-controller, and an infrared CO_2 detector (Cai and Wang 1998). Certified reference material (CRM batch 110; provided by A. Dickson at Scripps Institution of Oceanography) was used to calibrate the analyzer according to Dickson et al. (2007) daily during the transect surveys. Overall, the calibration ranged from 0.05 to 0.12 % (coefficient of variation) with an average standard deviation of ±1.5 μmol l^{-1}. In addition, the ratio of DO to argon were measured with a membrane inlet mass spectrometer (Kana et al. 1994) yielding a precision of <0.05 %. Thermostatted (±0.02 °C of incubation temperature) deionized water was used for standardization and gas ratios

were converted to gas concentrations using temperature and salinity-based argon concentrations (Colt 1984).

Pelagic respiration was estimated using a dark bottle incubation method (Smith and Kemp 2003). Samples for initial gas concentrations were preserved with 50 % saturated mercuric chloride in 12 ml vials with butyl rubber septum caps. We simultaneously incubated samples in triplicate 60 ml biochemical oxygen demand (BOD) bottles covered with opaque plastic bags in an opaque flow-through incubator at ambient water temperature (±1 °C) on shipboard for 24 h. The incubation was ended by adding Hg and samples were siphoned into the vials. Respiration rates were measured as the difference in DIC concentrations between initial and final samples divided by the incubation time, and eventually converted to equivalent nitrogen unit using the Redfield ratio (C:N = 6.62).

We collected sediment cores using an acrylic/PVC box corer to determine sediment-water flux of NH_4^+ and DIC. The sediment was subcored using two 7 × 30 cm (inner diameter × height) acrylic cylinders to a depth of ~15 cm. Sediment and blank (i.e., only water) cores were preincubated in a thermostated bath at bottom-water temperatures (±1 °C) for 24 h to minimize initial core disturbance artifacts. Each core was equipped with a Teflon magnetic stir bar rotating at 20 rpm to mix overlying water without resuspension. Overlying water was collected four times during 24 h of incubations. During each subsampling, 5 % water volume in each core was replaced with collected bottom water through a second port so that no bubbles formed within the tubes. Sediment-water fluxes were calculated using linear regressions of NH_4^+ and DIC

concentrations. The slopes of blank cores were used to account for water column processes and a dilution effect with the replacement bottom water.

Geochemical water properties monitored by the Chesapeake Bay Program were used to estimate NH_4^+ flux in longitudinal and vertical directions. Vertical profiles of temperature, salinity, and NH_4^+ from consecutive stations along the bay's longitudinal axis were obtained for June and July (Table 4.1). The following instruments or methods were used: Hydrolab Surveyor II for salinity, a thermistor or CTD for temperature, and the spectrophotometric phenol hypochlorite method for NH_4^+ concentration (EPA 1997). Salinity and temperature have been typically measured at ~1 m depth intervals during monthly or bimonthly surveys since 1984 (the Chesapeake Bay Program Water Quality database; http://www.chesapeakebay.net/data_waterquality.aspx). Simultaneously, the concentration of NH_4^+ was measured at four depths, including surface/bottom mixed layers and upper/lower boundary of pycnoclines.

Quantitative analysis of long-term sediment NH_4^+ flux became possible due to a routine sediment flux monitoring programs since the 1980s (Boynton and Bailey 2008). The monthly flux results were obtained at R-64 (CB4.3C) station for some years in June and July; it was reported in 1985-1996 for June and 1989-1998 for July in addition to our measurements in 2010 and 2011. The experimental method for collecting and analyzing NH_4^+ flux was similar to our experiment; however, the sediment NH_4^+ flux was not corrected for NH_4^+ regeneration in a blank core. Our flux results suggested that NH_4^+ flux in blank cores was an order of magnitude lower than that in sediment cores and insignificant during hypoxic events.

For each vertical CTD profile, we calculated density expressed as sigma-T (σ_T, kg m^{-3}) according to the following equations (US Navy 1956):

$\sigma_T = a(T) + b(T) \times S$

$a(T) = - 9.22 \times 10^{-3} + 5.59 \times 10^{-2} \times T - 7.88 \times 10^{-3} \times T^2 + 4.18 \times 10^{-5} \times T^3$

$b(T) = 8.04 \times 10^{-1} - 2.92 \times 10^{-3} \times T + 3.12 \times 10^{-5} \times T^2$

where T is water temperature (°C) and S is salinity. We defined the upper and lower pycnocline boundaries as the depth where the gradient of density ($d\sigma_T$ /dz) exceeds 0.2 kg m^{-4} for the first time towards bottom and surface mixed layers, respectively. Several studies have similarly used density gradients to define the depth of top and bottom of pycnoclines. Stratification was defined in Puget Sound (Culver and Perry 1999) and the Baltic Sea (Larsson et al. 2001) using similar threshold values ranging from 0.05 to 0.30 kg m^{-4}. In addition, the conductivity threshold used by the Chesapeake Bay Program resulted in identical results with the density threshold; the boundary was defined as a depth bounded by the threshold of conductivity gradients where the mean change in conductivity over sampling intervals exceeds 25 mS m^{-2} (the Chesapeake Bay Program Water Quality database; http://www.chesapeakebay.net/data_waterquality.aspx). This methodological consistency is possible because stratification in the region is strongly dependent on salinity, which is controlled by the spring freshet from the Susquehanna River (Officer et al. 1984).

Monthly phytoplankton taxonomic data used in this study were collected along the axis of the Bay. Field and laboratory methods are available at a website (http://www.chesapeakebay.net/data/downloads/baywide_cbp_plankton_database). We examined a percent contribution of phytoplankton carbon biomass reported for four

major taxonomic groups, including diatoms, dinoflagellates, cryptophytes, and cyanobacteria.

Results and Discussion

Stratification and Geochemical Distribution

Salinity below the pycnocline exhibited a steady decrease from 23 to 17 towards the north during summer from 1985 to 2011 (Fig. 4.1a). The interannual variability (i.e., error bar) in each station was consistent presumably because of damped effects of river flows and slow landward currents in the deeper portion of Chesapeake Bay in summer (Gibson and Najjar 2000). Consistent with the long-term observations, a 2.5-fold higher spring river discharge in 2011 relative to 2010 did not significantly affect salinity gradients ($p = 0.80$, analysis of covariance) (Fig. 4.1b). This observation seems to reflect conservative mixing in the bottom water during the seasonal anoxic event.

A diurnal variability in the extent of stratification in partially stratified estuaries is often observed because semidiurnal tidal currents enhance kinetic energy for turbulent mixing. However, our results from continuous CTD surveys using an undulating towed vehicle suggested that pycnocline depth and thickness were consistent over a tidal cycle (Fig. 4.2). The maintenance of stratification is a factor of dynamic balance between longitudinal salinity gradients and vertical velocity shear of the gravitational circulation (Fisher et al. 1988; Culver and Perry 1999). This observation suggested that once vertical stratification is established, shear stress might have not overturned stratification in the absence of strong weather event (Goodrich et al. 1987). Therefore, the potential influence

of short-term environmental variability on stratification would be minimum in summer, resulting in the persistent formation of pycnoclines on a daily basis.

Although strong pycnocline was usually observed throughout the mesohaline region in summer, pycnocline depth and thickness varied interannually. As an example of the variability, large salinity differences between water masses above and below the pycnocline resulted in a narrower band of high density gradients above the threshold (i.e., sigma-T) in July 1993 when spring discharge was a twofold higher than July 1992 (Fig. 4.3). In addition, stronger density gradients appeared to be associated with higher DO removal rate across the pycnocline in July 1993, resulting in a 1.5-fold greater hypoxic volume in 1993 than 1992 (Bever et al. 2013). The observation suggests that the formation and extent of hypoxia result from a tight biological and physical coupling in the Chesapeake Bay.

Correlation analysis provided evidence for the coupling of biological and physical processes, controlling NH_4^+ concentrations below pycnoclines (Table 4.2). In both June and July, spring river discharge was positively associated with NH_4^+ concentration and maximum sigma-T, a result of both elevated NH_4^+ recycling and retention efficiency. Also, note that maximum sigma-T exerted a significantly negative effect on pycnocline thickness and a positive effect on the thickness of bottom layers in July. These results suggest that higher river discharge in spring causes stronger (i.e., high sigma-T) and narrower pycnoclines, subsequently increasing NH_4^+ concentrations in the bottom mixed layers. Further, increases in the thickness of bottom mixed layers due to stronger stratification may extend the duration of pelagic anaerobic processes because the sinking rate is inversely correlated with depth (Hagy et al. 2005).

The long-term (1985-2011) average NH_4^+ concentrations below the pycnocline increased northward from 9.5 µmol l^{-1} at CB5.4 to 26.5 µmol l^{-1} at CB3.3C in June and July (Fig. 4.4). However, unlike the pattern of salinity (Fig. 4.1a), the gradient and variability of NH_4^+ concentrations varied interannually. For example, NH_4^+ gradients were significantly different between the transect surveys conducted in 2010 and 2011 (graph not shown, $p = 0.004$, analysis of covariance) because of a twofold higher NH_4^+ concentration in the northern mesohaline in 2011 despite similar NH_4^+ values in the southern mesohaline (Fig. 4.4). Overall, the relationship between NH_4^+ concentration and the distance between CB5.4 and CB3.3C along the Bay's axis averaged 0.12 µmol l^{-1} km^{-1}, suggesting a steady increase in longitudinal NH_4^+ transport.

It should be noted that NH_4^+ concentrations at the most southern (CB5.4) and northern (CB3.3C) end of mesohaline region were not included in the computation of NH_4^+ gradients in further analyses. Large water column depth changes near these stations (i.e., <10 to >30 m) and the topographies may exert control over density structure. For instance, occasional destratification may have occurred due to downward entrainment of surface water in the hydraulic control region located near CB5.4 (Chao and Paluszkiewicz 1991). It should be also noted that NH_4^+ data in August were not analyzed further due to lack of linearity in NH_4^+ gradients; the difference (i.e., early summer vs. August) appears to be caused by a difference in factors controlling the formation and maintenance of hypoxia in between the two periods (Murphy et al. 2011).

Pelagic Ammonium Metabolism

Pelagic respiration measured with the change of DIC concentrations in the dark was converted into nitrogen equivalent using the Redfield ratio, assuming a complete

oxidation of algae-driven organic matter without the loss of DIN (i.e., the absence of denitrification, anaerobic ammonium oxidation). Sediment-water flux data confirm this ratio (i.e., 6.8). Under anoxic condition, N_2 production was not detected because of the depletion of NO_3^- and the accumulation of reduced sulfur inhibited nitrogen-mediated processes (Jenkins and Kemp 1984).

Anaerobic respiration rates were consistently lower than aerobic rates and uniform throughout bottom mixed layers with an average of 28.8 nmol NH_4^+-N l^{-1} h^{-1} (Fig. 4.5). Multiple regression analysis revealed that only NO_2^- and DMn are significantly correlated with anaerobic respiration during the transect surveys, while other geochemical variables (e.g., temperature, DO, chlorophyll a, NO_3^-, NH_4^+, SRP, DS, DFe) were not significant predictors (Table 4.3). Changing redox conditions are reflected in the transition of different redox active species; for examples, dissimilatory reduction of NO_3^- and Mn(IV) can result in the secondary peak of NO_2^- and Mn(III) in oxic/anoxic interface (Trouwborst et al. 2006; Santoro 2009). Thus, the positive correlation between anaerobic respiration and the two redox species (i.e., NO_2^-, DMn) could be caused by up-regulation of microbial processes during the spatiotemporal transition of redox conditions. Because anaerobic respiration reached its annual minimum without horizontal (i.e., time, space) and vertical variability in summer, we examined the net balance under those conditions.

Benthic Ammonium Flux

Anoxic sediment-water NH_4^+ fluxes at CB4.3C ranged from 91.4 to 699.3 μmol m^{-2} h^{-1}, a twofold increase in NH_4^+ flux compared to that in oxic spring (Fig. 4.6). This is consistent with the significant correlation of NH_4^+ flux with DO ($r = -0.50$, $p < 0.001$) and temperature ($r = 0.59$, $p < 0.001$) in overlying waters. Similar to previous

observations (Cowan and Boynton 1996), multiple regression analysis using the anoxic dataset revealed that only temperature and sediment surficial chlorophyll a concentration are significantly correlated with NH_4^+ flux (Table 4.4). Overall, the results suggest benthic NH_4^+ recycling is predominantly controlled by both redox condition and labile organic matter input rates, while thermal kinetic control is consistently important regardless of redox conditions.

In addition to the strong association of benthic processes with redox and temperature, the seasonal variation in sediment-water NH_4^+ flux appears to be strongly associated with total water depth due to the variability in relative contribution of pelagic and benthic processes (Oviatt et al. 1986a; Kemp et al. 1992). There is strong evidence that eutrophication enhances the growth of smaller phytoplankton species (Harding 1994; Cooper 1995). The greater buoyancy of the small algae exerts a positive feedback effect on pelagic community respiration, while the relative contribution of benthic processes to total respiration tends to decrease with nutrient enrichment because of proportionally lower organic matter sedimentation (Kelly et al. 1985; Oviatt et al. 1986a; Hopkinson 1987). Nevertheless, higher anoxic benthic NH_4^+ fluxes suggest that even if the relative contribution of benthic processes on community respiration would be less during severe hypoxic (eutrophic) conditions, the amount of sedimentation and regeneration would be still higher in years with higher river discharge.

A positive feedback between nutrient loadings and hypoxia (Hagy et al. 2004) has been observed in recent decades coincident with over-enrichment of coastal and estuarine ecosystems (Boesch 2002). The relative release rate of NH_4^+ and SRP is of particular interest because of the shortage of DIN relative to SRP for summer phytoplankton growth

(Fisher et al. 1999). Unlike the release of SRP, which is predominantly controlled by geochemical properties of bottom waters (Middelburg and Levin 2009), benthic NH_4^+ flux appears to increase due to decreases in benthic microbial NH_4^+ transformation processes (i.e., nitrification, denitrification, assimilation) during summer anoxia (Cowan and Boynton 1996; Kemp et al. 1999; Testa et al. 2013). The loss of DO and NOx (NO_2^- + NO_3^-) prevents NH_4^+ oxidation which is coupled to denitrification (Kemp et al. 1990). In addition, DNRA would not occur due to the absence of NOx although DNRA becomes energetically more favored than denitrification under sulfidic conditions. Further, elevated NH_4^+ recycling per unit total nitrogen loading in hypoxic ecosystems (Turner et al. 2008; Conley et al. 2009; Testa and Kemp 2012) may increase the incidence and intensity of hypoxic waters due to enhanced phytoplankton growth (Conley et al. 2007). The enhanced NH_4^+ recycling can be caused geochemically by a reduction of NH_4^+ adsorption capacity in sediments (Seitzinger et al. 1991; Giblin et al. 2010). However, the similarity of the ratio of sediment DIC to DIN flux (6.8 ± 0.7, n = 12) to the Redfield ratio during the transect survey suggested that biological, rather than geochemical, processes were responsible for NH_4^+ flux.

Ammonium Balance during Summer Anoxic Event

Similar to the computation of the DO budget according to Kemp et al. (1992), a conceptual model was built to assess the relative contributions of biological and physical processes to determine interannual variations in NH_4^+ budgets at CB4.3C station below the pycnocline in June and July as follows:

$$(d[NH_4^+]/dt)Z_b = R_b + F_s - F_v - F_h$$

where Z_b represents the thickness of bottom mixed layer, R_b is depth-integrated anaerobic NH_4^+ remineralization, F_s is sediment-water NH_4^+ flux, F_v is vertical NH_4^+ dispersion across the pycnocline, and F_h is horizontal (longitudinal) NH_4^+ dispersion. We were able to estimate the changes in NH_4^+ over time ($d[NH_4^+]/dt$) because there have been bimonthly measurements of water quality from the Chesapeake Bay Program with some exceptions (1996-2003, 2009); because of lower temporal resolution, inter-month differences were used for those years. When actual measurement or monitoring was not conducted, we estimated a flux derived from reported empirical relationships. The thickness of the bottom mixed layer, Z_b, averaged 10.2 and 10.6 m in June and July, respectively.

We have used a constant value of anaerobic respiration (28.8 nmol N l^{-1} h^{-1}) to estimate depth-integrated rates, R_b, for both June and July based on previous estimates in 2010 and 2011. The results suggested that anaerobic respiration was uniform throughout bottom anoxic mixed layers likely because of the dominance of dissimilatory sulfate reduction and uniform geochemical conditions. The depth-integrated anaerobic respiration averaged 307 µmol N m^{-2} h^{-1}. Although the average is lower than the estimated value (547.5 µmol N m^{-2} h^{-1}) from an empirical relationship between temperature and respiration in the studied region (Fig. 8 in Smith and Kemp 1995), the latter is likely overestimated because water samples were collected in the higher respiration hypoxic zone.

Since direct measurements of sediment-water NH_4^+ flux, F_s, were limited in some years, we determined values in other years based on an empirical relationship. The relationship between measured and estimated NH_4^+ flux, using both temperature (Kemp

et al. 1992) and winter-spring discharge (Boynton and Kemp 2000) dependent linear regression, were not significantly correlated (graph now shown, $r^2 < 0.1$, $p > 0.05$). Instead, sediment DO demand and NH_4^+ flux are significantly correlated with surficial chlorophyll a concentration (Cowan and Boynton 1996); therefore, surficial chlorophyll a concentration was estimated for summer (Boynton and Kemp 2000) to derive the sediment-water NH_4^+ flux. The estimated flux was significantly correlated with measured flux ($r^2 = 0.65$, $p < 0.001$).

Vertical profiles of NH_4^+ exhibited strong gradients across pycnoclines with high interannual variation ranging from 0.7 to 5.2 μmol l^{-1} m^{-1} in June and July. The vertical NH_4^+ dispersion, F_v, was estimated by multiplying the NH_4^+ gradient by a vertical diffusion coefficient. Despite the highly variable nature of water column diffusion coefficients (Li et al. 2007), previous studies reported rather consistent values ranging from 0.1 to 0.2 cm^2 s^{-1} in summer (Pritchard 1967; Kemp et al. 1992). Assuming negligible anaerobic NH_4^+ oxidation in anoxic water, we used 0.2 cm^2 s^{-1} reported in Kemp et al. (1992). We must note that NH_4^+ upwelling can be as important as non-advective transport, in which the particular equation we used does not explicitly include it. According to a salt-water balance model result (Hagy 2002), a comparison between the two transport terms resulted in a ratio of 1.1 (upwelling : non-advective transport), suggesting similar contribution of upwelling compared to upward/downward non-advective transport. However, using the upper end of diffusion coefficient (0.2 cm^2 s^{-1}) appears to incorporate both advection and diffusion. To find out if our calculation would underestimate total vertical NH_4^+ dispersion by excluding an upwelling term, a diffusion coefficient (Y; cm^2 s^{-1}) was calculated for each year using an empirical equation

dependent of winter-spring river discharge (X; m^3 s^{-1}) from Susquehanna River ([Y = $0.20 – (3.3\times10^{-5})X$]) (Hagy 2002), resulting in average 0.1 cm^2 s^{-1}. Overall, vertical NH_4^+ diffusion calculated from the estimated coefficient resulted in the half of that calculated from the fixed coefficient, suggesting that the sum of the former and upwelling would not be different from the latter. As a result, net positive NH_4^+ dispersion was consistently estimated, suggesting vertical dispersion was usually directed from anoxic to oxic water columns.

Longitudinal profiles of NH_4^+ exhibited high interannual variability along the Bay's axis ranging from 0.04 to 0.22 μmol l^{-1} km^{-1}. Longitudinal NH_4^+ dispersion, F_h, was estimated by multiplying the NH_4^+ gradient by average landward current flow of 4 cm s^{-1} (Li et al. 2007). The dispersion averaged 370 μmol N m^{-2} h^{-1} in this study and was comparable to 402 μmol N m^{-2} h^{-1} estimated from DO concentration gradients (Kemp et al. 1992). The longitudinal dispersion of NH_4^+ would involve both diffusive and advective transport processes similar to vertical NH_4^+ dispersion, while the former is negligible due to much higher net landward flow. Consequently, elevated upstream NH_4^+ concentrations suggest that longitudinal advection would be the predominant force below the pycnocline during hypoxia as physical advection controls variability in DO concentration gradients in the same region (Sanford et al. 1990).

To validate the mass-balance equation, we compared longitudinal NH_4^+ gradient with calculated longitudinal NH_4^+ dispersion by substituting the known four other terms except F_h (i.e., $(d[NH_4^+]/dt)Z_b$, R_b, F_s, F_v) in the equation. It provides an independent means to calculate residual landward current flow (V_h); $V_h = (F_h)(dC/dy)^{-1}(Z_b)^{-1}$, where (dC/dy) is the longitudinal NH_4^+ gradient and Z_b is the average thickness of bottom

mixed layers. As the term $[(F_h)(dC/dy)^{-1}]$ is equal to the slope (2.09 (mmol m^{-2} h^{-1}) (µmol l^{-1} km^{-1})$^{-1}$) of the regression ($r^2 = 0.37$, $p < 0.001$), $V_h = (2.09 \times 10^3\ m^2\ h^{-1})(10.4\ m)^{-1} = 5$ cm s^{-1}, which is close to a typical current velocity in the bottom water (Pritchard 1967). The realistic magnitude of computed current velocity suggests that the equation is well balanced and the fluxes are within a range of realistic values.

Ammonium Budget Mediated by Biological and Physical Processes

The net NH_4^+ budget was computed by subtracting the sum of physical transport from that of biological NH_4^+ production, averaging 51 ± 116 µmol N m^{-2} h^{-1}. The large variability includes zero, suggesting that interactions between biological and physical mechanisms kept net NH_4^+ budgets in near balance. Similarly, DO budgets below Chesapeake Bay pycnoclines indicated that a gradient of DO is a fundamental force, driven by biological consumption and generating both longitudinal and vertical DO transport (Kemp et al. 1992). Therefore, our results consistently suggest that NH_4^+ production from benthic and pelagic biological processes creates concentration gradients, resulting in both longitudinal and vertical NH_4^+ dispersion. The interdependence would be strongly associated with the distribution and concentration of NH_4^+ below and above the pycnocline and further affect ecosystem production in summer and fall.

While anaerobic respiration was not correlated with spring river discharge, sediment-water NH_4^+ flux was negatively correlated (Fig. 4.7a, b), suggesting that the contribution of pelagic (aerobic and anaerobic) NH_4^+ production to total NH_4^+ pool would become even higher during severe hypoxic events because hypoxia is strongly associated with spring river discharge (Officer et al. 1984; Boynton and Kemp 2000; Hagy et al. 2004). However, the thickness of bottom layers was negatively correlated

with the thickness of both surface and pycnocline layers (Table 4.2), suggesting the compression of oxygenated water columns where respiration was about an order of magnitude higher than anoxic waters under wet spring conditions. Despite the decrease of oxic volumes, subsurface maximum respiration, consistently observed near the upper pycnocline only in summer (Lee et al. 2014), seems to counterbalance the expected decrease in depth-integrated pelagic respiration. For example, aerobic respiration increased exponentially from surface to the pycnocline with the highest rate of 2.5 and 4.3 μmol C l^{-1} h^{-1} at CB4.3C in July 2010 and 2011, respectively. Although the depth of the upper pycnocline was shallower in 2011 by 2 m, depth-integrated aerobic respiration increased 57 % in 2011 compared to 2010. These results suggest that aerobic respiration changes exponentially in response to spring river discharge, while depth-integrated anaerobic respiration changes linearly to the change of bottom water thickness. Therefore, observations that the sum of two anaerobic processes (i.e., pelagic, benthic) was insignificantly correlated with spring river discharge (graph not shown; $r^2 = 0.05$, $p > 0.05$) suggests low interannual variability. In addition, observations of the relationship between river discharge and phytoplankton deposition in mesohaline sediments were insignificant (Hagy et al. 2005). These lines of evidence suggest that the activity of aerobic processes increase exponentially in summer under wet spring conditions.

The relationship between physical fluxes and river discharges appears to offer an explanation for high aerobic respiration near the upper pycnocline. Although longitudinal dispersion was about a twofold higher than vertical dispersion (y-axis in Fig. 4.7c, d), only the latter was significantly correlated with spring river discharge, suggesting an increase of surface DIN pool and hence aerobic metabolism. In contrast, longitudinal

dispersion is a factor of NH_4^+ concentrations along a 140-km long axis. Considering average residual current flow in summer (4 cm s^{-1}), the dispersion likely has the longest time-scale (i.e., >32 days) among four flux terms. Thus, the high interannual variability of longitudinal dispersion would reflect a combination of variabilities of the three other flux terms.

The balance between longitudinal and vertical NH_4^+ dispersion may result from spatiotemporal differences in chlorophyll a distribution as it relates to primary production. For example, it can be speculated that elevated vertical NH_4^+ dispersion in the studied region would result in a relatively higher chlorophyll a concentrations in the mid (near CB4.3C) than northern (near CB3.3C) mesohaline region under wet spring conditions. It can be further speculated that chlorophyll a concentrations would be relatively lower in fall under wet than average-to-dry spring conditions because of relatively greater reduction of the total NH_4^+ pool available for fall phytoplankton bloom.

Vertical Ammonium Dispersion under Different Hypoxic Conditions

To facilitate a systematic comparison between years with different physical conditions, the long-term dataset in Fig. 4.7 was divided into four hypoxic categories representing <25th, 25-50th, 50-75th, and >75th percentile of recorded maximum hypoxic volumes according to Bever et al. (2013) for the period 1985-2011 (Fig. 4.8). Although the pattern is similar to Fig. 4.7, the only significant difference was found in vertical NH_4^+ dispersion between a group of highest hypoxic volume (>15.2 km^3) and all other groups at CB4.3C (Tukey's test, $p < 0.05$) (Fig. 4.8d). Therefore, the interannual difference in vertical dispersion could have been reflected in NH_4^+ and chlorophyll a

concentrations between high hypoxic (HH; above the 3rd quartile, >15.2 km^3) and intermediate to low hypoxic years (LH; below the 3rd quartile, <15.2 km^3).

Interannual variation in sub pycnocline NH_4^+ concentrations was substantially different for summer and fall (Fig. 4.9a, b). This observation suggests that higher vertical dispersion in HH years caused lower NH_4^+ concentrations before fall-turnover, consequently resulting in a 70 % reduction of the bottom NH_4^+ pool relative to summer (Fig. 4.9c). The fall decrease was considerably lower (50 %) in LH years, suggesting a higher and longer retention of NH_4^+ pool generated in summer. Therefore, higher vertical dispersion in HH years would have facilitated the growth of both primary and secondary producers in summer because both can fulfill nitrogen demand by assimilating NH_4^+ (Bronk et al. 2007; Bradley et al. 2010). These results combined with our NH_4^+ budget analysis appear to explain the pattern of chlorophyll a above the pycnocline. While chlorophyll a concentrations were higher in HH years throughout the mesohaline region except at CB3.3C in summer, those in LH years became comparable and even higher in the northern mesohaline regions in fall (Fig. 4.9d, e). As a result, an average reduction of chlorophyll a concentrations in fall relative to summer was 31 and 20 % under HH and LH conditions, respectively (Fig. 4.9f).

The lower chlorophyll a concentrations in fall under HH than LH conditions, however, was unexpected due to higher DIN in surface layers under HH conditions; the minimum difference was 4.7 µmol l^{-1} with always higher DIN under HH conditions. Although the decreased chlorophyll a under HH conditions could be caused by an increase in grazing pressure, hypoxia exerts various sub-lethal effects on the growth and reproduction of marine herbivores and omnivores despite species-specific differential

tolerance against hypoxia (Gobler et al. 2008; Elliott et al. 2013; Rocke and Liu 2014). Therefore, it is more likely that a combination of top-down and bottom-up effects, such as greater reduction of the SRP pool in fall due to greater summer consumption during HH condition, would limit phytoplankton growth.

Consequences of Elevated Vertical Ammonium Flux

Vertical NH_4^+ dispersion appear to have important implications regarding ecosystem metabolism and microbial food webs near the upper pycnocline. The function of pycnoclines is somewhat analogous to those of thin layers ubiquitously found in aquatic environments (McManus et al. 2003). Thin layers usually accumulate high concentrations of particulate and dissolved organic mainly due to similar biophysical mechanisms founding in stratified hypoxic ecosystems (Durham and Stocker 2012). Thus, there appears to be a positive feedback of elevated vertical NH_4^+ dispersion and stratification on microbial processes and the extent of hypoxia due to elevated the DO consumption near upper pycnoclines and increased organic matter supply for anaerobes.

However, we need to note that ratios of DIN to SRP in summer and fall were consistently higher than the Redfield ratio (16) at the depth of pycnoclines regardless of hypoxic conditions. Further, high NH_4^+ concentrations (e.g., >4 μmol l^{-1} in San Francisco Bay; Dugdale et al. 2007) can have negative effects on some phytoplankton groups because of a reduction of NO_3^- uptake (Berg et al. 2001; Glibert et al. 2006). In particular, high NH_4^+ concentrations inhibit the growth of diatoms, while many flagellates and cyanobacteria prefer reduced forms of nitrogen, such as NH_4^+ and urea (Fan et al. 2003; Yoshiyama and Sharp 2006; Glibert et al. 2006; Glibert 2010). Moreover, cellular carbon to both nitrogen and phosphorus composition in diatoms are lower than those in

dinoflagellates and cyanobacteria, suggesting the latter have lower phosphorus requirements (Bertilsson et al. 2003; Ho et al. 2003). Thus, it is likely that phytoplankton taxonomic composition would be changed interannually in response to variability in vertical NH_4^+ flux.

Although typical seasonality in phytoplankton composition prevailed, such as high dinoflagellates in summer and diatoms in fall (Fig. 4.10) (Adolf et al. 2006b), striking differences in the percent contribution of phytoplankton carbon biomass was observed at CB4.3C in summer (Fig. 4.10c); the contribution of dinoflagellates become dominant (52 %) under HH conditions, while that of dinoflagellates and diatoms become equivalent (40 %) under LH conditions. Such interannual variability in the composition was weaker in the northern mesohaline regions (e.g., CB3.3C) due to the close proximity to the source of anthropogenically oxidized forms of nitrogen. Further, we have measured highest chemoautotrophic production rates in the oxic/anoxic interface at CB3.3C in summer 2011 (i.e., HH year). Thus, even if high vertical NH_4^+ dispersion occurred under HH conditions, biological oxidation of NH_4^+ into NOx (nitrification) would be proportionally enhanced, alleviating a toxic effect of NH_4^+ on diatoms.

The changes in the phytoplankton community to those having a competitive advantage under high NH_4^+ concentrations suggests a shift of plankton assemblages toward heterotrophy. In particular, increasing biomass of dinoflagellate species, such as *Prorocentrum minimum* and *Karlodinium micrum*, in the Chesapeake Bay are linked to eutrophication (Killberg-Thoreson et al. 2013) and can alter food web dynamics due to changes in prey items for larger heterotrophs (Kleppel et al. 1991; Johnson et al. 2003); autotrophic and heterotrophic dinoflagellates are preferentially grazed by

mesozooplankton because dinoflagellates have a lower carbon to nitrogen ratio than other phytoplankton groups and contain other essential nutrients for egg production (Stoecker and Capuzzo 1990; White and Roman 1992). In addition, when the diet of *Acartia tonsa*, one of most abundant mesozooplankton in the Chesapeake Bay (Roman et al. 1993), is composed of dinoflagellates, the sinking speed of fecal pellets was slower than that with other diets, such as ciliates and diatoms (Feinberg and Dam 1998), increasing the retention and regeneration of organic matter near the pycnocline. More importantly, abundant dinoflagellates in the Chesapeake Bay, such as *P. minimum*, *K. micrum*, and *Heterocapsa rotundatum*, are mixotrophic dinoflagellates and can efficiently transfer microbial production into higher trophic levels due to swimming ability and a dual life strategy (Adolf et al. 2006a; Lee et al. 2012). These lines of evidence support the idea that changes in phytoplankton composition due to enhanced NH_4^+ concentrations will have a cascade effect on various community compositions and exert a positive influence on ecosystem production near the top of the pycnocline.

Conclusion

The relationships demonstrated here between NH_4^+ fluxes and phytoplankton biomass and composition can be conceptualized over hypoxic conditions (Fig. 4.11). Our mass-balance analysis combined with long-term monitoring dataset revealed that NH_4^+ budgets below the pycnocline during hypoxia is the product of dynamic balance between biological and physical NH_4^+ fluxes and affects ecosystem production in the mesohaline Chesapeake Bay. Under LH summer conditions, the balance between biological production and physical dispersion resulted in net positive NH_4^+ budget of 58.2 μmol m^{-2}

h^{-1} at CB4.3C (Fig. 4.11a). The result suggests that NH_4^+ had been accumulated at a rate of 4 μmol l^{-1} $month^{-1}$ below pycnoclines, using an average bottom water thickness of 10.4 m. This is supported by our observation in July 2010 when NH_4^+ concentrations increased approximately from 15 to 20 μmol l^{-1} in a month (Lee et al. 2014). The accumulation was contributed equivalently by both anaerobic respiration and sediment flux. Considering different time-scales and organic matter sources (Cowan and Boynton 1996), however, the similar values of two biological processes are likely coincidental. Under HH summer conditions, the balance between biological production and physical dispersion also resulted in net positive NH_4^+ budget of 27.4 μmol m^{-2} h^{-1}, equivalent to NH_4^+ accumulation at a rate of 2 μmol l^{-1} $month^{-1}$ below pycnoclines (Fig. 4.11c). The slower accumulation rate compared to that under LH conditions resulted in a 70 % removal of summer NH_4^+ pool in fall, which also resulted in proportionally greater reduction of chlorophyll a concentrations likely due to a relatively high reduction of SRP (Fig. 4.11d).

We presented dynamic NH_4^+ cycling processes and budgets during hypoxia using mass-balance analyses consisting of biological and physical components. Using the approach in the specific location where previous biophysical measurements are abundant, we were able to address a range of scientific questions raised in our previous studies. Overall, it seems clear that biophysical NH_4^+ fluxes in anoxic waters are tightly coupled despite different time-scales. It was also demonstrated that vertical NH_4^+ dispersion is strongly associated with environmental forces and hence affect ecosystem production and food web dynamics near upper pycnocline environments. If hypoxia increases throughout coastal and estuarine systems (Conley et al. 2009; Najjar et al. 2010), we would likely

observe a relative increase in aerobic metabolism to total metabolism due to elevated vertical NH_4^+ dispersion which may further exacerbate summer hypoxia.

Tables

Table 4.1: Sources of current and historical data used in the analysis.

Station	Year	Latitude (°N)	Longitude (°W)	Depth (m)	Data	Source
S1Y10	2010	37.775	76.175	23	salinity, temperature, NH_4^+, sediment NH_4^+ and DIC flux	This study
S2Y10	2010	38.224	76.243	21		
S3Y10	2010	38.312	76.287	21		
S4Y10*	2010	38.555	76.428	28		
S5Y10	2010	38.978	76.363	23		
S1Y11	2011	37.779	76.172	23		
S2Y11	2011	37.941	76.189	10		
S3Y11*	2011	38.555	76.428	28		
S4Y11	2011	38.975	76.366	21		
S5Y11	2011	39.041	76.356	12		
CB3.3C	1985-2011	38.996	76.359	26	salinity, temperature, NH_4^+, chlorophyll a, phytoplankton taxonomic composition	Chesapeake Bay Program database
CB4.1C	1985-2011	38.826	76.399	33		
CB4.2C	1985-2011	38.646	76.421	28		
CB4.3C*	1985-2011	38.555	76.428	28		
CB4.4	1985-2011	38.415	76.346	32		
CB5.1	1985-2011	38.319	76.292	26		
CB5.2	1985-2011	38.137	76.228	33		
CB5.3	1985-2011	37.910	76.171	29		
CB5.4	1985-2011	37.800	76.175	34		
R-64*	1989-1996, 1998	38.555	76.428	28	sediment NH_4^+ flux	Chesapeake Bay Sediment Water Flux database

* Station S4Y10, S3Y11, CB4.3C, and R-64 are identical and CB4.3C was used to represent all the stations in the text

Table 4.2: The relationship between environmental variables in the period of 1985 to 2011 was analyzed using Pearson correlation statistical method for June (n = 45; upper right side) and July (n = 54; lower left side) dataset. The thicknesses of surface, pycnocline, and bottom layers were defined using a threshold value of sigma-T gradient. Spring river discharge for June and July is the average of March to May and April to June discharge, respectively. Only the results with r > |0.2| are shown and bold coefficients indicate significant relationship ($p < 0.05$).

	NH_4^+	Maximum sigma-T	Pycnocline layer	Bottom layer	Surface layer	Spring river
	($\mu mol\ l^{-1}$)	($kg\ m^{-3}$)	(m)	(m)	(m)	($m^3\ s^{-1}$)
NH_4^+		-	-	-	-	**0.39**
Maximum sigma-T	-		-	0.24	-0.23	0.26
Pycnocline layer	0.23	**-0.47**		**-0.64**	**-0.35**	-
Bottom layer	**-0.29**	**0.53**	**-0.63**		**-0.46**	-
Surface layer	-	-	-0.25	**-0.57**		-
Spring river	**0.45**	**0.39**	-	-	-	

Table 4.3: Multiple linear regression analysis of anaerobic community respiration (µmol NH_4^+-N l^{-1} h^{-1}) in relation to environmental and geochemical variables in the Chesapeake Bay. (DS: total dissolved sulfide; DFe: dissolved iron; DMn: dissolved manganese).

# of variables	Temperature (°C)		NO_2^- (µM)		DS (µM)		DFe (µM)		DMn (µM)		intercept		r^2	p
2			0.001	***					0.004	*	0.001		0.38	<0.001
3	0.002		0.036	***					0.004	*	-0.066		0.42	<0.001
4			0.034	***	0.001		-0.003		0.004	*	0.002		0.42	<0.001

Table 4.4: Multiple linear regression analysis of sediment-water NH_4^+ flux (µmol N m^{-2} h^{-1}) in hypoxic and anoxic condition in relation to environmental and geochemical variables in the Chesapeake Bay. (SRP: soluble reactive phosphorus).

# of variables	Temperature (°C)		Salinity		NH_4^+ (µM)		SRP (µM)		Chlorophyll a (mg m-2)		intercept		r^2	p
2	30.5	***							1.6	***	-548.0	*	0.48	<0.01
3	30.9	***			2.4				1.6	**	-592.4	*	0.47	<0.01
4	33.9	**			3.0		-31.5		1.5	**	-623.3	*	0.45	<0.01
5	33.6	**	-2.3		2.7		-27.0		1.5	**	-571.1		0.41	<0.05

Figure Legends

Fig. 4.1: The distribution of average salinity in June and July in Chesapeake Bay mesohaline bottom waters (a) from 1985 to 2011 and (b) during the transect survey conducted in 2010 and 2011. The locations of S1Y10 and S1Y11, provided in Table 4.1, are close to CB5.4. Error bars represent standard errors of (a) the interannual mean for the long-term monitoring data and (b) the mean of vertical measurements.

Fig. 4.2: The contour map of density gradients (unit: kg m^{-4}) continuously measured during the transect survey using an undulating towed vehicle. The upper and lower line represent the boundary of pycnoclines where density gradients exceeds 0.2 kg m^{-4} for the first time.

Fig. 4.3: Vertical profiles of (a) dissolved oxygen and sigma-T, and (b) sigma-T gradients at CB4.3C station in 1992 and 1993. The dashed line in (b) represents a threshold (0.2 kg m^{-4}) for determining the top and bottom depth of pycnoclines.

Fig. 4.4: Average of June and July NH_4^+ concentrations below the pycnocline along the axial transect of the Chesapeake Bay.

Fig. 4.5: Pelagic aerobic and anaerobic respiration measured with the change of DIC was converted into nitrogen equivalent during the transect survey in (a) 2010 and (b) 2011. Empty circles represent sampling depths.

Fig. 4.6: Sediment-water NH_4^+ flux at CB4.3C in different (a) oxic conditions and (b) seasons in the period of 1985-1998 (excluding 1997) and 2010-2011. (Anoxic: <0.2 mg O_2 l^{-1} in overlying waters; hypoxic >0.2 and <2 mg O_2 l^{-1} in overlying waters).

Fig. 4.7: The average estimates of NH_4^+ flux in response to spring river discharge in June and July for (a) anaerobic respiration, (b) sediment-water regeneration, (c) longitudinal dispersion, and (d) vertical dispersion.

Fig. 4.8: Box-and-Whisker plots of NH_4^+ flux for hypoxic volume quartiles at CB4.3C. The fluxes includes (a) anaerobic water column respiration, (b) sediment-water regeneration, (c) longitudinal dispersion, and (d) vertical dispersion. The edges of the box are the 25^{th} and 75^{th} percentiles and the center line is the median. Whiskers at the both ends extend to the most extreme data points not including outliers that are marked with '+'. The asterisk in (d) represents significant difference ($p < 0.05$).

Fig. 4.9: Average NH_4^+ in bottom layers and chlorophyll a (Chl-a) in surface layers in (a, d) summer (June-August), (b, e) fall (September, October), and (c, f) the ratio of value in fall to value in summer. High and low hypoxic represent years with greater and less than 15.2 km^3 maximum hypoxic volume, respectively. Error bars represent standard errors of interannual mean for the long-term monitoring data.

Fig. 4.10: Percentage of phytoplankton carbon biomass contributed by four major phytoplankton groups in different seasons (summer (a, c), fall (b, d)) and stations (CB3.3C (a, b), CB4.3C (c, d)). Error bars represent standard errors of interannual mean. (Diat: diatoms; Dino: dinoflagellates; Cyan: cyanobacteria; Cryp: cryptophytes).

Fig. 4.11: Conceptual diagram of changes in (a, c) NH_4^+ fluxes and phytoplankton composition in response to summer hypoxic conditions in the Chesapeake Bay. Arrow size in (a) and (c) indicates relative magnitude only between the same fluxes (e.g., F_v between low and high hypoxic conditions). The gray scale of arrows indicates significant

(black; F_v) or insignificant difference (gray; R_b, F_s, F_h) in the respective flux between the two hypoxic conditions. The value beside the arrow indicates a flux (μmol N m^{-2} h^{-1}). The bottom panel shows a percent reduction of chlorophyll a (Chl-a) and NH_4^+ concentrations in (b) low and (d) high hypoxic conditions from summer to fall. The size of circles in summer is same, while that in fall is proportional to the percent reduction of summer concentrations. (R_b: depth-integrated anaerobic NH_4^+ remineralization; F_s: sediment-water NH_4^+ flux; F_v: vertical NH_4^+ dispersion; F_h: longitudinal NH_4^+ dispersion).

Figures

Fig. 4.1

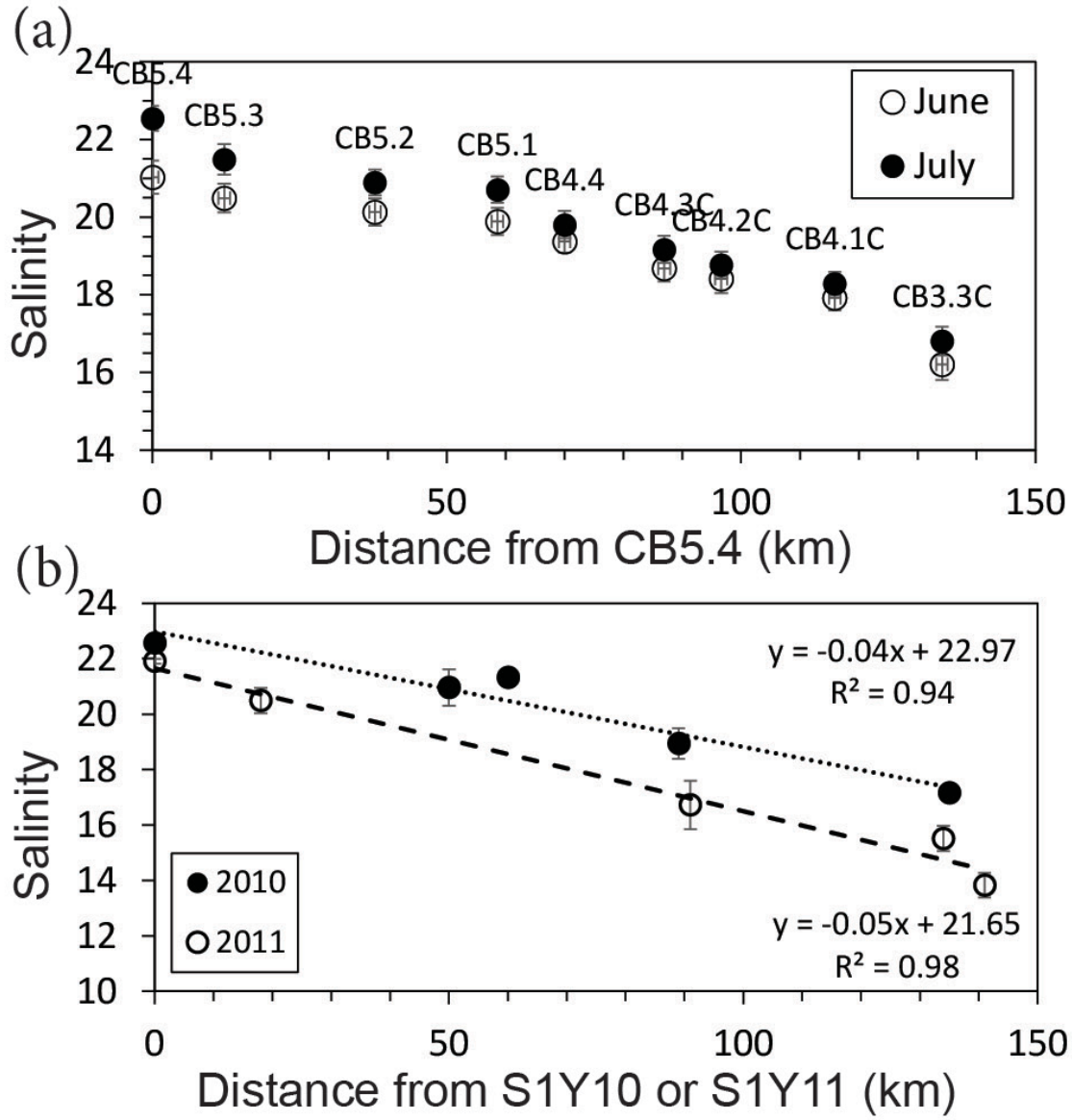

Fig. 4.2

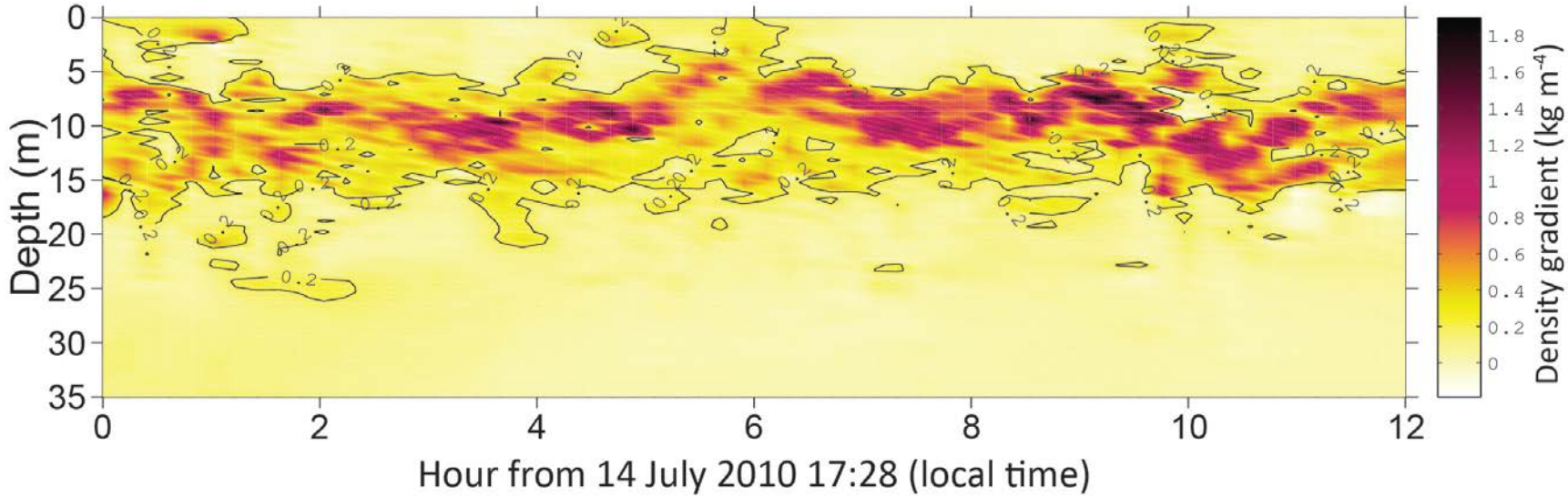
Depth (m)
0
5
10
15
20
25
30
35
0
2
4
6
8
10
12
Hour from 14 July 2010 17:28 (local time)
Density gradient (kg m-4)
1.8
1.6
1.4
1.2
1
0.8
0.6
0.4
0.2
0

Fig. 4.3

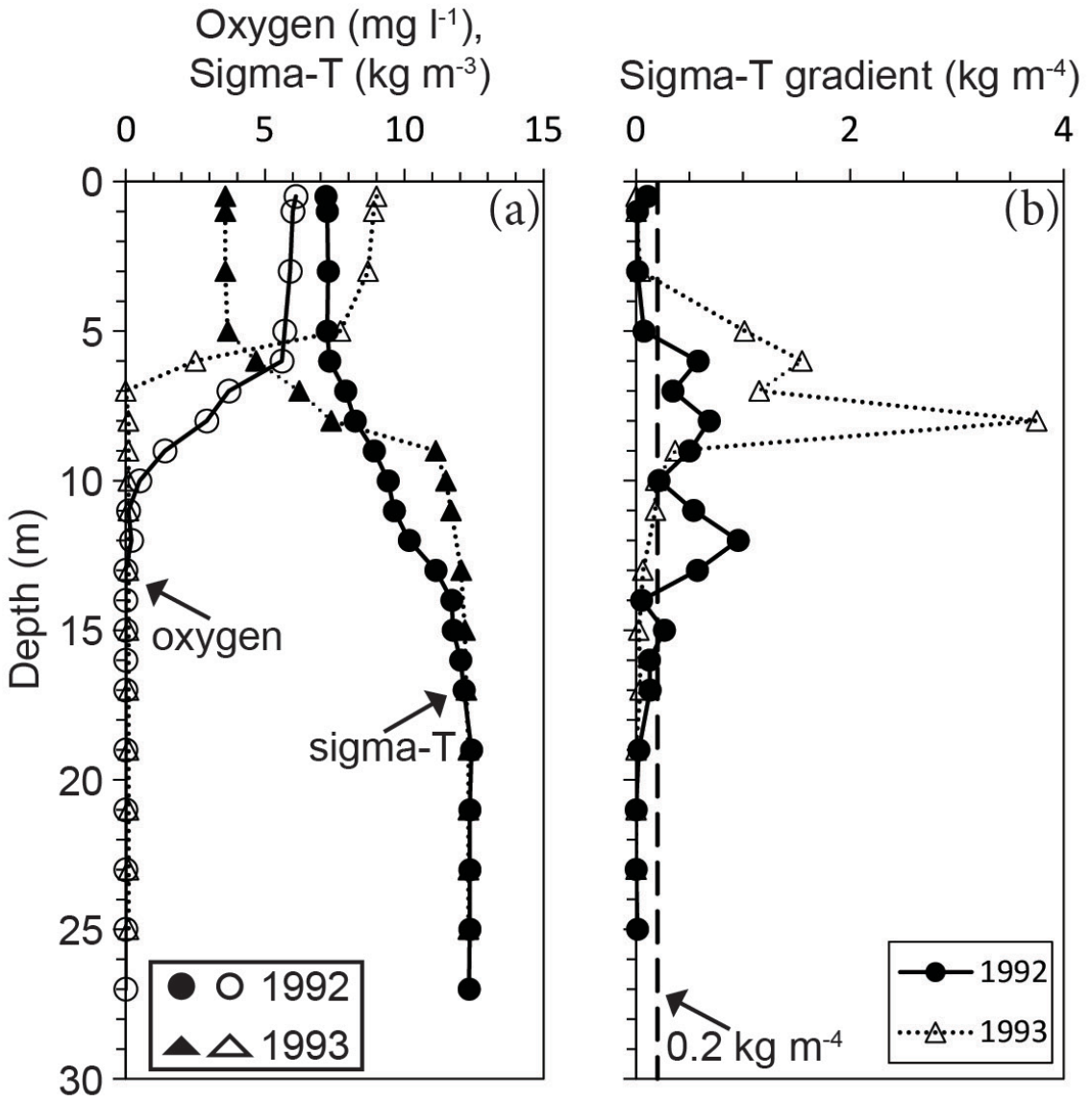
Oxygen (mg l-1),
Sigma-T (kg m-3)
0
5
10
15
Depth (m)
(a)
oxygen
sigma-T
1992
1993
Sigma-T gradient (kg m-4)
0
2
4
(b)
0.2 kg m-4
1992
1993

Fig. 4.4

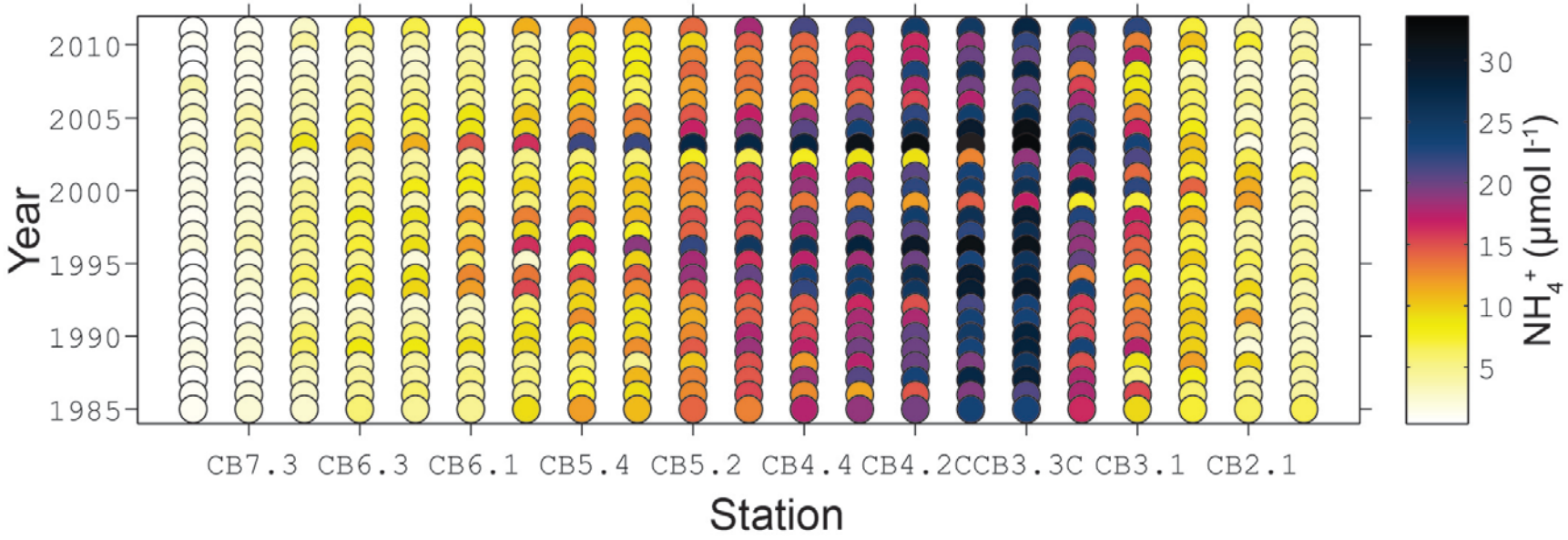
Year
2010
2005
2000
1995
1990
1985
CB7.3 CB6.3 CB6.1 CB5.4 CB5.2 CB4.4 CB4.2C CB3.3C CB3.1 CB2.1
Station
30
25
20
15
10
5
NH4+ (µmol l-1)

Fig. 4.5

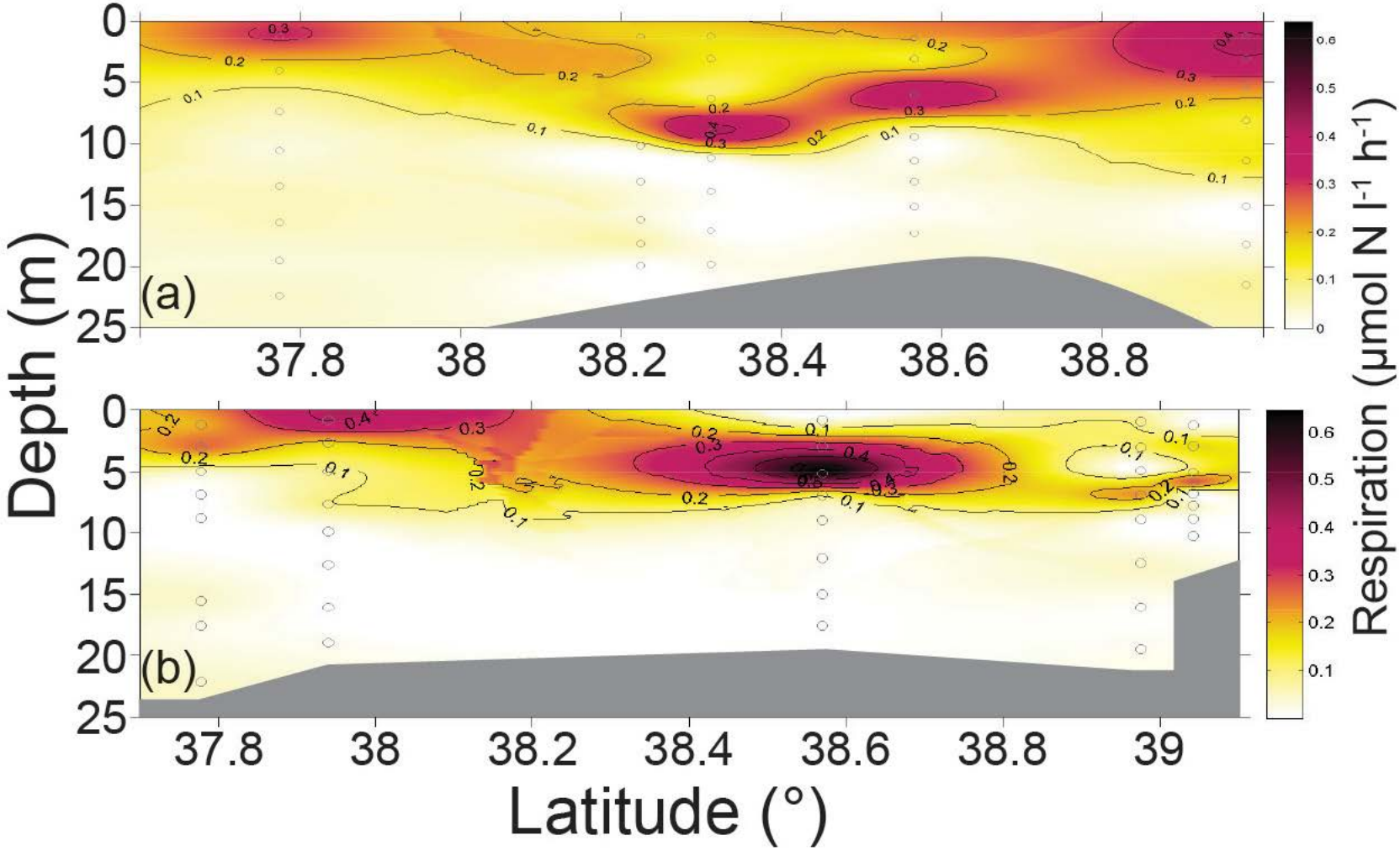
Depth (m)
0
5
10
15
20
25
(a)
(b)
37.8
38
38.2
38.4
38.6
38.8
39
Latitude (°)
Respiration (µmol N l-1 h-1)
0.6
0.5
0.4
0.3
0.2
0.1
0

Fig. 4.6

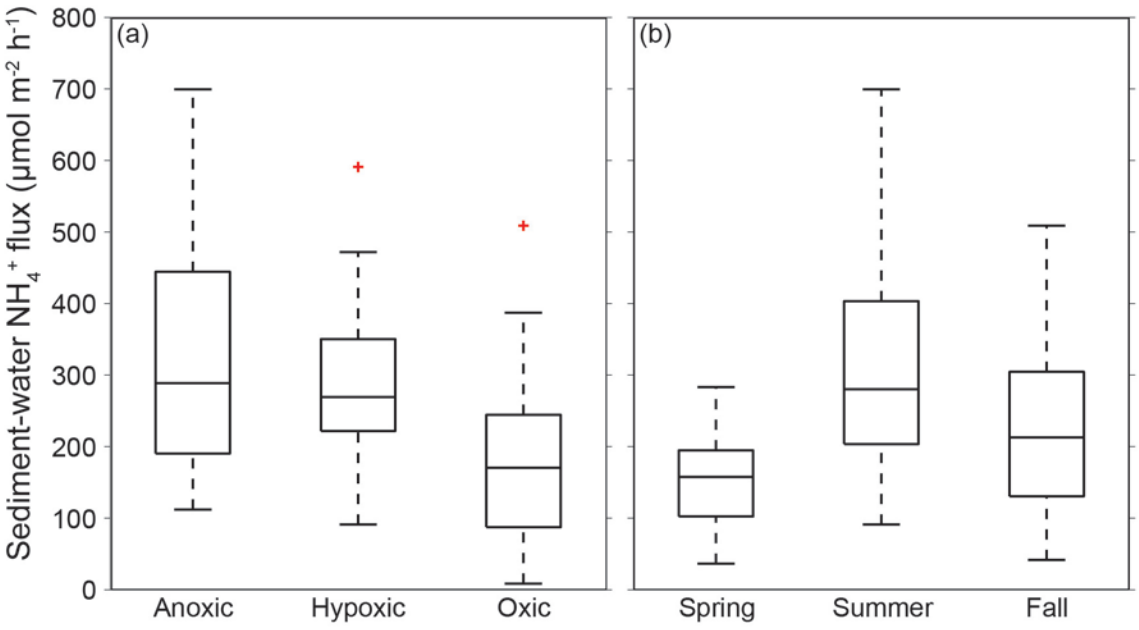
Sediment-water NH_4^+ flux (μmol m^{-2} h^{-1})
800
700
600
500
400
300
200
100
0
(a)
(b)
Anoxic
Hypoxic
Oxic
Spring
Summer
Fall

Fig. 4.7

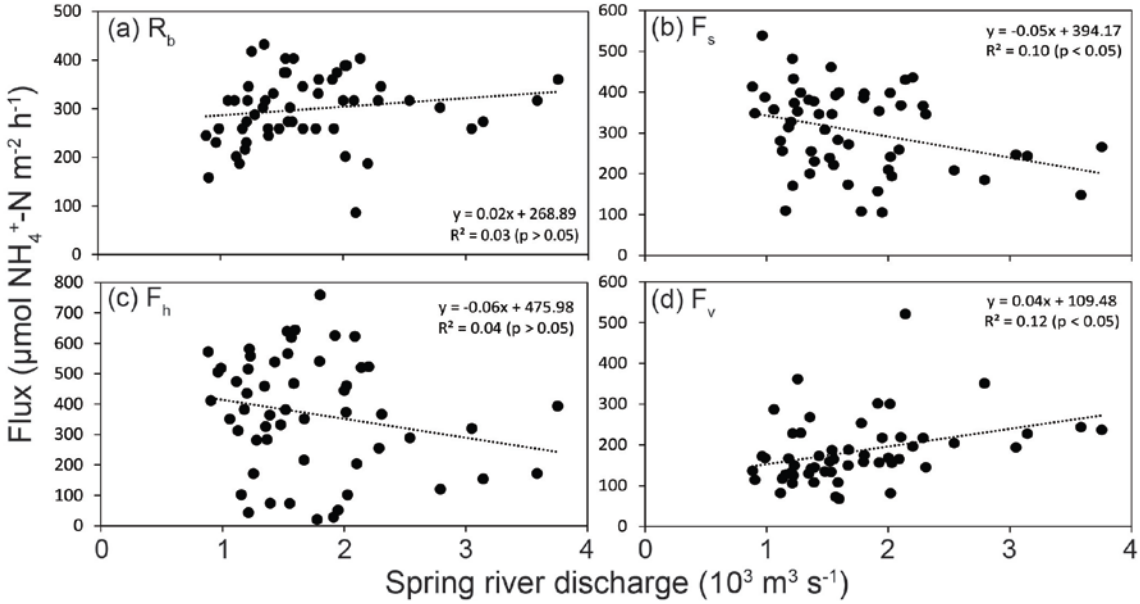
(a) R_b
y = 0.02x + 268.89
R^2 = 0.03 (p > 0.05)
(b) F_s
y = -0.05x + 394.17
R^2 = 0.10 (p < 0.05)
(c) F_h
y = -0.06x + 475.98
R^2 = 0.04 (p > 0.05)
(d) F_v
y = 0.04x + 109.48
R^2 = 0.12 (p < 0.05)
Flux (μmol NH_4^+-N m^{-2} h^{-1})
Spring river discharge (10^3 m^3 s^{-1})

Fig. 4.8

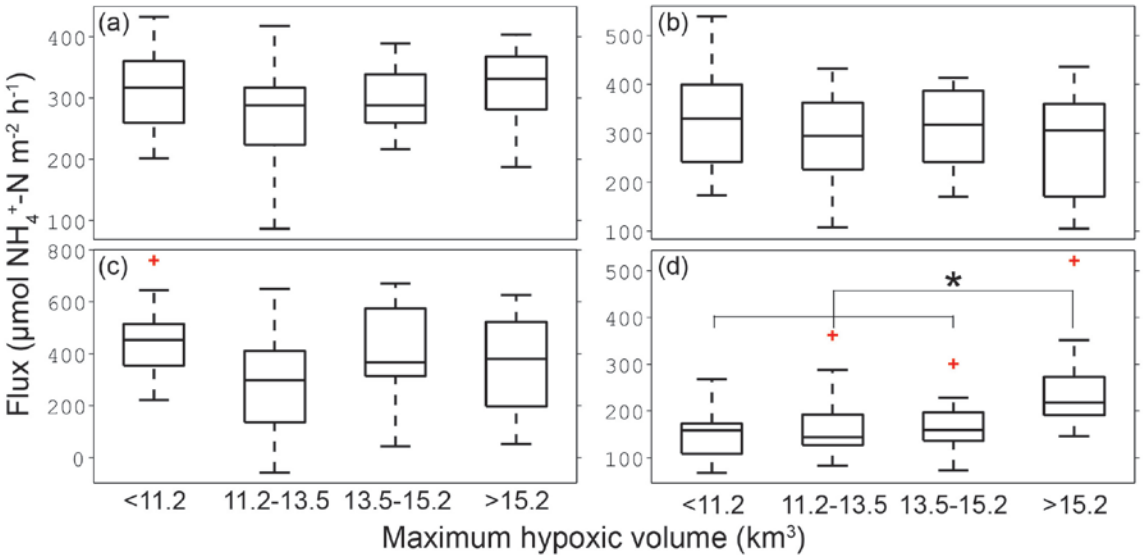
(a)
(b)
(c)
(d)
Flux (μmol NH4+-N m-2 h-1)
<11.2
11.2-13.5
13.5-15.2
>15.2
Maximum hypoxic volume (km3)
*

Fig. 4.9

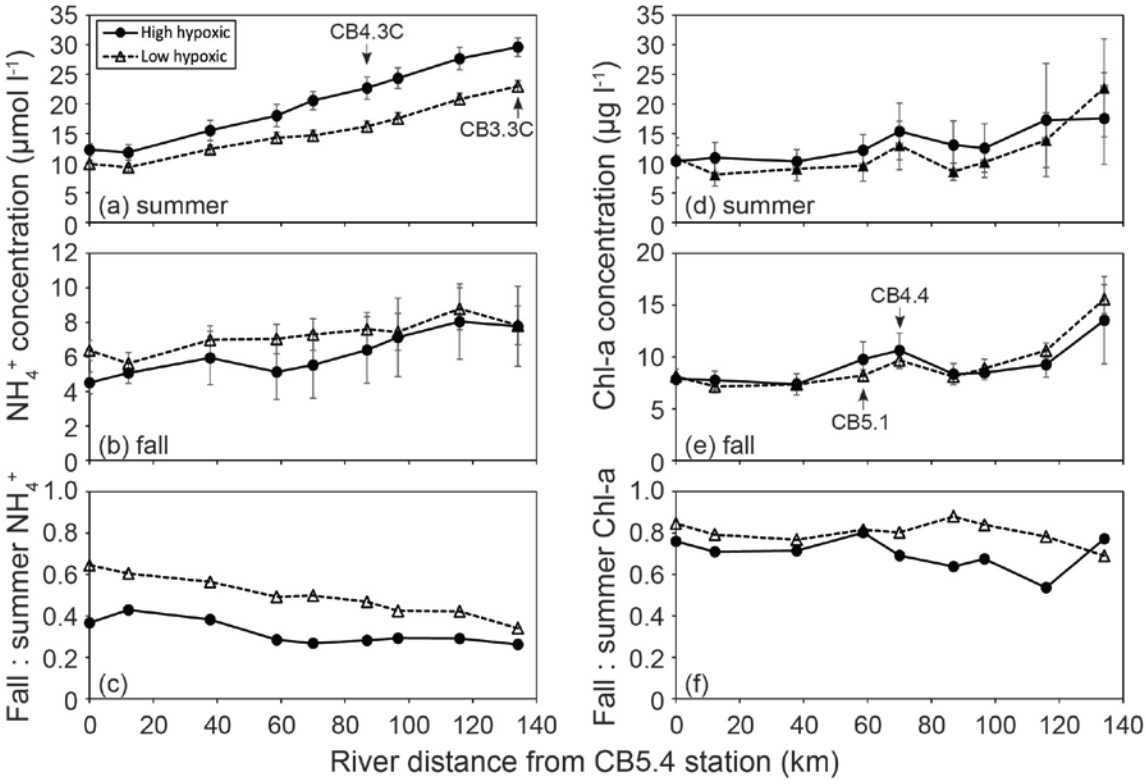
High hypoxic
Low hypoxic
CB4.3C
CB3.3C
(a) summer
(b) fall
(c)
(d) summer
(e) fall
(f)
CB4.4
CB5.1
NH4+ concentration (µmol l-1)
Fall : summer NH4+
Chl-a concentration (µg l-1)
Fall : summer Chl-a
River distance from CB5.4 station (km)

Fig. 4.10

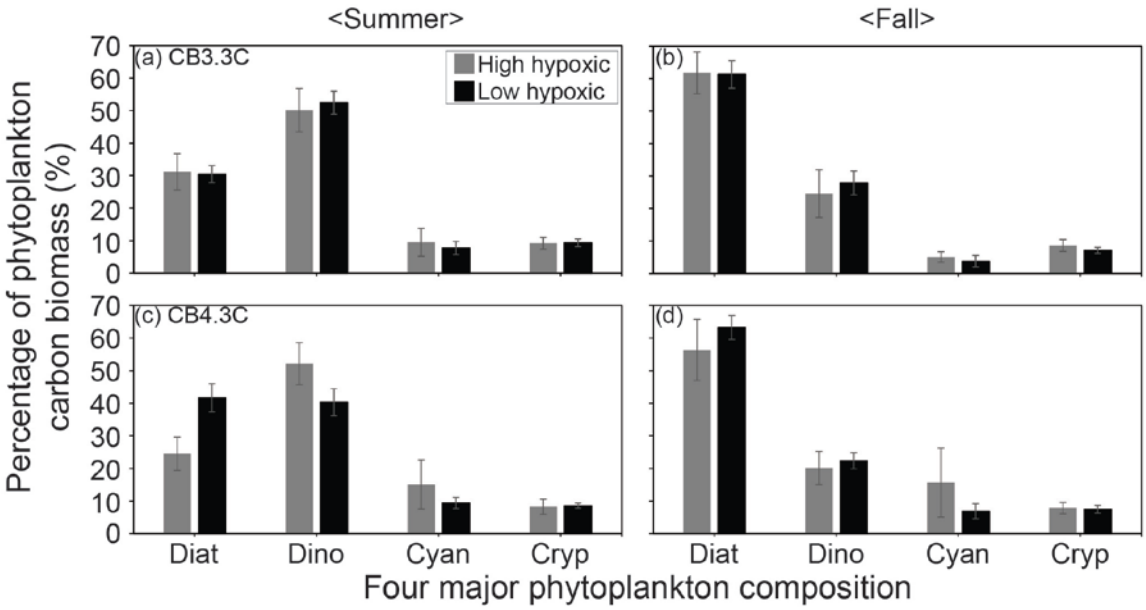
<Summer>
<Fall>
(a) CB3.3C
High hypoxic
Low hypoxic
(b)
(c) CB4.3C
(d)
Percentage of phytoplankton carbon biomass (%)
0
10
20
30
40
50
60
70
Diat
Dino
Cyan
Cryp
Four major phytoplankton composition

Fig. 4.11

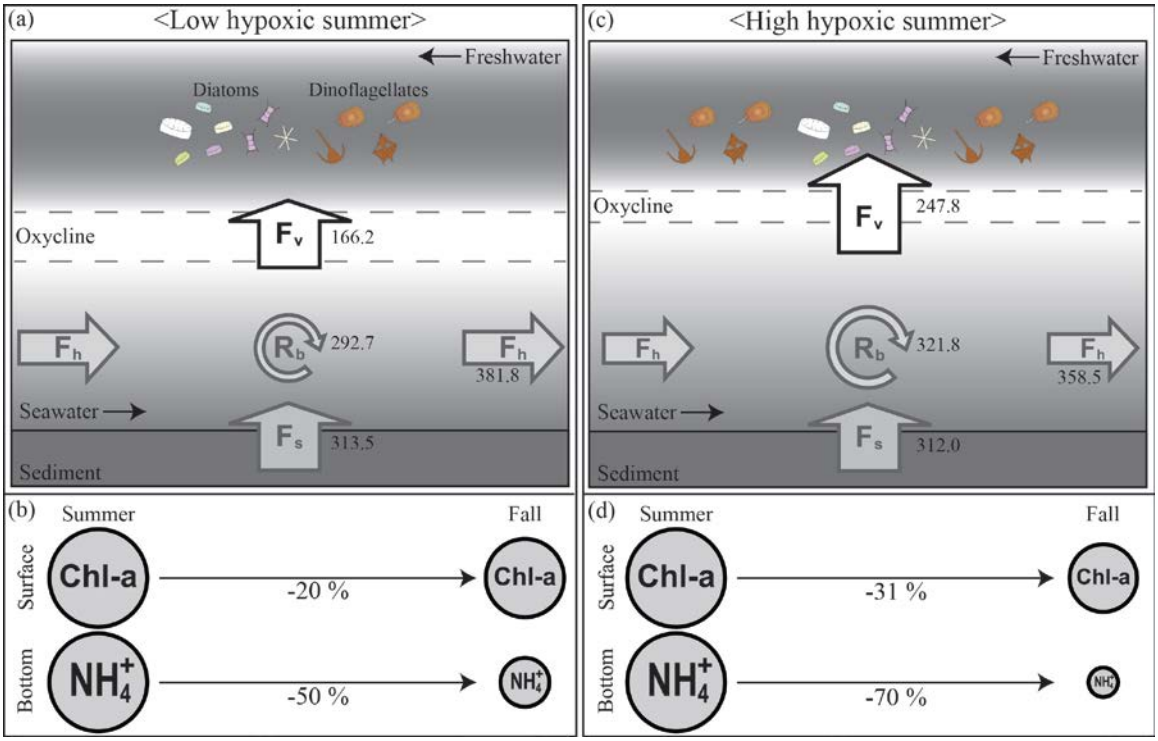
(a)
<Low hypoxic summer>
Freshwater
Diatoms
Dinoflagellates
Oxycline
F_v
166.2
F_h
R_b
292.7
F_h
381.8
Seawater
F_s
313.5
Sediment
(c)
<High hypoxic summer>
Freshwater
Oxycline
F_v
247.8
F_h
R_b
321.8
F_h
358.5
Seawater
F_s
312.0
Sediment
(b)
Summer
Fall
Surface
Chl-a
-20 %
Chl-a
Bottom
NH_4^+
-50 %
NH_4^+
(d)
Summer
Fall
Surface
Chl-a
-31 %
Chl-a
Bottom
NH_4^+
-70 %
NH_4^+

Chapter 5: Summary

Summary

Dissolved Inorganic Carbon as a Tool for Determining Respiration

The first application of DIC-based metabolic measures in the Chesapeake Bay was successfully carried out for an investigation of metabolic processes in both pelagic and benthic ecosystems. Due to the mixing of fresh water and seawater, DIC concentration ranged widely and was significantly correlated with salinity. At first the strong correlation appears to result from a conservative mixing between surface and bottom waters. But the relationship in both years was best fitted (i.e., highest coefficient of determination) with a second degree polynomial function; the relationship suggests the strong influence of biogeochemical processes in the middle of water column where the steepest gradient of geochemical compounds was usually observed. In addition, simultaneous incubations of DIC and DO samples under dark conditions resulted in higher respiration quotients in hypoxic (1.5) than oxic (1.1) water columns. Thus, the elevated DIC production relative to DO consumption in low oxic conditions could not be captured with DO incubation experiments, subsequently underestimating microaerobic metabolism by 50 %.

Transition of Terminal Electron Acceptors

To examine the contribution of different electron acceptors on community metabolism, a spatiotemporal transition of electron acceptors was either measured or estimated as part of this research. Contrary to DO and SO_4^{2-} that are dominant electron acceptors during oxic and anoxic conditions, respectively, other intermediates, such as NO_3^-, Mn(IV), Fe(III), are used and recycled by anaerobic processes. Although coupled geochemical analyses and genomic measurements may be required to identify all possible

processes, a flux of electron acceptors/donors across oxyclines can provide potential estimates of individual processes. The downward and upward flux of electron acceptors and donors, respectively, were further converted into electron equivalents to evaluate a redox balance (i.e., the flux of electron donors – acceptors). For example, net negative balances suggest higher fluxes of electron acceptors than donors, consistently resulting from the excess of DO fluxes throughout the present study. The net flux, however, was in near balance in summer, suggesting an increase of electron accepting processes, such as chemolithotrophic metabolism, utilizing DO as an oxidant. Such information is extremely useful if we are to understand the effect of stratification on community metabolism in stratified ecosystems where *in situ* incubation experiment is restricted.

Variability in Community Respiration

Despite large interannual differences in environmental conditions during the studied period, the spatiotemporal pattern of geochemical conditions was generally consistent. For example, the development of hypoxia in early spring was coincident with a decrease of oxidized redox-active species and followed by an increase of reduced forms, which were in turn reoxidized by mixing due to strong wind events in fall. This environmental setup appeared to exert a strong influence on pelagic and benthic biological processes because the transition of oxic and redox conditions was reflected in the availability of electron acceptors. Despite the interannual similarity in environmental conditions, however, the magnitude and variability in microbial respiration was different from those reported in previous studies and between studied years. Several studies reported temporal and vertical variations of respiration in surface and bottom waters of Chesapeake Bay, assuming a constant rate in each layer (Sampou and Kemp 1994; Smith

and Kemp 1995, 2001). In the present study, however, high vertical variability in aerobic respiration rates were consistently observed and exemplified by high rates near the top of oxyclines in summer. The zone of maximum respiration was usually coincident with the location of the steepest gradient of chemical compounds, such as ammonium; however, the zone was usually located above sulfidic waters. The consistent observation of subsurface maximum respiration strongly suggests that highly productive microbial food webs are developed due to the coexistence of oxidants and reduced compounds. In addition, the vertical variability in respiration was strongly associated with the degree of stratification; the depth of highest median respiration was coincident with that of maximum stratification (i.e., highest buoyancy frequency). The result indicates that the estimation of more accurate net ecosystem metabolism should take into consideration of the highly variable nature of community metabolism associated with both chemical gradients and stratification.

Variability of community respiration in estuarine systems is often associated with temperature and substrate supply due to a positive effect of temperature on cellular respiration fuelled by a decomposition of organic substrates (Pomeroy and Wiebe 2001; Apple et al. 2006). This positive relationship, however, appears to be limited for aerobic respiration and benthic DIC flux because there was no significant relationship between anaerobic respiration and both temperature and phytoplankton pigments. Similar results have been reported in estuarine sediments where biological processes strongly influence aerobic degradation of organic matter, while the combination of biological and geochemical processes control anaerobic degradation (Sun et al. 1993; Harvey et al. 1995). Thus, the insignificant association of anaerobic respiration with temperature and

organic matter is probably attributed to the mixed effect of biogeochemical processes in the absence of DO. Additionally, the present study provides evidence that a gradient of dissolved iron and manganese concentrations exerted a significant influence on anaerobic respiration; the results suggested higher variability in anaerobic respiration in both places and times where a transition of anoxic electron acceptors (e.g., iron, manganese) occurs before and after the accumulation of total dissolved sulfide. Further, the variability would have been caused by the adaptability of microbial community composition which appears to change dramatically during anoxic to sulfidic transitions (Brune et al. 2000; Crump et al. 2007; Hewson et al. 2014). Thus, prediction of the pattern and magnitude of anaerobic respiration needs to take into consideration the spatiotemporal variability in either redox conditions or microbial composition.

Variability in Autotrophic Production

Another important finding of the present study is that CO_2 fixation under dark conditions was elevated across the steepest geochemical gradients and in experimental incubations of anoxic waters with augmentation of terminal electron acceptors. The elevated fixation was observed with DO augmentation regardless of oxic conditions, while that was only observed with the augmentation of Mn(IV) and Fe(III) in sulfidic bottom waters. The result provides evidence that microbial phylogenetic and functional composition differ significantly across geochemical water properties, offering an explanation for a dramatic change in microbial community composition from anoxic to sulfidic condition (Crump et al. 2007).

Although four major taxonomic groups of phytoplankton (i.e., diatoms, dinoflagellates, cryptophytes, cyanobacteria) influence the variability in photoautotrophic

production (Adolf et al. 2006b), the close proximity of redoxclines from bottom euphotic depths could have facilitated the growth of anoxygenic photoautotrophs. My research employing inhibition of oxygenic photoautotrophic growth provides evidence that anoxygenic production rates were as high as oxygenic production near the bottom of redoxclines in summer. The elevated anoxygenic growth may have exerted a positive impact on deep microbial food webs by providing autochthonous organic substrates for heterotrophs. However, cyanobacterial anoxygenic processes have also been reported in reduced conditions (Jørgensen 1982), challenging the conclusion of the present study that anoxygenic photoautotrophic production can be an important source of organic matter. Thus, an incorporation of the experimental design with genomic measurements will be needed for determining the impact of anoxygenic photoautotrophs on ecosystem metabolism.

Although chemoautotrophic production has been considered as an important source of organic substrates for deep microbial food webs in other ecosystems (e.g., Taylor et al. 2001; García-Cantizano et al. 2005), little is known regarding the contribution, distribution, and function of the metabolism on ecosystem production. In addition, most previous studies using changes in DO concentrations as an index of both primary production and respiration could not detect chemoautotrophic metabolism without coupled genomic measurements. Thus, my research provides crucial evidence for chemoautotrophic activity and offers an explanation for occasional decreases of DIC during experimental incubations of anoxic waters and at times of elevated NO_2^- concentrations throughout water columns in early fall.

There appears much to learn about the distribution of chemoautotrophs in estuarine ecosystems because of the ubiquitous nature of oxic/anoxic interfaces in water column (Taylor et al. 2001), sediment (Mayer et al. 1995), and organic particle aggregate environments (Casamayor et al. 2001). Since hypoxia is an annually recurring environmental pattern, it is likely that there is a guild of pelagic chemoautotrophs shifting phylogenetic and functional composition according to thermodynamic energy requirements. Consistent with the results of community respiration and anoxygenic photoautotrophic production, a strong association of chemoautotrophic CO_2 fixation with the depth of oxyclines supports the idea that elevated chemoautotrophic metabolism likely results from the coexistence of oxidants and reduced compounds. Although vertical profiles of redox-active species differed among spatiotemporal surveys, chemoautotrophic production was significantly correlated with gradients of density, DO, total dissolved sulfide, iron, and manganese. Thus, the succession of chemoautotrophic metabolism is likely determined by metabolic adaptability to the transition of terminal electron acceptors.

The estimation of the total carbon budget, combining the total gain and loss of inorganic carbon, revealed that chemoautotrophs were insignificant influence because of the dominance of phytoplankton production and aerobic respiration. In particular, chemoautotrophic production was ~4.5-fold smaller than bacterial production and an order of magnitude smaller than gross phytoplankton production in summer. In comparison, significantly higher contributions of chemoautotrophy in other ecosystems (e.g., >30 %; Taylor et al. 2001; García-Cantizano et al. 2005) suggest that failing to consider chemoautotrophic primary production could result in incomplete organic carbon

budgets. Thus, understanding diverse microbial metabolism in the context of environmental conditions is essential especially in stratified hypoxic ecosystems because of a strong influence of environmental, physical, and geochemical characteristics on the formation of optimal growth conditions for aerobes, anaerobes, and microaerobes (Cloern et al. 1983; Taylor et al. 2001; Camacho et al. 2001).

Variability in Ammonium Fluxes

Mass balance analysis of ammonium budgets, consisting of anaerobic remineralization, sediment-water flux, vertical, and longitudinal dispersion of ammonium, appears to be in near balance; these data suggest a strong interdependence between biological and physical fluxes. Interannual variability in the contribution of biophysical fluxes caused significant differences in ammonium fluxes and budgets. The comparison of ammonium fluxes between high and low hypoxic years revealed that elevated vertical ammonium dispersion in wet spring and high hypoxic conditions caused elevated community metabolism near the upper boundary of pycnoclines. Although the effect of vertical ammonium dispersion on other microbial processes, such as nitrification, was not identified as part of this research, it is likely that vertical transport of bottom water chemical constituents would elevate the activity and diversity of other microbial processes.

Conclusion

The research described in this dissertation explored the spatiotemporal variability of microbial metabolism that controlled the cycling of estuarine carbon, nitrogen, and other redox-active species in relation to the transition of oxic conditions. My dissertation

work, conducted in pelagic and benthic systems of the mesohaline Chesapeake Bay, revealed that the variability is exceptionally high in the vicinity of oxyclines coincident with the steepest gradient of most geochemical compounds during seasonal hypoxia. The present study includes an observational and experimental approach to estimate microbially mediated processes as well as an incorporation of monitoring datasets to facilitate a comprehensive assessment of ecosystem-level metabolism. In particular, simultaneous assessments of changes in dissolved inorganic carbon (DIC) and oxygen (DO) concentration under dark conditions, and their relationships (i.e., respiration quotient), offers a way to investigate the relative contribution of aerobes and anaerobes on community respiration (Chapter 2). In addition, the present study includes a determination of various community metabolism in the oxycline based on estimates of both *in situ* experimental incubations and vertical profiles of microbially-mediated chemical compounds (Chapter 2, 3). When high-resolution of biogeochemical analyses were combined with long-term monitoring dataset of physical and geochemical variables, a comprehensive understanding of nutrient recycling influenced by hypoxia-related variables and stratification was possible (Chapter 4). Finally, this research has revealed highly dynamic microbial processes across redox gradients that will encourage further study of oxic/anoxic interfaces for a broad range of research topics, such as the diversity of microbial composition, distribution, functions, and metabolism.

Suggestions for Future Research

- Chemolithoautotrophic metabolism in the oligohaline region where estuarine turbidity maximum is consistently observed
- Metabolic efficiency of chemolithoautotrophic metabolism (i.e., yield factor)

- Contribution of cyanobacterial anoxygenic photosynthesis on total anoxygenic photosynthesis during seasonal hypoxia
- Role of interconnected processes in oxyclines on ecosystem production (e.g., nitrification, denitrification, electron shuttle using manganese)
- Fate of regenerated NH_4^+ in the upper mesohaline Chesapeake Bay when isopycnals turn upward due to large water column depth changes
- Biogeochemical fate of newly oxidized nitrogen (e.g., NO_2^-) after fall turnover
- More work on structure of microbial communities in conjunction with rate measurements

Appendix A: Assessment of centimeter-scale heterogeneities in microbial metabolism and geochemical properties in the oxic/anoxic interface

In stratified water columns during seasonal hypoxia, the zone of elevated microbial productivity and metabolic diversity was consistently observed across dissolved oxygen (DO) and redox gradients. I hypothesized that the coexistence of oxidants and reduced compounds is a fundamental mechanism developing biologically productive zone in the region (Chapter 2, 3). However, the thickness of oxyclines is usually <3 m in shallow estuaries and many conventional hydrographic bottles (e.g., Niskin bottles attached to a metal frame) are not designed for collecting samples in less than a meter scale.

To maximize the observation of various microbial metabolism in the oxic/anoxic interface, I collected samples within oxyclines using two high-resolution vertical sampling devices (Fig. A.1). The design of first sampler is a modified version of a 'syringe system' shown in Pedrós-Alió et al. (1993) to make it more stable by attaching a rudder and weight (Fig. A.1a). Duplicated 250 ml syringes were vertically fixed to a frame, and each syringe plunger was connected to a rotatable metal rod with string. To prevent bubble forming during syringe pumping, I used a well-pump motor connected to the rod to ensure slow and constant pumping speed (4 ml s^{-1}). Also a YSI sonde was attached (6600 V2) at the top sampling depth to monitor water properties (i.e., depth, DO, salinity) with a data logger (650 MDS, YSI). When the top of the sampler was positioned at 2 mg O_2 l^{-1} isopleth, syringes were filled simultaneously. Further, I designed another sampler equipped with a multi-channel peristaltic pump to draw water from eight depths across a 3 m range (Fig. A.1b). The new device can be operated by two people and has an advantage of continuous pumping up to 15 m deep. A total of eight surveys were

conducted in summer 2011-2013, and a series of metabolic and geochemical measurements were conducted similar to what I had reported in Chapter 3.

The results suggest that in less than a meter scale that metabolic processes, including community respiration and chemoautotrophic primary production in dark (DarkPP), varied vertically across DO gradients. Although DarkPP was consistently lower than community respiration, the vertical pattern of the two processes was somewhat similar when high total dissolved sulfide ($[S^{2-}] + [HS^{-}] + [H_2S]$) concentrations were measured below oxyclines (Fig. A.2a, b), suggesting that DarkPP can potentially serve as an energy source. This new production may provide labile organic carbon in unlit water columns and enhance heterotrophic metabolism.

Figures

Fig. A.1: High-resolution vertical sampling device made of (a) metal frame with syringes and (b) PVC pipe equipped with a multi-channel peristaltic pump.

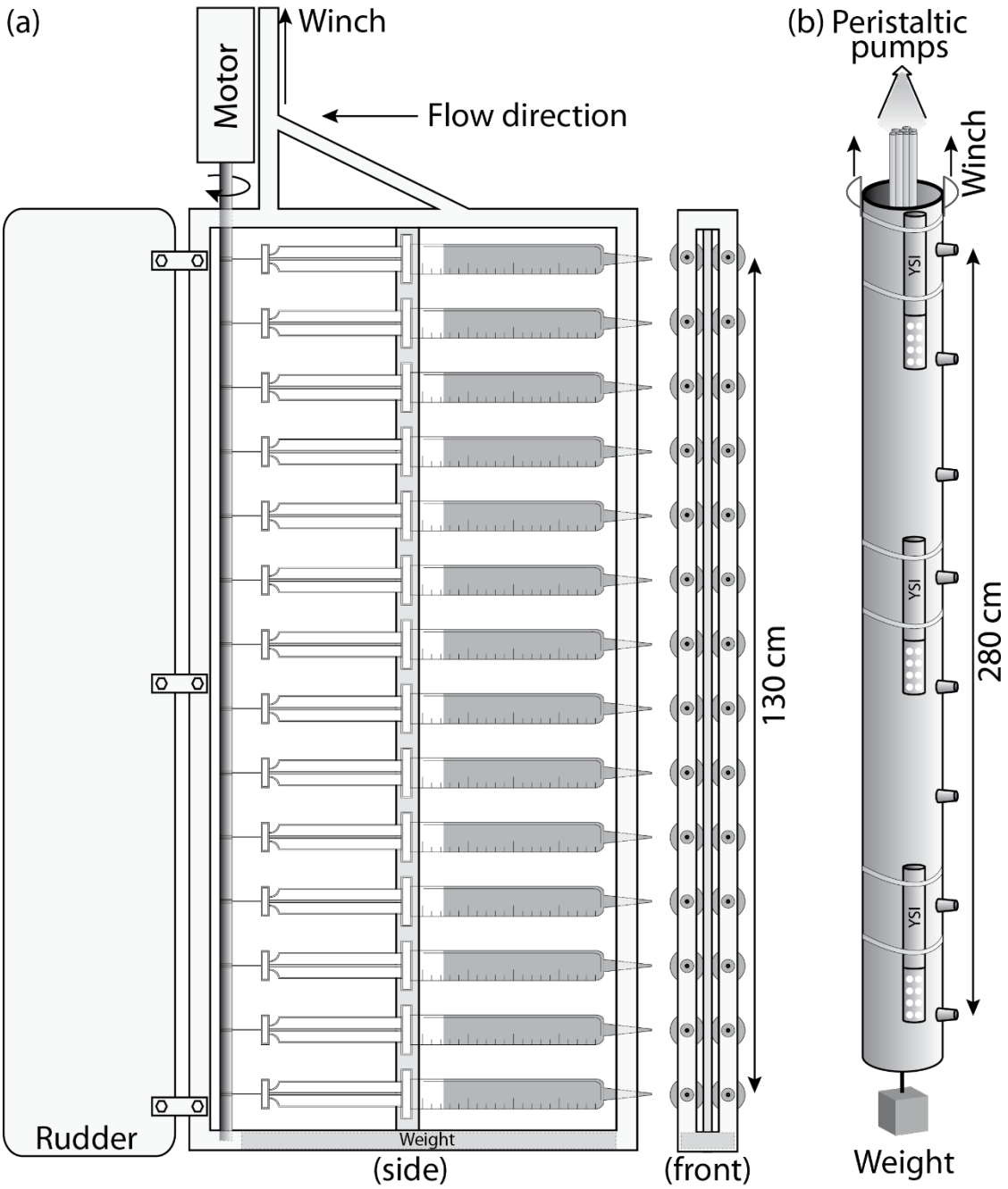

Fig. A.2: Dissolved oxygen concentration and microbial metabolic results in water samples collected within oxyclines.

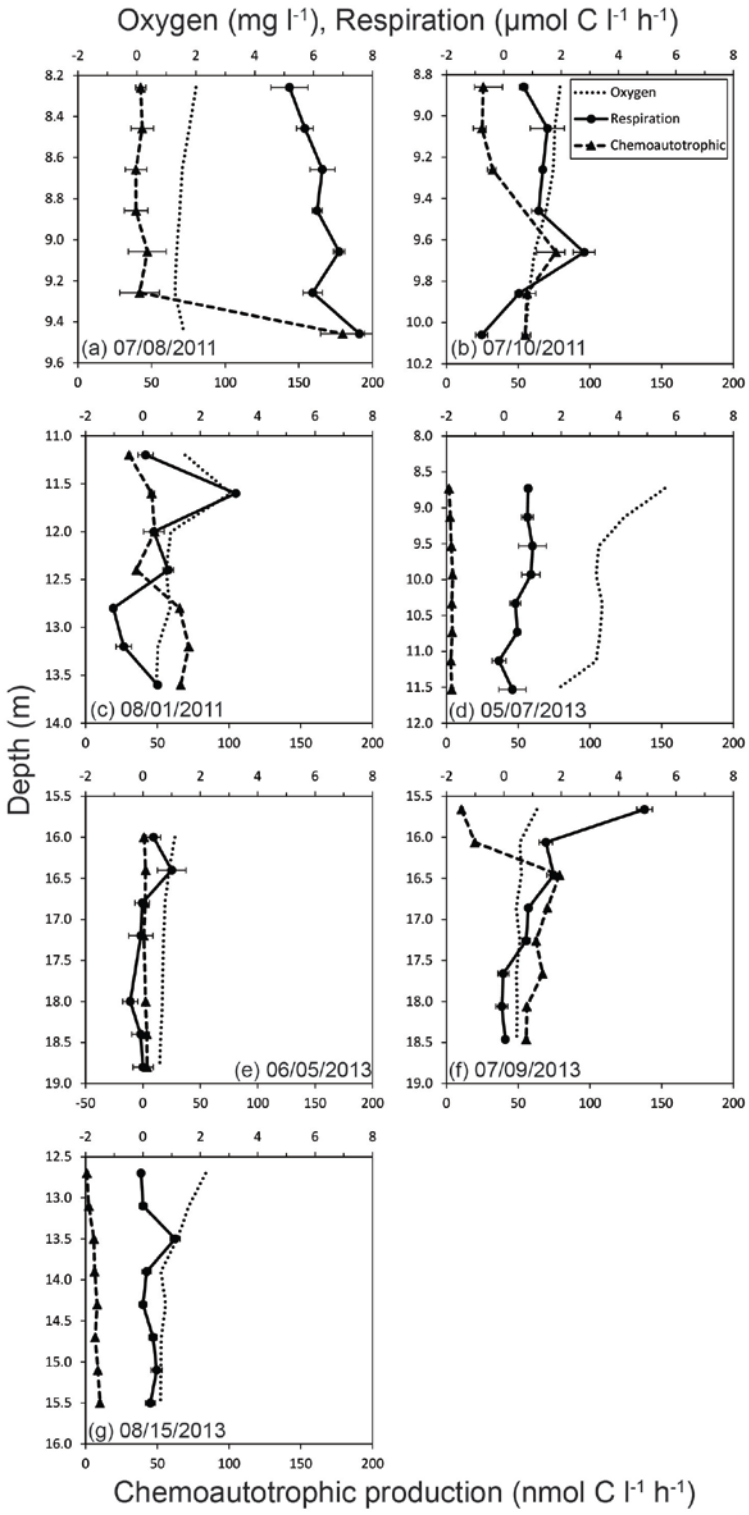

Appendix B: Determination of potential aerobic and anaerobic metabolism in experimental incubations with augmentation of terminal electron acceptors

Introduction

Upward and downward non-advective exchange is an important physical mechanism causing vertical dispersion of chemical compounds across pycnoclines in stratified water columns (Hagy 2002). The vertical flux is strongly associated with a concentration gradient across the pycnocline (Chapter 4) and may be a fundamental physical mechanism causing high chemoautotrophic and anoxygenic photoautotrophic production in the vicinity of oxyclines (Chapter 3). Chemoautotrophy is slow process because of the high energy requirement for the fixation of dissolved inorganic carbon taking place with the oxidation of a disproportionally large amount of reduced substrate. Thus, it is likely that the processes would be limited by the flux of terminal electron acceptors (TEA) in deep water column environments because the absence of TEA. To examine potential chemoautotrophic processes, collected water and sediment samples from the deepest portion of main stem of Chesapeake Bay were augmented with a series of TEA.

Materials and Methods

I used three methods to examine the effect of TEA augmentation: I injected a series of TEA into 300 ml biochemical oxygen demand (BOD) bottles, five liter gas-tight laminate bags, and sediment cores. First, water samples from sulfidic and anoxic environments were collected into BOD bottles and augmented with dissolved oxygen (DO) to near-saturation concentrations, while nitrate, Mn(IV), and Fe(III) were augmented to a final concentration of 20 μmol l^{-1}. The samples were incubated in a

temperature controlled bath (±1 °C in situ temperatures) for 24 and 4 h for community respiration and dark CO_2 fixation experiment, respectively.

I also used gas-tight bags (PMC Inc.) to simulate long-term changes of microbial metabolism. The experiment was a part of interdisciplinary projects combining metatranscriptome data analysis by colleagues at Cornell University to examine the change of active and abundant microbial community along with changes in the concentration of microbially mediated chemical compounds. Similar application of a gas-tight bag has been made for various experiments from bacterioplankton metabolism to sediment processes using a series of dissolved gas and inorganic compounds (e.g., Kruse 1993; Carlson et al. 1999; Hansen et al. 2000). The gas-tight laminate bag consists of a layer of polyethylene, aluminum foil, and Mylar film from inside to outside and has a total thickness of 127 μm with a polyethylene tube (inner diameter: 2.3mm, outer diameter: 3.9mm, wall thickness: 0.7mm) sealed into inner polyethylene layer of the bag. Water samples were collected at the Horn Point Laboratory dock in February 2013 and analyzed for biochemical properties (temperature: 3.3 °C, salinity: 11.3, density: 1006.3 kg m^{-3}, chlorophyll a: 19.4 μg l^{-1}). Bags filled with autoclaved oxic and anoxic water (purged with N_2 gas) had been incubated and monitored for the change of DO for 42 days using membrane inlet mass spectrometry.

I collected sediment cores from the deepest portion of main stem during temporal surveys in 2011 (Chapter 3) and augmented them with 100 μmol l^{-1} of nitrate in overlying waters. A series of fluxes in the treated sediment cores was compared with that in untreated (control) sediment cores.

Results and Discussion

The results of BOD experiments shown in Fig. 2.10 and Fig. B.1 suggest that the augmentation of TEA increased anaerobic respiration (e.g., dissimilatory NO_3^- reduction) and chemoautotrophic fixation. The responses of the bacterioplankton community were different in anoxic and sulfidic conditions, strongly suggesting functional or phylogenetic differences in community composition. Note that elevated chemoautotrophic fixation with augmentation of Mn(IV) and Fe(III) was as high as that with that of DO (Fig. B.1), suggesting high efficiency of metal oxides as electron acceptors (Schippers and Jørgensen 2001; Hulth et al. 2005; Trouwborst et al. 2006).

The long-term incubation experiment of anoxic and oxic water samples with gas-tight bags suggested that samples must be incubated in an anoxic space because non-linear DO changes in a bag incubated in air indicates air contamination across a film of bags (Fig. B.2). I speculated that the initial decrease in DO concentrations could have been caused by microbes located inside bags during manufacturing process rather than microbes originated from water samples. Thus, it is strongly recommended to rinse bags with weak acid or water samples prior to experiments. I also estimated a permeability of gas-tight bags according to Hansen et al. (2000),

$$P = (n \times x)\ (A \times t \times \Delta p)^{-1}$$

where P is a permeability, n is the amount of gas passing through a membrane, A is an area, x is a thickness of the membrane, and Δp is a difference in partial pressure of DO over the membrane. The estimated permeability in my experiment was close to the lower end of previously reported value (4.3×10^{-3} cm^3 cm m^{-2} d^{-1} bar^{-1}) (Hansen et al. 2000), suggesting that DO flux across the membrane is insignificant compared to biological

processes. I had further conducted incubation experiments with augmentation of other electron acceptors and acetate to determine whether microbes were limited by multiple factors. The results of TEA augmentation experiments will be combined with metatranscriptomic analyses to determine the response of microbial community composition and metabolism against changes in geochemical and environmental conditions.

One of most detrimental effects of hypoxia is the loss of nitrogen removal from ecosystem functions. The coupling of nitrification and denitrification is subsequently reduced in hypoxia because of low or absence of NO_3^- (Jenkins and Kemp 1984). The results of NO_3^- augmentation experiment into sediment cores appear to support the idea that NO_3^- limitation exerted significant negative influence on denitrification because the augmentation substantially increased denitrification rates (Fig. B.3e). The highest denitrification rate was measured in late spring taking place with the highest net influx (into sediments) of NOx (NO_2^- + NO_3^-) (Fig. B.3d). To determine the change of denitrification in response to NO_3^- augmentation, I calculated denitrification efficiency according to Eyre and Ferguson (2009):

Denitrification efficiency (%) = N_2 flux / (N_2 flux + NOx flux + NH_4^+ flux) × 100

The comparison of the efficiency before and after the augmentation revealed that the efficiency was increased by 60 % on average, suggesting denitrifying microbes were significantly limited by the lack of NO_3^-. However, denitrification rates were not enhanced in July and August, while the efflux (out of sediments) of ammonium increased exponentially in the same period (Fig. B.3c). The results seem to suggest that

dissimilatory nitrate reduction to ammonium (DNRA) prevailed in late summer because DNRA is energetically favorable under sulfidic condition (Gardner et al. 2006).

I have used different methods to test the effect of TEA limitation on a series of metabolic processes. The results present here support the idea that metabolic responses can be significantly different against the same TEA augmentation because of microbial phylogenetic and functional diversity, that are strongly dependent of environmental conditions (e.g., anoxic vs. sulfidic, early summer vs. late summer).

Figures

Fig. B.1: Augmentation of terminal electron acceptors into anoxic and sulfidic bottom waters was analyzed for cellular CO_2 fixation using radiolabeled $NaH^{14}CO_3$.

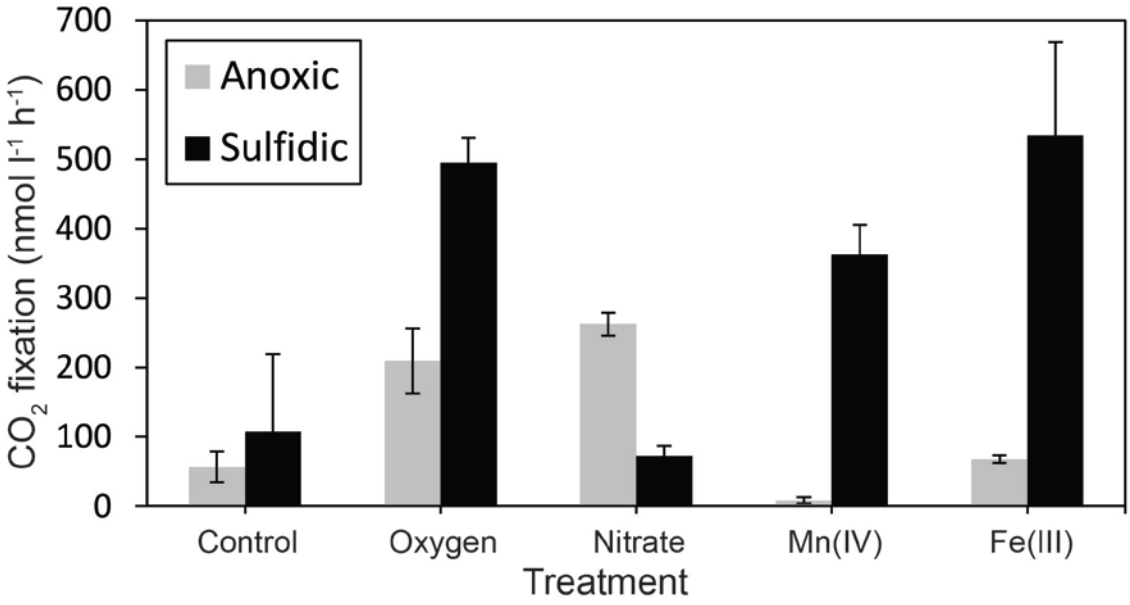

Fig. B.2: Results of long-term incubation experiments using gas-tight bags.

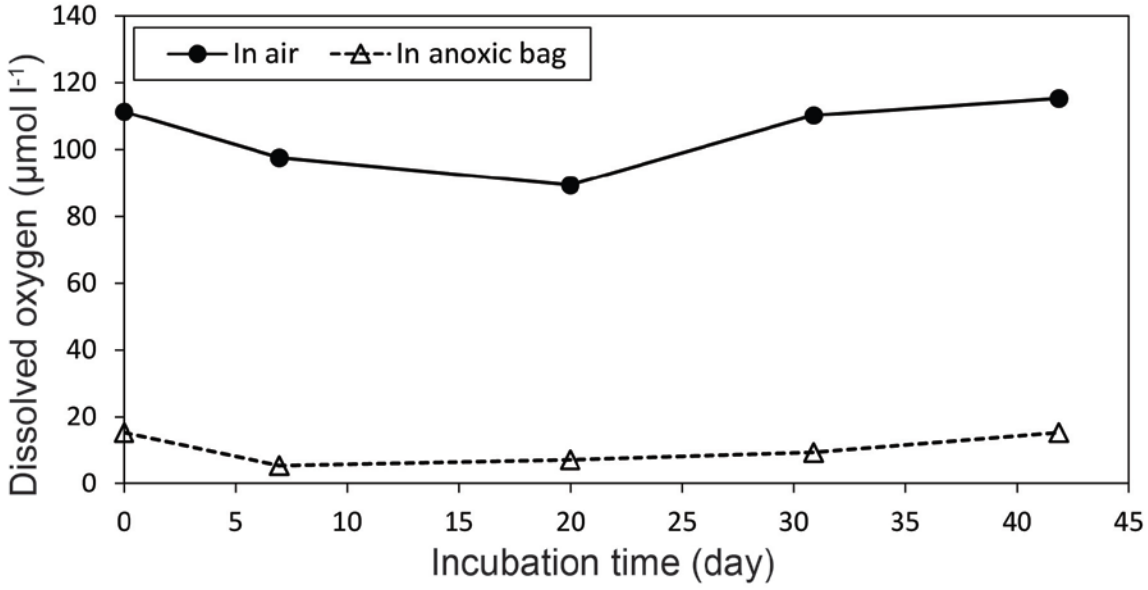

Fig. B.3: Sediment-water fluxes of a series of chemical compounds without (gray bars) and with (black bars) augmentation of 100 µmol l^{-1} of nitrate at a final concentration in overlying waters.

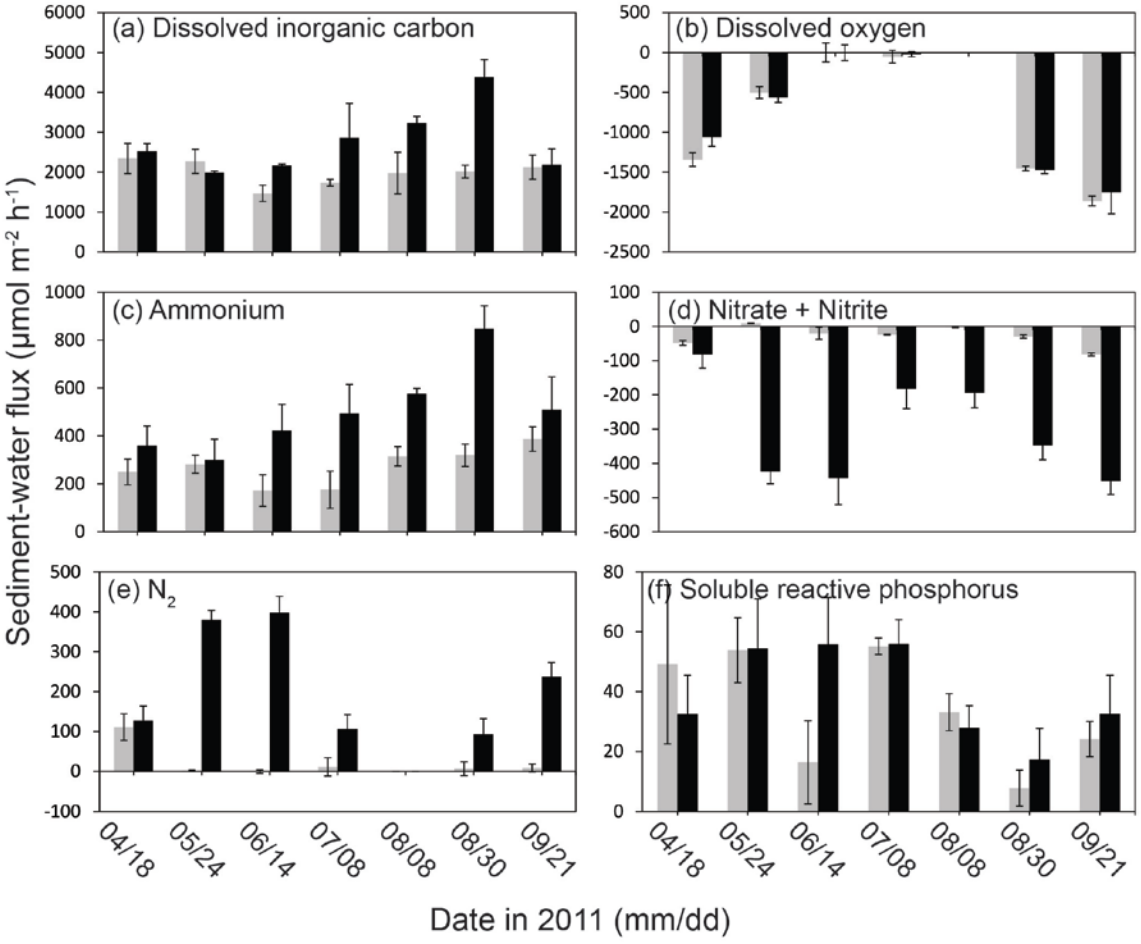

Appendix C: Complete dataset

The following section includes raw data collected for the present studies described in the chapters of this dissertation. These data include measures of water column biogeochemistry (Table C.1) and benthic biogeochemistry (Table C.2). Following abbreviations are used:

Oxic R.:	Respiration measured with changes in dissolved oxygen concentrations
DIC R.:	Respiration measured with changes in dissolved inorganic carbon concentrations
DIC:	dissolved inorganic carbon
SRP:	soluble reactive phosphorus
DS:	total dissolved sulfide (= $[S^{2-}] + [HS^{-}] + [H_2S]$)
DFe:	dissolved iron (= Fe(II)+ Fe(III))
DMn:	dissolved manganese (= [Mn(II)] + [Mn(III)])
Chl-a:	chlorophyll a
Pheo:	pheophytin
OxyPP:	oxygenic photoautotrophic production
AnoxyPP:	anoxygenic photoautotrophic production
DarkPP:	chemoautotrophic production
N_2:	nitrogen gas
O_2:	dissolved oxygen
NOx:	nitrite + nitrate
N_2:	nitrogen gas

Tables

Table C.1: Water column chemistry, dissolved nutrients, pelagic metabolism.

Date	Depth	Latitude	Longitude	Density	Conductivity	Temperature	Salinity	Oxygen	Fluorescence	Oxic R.	DIC R.	DIC
(mm/dd/yr)	(m)	(degree)		(Kg m^{-3})	(mS cm^{-1})	(°C)		(mg l^{-1})	(mg m^{-3})	(µmol l^{-1} h^{-1})		(µmol l^{-1})
5/17/10	1.0	38.6	-76.4	1006.4	14.6	17.5	10.1	9.8	24.1	0.9	0.6	1226.0
5/17/10	3.1	38.6	-76.4	1006.5	14.8	17.6	10.2	9.7	25.0	0.7	1.0	1223.4
5/17/10	5.0	38.6	-76.4	1006.8	15.4	17.6	10.6	8.8	20.2	0.5	0.9	1256.1
5/17/10	7.0	38.6	-76.4	1007.2	16.1	17.6	11.2	8.3	11.0	0.3	0.5	1282.9
5/17/10	9.0	38.6	-76.4	1008.2	17.1	16.6	12.2	5.3	9.0	0.2	0.0	1410.2
5/17/10	10.9	38.6	-76.4	1010.8	20.7	15.7	15.4	3.0	5.4	0.0	-0.4	1556.0
5/17/10	12.0	38.6	-76.4	1011.2	21.3	15.6	15.9	2.8	4.7	0.1	0.3	1573.7
5/17/10	12.9	38.6	-76.4	1011.5	21.6	15.5	16.2	2.4	4.6	0.0	-0.1	1598.1
6/7/10	0.9	38.6	-76.4	1005.0	17.5	24.6	10.4	8.3	15.1	0.9	1.3	1147.1
6/7/10	2.9	38.6	-76.4	1005.0	17.6	24.6	10.5	8.0	16.2	0.8	1.0	1153.0
6/7/10	6.1	38.6	-76.4	1005.2	17.5	24.1	10.5	7.1	13.0	0.4	0.9	1182.0
6/7/10	9.0	38.6	-76.4	1006.8	17.5	20.5	11.4	1.5	12.6	0.2	-0.2	1462.2
6/7/10	10.8	38.6	-76.4	1011.6	23.9	17.9	17.0	0.2	1.8	-0.1	-0.6	1651.6
6/7/10	12.9	38.6	-76.4	1012.8	25.7	17.7	18.5	0.3	1.6	-0.2	-0.4	1697.5
6/7/10	15.0	38.6	-76.4	1013.3	26.4	17.7	19.1	0.4	1.8	-0.2	-0.6	1714.0
6/7/10	16.4	38.6	-76.4	1013.3	-	17.7	19.1	0.6	0.0	-0.1	-0.4	1713.7
6/16/10	0.8	38.6	-76.4	1005.6	19.2	25.1	11.4	8.0	29.1	1.7	1.3	1158.0
6/16/10	3.3	38.6	-76.4	1005.6	19.2	25.0	11.4	9.2	26.0	1.5	1.2	1168.2
6/16/10	6.0	38.6	-76.4	1005.9	19.7	24.8	11.7	7.7	12.2	0.7	1.2	1205.3
6/16/10	9.5	38.6	-76.4	1008.2	21.0	21.5	13.6	0.1	16.4	-0.2	0.0	1510.6
6/16/10	10.5	38.6	-76.4	1010.1	23.8	20.7	15.8	0.1	4.7	-0.2	0.6	1581.9
6/16/10	13.2	38.6	-76.4	1011.6	25.5	19.8	17.5	0.1	2.2	-0.2	0.1	1629.4
6/16/10	15.2	38.6	-76.4	1012.0	26.0	19.5	18.0	0.1	1.9	-0.2	0.0	1657.4
6/16/10	16.8	38.6	-76.4	1012.3	26.2	19.3	18.2	0.2	1.7	-0.2	-0.1	1670.1
7/10/10	1.2	37.8	-76.2	1007.3	26.0	28.1	14.9	7.7	2.6	2.4	2.1	1415.6
7/10/10	4.0	37.8	-76.2	1007.7	26.7	27.9	15.3	7.0	1.0	1.1	1.0	1455.9
7/10/10	7.3	37.8	-76.2	1011.0	31.5	26.4	19.0	1.6	0.4	0.3	0.4	1724.7

Date	Depth	Latitude	Longitude	Density	Conductivity	Temperature	Salinity	Oxygen	Fluorescence	Oxic R.	DIC R.	DIC
(mm/dd/yr)	(m)	(degree)		(Kg m^{-3})	(mS cm^{-1})	(°C)		(mg l^{-1})	(mg m^{-3})	(µmol l^{-1} h^{-1})		(µmol l^{-1})
7/10/10	10.5	37.8	-76.2	1012.4	33.7	25.9	20.7	1.5	0.3	0.0	0.2	1771.0
7/10/10	13.4	37.8	-76.2	1013.7	35.6	25.4	22.2	1.2	0.3	0.1	0.3	1830.4
7/10/10	16.4	37.8	-76.2	1013.9	36.0	25.3	22.5	1.1	0.3	-0.2	0.4	1839.9
7/10/10	19.5	37.8	-76.2	1014.1	36.2	25.2	22.7	1.2	0.3	0.0	0.2	1840.5
7/10/10	22.4	37.8	-76.2	1014.1	36.3	25.2	22.8	1.1	0.3	-0.1	0.3	1839.4
7/11/10	1.4	38.6	-76.4	1005.6	21.3	27.2	12.2	6.8	1.4	1.6	1.4	1323.3
7/11/10	3.1	38.6	-76.4	1005.7	21.3	27.0	12.2	6.6	1.2	0.8	0.9	1315.5
7/11/10	6.0	38.6	-76.4	1005.9	21.7	26.9	12.5	5.8	0.8	3.0	2.5	1346.7
7/11/10	9.4	38.6	-76.4	1007.9	25.0	25.6	15.1	1.6	0.4	0.0	0.2	1569.8
7/11/10	11.4	38.6	-76.4	1010.0	28.3	25.0	17.4	0.1	0.3	-0.3	0.1	1731.6
7/11/10	13.1	38.6	-76.4	1010.9	29.7	25.0	18.3	0.1	0.2	-0.4	0.2	1758.6
7/11/10	15.1	38.6	-76.4	1011.9	31.9	25.1	19.8	0.1	0.3	-0.3	0.0	1806.5
7/11/10	17.4	38.6	-76.4	1012.2	32.4	25.2	20.2	0.1	0.2	-0.3	0.2	1816.8
7/12/10	1.3	38.2	-76.2	1006.8	23.9	27.2	13.8	6.8	1.6	1.1	1.2	1393.4
7/12/10	3.1	38.2	-76.2	1006.8	23.9	27.2	13.8	6.7	1.4	1.1	1.4	1391.4
7/12/10	6.6	38.2	-76.2	1007.1	24.5	27.1	14.2	6.0	1.0	0.9	1.3	1438.4
7/12/10	10.1	38.2	-76.2	1009.9	29.1	26.1	17.5	0.8	0.3	0.1	0.4	1695.0
7/12/10	13.1	38.2	-76.2	1010.8	30.8	26.0	18.7	0.2	0.2	-0.2	0.1	1744.2
7/12/10	16.1	38.2	-76.2	1013.1	35.0	25.7	21.6	0.2	0.2	-0.2	0.2	1832.5
7/12/10	18.2	38.2	-76.2	1013.2	35.1	25.7	21.7	0.2	0.2	-0.2	0.4	1833.5
7/12/10	19.9	38.2	-76.2	1013.3	35.2	25.7	21.8	0.3	0.2	-0.4	0.0	1834.9
7/13/10	1.2	38.3	-76.3	1006.8	24.1	27.3	13.9	6.9	1.2	1.1	1.1	1391.7
7/13/10	3.1	38.3	-76.3	1006.9	24.0	27.2	13.9	6.8	1.1	1.1	1.0	1392.8
7/13/10	6.3	38.3	-76.3	1007.0	24.0	27.0	13.9	6.3	0.9	0.9	0.8	1406.9
7/13/10	9.1	38.3	-76.3	1007.3	24.3	26.9	14.2	6.0	0.9	3.1	2.8	1419.3
7/13/10	11.2	38.3	-76.3	1012.8	34.6	25.9	21.3	0.1	0.2	-0.2	0.2	1824.9
7/13/10	13.9	38.3	-76.3	1012.9	34.9	25.9	21.5	0.1	0.2	-0.2	0.0	1830.1
7/13/10	17.1	38.3	-76.3	1013.1	35.1	25.9	21.6	0.1	0.2	-0.2	0.0	1835.3
7/13/10	19.8	38.3	-76.3	1013.1	35.2	25.9	21.7	0.1	0.3	-0.3	0.1	1835.9
7/14/10	1.2	39.0	-76.4	1005.1	19.8	26.8	11.4	7.2	5.0	2.2	2.7	1345.8
7/14/10	3.1	39.0	-76.4	1005.1	19.8	26.7	11.4	6.8	3.4	1.9	2.6	1343.8
7/14/10	5.2	39.0	-76.4	1005.2	19.9	26.7	11.4	6.3	2.1	1.4	1.7	1364.1

Date	Depth	Latitude	Longitude	Density	Conductivity	Temperature	Salinity	Oxygen	Fluorescence	Oxic R.	DIC R.	DIC
(mm/dd/yr)	(m)	(degree)		(Kg m^{-3})	(mS cm^{-1})	(°C)		(mg l^{-1})	(mg m^{-3})	(µmol l^{-1} h^{-1})		(µmol l^{-1})
7/14/10	8.1	39.0	-76.4	1006.2	21.3	25.9	12.5	2.8	1.0	0.6	0.9	1511.4
7/14/10	11.5	39.0	-76.4	1007.8	23.5	25.0	14.2	1.3	0.7	0.1	1.0	1584.4
7/14/10	15.1	39.0	-76.4	1010.0	26.9	24.0	16.8	0.1	0.3	-0.2	-0.5	1744.1
7/14/10	18.2	39.0	-76.4	1010.2	27.2	24.0	17.1	0.1	0.3	-0.3	0.2	1748.9
7/14/10	21.5	39.0	-76.4	1010.6	27.9	23.9	17.6	0.1	0.4	-0.3	0.5	1764.3
8/5/10	1.1	38.6	-76.4	1006.8	24.8	27.9	14.2	6.9	9.2	1.4	0.8	1422.1
8/5/10	3.0	38.6	-76.4	1006.9	24.7	27.7	14.2	7.0	10.5	5.0	6.2	1420.7
8/5/10	9.0	38.6	-76.4	1007.0	25.0	27.8	14.3	6.4	9.7	1.3	0.9	1447.3
8/5/10	14.0	38.6	-76.4	1007.9	26.0	27.1	15.2	2.4	3.5	0.5	0.7	1574.4
8/5/10	15.8	38.6	-76.4	1008.4	26.8	26.9	15.7	1.2	2.8	0.1	0.5	1661.1
8/5/10	18.2	38.6	-76.4	1009.8	29.0	26.3	17.4	0.0	1.8	-0.2	0.6	1782.9
8/5/10	19.7	38.6	-76.4	1010.0	29.2	26.2	17.6	0.0	1.8	-0.2	-0.8	1812.4
8/5/10	22.3	38.6	-76.4	1010.8	30.6	26.0	18.6	0.0	1.6	-0.6	0.9	1857.3
8/31/10	1.0	38.6	-76.4	1006.6	23.3	27.0	13.5	7.3	6.9	1.3	1.0	1324.8
8/31/10	2.8	38.6	-76.4	1006.9	23.5	26.6	13.7	5.4	14.2	1.2	1.2	1338.7
8/31/10	6.1	38.6	-76.4	1007.6	24.9	26.5	14.6	4.4	15.6	1.0	0.8	1420.8
8/31/10	9.0	38.6	-76.4	1009.9	29.5	26.4	17.6	1.3	5.7	0.4	1.2	1635.7
8/31/10	11.1	38.6	-76.4	1012.2	34.0	26.4	20.7	0.5	2.4	0.1	0.4	1769.7
8/31/10	13.9	38.6	-76.4	1013.5	36.5	26.3	22.4	0.1	1.0	-0.2	0.4	1833.0
8/31/10	17.1	38.6	-76.4	1013.9	37.1	26.2	22.8	0.1	0.9	-0.2	0.2	1840.8
8/31/10	20.3	38.6	-76.4	1014.0	37.1	26.2	22.9	0.1	1.0	-0.3	0.1	1846.6
10/18/10	0.8	38.6	-76.4	1009.7	20.8	18.0	14.6	9.3	8.1	0.7	0.4	1184.5
10/18/10	3.1	38.6	-76.4	1009.8	20.6	17.8	14.6	8.5	18.4	0.6	0.3	1184.2
10/18/10	5.0	38.6	-76.4	1009.8	20.6	17.7	14.6	8.5	23.5	0.5	0.5	1195.6
10/18/10	7.1	38.6	-76.4	1009.8	20.6	17.7	14.6	8.2	21.6	0.4	0.2	1199.9
10/18/10	9.0	38.6	-76.4	1009.8	20.7	17.7	14.6	8.1	19.6	0.2	0.2	1201.6
10/18/10	10.6	38.6	-76.4	1009.9	21.0	17.9	14.8	7.6	18.4	0.0	0.2	1206.1
10/18/10	11.5	38.6	-76.4	1010.0	21.2	18.1	14.9	7.5	17.7	0.2	0.3	1216.6
10/18/10	12.7	38.6	-76.4	1011.1	23.8	18.8	16.6	6.1	11.5	0.3	0.4	1330.3
4/18/11	0.9	38.6	-76.4	1004.8	9.1	12.5	6.9	10.4	18.9	0.6	0.3	1152.5
4/18/11	3.0	38.6	-76.4	1005.3	9.8	12.1	7.5	9.9	38.2	0.5	0.3	1194.5
4/18/11	5.2	38.6	-76.4	1006.5	11.7	12.2	9.1	9.8	47.7	0.3	0.5	1255.9

Date	Depth	Latitude	Longitude	Density	Conductivity	Temperature	Salinity	Oxygen	Fluorescence	Oxic R.	DIC R.	DIC
(mm/dd/yr)	(m)	(degree)		(Kg m^{-3})	(mS cm^{-1})	(°C)		(mg l^{-1})	(mg m^{-3})	(µmol l^{-1} h^{-1})		(µmol l^{-1})
4/18/11	7.3	38.6	-76.4	1007.5	13.0	11.9	10.2	9.1	51.8	0.3	0.4	1324.1
4/18/11	8.8	38.6	-76.4	1008.3	13.9	11.3	11.1	7.7	50.2	0.4	0.6	1401.6
4/18/11	9.9	38.6	-76.4	1008.6	14.2	11.1	11.5	7.0	47.2	0.3	0.5	1441.2
4/18/11	11.9	38.6	-76.4	1009.6	15.2	10.3	12.7	4.8	38.1	0.2	0.5	1570.8
4/18/11	13.5	38.6	-76.4	1009.8	15.4	10.2	12.9	4.6	35.2	-0.2	0.0	1615.4
5/24/11	0.8	38.6	-76.4	1001.2	7.2	21.1	4.3	11.2	136.0	3.5	3.5	715.0
5/24/11	3.0	38.6	-76.4	1001.4	7.0	20.4	4.3	9.1	88.4	0.9	0.9	820.8
5/24/11	5.3	38.6	-76.4	1001.5	7.1	20.3	4.3	8.1	51.1	0.7	0.8	831.7
5/24/11	8.0	38.6	-76.4	1004.8	11.9	17.6	8.0	1.3	57.8	0.8	0.4	1399.8
5/24/11	11.4	38.6	-76.4	1006.8	14.7	16.7	10.4	0.2	9.5	0.1	-0.1	1557.3
5/24/11	14.3	38.6	-76.4	1008.1	16.8	16.6	12.0	0.1	6.6	0.0	0.2	1619.8
5/24/11	17.1	38.6	-76.4	1008.9	18.0	16.5	13.0	0.1	6.1	0.0	0.1	1669.2
5/24/11	19.1	38.6	-76.4	1009.9	19.5	16.3	14.2	0.3	4.8	0.0	0.2	1720.1
6/14/11	0.8	38.6	-76.4	1001.1	9.3	24.5	5.2	7.8	20.8	1.7	1.4	1111.0
6/14/11	2.9	38.6	-76.4	1001.2	9.3	24.3	5.3	7.3	27.4	1.3	1.1	1120.5
6/14/11	4.9	38.6	-76.4	1001.5	9.7	24.1	5.6	6.6	26.3	1.3	0.8	1141.4
6/14/11	8.9	38.6	-76.4	1002.7	11.8	23.5	7.0	4.3	23.7	0.7	3.2	1252.0
6/14/11	10.9	38.6	-76.4	1009.5	22.1	20.2	14.8	0.2	6.3	-0.1	0.8	1729.4
6/14/11	14.7	38.6	-76.4	1012.1	26.4	19.8	18.2	0.0	4.1	-0.7	-0.3	1852.1
6/14/11	15.8	38.6	-76.4	1012.3	26.8	19.8	18.4	0.0	4.0	-0.2	0.3	1861.5
6/14/11	17.7	38.6	-76.4	1012.4	27.0	19.8	18.6	0.1	4.1	-0.3	-0.4	1871.1
7/7/11	1.2	37.8	-76.2	1004.4	18.3	26.8	10.4	8.3	4.3	1.9	1.4	1288.0
7/7/11	3.1	37.8	-76.2	1004.7	18.8	26.6	10.7	6.8	2.7	2.1	1.7	1327.4
7/7/11	5.0	37.8	-76.2	1008.7	26.2	25.7	15.8	2.9	1.3	0.0	0.3	1683.5
7/7/11	6.9	37.8	-76.2	1010.5	29.0	25.0	17.9	1.8	0.8	-0.4	-0.6	1719.8
7/7/11	8.8	37.8	-76.2	1011.6	30.7	24.6	19.2	1.3	0.7	-0.7	0.0	1772.2
7/7/11	15.5	37.8	-76.2	1013.8	33.7	23.6	21.8	0.9	0.7	-0.7	0.3	1877.1
7/7/11	17.6	37.8	-76.2	1013.9	33.7	23.5	21.8	0.9	0.7	-0.7	0.1	1891.8
7/7/11	22.1	37.8	-76.2	1014.2	34.0	23.4	22.1	0.8	0.6	-0.9	0.3	1904.6
7/8/11	0.9	38.6	-76.4	1003.1	15.7	27.0	8.8	7.2	1.8	1.1	0.2	1263.6
7/8/11	3.0	38.6	-76.4	1003.2	15.9	26.9	8.9	6.7	1.8	-0.1	2.4	1254.3
7/8/11	5.2	38.6	-76.4	1004.6	17.9	26.0	10.3	4.4	1.5	0.3	4.3	1367.8

Date	Depth	Latitude	Longitude	Density	Conductivity	Temperature	Salinity	Oxygen	Fluorescence	Oxic R.	DIC R.	DIC
(mm/dd/yr)	(m)	(degree)		(Kg m^{-3})	(mS cm^{-1})	(°C)		(mg l^{-1})	(mg m^{-3})	(µmol l^{-1} h^{-1})		(µmol l^{-1})
7/8/11	7.0	38.6	-76.4	1006.8	20.6	24.0	12.6	0.6	0.7	0.0	0.8	1592.3
7/8/11	9.0	38.6	-76.4	1008.7	23.0	22.6	14.7	0.2	0.5	-0.2	0.2	1734.9
7/8/11	12.1	38.6	-76.4	1009.7	24.7	22.5	15.9	0.1	0.5	-0.6	0.1	1769.9
7/8/11	15.0	38.6	-76.4	1010.5	26.3	22.7	16.9	0.1	0.5	-0.7	0.0	1777.2
7/8/11	17.6	38.6	-76.4	1012.3	29.9	22.9	19.4	0.1	0.5	-0.5	0.0	1854.6
7/9/11	0.9	37.9	-76.2	1004.0	18.3	27.6	10.3	9.0	6.5	2.9	2.7	1265.8
7/9/11	2.7	37.9	-76.2	1004.1	18.2	27.3	10.3	8.5	3.6	2.3	1.2	1279.8
7/9/11	5.0	37.9	-76.2	1004.4	18.2	26.7	10.4	7.6	2.3	1.6	0.6	1316.1
7/9/11	7.7	37.9	-76.2	1004.9	19.0	26.5	10.9	4.9	1.4	-0.4	0.6	1400.9
7/9/11	9.9	37.9	-76.2	1010.1	27.5	24.4	17.1	0.3	0.7	-0.9	-0.7	1760.3
7/9/11	12.6	37.9	-76.2	1012.1	30.6	23.8	19.5	0.2	0.6	-0.7	-0.8	1855.1
7/9/11	16.0	37.9	-76.2	1012.9	32.0	23.6	20.5	0.1	0.5	-0.7	-0.1	1877.9
7/9/11	18.9	37.9	-76.2	1013.6	33.1	23.5	21.4	0.2	0.5	-0.6	0.1	1903.8
7/10/11	1.0	39.0	-76.4	1002.1	13.0	26.5	7.2	6.3	3.6	1.2	0.6	1311.3
7/10/11	3.1	39.0	-76.4	1002.2	13.0	26.2	7.2	5.8	1.8	0.7	0.7	1316.2
7/10/11	5.0	39.0	-76.4	1004.0	16.1	25.3	9.3	3.3	1.1	-0.3	0.0	1446.7
7/10/11	7.0	39.0	-76.4	1005.5	18.3	24.3	11.0	1.7	0.9	-0.3	1.5	1544.2
7/10/11	9.0	39.0	-76.4	1009.4	24.1	22.4	15.5	0.3	0.6	-0.6	0.0	1761.9
7/10/11	12.5	39.0	-76.4	1010.5	25.8	22.1	16.8	0.2	0.6	-0.8	0.3	1807.5
7/10/11	16.0	39.0	-76.4	1011.0	26.8	22.1	17.5	0.1	0.5	-1.1	0.0	1829.5
7/10/11	19.5	39.0	-76.4	1011.3	27.4	22.2	17.9	0.1	0.5	-2.0	0.1	1841.5
7/11/11	1.3	39.0	-76.4	1002.1	13.1	26.5	7.3	6.0	3.6	0.4	0.1	1335.2
7/11/11	2.9	39.0	-76.4	1002.3	13.6	26.6	7.6	6.2	2.8	0.7	1.2	1307.4
7/11/11	5.1	39.0	-76.4	1002.6	14.0	26.4	7.9	6.1	2.5	1.5	0.9	1318.3
7/11/11	6.0	39.0	-76.4	1003.0	14.7	26.2	8.3	5.6	2.4	3.7	1.9	1345.2
7/11/11	6.9	39.0	-76.4	1005.4	18.3	24.5	10.9	2.6	1.2	1.0	-0.8	1498.6
7/11/11	7.8	39.0	-76.4	1006.5	19.9	23.9	12.2	1.3	1.0	0.8	0.3	1593.7
7/11/11	8.9	39.0	-76.4	1007.5	21.1	23.4	13.2	0.8	1.0	0.2	0.1	1638.6
7/11/11	10.3	39.0	-76.4	1008.5	22.9	22.8	14.5	0.1	0.8	-1.0	0.0	1751.6
8/8/11	0.8	38.6	-76.4	1005.6	22.3	28.0	12.5	8.8	104.6	3.3	3.0	1436.2
8/8/11	3.0	38.6	-76.4	1005.7	22.3	27.8	12.6	7.0	43.9	1.6	1.4	1493.1
8/8/11	5.1	38.6	-76.4	1005.8	22.2	27.5	12.7	5.9	21.9	0.7	0.8	1506.4

Date	Depth	Latitude	Longitude	Density	Conductivity	Temperature	Salinity	Oxygen	Fluorescence	Oxic R.	DIC R.	DIC
(mm/dd/yr)	(m)	(degree)		(Kg m^{-3})	(mS cm^{-1})	(°C)		(mg l^{-1})	(mg m^{-3})	(µmol l^{-1} h^{-1})		(µmol l^{-1})
8/8/11	8.1	38.6	-76.4	1005.9	22.3	27.5	12.7	5.6	17.3	0.8	0.3	1521.5
8/8/11	10.9	38.6	-76.4	1007.4	24.5	26.6	14.3	1.5	6.0	-0.1	0.1	1677.8
8/8/11	14.0	38.6	-76.4	1010.9	30.0	25.3	18.4	0.0	3.3	-0.4	0.5	1874.8
8/8/11	16.0	38.6	-76.4	1011.6	31.2	25.1	19.4	0.0	3.0	-0.4	0.0	1904.3
8/8/11	18.1	38.6	-76.4	1011.8	31.5	25.1	19.6	0.1	3.5	-0.4	0.4	1907.1
8/30/11	1.0	38.6	-76.4	1005.8	19.5	24.9	11.6	10.5	76.7	3.0	2.7	1396.1
8/30/11	3.0	38.6	-76.4	1006.3	20.3	24.6	12.2	7.1	23.2	2.9	2.1	1509.6
8/30/11	5.0	38.6	-76.4	1006.5	20.5	24.6	12.4	7.0	16.1	0.7	0.3	1521.3
8/30/11	8.5	38.6	-76.4	1006.7	21.1	24.7	12.7	6.7	12.1	0.6	0.3	1539.8
8/30/11	10.9	38.6	-76.4	1007.4	22.8	25.0	13.7	5.6	8.6	0.3	0.2	1597.0
8/30/11	12.9	38.6	-76.4	1008.0	24.2	25.1	14.6	4.3	7.4	0.8	0.4	1656.5
8/30/11	14.8	38.6	-76.4	1008.5	25.4	25.3	15.4	4.0	5.3	0.3	0.2	1684.5
8/30/11	17.6	38.6	-76.4	1008.9	26.1	25.4	15.8	3.7	4.7	0.1	0.1	1708.3
9/21/11	0.9	38.6	-76.4	1002.2	9.2	21.1	5.6	8.9	26.6	0.7	0.5	1065.2
9/21/11	3.0	38.6	-76.4	1002.7	10.2	21.2	6.3	7.8	13.3	0.5	0.1	1144.4
9/21/11	4.9	38.6	-76.4	1004.2	13.5	21.8	8.4	6.8	6.6	0.4	0.0	1290.5
9/21/11	8.4	38.6	-76.4	1005.4	16.6	22.6	10.3	6.1	6.5	0.4	0.0	1408.8
9/21/11	11.6	38.6	-76.4	1006.3	19.2	23.6	11.7	3.8	4.9	0.4	0.1	1529.6
9/21/11	12.9	38.6	-76.4	1007.0	21.1	24.2	12.8	2.9	4.0	0.2	0.2	1581.9
9/21/11	15.5	38.6	-76.4	1007.3	21.9	24.5	13.3	2.4	3.8	0.3	0.0	1616.3
9/21/11	16.6	38.6	-76.4	1007.3	22.0	24.5	13.4	2.4	3.7	0.2	0.3	1618.4

Table C.1: Water column chemistry, dissolved nutrients, pelagic metabolism (continued).

Date	Depth	Latitude	Longitude	NO_2^-	NO_3^-	NH_4^+	SRP	DS	DFe	DMn	Chl-a	Pheo	OxyPP	AnoxyPP	DarkPP
(mm/dd/yr)	(m)	(degree)				(µmol l^{-1})					(µg l^{-1})			(nmol l^{-1} h^{-1})	
5/17/10	1.0	38.6	-76.4	0.9	25.4	0.2	0.1	-	-	0.0	-	-	-	-	-
5/17/10	3.1	38.6	-76.4	0.9	24.8	0.8	0.0	-	-	0.0	-	-	-	-	-
5/17/10	5.0	38.6	-76.4	0.9	23.8	1.5	0.0	-	-	0.0	-	-	-	-	-
5/17/10	7.0	38.6	-76.4	0.8	21.1	3.2	0.0	-	-	0.0	-	-	-	-	-
5/17/10	9.0	38.6	-76.4	0.9	17.2	10.6	0.0	-	-	0.0	-	-	-	-	-
5/17/10	10.9	38.6	-76.4	0.8	11.3	15.4	0.1	-	-	0.0	-	-	-	-	-
5/17/10	12.0	38.6	-76.4	0.7	10.7	15.6	0.1	-	-	0.0	-	-	-	-	-
5/17/10	12.9	38.6	-76.4	0.8	10.1	17.1	0.1	-	-	0.0	-	-	-	-	-
6/7/10	0.9	38.6	-76.4	0.4	5.8	2.2	0.1	-	-	0.0	-	-	-	-	-
6/7/10	2.9	38.6	-76.4	0.3	5.2	2.4	0.1	-	-	0.0	-	-	-	-	-
6/7/10	6.1	38.6	-76.4	0.4	5.6	3.9	0.0	-	-	0.0	-	-	-	-	-
6/7/10	9.0	38.6	-76.4	0.8	6.2	18.2	0.1	-	-	2.1	-	-	-	-	-
6/7/10	10.8	38.6	-76.4	0.6	3.4	20.2	0.8	-	-	0.3	-	-	-	-	-
6/7/10	12.9	38.6	-76.4	0.4	2.2	18.6	1.0	-	-	0.1	-	-	-	-	-
6/7/10	15.0	38.6	-76.4	0.4	1.9	18.2	1.1	-	-	0.1	-	-	-	-	-
6/7/10	16.4	38.6	-76.4	0.4	1.8	18.2	1.1	-	-	0.1	-	-	-	-	-
6/16/10	0.8	38.6	-76.4	0.2	1.6	3.6	0.1	-	-	0.0	-	-	-	-	-
6/16/10	3.3	38.6	-76.4	0.2	1.6	0.2	0.2	-	-	0.0	-	-	-	-	-
6/16/10	6.0	38.6	-76.4	0.2	2.5	1.4	0.1	-	-	0.0	-	-	-	-	-
6/16/10	9.5	38.6	-76.4	0.6	3.2	12.7	0.1	-	-	0.0	-	-	-	-	-
6/16/10	10.5	38.6	-76.4	1.2	0.9	15.3	0.2	-	-	0.0	-	-	-	-	-
6/16/10	13.2	38.6	-76.4	0.8	0.8	16.4	0.5	-	-	0.2	-	-	-	-	-
6/16/10	15.2	38.6	-76.4	0.9	0.4	17.2	0.6	-	-	0.4	-	-	-	-	-
6/16/10	16.8	38.6	-76.4	0.9	0.4	17.7	0.7	-	-	0.5	-	-	-	-	-
7/10/10	1.2	37.8	-76.2	0.1	0.1	0.0	0.0	-	0.0	0.0	-	-	-	-	-
7/10/10	4.0	37.8	-76.2	0.1	0.5	0.0	0.0	-	0.0	0.0	-	-	-	-	-
7/10/10	7.3	37.8	-76.2	0.2	0.2	4.8	0.4	-	0.9	0.0	-	-	-	-	-

Date	Depth	Latitude	Longitude	NO_2^-	NO_3^-	NH_4^+	SRP	DS	DFe	DMn	Chl-a	Pheo	OxyPP	AnoxyPP	DarkPP
(mm/dd/yr)	(m)	(degree)					(µmol l^{-1})				(µg l^{-1})			(nmol l^{-1} h^{-1})	
7/10/10	10.5	37.8	-76.2	0.3	0.5	9.8	0.7	-	0.0	0.0	-	-	-	-	-
7/10/10	13.4	37.8	-76.2	0.3	0.6	9.0	1.0	-	0.0	0.0	-	-	-	-	-
7/10/10	16.4	37.8	-76.2	0.4	0.7	10.9	1.4	-	0.4	0.0	-	-	-	-	-
7/10/10	19.5	37.8	-76.2	0.4	0.7	9.4	1.3	-	0.5	0.0	-	-	-	-	-
7/10/10	22.4	37.8	-76.2	0.3	0.8	9.5	1.3	-	0.0	3.5	-	-	-	-	-
7/11/10	1.4	38.6	-76.4	0.1	0.2	0.0	0.2	0.0	0.0	0.0	-	-	-	-	-
7/11/10	3.1	38.6	-76.4	0.1	0.0	0.0	0.1	0.0	0.0	0.0	-	-	-	-	-
7/11/10	6.0	38.6	-76.4	0.1	0.1	0.4	0.2	0.0	0.0	0.0	-	-	-	-	-
7/11/10	9.4	38.6	-76.4	0.1	0.0	9.3	1.2	0.0	1.2	0.0	-	-	-	-	-
7/11/10	11.4	38.6	-76.4	0.1	0.1	14.4	2.0	2.4	0.0	2.9	-	-	-	-	-
7/11/10	13.1	38.6	-76.4	0.1	0.1	14.2	1.9	4.5	0.0	2.6	-	-	-	-	-
7/11/10	15.1	38.6	-76.4	0.1	0.2	13.7	1.9	5.6	0.0	2.4	-	-	-	-	-
7/11/10	17.4	38.6	-76.4	0.1	0.1	14.2	2.0	5.1	0.0	2.3	-	-	-	-	-
7/12/10	1.3	38.2	-76.2	0.1	0.1	0.0	0.1	-	0.0	0.0	-	-	-	-	-
7/12/10	3.1	38.2	-76.2	0.1	0.0	0.0	0.1	-	0.0	0.0	-	-	-	-	-
7/12/10	6.6	38.2	-76.2	0.1	0.0	0.0	0.1	-	0.0	0.1	-	-	-	-	-
7/12/10	10.1	38.2	-76.2	0.2	0.2	7.9	0.7	-	0.0	0.4	-	-	-	-	-
7/12/10	13.1	38.2	-76.2	0.3	0.2	14.6	1.4	-	0.0	0.1	-	-	-	-	-
7/12/10	16.1	38.2	-76.2	0.4	0.6	15.0	1.3	-	0.0	0.9	-	-	-	-	-
7/12/10	18.2	38.2	-76.2	0.4	0.5	14.3	1.3	-	0.0	0.6	-	-	-	-	-
7/12/10	19.9	38.2	-76.2	0.4	0.5	14.2	1.0	-	0.0	0.6	-	-	-	-	-
7/13/10	1.2	38.3	-76.3	0.1	0.2	0.0	0.2	0.0	0.0	0.0	-	-	-	-	-
7/13/10	3.1	38.3	-76.3	0.1	0.2	0.0	0.1	0.0	0.0	0.0	-	-	-	-	-
7/13/10	6.3	38.3	-76.3	0.1	0.1	0.0	0.1	0.0	0.0	0.0	-	-	-	-	-
7/13/10	9.1	38.3	-76.3	0.1	0.2	0.0	0.2	0.0	0.0	0.0	-	-	-	-	-
7/13/10	11.2	38.3	-76.3	0.1	0.0	16.7	2.0	1.2	0.0	0.0	-	-	-	-	-
7/13/10	13.9	38.3	-76.3	0.1	0.0	16.9	2.0	0.5	0.4	0.0	-	-	-	-	-
7/13/10	17.1	38.3	-76.3	0.1	0.1	17.7	2.2	0.9	0.1	0.0	-	-	-	-	-
7/13/10	19.8	38.3	-76.3	0.1	0.1	17.8	2.0	0.7	0.0	2.0	-	-	-	-	-
7/14/10	1.2	39.0	-76.4	0.1	0.0	0.0	0.3	0.0	0.0	0.0	-	-	-	-	-
7/14/10	3.1	39.0	-76.4	0.1	0.1	0.0	0.2	0.0	0.0	0.0	-	-	-	-	-
7/14/10	5.2	39.0	-76.4	0.1	0.1	0.5	0.2	0.0	0.0	0.2	-	-	-	-	-

Date	Depth	Latitude	Longitude	NO_2^-	NO_3^-	NH_4^+	SRP	DS	DFe	DMn	Chl-a	Pheo	OxyPP	AnoxyPP	DarkPP
(mm/dd/yr)	(m)	(degree)				(µmol l^{-1})					(µg l^{-1})		(nmol l^{-1} h^{-1})		
7/14/10	8.1	39.0	-76.4	0.1	0.1	8.8	0.1	0.0	0.0	0.2	-	-	-	-	-
7/14/10	11.5	39.0	-76.4	0.1	0.1	14.0	0.7	0.0	0.0	0.2	-	-	-	-	-
7/14/10	15.1	39.0	-76.4	0.1	0.1	21.1	2.8	1.0	0.0	6.9	-	-	-	-	-
7/14/10	18.2	39.0	-76.4	0.1	0.1	22.1	3.1	3.6	0.0	7.3	-	-	-	-	-
7/14/10	21.5	39.0	-76.4	0.1	0.2	23.8	3.2	3.9	0.0	7.1	-	-	-	-	-
8/5/10	1.1	38.6	-76.4	0.1	0.0	0.0	0.3	0.0	-	0.3	-	-	-	-	-
8/5/10	3.0	38.6	-76.4	0.1	0.1	0.0	0.2	0.0	-	0.2	-	-	-	-	-
8/5/10	9.0	38.6	-76.4	0.1	0.1	0.0	0.3	0.0	-	0.2	-	-	-	-	-
8/5/10	14.0	38.6	-76.4	0.2	0.1	10.3	1.5	0.0	-	0.3	-	-	-	-	-
8/5/10	15.8	38.6	-76.4	0.1	0.3	14.7	2.1	1.3	-	1.9	-	-	-	-	-
8/5/10	18.2	38.6	-76.4	0.1	0.2	24.1	5.0	8.7	-	2.1	-	-	-	-	-
8/5/10	19.7	38.6	-76.4	0.1	0.4	24.8	4.3	8.9	-	2.4	-	-	-	-	-
8/5/10	22.3	38.6	-76.4	0.2	0.2	27.4	4.7	9.1	-	2.7	-	-	-	-	-
8/31/10	1.0	38.6	-76.4	0.1	0.2	0.0	0.4	0.0	0.0	0.5	-	-	-	-	-
8/31/10	2.8	38.6	-76.4	0.1	0.1	0.0	0.3	0.0	0.0	0.5	-	-	-	-	-
8/31/10	6.1	38.6	-76.4	0.1	0.1	0.0	0.2	0.0	0.0	0.4	-	-	-	-	-
8/31/10	9.0	38.6	-76.4	3.9	0.2	0.0	0.6	0.0	2.5	0.6	-	-	-	-	-
8/31/10	11.1	38.6	-76.4	3.4	0.2	0.2	1.3	0.0	0.0	1.0	-	-	-	-	-
8/31/10	13.9	38.6	-76.4	3.8	0.2	0.5	1.5	0.0	0.0	1.6	-	-	-	-	-
8/31/10	17.1	38.6	-76.4	5.5	0.3	0.2	1.5	0.1	0.0	2.4	-	-	-	-	-
8/31/10	20.3	38.6	-76.4	3.7	0.1	0.4	1.7	0.0	0.0	3.1	-	-	-	-	-
10/18/10	0.8	38.6	-76.4	2.1	1.5	0.4	0.1	-	0.2	1.7	-	-	-	-	-
10/18/10	3.1	38.6	-76.4	2.1	1.7	0.1	0.3	-	0.5	1.7	-	-	-	-	-
10/18/10	5.0	38.6	-76.4	2.1	1.6	0.2	0.4	-	1.5	1.8	-	-	-	-	-
10/18/10	7.1	38.6	-76.4	2.1	1.9	0.2	0.2	-	0.0	1.9	-	-	-	-	-
10/18/10	9.0	38.6	-76.4	2.2	1.7	0.4	0.1	-	0.9	1.9	-	-	-	-	-
10/18/10	10.6	38.6	-76.4	2.1	1.4	1.2	0.1	-	19.7	2.0	-	-	-	-	-
10/18/10	11.5	38.6	-76.4	2.4	1.6	2.3	0.1	-	0.1	2.0	-	-	-	-	-
10/18/10	12.7	38.6	-76.4	5.7	2.1	7.9	0.3	-	0.7	2.2	-	-	-	-	-
4/18/11	0.9	38.6	-76.4	0.6	39.0	5.4	0.0	0.0	1.2	0.0	9.9	4.3	-	-	-
4/18/11	3.0	38.6	-76.4	0.6	35.5	3.8	0.0	0.0	0.9	0.0	12.5	4.1	-	-	-
4/18/11	5.2	38.6	-76.4	0.5	27.6	4.0	0.0	0.0	0.1	0.0	12.5	4.6	60.8	0.0	12.5

Date	Depth	Latitude	Longitude	NO_2^-	NO_3^-	NH_4^+	SRP	DS	DFe	DMn	Chl-a	Pheo	OxyPP	AnoxyPP	DarkPP
(mm/dd/yr)	(m)	(degree)					($\mu mol\ l^{-1}$)				($\mu g\ l^{-1}$)			($nmol\ l^{-1}\ h^{-1}$)	
4/18/11	7.3	38.6	-76.4	0.6	22.2	4.4	0.7	0.0	10.2	0.0	17.2	4.0	112.5	0.0	13.4
4/18/11	8.8	38.6	-76.4	0.5	19.1	7.4	0.0	0.0	0.3	0.0	14.5	6.8	13.2	0.0	18.2
4/18/11	9.9	38.6	-76.4	0.6	17.8	8.6	0.0	0.0	0.1	0.0	12.6	6.3	0.8	0.0	12.2
4/18/11	11.9	38.6	-76.4	0.6	15.2	14.5	0.0	0.0	1.6	0.0	8.5	4.8	-	-	-
4/18/11	13.5	38.6	-76.4	0.6	14.6	16.1	0.0	0.0	3.5	0.0	15.6	16.8	-	-	-
5/24/11	0.8	38.6	-76.4	0.4	20.5	0.0	0.2	0.0	0.0	0.2	81.3	13.3	-	-	-
5/24/11	3.0	38.6	-76.4	0.4	22.0	0.0	0.1	0.0	0.5	0.1	20.7	4.7	-	-	-
5/24/11	5.3	38.6	-76.4	0.4	21.4	0.1	0.0	0.0	0.4	0.0	12.0	3.5	100.2	51.2	54.1
5/24/11	8.0	38.6	-76.4	0.5	15.1	15.6	0.1	0.0	0.4	2.0	12.5	4.6	48.9	0.0	131.0
5/24/11	11.4	38.6	-76.4	1.5	6.3	17.8	0.4	0.0	0.7	2.3	2.4	1.7	0.0	48.0	90.8
5/24/11	14.3	38.6	-76.4	1.7	2.2	16.1	0.6	0.0	1.3	2.2	1.8	1.4	31.5	0.0	134.9
5/24/11	17.1	38.6	-76.4	1.3	2.2	15.4	0.6	0.0	1.2	1.9	1.8	1.3	-	-	146.2
5/24/11	19.1	38.6	-76.4	1.2	1.0	16.0	0.4	0.0	1.4	0.9	1.4	1.3	-	-	173.5
6/14/11	0.8	38.6	-76.4	0.7	10.6	3.1	0.0	0.0	0.4	0.0	18.0	5.8	-	-	-
6/14/11	2.9	38.6	-76.4	0.7	10.2	2.6	0.0	0.0	0.9	0.0	17.4	4.5	-	-	-
6/14/11	4.9	38.6	-76.4	0.7	9.4	3.7	0.1	0.0	0.8	0.0	16.3	5.1	160.4	0.0	36.4
6/14/11	8.9	38.6	-76.4	0.6	6.7	8.7	0.1	0.0	0.6	0.0	14.2	5.1	40.0	0.0	26.9
6/14/11	10.9	38.6	-76.4	3.3	6.4	21.4	1.5	1.2	1.2	1.5	3.8	2.7	187.4	180.8	278.3
6/14/11	14.7	38.6	-76.4	0.1	0.3	20.5	2.4	11.0	1.8	1.1	2.2	3.3	83.7	0.0	147.9
6/14/11	15.8	38.6	-76.4	0.1	0.3	18.7	1.0	11.5	3.1	0.9	2.0	3.0	-	-	69.7
6/14/11	17.7	38.6	-76.4	0.1	0.3	19.6	1.1	4.5	2.0	1.7	1.9	2.7	-	-	120.5
7/7/11	1.2	37.8	-76.2	0.1	0.2	0.0	0.5	0.0	0.3	0.0	16.5	2.5	-	-	-
7/7/11	3.1	37.8	-76.2	0.1	0.1	0.0	0.5	0.0	1.8	0.0	16.1	2.4	-	-	-
7/7/11	5.0	37.8	-76.2	0.2	0.1	4.2	0.5	0.0	3.0	0.0	6.3	2.5	673.3	353.2	57.1
7/7/11	6.9	37.8	-76.2	0.2	0.3	4.1	0.6	0.0	0.5	0.0	3.3	1.7	204.0	106.2	98.7
7/7/11	8.8	37.8	-76.2	0.2	0.4	6.4	1.3	0.0	0.9	0.0	3.3	1.3	384.9	41.8	48.4
7/7/11	15.5	37.8	-76.2	0.3	0.4	11.2	1.9	0.0	0.2	0.0	2.2	0.9	43.5	45.4	53.7
7/7/11	17.6	37.8	-76.2	0.3	0.5	9.5	1.8	0.0	0.1	0.0	2.3	0.9	-	-	29.6
7/7/11	22.1	37.8	-76.2	0.3	0.6	10.7	2.6	0.0	1.2	0.0	2.1	0.9	-	-	179.3
7/8/11	0.9	38.6	-76.4	0.1	0.1	0.0	0.6	0.0	1.8	0.0	15.0	2.4	-	-	-
7/8/11	3.0	38.6	-76.4	0.1	0.1	0.0	0.6	0.0	0.6	0.0	15.1	3.1	-	-	-
7/8/11	5.2	38.6	-76.4	0.1	0.1	4.9	0.8	0.0	0.9	0.0	10.1	2.4	0.0	0.0	88.4

Date	Depth	Latitude	Longitude	NO_2^-	NO_3^-	NH_4^+	SRP	DS	DFe	DMn	Chl-a	Pheo	OxyPP	AnoxyPP	DarkPP
(mm/dd/yr)	(m)	(degree)				(µmol l^{-1})					(µg l^{-1})			(nmol l^{-1} h^{-1})	
7/8/11	7.0	38.6	-76.4	0.1	0.1	17.3	1.9	0.0	0.1	0.0	2.8	2.2	483.7	120.2	302.3
7/8/11	9.0	38.6	-76.4	0.1	0.2	29.1	4.0	16.4	1.7	3.7	1.7	0.8	154.6	249.0	306.9
7/8/11	12.1	38.6	-76.4	0.1	0.1	29.6	3.6	19.9	1.8	2.5	1.5	0.8	0.0	119.8	102.4
7/8/11	15.0	38.6	-76.4	0.1	0.1	25.6	2.6	11.6	1.4	1.7	1.5	0.9	-	-	102.4
7/8/11	17.6	38.6	-76.4	0.1	0.0	22.0	2.5	9.2	1.8	0.8	1.5	1.1	-	-	217.0
7/9/11	0.9	37.9	-76.2	0.1	0.1	0.1	0.3	0.0	1.3	0.0	19.0	3.1	-	-	-
7/9/11	2.7	37.9	-76.2	0.1	0.0	0.0	0.5	0.0	0.1	0.0	16.7	2.6	-	-	-
7/9/11	5.0	37.9	-76.2	0.1	0.0	1.5	0.6	0.0	4.3	0.0	13.6	2.5	1497.1	560.3	209.2
7/9/11	7.7	37.9	-76.2	0.1	0.1	0.0	0.7	0.0	11.8	0.0	9.4	2.8	480.1	357.9	59.8
7/9/11	9.9	37.9	-76.2	0.1	0.1	0.0	1.1	0.1	0.8	0.0	2.1	1.3	497.4	0.0	402.1
7/9/11	12.6	37.9	-76.2	0.2	0.0	12.0	1.8	0.0	1.4	0.0	1.7	1.0	84.5	0.0	181.9
7/9/11	16.0	37.9	-76.2	0.3	1.3	11.5	1.4	0.0	0.5	0.1	1.8	1.2	-	-	49.2
7/9/11	18.9	37.9	-76.2	0.4	0.2	11.6	1.5	0.0	0.6	0.0	1.7	1.0	-	-	69.4
7/10/11	1.0	39.0	-76.4	0.2	1.5	4.4	0.4	0.0	0.4	0.0	17.9	5.1	-	-	-
7/10/11	3.1	39.0	-76.4	0.2	1.1	5.5	0.7	0.0	0.2	0.0	11.2	4.6	-	-	-
7/10/11	5.0	39.0	-76.4	0.1	0.4	12.5	1.1	0.0	1.1	0.0	5.8	4.0	1567.8	386.0	43.0
7/10/11	7.0	39.0	-76.4	0.1	0.4	19.1	1.3	0.0	1.7	0.9	4.0	2.9	391.7	51.5	192.6
7/10/11	9.0	39.0	-76.4	0.1	0.2	28.6	3.4	5.8	4.8	3.9	1.6	1.0	831.5	0.0	435.5
7/10/11	12.5	39.0	-76.4	0.1	0.0	28.7	3.7	14.2	2.3	3.0	1.5	1.1	0.0	369.6	172.5
7/10/11	16.0	39.0	-76.4	0.1	0.9	28.6	3.5	15.7	2.4	2.6	1.3	1.0	-	-	133.5
7/10/11	19.5	39.0	-76.4	0.1	0.1	28.7	3.3	21.1	2.0	1.9	1.3	1.0	-	-	206.7
7/11/11	1.3	39.0	-76.4	0.2	0.7	5.3	0.2	0.0	3.2	0.0	16.7	5.5	-	-	-
7/11/11	2.9	39.0	-76.4	0.2	0.8	3.4	0.2	0.0	1.5	0.0	16.7	5.0	-	-	-
7/11/11	5.1	39.0	-76.4	0.1	0.7	4.1	5.2	0.0	0.7	0.0	14.4	4.9	2808.6	488.9	167.5
7/11/11	6.0	39.0	-76.4	0.2	5.7	6.4	0.9	0.0	0.6	0.0	12.8	4.6	1441.7	371.8	93.5
7/11/11	6.9	39.0	-76.4	0.2	0.4	20.4	1.1	0.0	0.7	1.0	7.0	3.0	1961.3	327.9	82.0
7/11/11	7.8	39.0	-76.4	0.2	0.2	21.7	1.8	0.3	0.8	1.8	4.7	2.3	556.0	21.3	106.5
7/11/11	8.9	39.0	-76.4	0.1	0.2	23.9	2.2	0.1	2.3	2.8	4.1	2.2	-	-	328.2
7/11/11	10.3	39.0	-76.4	0.1	0.0	29.0	3.9	1.4	9.8	4.8	2.5	1.7	-	-	435.5
8/8/11	0.8	38.6	-76.4	0.0	0.2	0.0	-0.3	0.0	2.1	0.0	46.5	7.2	-	-	-
8/8/11	3.0	38.6	-76.4	0.0	0.3	0.0	-0.3	0.0	2.0	0.0	18.0	6.0	-	-	-
8/8/11	5.1	38.6	-76.4	0.1	0.1	0.2	0.2	0.0	1.0	0.0	12.2	4.6	127.9	19.8	13.5

Date	Depth	Latitude	Longitude	NO_2^-	NO_3^-	NH_4^+	SRP	DS	DFe	DMn	Chl-a	Pheo	OxyPP	AnoxyPP	DarkPP
(mm/dd/yr)	(m)	(degree)				($\mu mol\ l^{-1}$)					($\mu g\ l^{-1}$)			($nmol\ l^{-1}\ h^{-1}$)	
8/8/11	8.1	38.6	-76.4	0.1	0.2	0.2	-0.2	0.0	6.3	0.0	10.1	4.7	91.0	10.6	14.3
8/8/11	10.9	38.6	-76.4	0.1	0.1	9.6	0.8	0.0	0.1	0.0	3.0	3.1	38.6	0.0	10.3
8/8/11	14.0	38.6	-76.4	0.0	0.3	21.4	2.6	6.9	3.5	2.7	1.8	1.3	75.4	0.0	60.3
8/8/11	16.0	38.6	-76.4	0.0	0.1	22.2	7.1	9.6	1.7	1.9	1.5	1.1	-	-	28.3
8/8/11	18.1	38.6	-76.4	0.1	0.3	22.1	2.7	9.9	1.2	1.7	2.3	1.8	-	-	45.3
8/30/11	1.0	38.6	-76.4	0.8	0.3	0.0	9.2	0.0	0.0	0.0	37.5	5.7	-	-	-
8/30/11	3.0	38.6	-76.4	4.6	0.9	1.4	0.6	0.0	0.0	0.0	12.3	3.7	-	-	-
8/30/11	5.0	38.6	-76.4	4.5	1.1	2.5	0.2	0.0	0.0	0.0	8.2	3.2	37.8	5.1	24.7
8/30/11	8.5	38.6	-76.4	4.1	0.8	2.9	0.2	0.0	0.2	0.0	4.8	3.0	28.9	4.1	23.9
8/30/11	10.9	38.6	-76.4	3.7	0.6	5.2	0.3	0.0	0.0	0.0	4.0	3.0	16.1	0.0	21.7
8/30/11	12.9	38.6	-76.4	3.2	0.6	7.7	0.4	0.0	0.5	0.0	2.9	3.5	12.9	0.0	23.4
8/30/11	14.8	38.6	-76.4	3.1	0.4	6.5	1.3	0.0	1.5	0.0	1.6	3.0	-	-	27.5
8/30/11	17.6	38.6	-76.4	3.1	0.5	6.8	0.7	0.0	0.0	0.0	1.6	3.0	-	-	23.2
9/21/11	0.9	38.6	-76.4	2.8	45.6	0.2	0.1	0.0	0.1	0.0	14.7	3.2	-	-	-
9/21/11	3.0	38.6	-76.4	2.8	40.4	1.5	0.4	0.0	0.3	0.0	5.9	1.7	-	-	-
9/21/11	4.9	38.6	-76.4	3.1	32.2	0.1	0.2	0.0	0.0	0.0	2.4	2.1	1.9	0.0	9.2
9/21/11	8.4	38.6	-76.4	2.8	21.2	0.0	-0.1	0.0	0.0	0.0	3.0	2.9	5.5	0.0	17.3
9/21/11	11.6	38.6	-76.4	3.3	18.6	2.4	0.2	0.0	1.5	0.0	2.3	3.6	8.5	0.0	18.3
9/21/11	12.9	38.6	-76.4	3.0	18.8	0.2	0.4	0.0	0.0	0.0	1.7	2.8	7.2	0.0	15.9
9/21/11	15.5	38.6	-76.4	2.5	18.8	0.3	0.5	0.0	0.0	0.0	1.6	2.6	-	-	19.2
9/21/11	16.6	38.6	-76.4	2.5	18.9	0.0	0.5	0.0	0.0	0.0	1.6	2.5	-	-	17.3

Table C.2: Bottom water chemistry and sediment-water flux.

Date	Cast	Latitude	Longitude	Temperature	Salinity	Oxygen	N_2	O_2	DIC	NOx	NH_4^+	SRP	DS
(mm/dd/yr)		(degree)		(°C)		(mg l^{-1})	(µmol N_2-N m^{-2} h^{-1})			(µmol m^{-2} h^{-1})			
05/17/10	Channel	38.6	-76.4	15.5	16.2	2.4	14.9	-1386.3	674.8	-34.1	283.2	-	-
06/07/10	Channel	38.6	-76.4	17.7	19.1	0.6	-	-	1715.0	-10.2	278.0	-	-
06/16/10	Channel	38.6	-76.4	19.3	18.2	0.2	-	-	1258.7	0.4	206.8	-	-
07/10/10	Shoal	37.8	-76.2	26.3	19.6	0.4	-	-	2488.1	19.8	221.5	36.8	-
07/10/10	Middle	37.8	-76.2	25.4	22.5	1.1	-	-	1756.6	-20.3	254.0	23.9	-
07/10/10	Channel	37.8	-76.2	25.2	22.9	1.1	-	-	2383.2	24.7	288.3	9.0	-
07/11/10	Shoal	38.6	-76.5	26.7	12.2	5.3	17.6	-790.1	1648.5	0.1	242.8	-3.2	-
07/11/10	Middle	38.6	-76.5	25.0	17.5	0.1	-	-	623.0	-4.4	164.4	15.1	-
07/11/10	Channel	38.6	-76.4	25.2	20.2	0.1	-	-	6894.2	0.8	1319.4	329.1	478.2
07/12/10	Shoal	38.2	-76.4	27.1	13.9	5.6	22.5	-242.1	55.7	-1.1	88.7	-34.4	-
07/12/10	Middle	38.2	-76.3	25.4	19.8	0.1	-	-	948.5	-3.4	169.1	12.7	-
07/12/10	Channel	38.2	-76.3	25.7	21.7	0.3	-	-	958.7	-16.8	260.2	104.7	-
07/13/10	Shoal	38.3	-76.3	26.0	17.3	0.8	-	-	710.5	-0.7	179.9	-13.3	-
07/13/10	Middle	38.3	-76.3	25.7	19.8	0.1	-	-	1310.9	-4.9	86.7	30.1	151.7
07/13/10	Channel	38.3	-76.3	25.9	21.1	0.1	-	-	2771.5	-14.3	316.2	67.1	230.5
07/14/10	Shoal	39.0	-76.4	26.7	11.4	5.6	-51.4	-1646.8	7591.8	-6.9	1144.6	233.3	-
07/14/10	Middle	39.0	-76.4	23.9	17.7	0.1	-	-	179.2	4.9	48.2	-2.1	0.0
07/14/10	Channel	39.0	-76.4	23.9	17.1	0.1	-	-	104.4	1.8	139.4	5.0	0.0
08/05/10	Channel	38.6	-76.4	26.0	18.6	0.0	-	-	-	-	-	-	-
08/31/10	Channel	38.6	-76.4	26.2	22.9	0.1	-	-	3404.1	-10.6	474.0	63.0	253.9
10/18/10	Channel	38.6	-76.4	18.8	16.6	6.1	46.5	-752.3	786.3	-9.7	144.4	-2.8	-
04/18/11	Channel	38.6	-76.4	10.2	12.9	4.6	111.5	-1342.6	2346.7	-48.1	249.1	49.1	-
04/18/11	Channel	38.6	-76.4	10.2	12.9	4.6	127.6	-1055.8	2523.8	-82.2	358.7	32.6	-
05/24/11	Channel	38.6	-76.4	16.3	14.2	0.3	2.2	-501.6	2271.8	9.2	281.7	53.8	452.5
05/24/11	Channel	38.6	-76.4	16.3	14.2	0.3	379.8	-562.8	1984.8	-423.8	299.6	54.4	0.9
6/14/11	Channel	38.6	-76.4	19.8	18.6	0.1	-0.2	0.0	1468.5	-20.2	172.3	16.4	544.1
6/14/11	Channel	38.6	-76.4	19.8	18.6	0.1	398.5	-3.0	2164.8	-442.4	423.6	55.8	-4.0

Date (mm/dd/yr)	Cast	Latitude (degree)	Longitude	Temperature (°C)	Salinity	Oxygen (mg l^{-1})	N_2 (µmol N_2-N m^{-2} h^{-1})	O_2	DIC	NOx (µmol m^{-2} h^{-1})	NH_4^+	SRP	DS
7/8/11	Channel	38.6	-76.4	22.9	19.4	0.1	11.5	-51.4	1733.0	-23.9	175.6	55.1	460.2
7/8/11	Channel	38.6	-76.4	22.9	19.4	0.1	106.6	-23.5	2855.8	-181.8	494.6	55.9	64.0
08/08/11	Channel	38.6	-76.4	25.1	19.6	0.1	-	-	1975.8	-1.6	314.9	33.1	-79.8
08/08/11	Channel	38.6	-76.4	25.1	19.6	0.1	-	-	3232.7	-193.3	576.0	27.9	-24.3
8/30/11	Channel	38.6	-76.4	25.4	15.8	3.7	6.8	-1454.3	2017.4	-29.4	319.1	7.8	-
8/30/11	Channel	38.6	-76.4	25.4	15.8	3.7	93.7	-1472.9	4389.1	-348.3	848.2	17.3	-
09/21/11	Channel	38.6	-76.4	24.5	13.4	2.4	8.8	-1860.4	2126.9	-81.7	387.1	24.2	-
09/21/11	Channel	38.6	-76.4	24.5	13.4	2.4	237.7	-1752.6	2192.5	-451.4	509.0	32.6	-

Bibliography

Abril, G., M. Nogueira, H. Etcheber, G. Cabeçadas, E. Lemaire, and M. J. Brogueira. 2002. Behaviour of organic carbon in nine contrasting European estuaries. Estuar. Coast. Shelf Sci. **54**: 241–262.

Adolf, J. E., D. K. Stoecker, and L. W. Harding. 2006a. The balance of autotrophy and heterotrophy during mixotrophic growth of *Karlodinium micrum* (Dinophyceae). J. Plankton Res. **28**: 737–751.

Adolf, J. E., C. L. Yeager, W. D. Miller, M. E. Mallonee, and L. W. J. Harding. 2006b. Environmental forcing of phytoplankton floral composition, biomass, and primary productivity in Chesapeake Bay, USA. Estuar. Coast. Shelf Sci. **67**: 108–122.

Alldredge, A., T. Cowles, S. MacIntyre S, J. Rines, P. Donaghay, C. Greenlaw, D. Holliday, M. Dekshenieks, J. Sullivan, and J. Zaneveld. 2002. Occurrence and mechanisms of formation of a dramatic thin layer of marine snow in a shallow Pacific fjord. Mar. Ecol. Prog. Ser. **233**: 1–12.

Alonso-Sáez, L., P. E. Galand, E. O. Casamayor, C. Pedrós-Alió, and S. Bertilsson. 2010. High bicarbonate assimilation in the dark by Arctic bacteria. ISME J. **4**: 1581–1590.

Anderson, L. G., P. O. J. Hall, A. Iverfeldt, M. M. R. van der Loeff, B. Sundby, and S. F. G. Westerlund. 1986. Benthic respiration measured by total carbonate production. Limnol. Oceanogr. **31**: 319–329.

Andersson, M. G. I., N. Brion, and J. J. Middelburg. 2006. Comparison of nitrifier activity versus growth in the Scheldt estuary—a turbid, tidal estuary in northern Europe. Aquat. Microb. Ecol. **42**: 149–158.

An, S. M., and W. S. Gardner. 2002. Dissimilatory nitrate reduction to ammonium (DNRA) as a nitrogen link, versus denitrification as a sink in a shallow estuary (Laguna Madre/Baffin Bay, Texas). Mar. Ecol. Prog. Ser. **237**: 41–50.

Apple, J. K., P. A. del Giorgio, and W. M. Kemp. 2006. Temperature regulation of bacterial production, respiration, and growth efficiency in a temperate salt-marsh estuary. Aquat. Microb. Ecol. **43**: 243–254.

Arar, E. J., and G. B. Collins. 1997. In vitro determination of chlorophyll a and pheophytin a in marine and freshwater algae by fluorescence. U.S. Environmental Protection Agency method 445.0.

Baines, and M. L. Pace. 1991. The production of dissolved organic matter by phytoplankton and its importance to bacteria: patterns across marine and freshwater systems. Limnol. Oceanogr. **36**: 1078–1090.

Baird, D., R. R. Christian, C. H. Peterson, and G. A. Johnson. 2004. Consequences of hypoxia on estuarine ecosystem function: energy diversion from consumers to microbes. Ecol. Appl. **14**: 805–822.

Baird, D., R. E. Ulanowicz, and W. R. Boynton. 1995. Seasonal nitrogen dynamics in Chesapeake Bay: a network approach. Estuar. Coast. Shelf Sci. **41**: 137–162.

Bastviken, D., M. Olsson, and L. Tranvik. 2003. Simultaneous measurements of organic carbon mineralization and bacterial production in oxic and anoxic lake sediments. Microb. Ecol. **46**: 73–82.

Bauer, J. E., W.-J. Cai, P. A. Raymond, T. S. Bianchi, C. S. Hopkinson, and P. A. G. Regnier. 2013. The changing carbon cycle of the coastal ocean. Nature **504**: 61–70.

Benz, M., A. Brune, and B. Schink. 1998. Anaerobic and aerobic oxidation of ferrous iron at neutral pH by chemoheterotrophic nitrate-reducing bacteria. Arch. Microbiol. **169**: 159–165.

Berg, G. M., P. M. Glibert, N. O. G. Jorgensen, M. Balode, and I. Purina. 2001. Variability in inorganic and organic nitrogen uptake associated with riverine nutrient input in the Gulf of Riga, Baltic Sea. Estuaries **24**: 204.

Bertilsson, S., O. Berglund, D. M. Karl, and S. W. Chisholm. 2003. Elemental composition of marine *Prochlorococcus* and *Synechococcus*: Implications for the ecological stoichiometry of the sea. Limnol. Oceanogr. **48**: 1721–1731.

Bever, A. J., M. A. M. Friedrichs, C. T. Friedrichs, M. E. Scully, and L. W. J. Lanerolle. 2013. Combining observations and numerical model results to improve estimates of hypoxic volume within the Chesapeake Bay, USA. J. Geophys. Res. Oceans **118**: 4924–4944.

Bochdansky, A. B., and S. M. Bollens. 2009. Thin layer formation during runaway stratification in the tidally dynamic San Francisco Estuary. J. Plankton Res. **31**: 1385 – 1390.

Bock, E. 1976. Growth of *Nitrobacter* in the presence of organic matter. II. Chemoorganotrophic growth of *Nitrobacter agilis*. Arch. Microbiol. **108**: 305–312.

Boesch, D. F. 2002. Challenges and opportunities for science in reducing nutrient over-enrichment of coastal ecosystems. Estuaries **25**: 886–900.

Boicourt, W. C. 1992. The influences of circulation processes on dissolved oxygen in Chesapeake Bay, p. 7–59. *In* Dissolved Oxygen in Chesapeake Bay. Maryland Sea Grant, College Park, MD.

Bourgault, D., F. Cyr, P. S. Galbraith, and E. Pelletier. 2012. Relative importance of pelagic and sediment respiration in causing hypoxia in a deep estuary. J. Geophys. Res. **117**: C08033.

Bouskill, N. J., D. Eveillard, G. O'Mullan, G. A. Jackson, and B. B. Ward. 2011. Seasonal and annual reoccurrence in betaproteobacterial ammonia-oxidizing bacterial population structure. Environ. Microbiol. **13**: 872–886.

Bouvier, T. C., and P. A. Del Giorgio. 2002. Compositional changes in free-living bacterial communities along a salinity gradient in two temperate estuaries. Limnol. Oceanogr. **47**: 453–470.

Boynton, W. R., and E. M. Bailey. 2008. Sediment oxygen and nutrient exchange measurements from Chesapeake Bay, tributary rivers and Maryland coastal bays: development of a comprehensive database and analysis of factors controlling patterns and magnitude of sediment-water exchanges. Technical Report No. TS-542-08. Technical Report No. TS-542-08 University of Maryland Center for Environmental Science.

Boynton, W. R., and W. M. Kemp. 1985. Nutrient regeneration and oxygen consumption by sediments along an estuarine salinity gradient. Mar. Ecol. Prog. Ser. **23**: 45–55.

Boynton, W. R., and W. M. Kemp. 2000. Influence of river flow and nutrient loads on selected ecosystem processes, p. 269–298. *In* Estuarine science: a synthetic approach to research and practice. Island Press, Washington, DC, USA.

Bradley, P. B., M. P. Sanderson, M. E. Frischer, J. Brofft, M. G. Booth, L. J. Kerkhof, and D. A. Bronk. 2010. Inorganic and organic nitrogen uptake by phytoplankton and heterotrophic bacteria in the stratified Mid-Atlantic Bight. Estuar. Coast. Shelf Sci. **88**: 429–441.

Bräuer, S. L., K. Kranzler, N. Goodson, D. Murphy, H. M. Simon, A. M. Baptista, and B. M. Tebo. 2013. Dark carbon fixation in the Columbia River's estuarine turbidity maxima: molecular characterization of red-type *cbbL* genes and measurement of DIC uptake rates in response to added electron donors. Estuaries Coasts **36**: 1073–1083.

Brewer, P. G., and D. W. Spencer. 1971. Colorimetric determination of manganese in anoxic waters. Limnol. Oceanogr. **16**: 107–110.

Bronk, D. A., J. H. See, P. Bradley, and L. Killberg. 2007. DON as a source of bioavailable nitrogen for phytoplankton. Biogeosciences **4**: 283–296.

Bruckner, C. G., K. Mammitzsch, G. Jost, J. Wendt, M. Labrenz, and K. Jürgens. 2013. Chemolithoautotrophic denitrification of epsilonproteobacteria in marine pelagic redox gradients. Environ. Microbiol. **15**: 1505–1513.

Brune, A., P. Frenzel, and H. Cypionka. 2000. Life at the oxic–anoxic interface: microbial activities and adaptations. FEMS Microbiol. Rev. **24**: 691–710.

Burdige, D. J. 1993. The biogeochemistry of manganese and iron reduction in marine sediments. Earth-Sci. Rev. **35**: 249–284.

Caffrey, J. M. 2004. Factors controlling net ecosystem metabolism in U.S. estuaries. Estuaries **27**: 90–101.

Cai, W.-J., and Y. Wang. 1998. The chemistry, fluxes, and sources of carbon dioxide in the estuarine waters of the Satilla and Altamaha Rivers, Georgia. Limnol. Oceanogr. **43**: 657–668.

Camacho, A., J. Erez, A. Chicote, M. Florín, M. M. Squires, C. Lehmann, and R. Backofen. 2001. Microbial microstratification, inorganic carbon photoassimilation and dark carbon fixation at the chemocline of the meromictic Lake Cadagno (Switzerland) and its relevance to the food web. Aquat. Sci. **63**: 91–106.

Canfield, D. E., E. Kristensen, and B. Thamdrup. 2005. Aquatic geomicrobiology, Elsevier Academic Press, San Diego, California, USA.

Capone, D. G., and R. P. Kiene. 1988. Comparison of microbial dynamics in marine and freshwater sediments: contrasts in anaerobic carbon catabolism. Limnol. Oceanogr. **33**: 725–749.

Carlson, C. A., N. R. Bates, H. W. Ducklow, and D. A. Hansell. 1999. Estimation of bacterial respiration and growth efficiency in the Ross Sea, Antarctica. Aquat. Microb. Ecol. **19**: 229–244.

Casamayor, E. O. 2010. Vertical distribution of planktonic autotrophic thiobacilli and dark CO_2 fixation rates in lakes with oxygen-sulfide interfaces. Aquat. Microb. Ecol. **59**: 217–228.

Casamayor, E. O., J. García-Cantizano, J. Mas, and C. Pedrós-Alió. 2001. Primary production in estuarine oxic/anoxic interfaces: contribution of microbial dark CO_2 fixation in the Ebro River salt wedge estuary. Mar. Ecol. Prog. Ser. **215**: 49–56.

Casamayor, E. O., M. Lliros, A. Picazo, A. Barberan, C. M. Borrego, and A. Camacho. 2012. Contribution of deep dark fixation processes to overall CO_2 incorporation and large vertical changes of microbial populations in stratified karstic lakes. Aquat. Sci. **74**: 61–75.

Chao, S.-Y., and T. Paluszkiewicz. 1991. The hydraulics of density currents over estuarine sills. J. Geophys. Res. Oceans **96**: 7065–7076.

Christensen, P. B., S. Rysgaard, N. P. Sloth, T. Dalsgaard, and S. Schwrter. 2000. Sediment mineralization, nutrient fluxes, denitrification and dissimilatory nitrate reduction to ammonium in an estuarine fjord with sea cage trout farms. Aquat. Microb. Ecol. **21**: 73–84.

Chrost, R. H., and M. A. Faust. 1983. Organic carbon release by phytoplankton: its composition and utilization by bacterioplankton. J. Plankton Res. **5**: 477–493.

Church, M. J., D. A. Hutchins, and H. W. Ducklow. 2000. Limitation of bacterial growth by dissolved organic matter and iron in the Southern Ocean. Appl. Environ. Microbiol. **66**: 455 –466.

Cloern, J. E. 2001. Our evolving conceptual model of the coastal eutrophication problem. Mar. Ecol. Prog. Ser. **210**: 223–253.

Cloern, J. E., B. E. Cole, and R. S. Oremland. 1983. Autotrophic processes in meromictic Big Soda Lake, Nevada. Limnol. Oceanogr. **28**: 1049–1061.

Colt, J. 1984. Computation of dissolved gas concentrations in water as functions of temperature, salinity, and pressure. Am. Fish. Soc. Spec. Publ. **no. 14**.

Conley, D. J., J. Carstensen, G. Ærtebjerg, P. B. Christensen, T. Dalsgaard, J. L. S. Hansen, and A. B. Josefson. 2007. Long-term changes and impacts of hypoxia in Danish coastal waters. Ecol. Appl. **17**: S165–S184.

Conley, D. J., J. Carstensen, R. Vaquer-Sunyer, and C. M. Duarte. 2009. Ecosystem thresholds with hypoxia, p. 21–29. *In* J.H. Andersen and D.J. Conley [eds.], Eutrophication in Coastal Ecosystems. Springer Netherlands.

Cooper, S. R. 1995. Chesapeake Bay watershed historical land use: impact on water quality and diatom communities. Ecol. Appl. **5**: 703.

Cooper, S. R., and G. S. Brush. 1993. A 2,500-year history of anoxia and eutrophication in Chesapeake Bay. Estuaries **16**: 617.

Cornwell, J. C., D. J. Conley, M. S. Owens, and J. C. Stevenson. 1996. A sediment chronology of the eutrophication of Chesapeake Bay. Estuaries **19**: 488.

Cornwell, J. C., W. M. Kemp, and T. M. Kana. 1999. Denitrification in coastal ecosystems: methods, environmental controls, and ecosystem level controls, a review. Aquat. Ecol. **33**: 41–54.

Cornwell, J. C., and P. A. Sampou. 1995. Environmental controls on iron sulfide mineral formation in a coastal plain estuary, p. 224–242. *In* Geochemical transformations of sedimentary sulfur. American Chemical Society.

Cowan, J. I., and W. Boynton. 1996. Sediment-water oxygen and nutrient exchanges along the longitudinal axis of Chesapeake Bay: seasonal patterns, controlling factors and ecological significance. Estuaries **19**: 562–580.

Cronin, W. B., and D. W. Pritchard. 1975. Additional statics on the dimensions of the Chesapeake Bay and its tributaries: cross-section widths and segment volumes per meter depth. Chesap. Bay Inst. Special Report **42**, Reference 75-3.

Crump, B. C., J. A. Baross, and C. A. Simenstad. 1998. Dominance of particle-attached bacteria in the Columbia River estuary, USA. Aquat. Microb. Ecol. **14**: 7–18.

Crump, B. C., C. S. Hopkinson, M. L. Sogin, and J. E. Hobbie. 2004. Microbial biogeography along an estuarine salinity gradient: combined influences of bacterial growth and residence time. Appl. Environ. Microbiol. **70**: 1494–1505.

Crump, B. C., C. Peranteau, B. Beckingham, and J. C. Cornwell. 2007. Respiratory succession and community succession of bacterioplankton in seasonally anoxic estuarine waters. Appl. Environ. Microbiol. **73**: 6802–6810.

Culver, M. E., and M. J. Perry. 1999. The response of photosynthetic absorption coefficients to irradiance in culture and in tidally mixed estuarine waters. Limnol. Oceanogr. **44**: 24–36.

Diaz, R. J., and R. Rosenberg. 2008. Spreading dead zones and consequences for marine ecosystems. Science **321**: 926 –929.

Dickson, A. G., C. L. Sabine, and J. R. Christian. 2007. Guide to best practices for ocean CO_2 measurements. PICES Spec. Publ. **3**: 191.

Drake, L. A., K. H. Choi, A. G. E. Haskell, and F. C. Dobbs. 1998. Vertical profiles of virus-like particles and bacteria in the water column and sediments of Chesapeake Bay. Aquat. Microb. Ecol. **16**: 17–25.

Dugdale, R. C., F. P. Wilkerson, V. E. Hogue, and A. Marchi. 2007. The role of ammonium and nitrate in spring bloom development in San Francisco Bay. Estuar. Coast. Shelf Sci. **73**: 17–29.

Durham, W. M., and R. Stocker. 2012. Thin phytoplankton layers: characteristics, mechanisms, and consequences. Annu. Rev. Mar. Sci. **4**: 177–207.

Elliott, D. T., J. J. Pierson, and M. R. Roman. 2013. Copepods and hypoxia in Chesapeake Bay: abundance, vertical position and non-predatory mortality. J. Plankton Res. **35**: 1027–1034.

Van den Ende, F. P., J. Meier, and H. van Gemerden. 1997. Syntrophic growth of sulfate-reducing bacteria and colorless sulfur bacteria during oxygen limitation. FEMS Microbiol. Ecol. **23**: 65–80.

EPA. 1997. Methods for the determination of chemical substances in marine and estuarine environmental matrices - 2nd edition.

Epping, E. H. G., V. Schoemann, and H. de Heij. 1998. Manganese and iron oxidation during benthic oxygenic photosynthesis. Estuar. Coast. Shelf Sci. **47**: 753–767.

Etemad-Shahidi, A., and J. Imberger. 2002. Anatomy of turbulence in a narrow and strongly stratified estuary. J. Geophys. Res. Oceans **107**: 7–1–7–16.

Eyre, B. D., and A. J. P. Ferguson. 2009. Denitrification efficiency for defining critical loads of carbon in shallow coastal ecosystems. Hydrobiologia **629**: 137–146.

Fan, C., P. M. Glibert, and J. M. Burkholder. 2003. Characterization of the affinity for nitrogen, uptake kinetics, and environmental relationships for Prorocentrum minimum in natural blooms and laboratory cultures. Harmful Algae **2**: 283–299.

Feinberg, L., and H. Dam. 1998. Effects of diet on dimensions, density and sinking rates of fecal pellets of the copepod *Acartia tonsa*. Mar. Ecol. Prog. Ser. **175**: 87–96.

Fisher, T. R., A. B. Gustafson, K. Sellner, R. Lacouture, L. W. Haas, R. L. Wetzel, R. Magnien, D. Everitt, B. Michaels, and R. Karrh. 1999. Spatial and temporal variation of resource limitation in Chesapeake Bay. Mar. Biol. **133**: 763–778.

Fisher, T. R., J. D. Hagy, and E. Rochelle-Newall. 1998. Dissolved and particulate organic carbon in Chesapeake Bay. Estuaries **21**: 215–229.

Fisher, T. R., L. W. Harding, D. W. Stanley, and L. G. Ward. 1988. Phytoplankton, nutrients, and turbidity in the Chesapeake, Delaware and Hudson estuaries. Estuar. Coast. Shelf Sci. **27**: 61–93.

Fisher, T. R., E. R. Peele, J. W. Ammerman, and L. W. J. Harding. 1992. Nutrient limitation of phytoplankton in Chesapeake Bay. Mar. Ecol. Prog. Ser. **82**: 51–63.

Fortunato, C. S., and B. C. Crump. 2011. Bacterioplankton community variation across river to ocean environmental gradients. Microb. Ecol. **62**: 374–382.

García-Cantizano, J., E. O. Casamayor, J. M. Gasol, R. Guerrero, and C. Pedrós-Alió. 2005. Partitioning of CO_2 incorporation among planktonic microbial guilds and estimation of in situ specific growth rates. Microb. Ecol. **50**: 230–241.

Gardner, W. S., M. J. McCarthy, S. An, D. Sobolev, K. S. Sell, and D. Brock. 2006. Nitrogen fixation and dissimilatory nitrate reduction to ammonium (DNRA) support nitrogen dynamics in Texas estuaries. Limnol. Oceanogr. **51**: 558–568.

Gattuso, J.-P., M. Frankignoulle, and R. Wollast. 1998. Carbon and carbonate metabolism in coastal aquatic ecosystems. Annu. Rev. Ecol. Syst. **29**: 405–434.

Gavis, J., and V. Grant. 1986. Sulfide, iron, manganese, and phosphate in the deep water of the Chesapeake Bay during anoxia. Estuar. Coast. Shelf Sci. **23**: 451–463.

Giblin, A. E., C. R. Tobias, B. Song, N. Weston, G. T. Banta, and V. H. Rivera-Monroy. 2013. The importance of dissimilatory nitrate reduction to ammonium (DNRA) in the nitrogen cycle of coastal ecosystems. Oceanography **26**: 124–131.

Giblin, A. E., N. B. Weston, G. T. Banta, J. Tucker, and C. S. Hopkinson. 2010. The effects of salinity on nitrogen losses from an oligohaline estuarine sediment. Estuaries Coasts **33**: 1054–1068.

Gibson, J. r., and R. G. Najjar. 2000. The response of Chesapeake Bay salinity to climate-induced changes in streamflow. Limnol Ocean. **45**: 1764–1772.

Gilmour, S. G. 1996. The interpretation of Mallows's C_p-statistic. J. R. Stat. Soc. Ser. Stat. **45**: 49–56.

Del Giorgio, P. A., and T. C. Bouvier. 2002. Linking the physiologic and phylogenetic successions in free-living bacterial communities along an estuarine salinity gradient. Limnol. Oceanogr. **47**: 471–486.

Glibert, P. M. 1982. Regional studies of daily, seasonal and size fraction variability in ammonium remineralization. Mar. Biol. **70**: 209–222.

Glibert, P. M. 2010. Long-term changes in nutrient loading and stoichiometry and their relationships with changes in the food web and dominant pelagic fish species in the San Francisco estuary, California. Rev. Fish. Sci. **18**: 211–232.

Glibert, P. M., J. Harrison, C. Heil, and S. Seitzinger. 2006. Escalating worldwide use of urea – a global change contributing to coastal eutrophication. Biogeochemistry **77**: 441–463.

Gobler, C., T. Davis, S. Deonarine, M. Saxton, P. Lavrentyev, and F. Jochem. 2008. Grazing and virus-induced mortality of microbial populations before and during the onset of annual hypoxia in Lake Erie. Aquat. Microb. Ecol. 117–128.

Goodrich, D. M., W. C. Boicourt, P. Hamilton, and D. W. Pritchard. 1987. Wind-induced destratification in Chesapeake Bay. J. Phys. Oceanogr. **17**: 2232–2240.

Gottschal, J. C., and R. Szewzyk. 1985. Growth of a facultative anaerobe under oxygen-limiting conditions in pure culture and in co-culture with a sulfate-reducing bacterium. FEMS Microbiol. Lett. **31**: 159–170.

Goyet, C., and S. D. Hacker. 1992. Procedure for calibration of a coulometric system used for total inorganic carbon measurements of seawater. Mar. Chem. **38**: 37–51.

Goyet, C., and A. K. Snover. 1993. High-accuracy measurements of total dissolved inorganic carbon in the ocean: comparison of alternate detection methods. Mar. Chem. **44**: 235–242.

Griffin, B. M., J. Schott, and B. Schink. 2007. Nitrite, an electron donor for anoxygenic photosynthesis. Science **316**: 1870.

Hagy, J. D. 2002. Eutrophication, hypoxia, and trophic transfer efficiency in Chesapeake Bay. Ph.D. thesis. University of Maryland Center for Environmental Science.

Hagy, J. D., W. R. Boynton, and D. A. Jasinski. 2005. Modelling phytoplankton deposition to Chesapeake Bay sediments during winter–spring: interannual variability in relation to river flow. Estuar. Coast. Shelf Sci. **62**: 25–40.

Hagy, J. D., W. R. Boynton, C. W. Keefe, and K. V. Wood. 2004. Hypoxia in Chesapeake Bay, 1950-2001: long-term change in relation to nutrient loading and river flow. Estuaries **27**: 634–658.

Hamdan, L. J., and R. B. Jonas. 2006. Seasonal and interannual dynamics of free-living bacterioplankton and microbially labile organic carbon along the salinity gradient of the Potomac River. Estuaries Coasts **29**: 40–53.

Hansen, J. W., B. Thamdrup, and B. B. Jørgensen. 2000. Anoxic incubation of sediment in gas-tight plastic bags: a method for biogeochemical process studies. Mar. Ecol. Prog. Ser. **208**: 273–282.

Harding, L. W. 1994. Long-term trends in the distribution of phytoplankton in Chesapeake Bay: roles of light, nutrients and streamflow. Mar. Ecol. Prog. Ser. **104**: 267–291.

Harding, L. W., M. E. Mallonee, and E. S. Perry. 2002. Toward a predictive understanding of primary productivity in a temperate, partially stratified estuary. Estuar. Coast. Shelf Sci. **55**: 437–463.

Hargrave, B. T., and G. A. Phillips. 1981. Annual in situ carbon dioxide and oxygen flux across a subtidal marine sediment. Estuar. Coast. Shelf Sci. **12**: 725–737.

Harvey, H. R., J. H. Tuttle, and J. T. Bell. 1995. Kinetics of phytoplankton decay during simulated sedimentation: changes in biochemical composition and microbial activity under oxic and anoxic conditions. Geochim. Cosmochim. Acta **59**: 3367–3377.

Hewson, I., E. M. Eggleston, M. Doherty, D. Y. Lee, M. Owens, J. P. Shapleigh, J. C. Cornwell, and B. C. Crump. 2014. Metatranscriptomic analyses of plankton communities inhabiting surface and subpycnocline waters of the Chesapeake Bay during oxic-anoxic-oxic transitions. Appl. Environ. Microbiol. **80**: 328–338.

Holland, A., A. Shaughnessy, and M. Hiegel. 1987. Long-term variation in mesohaline Chesapeake Bay macrobenthos: spatial and temporal patterns. Estuaries Coasts **10**: 227–245.

Hopkinson, C. S. 1987. Nutrient regeneration in shallow-water sediments of the estuarine plume region of the nearshore Georgia Bight, USA. Mar. Biol. **94**: 127–142.

Hopkinson, C. S., I. Buffam, J. Hobbie, J. Vallino, M. Perdue, B. Eversmeyer, F. Prahl, J. Covert, R. Hodson, M. A. Moran, E. Smith, J. Baross, B. Crump, S. Findlay, and K. Foreman. 1998. Terrestrial inputs of organic matter to coastal ecosystems: an intercomparison of chemical characteristics and bioavailability. Biogeochemistry **43**: 211–234.

Hopkinson, C. S., and E. M. Smith. 2005. Estuarine respiration: an overview of benthic, pelagic, and whole system respiration, *In* Respiration in aquatic ecosystems. Oxford University Press, New York, NY.

Hopkinson, C. S., and J. J. Vallino. 1995. The relationships among man's activities in watersheds and estuaries: a model of runoff effects on patterns of estuarine community metabolism. Estuaries **18**: 598–621.

Horrigan, S. G., J. P. Montoya, J. L. Nevins, J. J. McCarthy, H. Ducklow, R. Goericke, and T. Malone. 1990. Nitrogenous nutrient transformations in the spring and fall in the Chesapeake Bay. Estuar. Coast. Shelf Sci. **30**: 369–391.

Ho, T., A. Quigg, Z. V. Finkel, A. J. Milligan, K. Wyman, P. G. Falkowski, and F. M. M. Morel. 2003. The elemental composition of some marine phytoplankton. J. Phycol. **39**: 1145–1159.

Ho, T.-Y., G. T. Taylor, Y. Astor, R. Varela, F. Müller-Karger, and M. I. Scranton. 2004. Vertical and temporal variability of redox zonation in the water column of the Cariaco Basin: implications for organic carbon oxidation pathways. Mar. Chem. **86**: 89–104.

Howarth, R., F. Chan, D. J. Conley, J. Garnier, S. C. Doney, R. Marino, and G. Billen. 2011. Coupled biogeochemical cycles: eutrophication and hypoxia in temperate estuaries and coastal marine ecosystems. Front. Ecol. Environ. **9**: 18–26.

Huang, W.-J., Y. Wang, and W.-J. Cai. 2012. Assessment of sample storage techniques for total alkalinity and dissolved inorganic carbon in seawater. Limnol. Oceanogr. Methods **10**: 711–717.

Hulth, S., R. C. Aller, D. E. Canfield, T. Dalsgaard, P. Engström, F. Gilbert, K. Sundbäck, and B. Thamdrup. 2005. Nitrogen removal in marine environments: recent findings and future research challenges. Mar. Chem. **94**: 125–145.

Jenkins, M. C., and W. M. Kemp. 1984. The coupling of nitrification and denitrification in two estuarine sediments. Limnol. Oceanogr. **29**: 609–619.

Jiang, L.-Q., W.-J. Cai, and Y. Wang. 2008. A comparative study of carbon dioxide degassing in river- and marine-dominated estuaries. Limnol. Oceanogr. **53**: 2603–2615.

Jiang, L.-Q., W.-J. Cai, Y. Wang, J. Diaz, P. L. Yager, and X. Hu. 2010. Pelagic community respiration on the continental shelf off Georgia, USA. Biogeochemistry **98**: 101–113.

Johnson, M. D., M. Rome, and D. K. Stoecker. 2003. Microzooplankton grazing on *Prorocentrum minimum* and *Karlodinium micrum* in Chesapeake Bay. Limnol. Oceanogr. **48**: 238–248Purchase.

Jonas, R. B. 1997. Bacteria, dissolved organics and oxygen consumption in salinity stratified Chesapeake Bay, an anoxia paradigm. Am. Zool. **37**: 612–620.

Jonas, R. B., and J. H. Tuttle. 1990. Bacterioplankton and organic carbon dynamics in the lower mesohaline Chesapeake Bay. Appl. Environ. Microbiol. **56**: 747–757.

Jordan, T. E., J. C. Cornwell, W. R. Boynton, and J. T. Anderson. 2008. Changes in phosphorus biogeochemistry along an estuarine salinity gradient: The iron conveyer belt. Limnol. Oceanogr. **53**: 172–184.

Jørgensen, B. B. 1982. Ecology of the bacteria of the sulphur cycle with special reference to anoxic-oxic interface environments. Philos. Trans. R. Soc. Lond. B. Biol. Sci. **298**: 543–561.

Joye, S. B., and J. T. Hollibaugh. 1995. Influence of sulfide inhibition of nitrification on nitrogen regeneration in sediments. Science **270**: 623–625.

Kana, T. M., C. Darkangelo, M. D. Hunt, J. B. Oldham, G. E. Bennett, and J. C. Cornwell. 1994. Membrane inlet mass spectrometer for rapid high-precision determination of N_2, O_2, and Ar in environmental water samples. Anal. Chem. **66**: 4166–4170.

Kan, J., B. C. Crump, K. Wang, and F. Chen. 2006. Bacterioplankton community in Chesapeake Bay: predictable or random assemblages. Limnol. Oceanogr. **51**: 2157–2169.

Kass, R. E., and A. E. Raftery. 1995. Bayes factors. J. Am. Stat. Assoc. **90**: 773–795.

Kelly, J. R., V. M. Berounsky, S. W. Nixon, and C. A. Oviatt. 1985. Benthic-pelagic coupling and nutrient cycling across an experimental eutrophication gradient. Mar. Ecol. Prog. Ser. **26**: 207–219.

Kemp, P. F., J. J. Cole, B. F. Sherr, and E. B. Sherr. 1993. Handbook of methods in aquatic microbial ecology, CRC Press.

Kemp, W. M., J. Faganeli, S. Puskaric, E. Smith, and W. Boynton. 1999. Pelagic-benthic coupling and nutrient cycling. In: Malone T, Malej A, Harding L, Smodlaka N, Turner R (eds) Ecosystems at the land-sea margin: drainage basin to coastal sea., American Geophysical Union, Washington, DC.

Kemp, W. M., P. A. Sampou, J. Garber, J. Tuttle, and W. R. Boynton. 1992. Seasonal depletion of oxygen from bottom waters of Chesapeake Bay: roles of benthic and planktonic respiration and physical exchange processes. Mar. Ecol. Prog. Ser. **85**: 137–152.

Kemp, W. M., P. Sampou, J. Caffrey, M. Mayer, K. Henriksen, and W. R. Boynton. 1990. Ammonium recycling versus denitrification in Chesapeake Bay sediments. Limnol. Oceanogr. **35**: 1545–1563.

Kemp, W. M., E. M. Smith, M. Marvin-Dipasquale, and W. R. Boynton. 1997. Organic carbon balance and net ecosystem metabolism in Chesapeake Bay. Mar. Ecol. Prog. Ser. **150**: 229–248.

Kepkay, P. E., and K. H. Nealson. 1987. Growth of a manganese oxidizing *Pseudomonas* sp. in continuous culture. Arch. Microbiol. **148**: 63–67.

Killberg-Thoreson, L., R. E. Sipler, and D. A. Bronk. 2013. Anthropogenic nutrient sources supplied to a Chesapeake Bay tributary support algal growth: a bioassay and high-resolution mass spectrometry approach. Estuaries Coasts **36**: 966–980.

Kirchman, D. L. 1993. Leucine incorporation as a measure of biomass production by heterotrophic bacteria, *In* Handbook of methods in aquatic microbial ecology. CRC Press.

Kleppel, G. S., D. V. Holliday, and R. E. Pieper. 1991. Trophic interactions between copepods and microplankton: a question about the role of diatoms. Limnol. Oceanogr. **36**: 172–178.

Kruse, B. 1993. Measurement of plankton O_2 respiration in gas-tight plastic bags. Mar. Ecol. Prog. Ser. **94**: 155–163.

Labrenz, M., G. Jost, C. Pohl, S. Beckmann, W. Martens-Habbena, and K. Jürgens. 2005. Impact of different in vitro electron donor/acceptor conditions on potential chemolithoautotrophic communities from marine pelagic redoxclines. Appl. Environ. Microbiol. **71**: 6664–6672.

Lane, L., S. Rhoades, C. Thomas, and L. Van Heukelem. 2000. Standard operating procedures 2000. University of Maryland Horn Point Laboratory Technical Report No. TS-264-00.

Larsson, U., S. Hajdu, J. Walve, and R. Elmgren. 2001. Baltic Sea nitrogen fixation estimated from the summer increase in upper mixed layer total nitrogen. Limnol. Oceanogr. **46**: 811–820.

Lee, D. Y., D. P. Keller, B. C. Crump, and R. R. Hood. 2012. Community metabolism and energy transfer in the Chesapeake Bay estuarine turbidity maximum. Mar. Ecol. Prog. Ser. **449**: 65–82.

Lee, D. Y., M. S. Owens, M. Doherty, E. M. Eggleston, I. Hewson, B. C. Crump, and J. C. Cornwell. 2014. The effects of oxygen transition on community respiration and potential chemoautotrophic production in a seasonally stratified anoxic estuary. Estuaries Coasts, doi:10.1007/s12237-014-9803-8.

Li, M., L. Zhong, W. C. Boicourt, S. Zhang, and D.-L. Zhang. 2007. Hurricane-induced destratification and restratification in a partially-mixed estuary. J. Mar. Res. **65**: 169–192.

Lin, X., M. I. Scranton, A. Y. Chistoserdov, R. Varela, and G. T. Taylor. 2008. Spatiotemporal dynamics of bacterial populations in the anoxic Cariaco Basin. Limnol. Oceanogr. **53**: 37–51.

Lipschultz, F., S. C. Wofsy, and L. E. Fox. 1986. Nitrogen metabolism of the eutrophic Delaware River ecosystem. Limnol. Oceanogr. **31**: 701–716.

Li, W. K. W. 1982. Estimating heterotrophic bacterial productivity by inorganic radiocarbon uptake: importance of establishing time courses of uptake. Mar. Ecol. Prog. Ser. **8**: 167–172.

Llirós, M., L. Alonso-Sáez, F. Gich, A. Plasencia, O. Auguet, E. O. Casamayor, and C. M. Borrego. 2011. Active bacteria and archaea cells fixing bicarbonate in the dark along the water column of a stratified eutrophic lagoon. FEMS Microbiol. Ecol. **77**: 370–384.

Lomas, M. W., and F. Lipschultz. 2006. Forming the primary nitrite maximum: nitrifiers or phytoplankton? Limnol. Oceanogr. **51**: 2453–2467.

Malone, T. C., L. Crocker, S. Pike, and B. Wendler. 1988. Influences of river flow on the dynamics of phytoplankton production in a partially stratified estuary. Mar. Ecol. Prog. Ser. **48**: 235–249.

Malone, T. C., W. M. Kemp, H. W. Ducklow, W. R. Boynton, J. H. Tuttle, and R. B. Jonas. 1986. Lateral variation in the production and fate of phytoplankton in a partially stratified estuary. Mar. Ecol. Prog. Ser. **32**: 149–160.

Malone, T., D. Conley, T. Fisher, P. Glibert, L. Harding, and K. Sellner. 1996. Scales of nutrient-limited phytoplankton productivity in Chesapeake Bay. Estuaries Coasts **19**: 371–385.

Martens-Habbena, W., P. M. Berube, H. Urakawa, J. R. de la Torre, and D. A. Stahl. 2009. Ammonia oxidation kinetics determine niche separation of nitrifying Archaea and Bacteria. Nature **461**: 976–979.

Marvin-DiPasquale, M. C., and D. G. Capone. 1998. Benthic sulfate reduction along the Chesapeake Bay central channel. I. Spatial trends and controls. Mar. Ecol. Prog. Ser. **168**: 213–228.

Mayer, M. S., L. Schaffner, and W. M. Kemp. 1995. Nitrification potentials of benthic macrofaunal tubes and burrow walls: effects of sediment NH_4^+ and animal irrigation behavior. Mar Ecol Prog Ser **121**: 157–169.

McCallister, S. L., J. E. Bauer, H. W. Ducklow, and E. A. Canuel. 2006. Sources of estuarine dissolved and particulate organic matter: A multi-tracer approach. Org. Geochem. **37**: 454–468.

McCarthy, J. J., W. Kaplan, and J. L. Nevins. 1984. Chesapeake Bay Nutrient and Plankton Dynamics. 2. Sources and Sinks of Nitrite. Limnol. Oceanogr. **29**: 84–98.

McDonough, R. J., R. W. Sanders, K. G. Porter, and D. L. Kirchman. 1986. Depth distribution of bacterial production in a stratified lake with an anoxic hypolimnion. Appl. Environ. Microbiol. **52**: 992–1000.

McManus, M. A., O. M. Cheriton, P. J. Drake, D. V. Holliday, C. D. Storlazzi, P. L. Donaghay, and C. F. Greenlaw. 2005. Effects of physical processes on structure and

transport of thin zooplankton layers in the coastal ocean. Mar. Ecol. Prog. Ser. **301**: 199–215.

McManus, M., A. Alldredge, A. Barnard, E. Boss, J. Case, T. Cowles, P. Donaghay, L. Eisner, D. Gifford, C. Greenlaw, C. Herren, D. Holliday, D. Johnson, S. MacIntyre, D. McGehee, T. Osborn, M. Perry, R. Pieper, J. Rines, D. Smith, J. Sullivan, M. Talbot, M. Twardowski, A. Weidemann, and J. Zaneveld. 2003. Characteristics, distribution and persistence of thin layers over a 48 hour period. Mar. Ecol. Prog. Ser. **261**: 1–19.

Middelburg, J. J., and L. A. Levin. 2009. Coastal hypoxia and sediment biogeochemistry. Biogeosciences **6**: 1273–1293.

Morris, R. L., and T. M. Schmidt. 2013. Shallow breathing: bacterial life at low O_2. Nat. Rev. Microbiol. **11**: 205–212.

Murphy, R. R., W. M. Kemp, and W. P. Ball. 2011. Long-term trends in Chesapeake Bay seasonal hypoxia, stratification, and nutrient loading. Estuaries Coasts **34**: 1293–1309.

Najjar, R. G., C. R. Pyke, M. B. Adams, D. Breitburg, C. Hershner, M. Kemp, R. Howarth, M. R. Mulholland, M. Paolisso, D. Secor, K. Sellner, D. Wardrop, and R. Wood. 2010. Potential climate-change impacts on the Chesapeake Bay. Estuar. Coast. Shelf Sci. **86**: 1–20.

Najjar, R. G., H. A. Walker, P. J. Anderson, E. J. Barron, R. J. Bord, J. R. Gibson, V. S. Kennedy, C. G. Knight, J. P. Megonigal, R. E. OConnor, C. D. Polsky, N. P. Psuty, B. A. Richards, L. G. Sorenson, E. M. Steele, and R. S. Swanson. 2000. The potential impacts of climate change on the mid-Atlantic coastal region. Clim. Res. **14**: 219–233.

Nealson, K. H., and C. R. Myers. 1992. Microbial reduction of manganese and iron: new approaches to carbon cycling. Appl. Environ. Microbiol. **58**: 439–443.

Odum, H. T. 1956. Primary production in flowing waters. Limnol. Oceanogr. **1**: 102–117.

Officer, C. B. 1979. Discussion of the behaviour of nonconservative dissolved constituents in estuaries. Estuar. Coast. Mar. Sci. **9**: 91–94.

Officer, C. B., R. B. Biggs, J. L. Taft, L. E. Cronin, M. A. Tyler, and W. R. Boynton. 1984. Chesapeake Bay anoxia: origin, development, and significance. Science **223**: 22–27.

Oviatt, C. A., A. A. Keller, P. A. Sampou, and L. L. Beatty. 1986a. Patterns of productivity during eutrophication: a mesocosm experiment. Mar. Ecol. Prog. Ser. **28**: 69–8.

Oviatt, C. A., D. T. Rudnick, A. A. Keller, P. A. Sampou, and G. T. Almquist. 1986b. A comparison of system (O_2 and CO_2) and C-14 measurements of metabolism in estuarine mesocosms. Mar. Ecol. Prog. Ser. **28**: 57–67.

Parsons, T. R., Y. Maita, and C. M. Lalli. 1984. A manual of chemical and biological methods for seawater analysis, Pergamon Press, Elmsford, New York, USA.

Passow, U. 2002. Transparent exopolymer particles (TEP) in aquatic environments. Prog. Oceanogr. **55**: 287–333.

Pedrós-Alió, C., J. García-Cantizano, and J. I. Calderón. 1993. Bacterial production in anaerobic water column, p. 519–530. *In* Handbook of methods in aquatic microbial ecology. CRC Press.

Perez, R. C., and A. Matin. 1982. Carbon dioxide assimilation by *Thiobacillus novellus* under nutrient-limited mixotrophic conditions. J. Bacteriol. **150**: 46–51.

Pierson, J. J., M. R. Roman, D. G. Kimmel, W. C. Boicourt, and X. Zhang. 2009. Quantifying changes in the vertical distribution of mesozooplankton in response to hypoxic bottom waters. J. Exp. Mar. Biol. Ecol. **381**: S74–S79.

Pomeroy, L. R., and W. J. Wiebe. 2001. Temperature and substrates as interactive limiting factors for marine heterotrophic bacteria. Aquat. Microb. Ecol. **23**: 187–204.

Pritchard, D. W. 1967. Observations of circulation in coastal plain estuaries, p. 37–44. *In* Estuaries.

Regnier, P., P. Friedlingstein, P. Ciais, F. T. Mackenzie, N. Gruber, I. A. Janssens, G. G. Laruelle, R. Lauerwald, S. Luyssaert, A. J. Andersson, S. Arndt, C. Arnosti, A. V. Borges, A. W. Dale, A. Gallego-Sala, Y. Goddéris, N. Goossens, J. Hartmann, C. Heinze, T. Ilyina, F. Joos, D. E. LaRowe, J. Leifeld, F. J. R. Meysman, G. Munhoven, P. A. Raymond, R. Spahni, P. Suntharalingam, and M. Thullner. 2013. Anthropogenic perturbation of the carbon fluxes from land to ocean. Nat. Geosci. **6**: 597–607.

Rich, J., O. Dale, B. Song, and B. Ward. 2008. Anaerobic ammonium oxidation (Anammox) in Chesapeake Bay sediments. Microb. Ecol. **55**: 311–320.

Robinson, C. 2008. Heterotrophic bacterial respiration, p. 299–334. *In* Microbial Ecology of the Oceans. John Wiley & Sons, Inc., Hoboken, NJ, USA.

Rocke, E., and H. Liu. 2014. Respiration, growth and grazing rates of three ciliate species in hypoxic conditions. Mar. Pollut. Bull. **85**: 410–417.

Roden, E. E., and J. H. Tuttle. 1992. Sulfide release from estuarine sediments underlying anoxic bottom water. Limnol. Oceanogr. **37**: 725–738.

Roden, E. E., J. H. Tuttle, W. R. Boynton, and W. M. Kemp. 1995. Carbon cycling in mesohaline Chesapeake Bay sediments. 1. POC deposition rates and mineralization pathways. J. Mar. Res. **53**: 799–819.

Roman, M. R., A. L. Gauzens, W. K. Rhinehart, and J. R. White. 1993. Effects of low oxygen waters on Chesapeake Bay zooplankton. Limnol. Oceanogr. **38**: 1603–1614.

Roslev, P., M. B. Larsen, D. Jørgensen, and M. Hesselsoe. 2004. Use of heterotrophic CO_2 assimilation as a measure of metabolic activity in planktonic and sessile bacteria. J. Microbiol. Methods **59**: 381–393.

Rysgaard, S., N. Risgaard-Petersen, and N. P. Sloth. 1996. Nitrification, denitrification, and nitrate ammonification in sediments of two coastal lagoons in Southern France. Hydrobiologia **329**: 133–141.

Sampou, P., and W. M. Kemp. 1994. Factors regulating plankton community respiration in Chesapeake Bay. Mar. Ecol. Prog. Ser. **110**: 249–258.

Sanford, L. P., K. G. Sellner, and D. L. Breitburg. 1990. Covariability of dissolved oxygen with physical processes in the summertime Chesapeake Bay. J. Mar. Res. **48**: 567–590.

Santoro, A. E. 2009. Microbial nitrogen cycling at the saltwater–freshwater interface. Hydrogeol. J. **18**: 187–202.

Schippers, A., and B. B. Jørgensen. 2001. Oxidation of pyrite and iron sulfide by manganese dioxide in marine sediments. Geochim. Cosmochim. Acta **65**: 915–922.

Scully, M. E. 2010. Wind modulation of dissolved oxygen in Chesapeake Bay. Estuaries Coasts **33**: 1164–1175.

Seitzinger, S., W. Gardner, and A. Spratt. 1991. The effect of salinity on ammonium sorption in aquatic sediments: Implications for benthic nutrient recycling. Estuaries Coasts **14**: 167–174.

Shiah, F.-K., and H. W. Ducklow. 1994. Temperature regulation of heterotrophic bacterioplankton abundance, production, and specific growth rate in Chesapeake Bay. Limnol. Oceanogr. **39**: 1243–1258.

Shively, J. M., G. van Keulen, and W. G. Meijer. 1998. Something from almost nothing: carbon dioxide fixation in chemoautotrophs. Annu. Rev. Microbiol. **52**: 191–230.

Sieracki, M. E., I. C. Gilg, E. C. Thier, N. J. Poulton, and R. Goericke. 2006. Distribution of planktonic aerobic anoxygenic photoheterotrophic bacteria in the Northwest Atlantic. Limnol. Oceanogr. **51**: 38–46.

Smith, E. M., and W. M. Kemp. 1995. Seasonal and regional variations in plankton community production and respiration for Chesapeake Bay. Mar. Ecol. Prog. Ser. **116**: 217–231.

Smith, E. M., and W. M. Kemp. 2001. Size structure and the production/respiration balance in a coastal plankton community. Limnol. Oceanogr. **46**: 473–485.

Smith, E. M., and W. M. Kemp. 2003. Planktonic and bacterial respiration along an estuarine gradient: responses to carbon and nutrient enrichment. Aquat. Microb. Ecol. **30**: 251–261.

Smith, S. V., and J. Hollibaugh. 1993. Coastal metabolism and the oceanic organic carbon balance. Rev Geophys **31**: 75–89.

Sorokin, Y. I., P. Y. Sorokin, V. A. Avdeev, D. Y. Sorokin, and S. V. Ilchenko. 1995. Biomass, production and activity of bacteria in the Black Sea, with special reference to chemosynthesis and the sulfur cycle. Hydrobiologia **308**: 61–76.

Stanley, D. W., and S. W. Nixon. 1992. Stratification and bottom-water hypoxia in the Pamlico River estuary. Estuaries **15**: 270–281.

Starkenburg, S. R., P. S. G. Chain, L. A. Sayavedra-Soto, L. Hauser, M. L. Land, F. W. Larimer, S. A. Malfatti, M. G. Klotz, P. J. Bottomley, D. J. Arp, and W. J. Hickey. 2006. Genome sequence of the chemolithoautotrophic nitrite-oxidizing bacterium *Nitrobacter winogradskyi* Nb-255. Appl. Environ. Microbiol. **72**: 2050–2063.

Stoecker, D. K., and J. M. Capuzzo. 1990. Predation on protozoa: its importance to zooplankton. J. Plankton Res. **12**: 891–908.

Straub, K. L., M. Benz, B. Schink, and F. Widdel. 1996. Anaerobic, nitrate-dependent microbial oxidation of ferrous iron. Appl. Environ. Microbiol. **62**: 1458–1460.

Sundbäck, K., A. Miles, and E. Göransson. 2000. Nitrogen fluxes, denitrification and the role of microphytobenthos in microtidal shallow-water sediments: an annual study. Mar. Ecol. Prog. Ser. **200**: 59–76.

Sun, M.-Y., C. Lee, and R. C. Aller. 1993. Laboratory studies of oxic and anoxic degradation of chlorophyll-a in Long Island Sound sediments. Geochim. Cosmochim. Acta **57**: 147–157.

Swan, B. K., M. Martinez-Garcia, C. M. Preston, A. Sczyrba, T. Woyke, D. Lamy, T. Reinthaler, N. J. Poulton, E. D. P. Masland, M. L. Gomez, M. E. Sieracki, E. F. DeLong, G. J. Herndl, and R. Stepanauskas. 2011. Potential for chemolithoautotrophy among ubiquitous bacteria lineages in the dark ocean. Science **333**: 1296–1300.

Taft, J., W. Taylor, E. Hartwig, and R. Loftus. 1980. Seasonal oxygen depletion in Chesapeake Bay. Estuaries Coasts **3**: 242–247.

Taylor, G. T., M. Iabichella, T.-Y. Ho, M. I. Scranton, R. C. Thunell, F. Muller-Karger, and Ramon Varela. 2001. Chemoautotrophy in the redox transition zone of the Cariaco Basin: a significant midwater source of organic carbon production. Limnol. Oceanogr. **46**: 148–163.

Tebo, B. M., H. A. Johnson, J. K. McCarthy, and A. S. Templeton. 2005. Geomicrobiology of manganese(II) oxidation. Trends Microbiol. **13**: 421–428.

Testa, J. M., D. C. Brady, D. M. Di Toro, W. R. Boynton, J. C. Cornwell, and W. M. Kemp. 2013. Sediment flux modeling: Simulating nitrogen, phosphorus, and silica cycles. Estuar. Coast. Shelf Sci. **131**: 245–263.

Testa, J. M., and W. M. Kemp. 2012. Hypoxia-induced shifts in nitrogen and phosphorus cycling in Chesapeake Bay. Limnol. Oceanogr. **57**: 835–850.

Trouwborst, R. E., B. G. Clement, B. M. Tebo, B. T. Glazer, and G. W. Luther. 2006. Soluble Mn(III) in suboxic zones. Science **313**: 1955–1957.

Turner, R. E., N. N. Rabalais, and D. Justic. 2008. Gulf of Mexico hypoxia: alternate states and a legacy. Environ. Sci. Technol. **42**: 2323–2327.

US Navy. 1956. Tables for rapid computation of density and electrical conductivity of sea water. Oceanographic Survey Branch, Division of Oceanography, U.S. Navy Hydrographic Office.

Veuger, B., A. Pitcher, S. Schouten, J. S. Sinninghe Damsté, and J. J. Middelburg. 2013. Nitrification and growth of autotrophic nitrifying bacteria and *Thaumarchaeota* in the coastal North Sea. Biogeosciences **10**: 1775–1785.

Watson, S. W., E. Bock, F. W. Valois, J. B. Waterbury, and U. Schlosser. 1986. *Nitrospira marina* gen. nov. sp. nov.: a chemolithotrophic nitrite-oxidizing bacterium. Arch. Microbiol. **144**: 1–7.

White, J. R., and M. R. Roman. 1992. Egg production by the calanoid copepod *Arcartia tonsa* in the mesohaline Chesapeake Bay: the importance of food resources and temperature. Mar. Ecol. Prog. Ser. **86**: 239–249.

Wienke, S. M., and J. E. Cloern. 1987. The phytoplankton component of seston in San Francisco Bay. Neth. J. Sea Res. **21**: 25–33.

Williams, P. J. leB., and P. A. del Giorgio. 2005. Respiration in aquatic ecosystems: history and background, p. 1–17. *In* Respiration in aquatic ecosystems. Oxford University Press, New York, NY.

Wissel, B., Quiones-Rivera, J. Zoraida, and F. Brian. 2008. Combined analyses of O_2 and CO_2 for studying the coupling of photosynthesis and respiration in aquatic systems. Can. J. Fish. Aquat. Sci. **65**: 2378–2388.

Wright, J. J., K. M. Konwar, and S. J. Hallam. 2012. Microbial ecology of expanding oxygen minimum zones. Nat. Rev. Microbiol. **10**: 381–394.

Yeager, C. L. J., L. W. H. Jr, and M. E. Mallonee. 2005. Phytoplankton production, biomass and community structure following a summer nutrient pulse in Chesapeake Bay. Aquat. Ecol. **39**: 135–149.

Yoshiyama, K., and J. H. Sharp. 2006. Phytoplankton response to nutrient enrichment in an urbanized estuary: Apparent inhibition of primary production by overeutrophication. Limnol. Oceanogr. **51**: 424–434.

Zaikova, E., D. A. Walsh, C. P. Stilwell, W. W. Mohn, P. D. Tortell, and S. J. Hallam. 2010. Microbial community dynamics in a seasonally anoxic fjord: Saanich Inlet, British Columbia. Environ. Microbiol. **12**: 172–191.

Zhai, W., M. Dai, and X. Guo. 2007. Carbonate system and CO_2 degassing fluxes in the inner estuary of Changjiang (Yangtze) River, China. Mar. Chem. **107**: 342–356.

Zimmerman, A. R., and E. A. Canuel. 2000. A geochemical record of eutrophication and anoxia in Chesapeake Bay sediments: anthropogenic influence on organic matter composition. Mar. Chem. **69**: 117–137.

Zopfi, J., T. G. Ferdelman, B. B. Jørgensen, A. Teske, and B. Thamdrup. 2001. Influence of water column dynamics on sulfide oxidation and other major biogeochemical processes in the chemocline of Mariager Fjord (Denmark). Mar. Chem. **74**: 29–51.